PREVENTING BIOFILM IMPLANT-RELATED OSTEOMYELITIS USING A NOVEL SYNTHETIC ANALOG OF ANTIMICROBIAL PEPTIDES

by

Dustin Lee Williams

A dissertation submitted to the faculty of
The University of Utah
in partial fulfillment of the requirements for the degree of

Doctor of Philosophy

Department of Bioengineering

The University of Utah

August 2012

The University of Utah Graduate School

STATEMENT OF DISSERTATION APPROVAL

The dissertation of **Dustin Williams**

has been approved by the following supervisory committee members:

Roy Bloebaum	, Chair	**April 18, 2012** Date Approved
Patrick Tresco	, Member	**April 18, 2012** Date Approved
Larry Meyer	, Member	**April 18, 2012** Date Approved
Susan Bock	, Member	**April 18, 2012** Date Approved
John Hibbs	, Member	**April 18, 2012** Date Approved

and by **Patrick Tresco**, Chair of the Department of **Bioengineering**

and by Charles A. Wight, Dean of The Graduate School.

ABSTRACT

Biofilm implant-related infections represent one of the most difficult-to-treat pathologies in current healthcare systems. According to the National Institutes of Health, over 80% of infections in the human body are biofilm related. Biofilms are dynamic communities of bacterial cells that are often polymicrobial and which typically develop into three-dimensional structures that are attached to a surface. Due to the morphological, physiological and genotypic characteristics of biofilms, they are highly resistant to antibiotic therapies.

One of the most practical strategies that has been undertaken to prevent these biofilm implant-related infections has been the development of active release coatings on biomaterial devices. Unfortunately, to date, active release coatings have had limited *in vivo* and clinical success due to several important limitations.

To address these limitations, the work that was performed in this dissertation has led to or may lead to five areas of development that have the potential to contribute to the fields of bioengineering and biofilm research. First, a membrane biofilm reactor was developed to grow biofilms for use as initial inocula both *in vitro* and *in vivo*. Second, in contrast to the common use of planktonic bacteria for *in vitro* and *in vivo* testing, all aspects of this project used well-established biofilms of methicillin-resistant *Staphylococcus aureus* using the membrane biofilm reactor to more closely model the phenotype of bacteria that reside in natural ecosystem. Third, a novel antimicrobial

compound was used as an active release agent. Fourth, the *in vitro* work performed in this study was done using a flow cell system to more closely model an *in vivo* paradigm. Fifth, the animal model that was established for this project presents the first animal model in the published literature to use well-established biofilms of MRSA that were grown under fluid sheer forces as initial inocula in an animal model of biofilm-related infection.

The *in vitro* results demonstrated that the active release coating was able to significantly eradicate biofilms within a 24-hour period. These results translated to the *in vivo* model wherein the active release coating was able to prevent biofilm implant-related infection in 100% of animals tested. Taken together, these results provide a promising outlook for the future use of this active release coating to prevent biofilm implant-related infections.

In loving memory of my father, Don Carlos Williams, who passed away just four days before I was to start my trying Graduate School experience. To my mother who is everything that a mother and grandmother should be. To my family, extended and immediate, who have never given up on me. To my wife, who has never allowed me to quit, who is beautiful inside and out, who has been my rock and support; and to my kids who bring joy to the world and who have been my motivation to make the world a better place. And most importantly to my Father in Heaven. The fact that I have made it through this experience and accomplished all that I have is a testament to the power of prayer.

TABLE OF CONTENTS

ABSTRACT.....iii

SYMBOLS.....ix

ACKNOWLEDGMENTS xi

1. THE IMPACT OF BIOFILMS ON BIOMEDICAL DEVICES 1

1.1 The Birth of Germ Theory 1
1.2 From Germ Theory to Biofilm Theory 6
1.3 Early Observation of Biofilm on a Medical Implant 8
1.4 The Biofilm Theory Applied to Orthopaedics 10
1.5 Characteristics of Biofilms and Antibiotic Resistance 11
1.6 The Rise of an Antibiotic Resistance Era 21
1.7 The Current Impact of Biofilms on Biomedical Devices 23
1.8 Prevalence of Open Fractures and Rates of Infection.....25
1.9 Rationale for Study Design and Dissertation Outline.....28

2. PREANTIBIOTIC THERAPIES, THE DEVELOPMENT OF NOVEL ANTIMICROBIAL COMPOUNDS, AND ACTIVE RELEASE COATINGS 38

2.1 Methods of Treating Infection Prior to the Discovery of Antibiotics 38
2.2 A Novel Class of Antimicrobial Compounds Discovered.....44
2.3 CSA-13 Ceragenin: A Novel Synthetic Analog of AMPs.....49
2.4 General Hypothesis of Dissertation and Specific Aims.....51
2.5 A Practical Approach to Delivering Antimicrobials: Active Release Coatings 53
2.6 The Selection of Polymer for an Active Release Coating 67

3. USING BIOFILMS AS INITIAL INOCULA IN ANIMAL MODELS OF BIOFILM-RELATED INFECTIONS 77

3.1 The Use of Planktonic Cells in Animal Models 77
3.2 Limitations of Using Planktonic Cells as Initial Inocula 78
3.3 Number of Bacteria in a Biofilm That May Be Used as Initial Inocula 80
3.4 The 10^5 Rule May Not Apply to Biofilm.....83
3.5 Future Methods of Growing Biofilm for Use as Initial Inocula 84

3.6 Concluding Discussion 85

4. A MEMBRANE BIOFILM REACTOR TO PRODUCE MATURE BIOFILMS ON THE SURFACE OF PEEK MEMBRANES FOR THE *IN VIVO* ANIMAL MODEL APPLICATION 89

4.1 Introduction 89
4.2 Materials and Methods 91
4.3 Results 95
4.4 Discussion 96

5. *IN VITRO* ANALYSIS OF THE CSA-13 ACTIVE RELEASE COATING TO ERADICATE BIOFILMS OF MRSA 103

5.1 Introduction 103
5.2 Materials and Methods 104
5.3 Results 114
5.4 Discussion 118

6. CHARACTERIZATION OF THE CSA-13 ACTIVE RELEASE COATING 128

6.1 Introduction 128
6.2 Materials and Methods 129
6.3 Results 133
6.4 Discussion 139

7. ESTABLISHING AN *IN VIVO* ANIMAL MODEL OF BIOFILM IMPLANT-RELATED OSTEOMYELITIS TO TEST COMBINATION BIOMATERIALS USING BIOFILMS AS INITIAL INOCULA 151

7.1 Introduction 151
7.2 Materials and Methods 152
7.3 Results 164
7.4 Discussion 168

8. *IN VIVO* EFFICACY OF THE NOVEL CSA-13 ACTIVE RELEASE COATING TO PREVENT BIOFILM IMPLANT-RELATED OSTEOMYELITIS 182

8.1 Introduction 182
8.2 Materials and Methods 182
8.3 Results 185
8.4 Discussion 192

9. CONCLUDING REMARKS 203

9.1 Dissertation Highlights 203
9.2 Future Work 207
9.3 Conclusion 209

Appendices

A: USING BIOFILMS AS INITIAL INOCULA IN ANIMAL MODELS OF BIOFILM-RELATED INFECTIONS 211

B: A MODIFIED CDC BIOFILM REACTOR TO PRODUCE MATURE BIOFILMS ON THE SURFACE OF PEEK MEMBRANES FOR AN *IN VIVO* ANIMAL MODEL APPLICATION 219

C: USE OF DELRIN PLASTIC IN A MODIFIED CDC BIOFILM REACTOR 227

D: OBSERVING THE BIOFILM MATRIX OF *Staphylococcus epidermidis* ATCC 35984 GROWN USING THE CDC BIOFILM REACTOR 233

E: EXPERIMENTAL MODEL OF BIOFILM IMPLANT-RELATED OSTEOMYELITIS TO TEST COMBINATION BIOMATERIALS USING BIOFILMS AS INITIAL INOCULA 244

REFERENCES 258

SYMBOLS

PhD	Doctor of Philosophy
mL	Milliliter
MD	Medical Doctor
SEM	Scanning Electron Microscopy
SCLM	Scanning Confocal Laser Microscopy
ECM	Extracellular Matrix
DNA	Deoxyribonucleic acid
NIH	National Institutes of Health
CDC	Centers for Disease Control
U.S.	United States
OIF	Operation Iraqi Freedom
OEF	Operation Enduring Freedom
CSA-13	Cationic Steroid Antimicrobial-13
UHMWPE	Ultrahighmolecularweightpolyethylene
MRSA	Methicillin-Resistant *Staphylococcus aureus*
FDA	Food and Drug Administration
AMPs	Antimicrobial Peptides
AFM	Atomic Force Microscopy
mg	Milligram
MIC	Minimum Inhibitory Concentration
PU	Polyurethane
PMMA	Polymethylmethacrylate
PHEMA	Polyhydroxyethylmethacrylate
HA	Hydroxyapatite
PLLA	Polylactic Acid
PLGA	Polyglycolactic Acid
PV	Polyvinyl
PDMS	Polydimethylsiloxane
RTV-1	One Part Room Temperature Vulcanizing
ETO	Ethylene Oxide
PEG	Polyethyleneglycol
mm	Millimeter
w/w	Weight-To-Weight
nm	Nanometer

µm	Micrometer
CLSI	Clinical and Laboratory Standards Institute
SOP	Standard Operating Procedure
ASTM	American Society for Testing and Materials
PEEK	Polyetheretherketone
PCR	Polymerase Chain Reaction
PIA	Polysaccharide Intercellular Adhesin
cm	Centimeter
BHI	Brain Heart Infusion
C	Celsius
min	Minute
Hz	Hertz
µL	Microliter
CFU	Colony Forming Units
ANOVA	Analysis of Variance
SD	Standard Deviation
SS	Stainless Steel
inHg	Inches of Mercury
D/E	Dey Engley
LC/MS	High Pressure Liquid Chromatography/Time of Flight Mass Spectrometry
dCSA-13	Deuterated CSA-13
ATR-FTIR	Attenuated Total Reflectance Fourier Transformed Infrared Spectroscopy
TGA	Thermal Gravimetric Analysis
SE	Secondary Electron
BSE	Backscatter Electron
EDX	Electron Dispersive X-Ray
Cl	Chlorine
IACUC	Institutional Animal Care and Use Committee
EHS	Environmental Health and Safety
IV	Intravenous
kg	Kilogram
hr	Hour
F	Fahrenheit
MAR	Mineral Apposition Rate
kV	Kilovolts
L	Liter
H&E	Hematoxylin and Eosin

ACKNOWLEDGMENTS

This work would not have been possible without the help of a flexibly rigid, merciful yet stern, and accepting mentor, Dr. Roy Bloebaum. I cannot imagine having made it through this process, having accomplished any of the goals I set out to achieve or undertaking any of my experiments without the help of Roy. The day I met him, he said he would treat me like one who had already received a Nobel Prize. I was expected to advance science, not just dabble in it, and to know every detail of my work so that I could defend it astutely. Nevertheless, all who know him have learned that he has a heart of gold and he allowed me to fail at times so that I could grow when I needed to, especially in the face of adversity. Despite those failures, I am especially grateful to have had minimal "come to Jesus" moments with him.

I also cannot express a sufficient amount of gratitude to my brothers and sisters for their support. All my life they have teased me for being a "nerd," despite my mother's protests. Now they will have even more ammunition to do so, but I embrace their jovial teases and hope to share my "nerdiness" in potentially helping millions who suffer from infection to be healed. My family, with my mother and father as the figure heads, constitutes the fiber of who I have become and I acknowledge their examples for building the foundation upon which I have lived my life.

There is perhaps no one who kept me from quitting Graduate School more than my wife, Marianne. I remember the very day when I suggested to her that I should just get a job and get on with life. She told me, "Science is your life." She went on to say that if I could see the potential that others see in me, I would not quit. I followed her counsel and as a result dedicated my whole heart to my PhD work. I believe that it was because of what she did for me that Dr. Bill Costerton, the world leader in biofilm discovery and research, told me that "Your work represents one of the top 10 PhD dissertations I have seen in my lifetime." But I am even more grateful for the work that my wife has performed to make my life wonderful. As a homemaker, she has embraced the most influential career in life and has raised two of the most caring, kind and delightful children that I have ever known: my boy, Jaden, and my self-proclaimed princess, Telia. They are great because she is great and we have another great one pending.

It would be inappropriate for me to not acknowledge the tremendous amount of confidence and encouragement that I received from Dr. Paul Savage and his team members, Jake Pollard, Jason Snarr, and Vinod Chaudhary. The fact that Paul was able to develop one of the most promising antimicrobial compounds of our time, and the fact that our team has had the opportunity to work with him, is a treasure. In addition to providing their time, supplies and lab space, they have influenced the advancement of this work and "bent over backwards" at times to help us in any way possible.

Those from the Bone and Joint Research Lab have likewise contributed more than can be said to this work. From the expertise of Richard Tyler Epperson in generating world-class histological sections for data analysis to Amber Wood, the one who keeps

Roy in line and makes it all happen in the front office: and from Bryan Haymond who always has some life application to Rugby or a controversial comment to make, to Sujee Jeyapalina, who is one of the most esoteric and unfiltered individuals this world has ever known. Dr. Peter Beck should also be given an enormous amount of appreciation for volunteering his valuable time for several years to perform surgeries on more than 100 animals in the lab. The list could go on, but in the end all I can say is Thank You to you all: Roy, Bryan, Kassie, Lucy, Nate, Julia, Andrew, Amber, Gwen, Andy, Sam, Peter, Dave, Sujee, Taylor, Steven, Dan, Brian, Tyler, Brooke, Adrian, Ryan, Kris, Sarina, Catherine, Teri, Emily, and all of those who have volunteered and served in our lab.

Because I would fail to receive multiple unwanted flying hugs for the rest of my life if I did not express my gratitude, I must also acknowledge the help of Dr. Brad Isaacson who has been a support and real friend to me throughout my graduate career. Brad is my unofficial brother who started Graduate School with me in the Fall of 2007 and has since become the self-proclaimed godfather of my children. Working synergistically off of each others' passion for science, we were able to develop research projects of our own thinking, bring in more than a million dollars of funding, publish more manuscripts than most graduate students, make Roy's life miserable and develop a lasting friendship despite stark differences in our ideologies that many would find to be irreconcilable.

The work presented in this dissertation was made particularly strong due to the many insights provided to us by our collaborators, consultants and colleagues. Dr. Bill Costerton traveled from the East Coast and Canada to provide us insights into the growth of biofilms and the development of our animal model. Dr. Lutz Claes traveled from

Germany to review our work and help optimize our surgical methods. Similar insights were given to us by Dr. Paul Savage, Dr. Jack Taylor, Dr. Charles Saltzman, Dr. Peter Beck, Dr. Albert Parker, Dr. Darla Goeres, Dr. David Moore, and many others.

Significant contributions and refinements to this work were also made by my advisory committee members. Dr. Larry Meyer provided us with the suggestion to use bone pieces in our *in vitro* testing. Dr. John Hibbs brainstormed with me to develop the concept of a flow cell system to test our antimicrobial coating *in vitro* as well as the method of creating infection in our animal model. Dr. Patrick Tresco and Dr. Susan Bock ensured that optimized controls were included in our animal work as well as in the *in vitro* testing. Dr. Tresco has also helped in the development of other projects in our lab and collaborated with me and Dr. Brian Holt on a potential project to develop a novel socket prosthetic for amputees. I am particularly grateful to my committee for giving me more than one chance to develop my knowledge and this project.

I also thank the technical, surgical and veterinary staff at the University of Utah's Comparative Medicine Center. The care that they provided to our animals was world-class and their genuine concern for animals' well being in general makes the research at the University of Utah successful.

Finally, I give my deep appreciation to the George E. Wahlen Department of Veterans Affairs in Salt Lake City for providing space and facilities for this work to be performed, as well as for awarding me the Predoctoral Associated Health Rehabilitation Research Fellowship, which funded my salary and benefits for a one-year period. Likewise, it is impossible to appropriately thank the National Institutes of Health for

awarding us $1.25 million of funding over five years to accomplish this work. After reading this dissertation, it should be seen that this funding was not used unwisely.

This project was largely successful due to the contributions of these people and institutions, and I openly express my gratitude for all that they have done.

CHAPTER 1

THE IMPACT OF BIOFILMS ON BIOMEDICAL DEVICES

1.1 The Birth of Germ Theory

One decade prior to the birth of Johann Sebastian Bach (1685-1750) and George Frideric Handel (1685-1759), amateur microscopist Antony van Leeuwenhoek (1632-1723) of Delft, Holland observed microscopic "animalcules" for the first time.[1] Using rudimentary techniques of hand-grinding glass into microscope lenses, van Leeuwenhoek viewed the constituents of scrapings from his own teeth. Based on what he saw, he drew pictures of what he believed to be living organisms. His drawings depicted rod-shaped matter and cone-like structures, one of which he drew with a squiggly line trailing behind it to indicate that it had motion (Figure 1.1). The pictures he drew were revolutionary at the time, but have since become archaic compared to technological advances that now permit scientists to look beyond the microcosm to the nanostructures of microbial cells.

Nevertheless, van Leeuwenhoek's observations are regarded as the benchmark of cellular discovery, for, prior to his observations there was no physical evidence that living matter existed beyond what the human eye could observe visually. Although these direct observations were unique, van Leeuwenhoek was not the first to conceptualize the existence of microscopic living matter. For centuries, philosophers and physicians had speculated that invisible, living creatures did in fact exist.

Nearly two millennia prior to the birth of van Leeuwenhoek, Titus Lucretius Carus (about 98-55 B.C.), the Roman poet and philosopher, suspected that invisible, living creatures were responsible for human disease.[2] Lucretius' belief was furthered by Girolamo Fracastoro (1478-1553), an Italian physician, scholar and poet who suggested that fomites could foster the seeds, or spores, of contagion and cause infection.[3] Lucretius' and Fracastoro's theories would later be described as atomist—a theory suggesting that minute, discrete, finite and indivisible elements are the ultimate constituents of all matter.

Unfortunately, the intuitive thinking of Carus and Fracastoro, and even the visual observations of animalcules by van Leeuwenhoek–all of which suggested that living matter did exist beyond the bounds of the naked eye–were not widely accepted. Indeed, their ideas were considered fanciful at best. This lack of acceptance stemmed from the fact that the world had a firm, and long-standing trust in the teachings of one of the most well known scholars in history: Aristotle Stagiritis, son of Nicomachus (384-322 B.C.). Indeed, the inaccurate observations of Aristotle were the root cause of a millennium-long debate surrounding one of the most important developments of human thought–the theory of spontaneous generation.[2]

Near 343 B.C., in volume VI, section 15, S4v of his *Historia Animalia*, Aristotle wrote that "There is a species of mullet that grows spontaneously out of mud and sand." He wrote further, "From the facts above enumerated it is quite proved that certain fishes come spontaneously into existence, not being derived from eggs or from copulation. Such fish as are neither oviparous nor viviparous arise all from one of two sources, from mud, or from sand and from decayed matter that rises thence as a scum; for instance, the

so-called froth of the small fry comes out of sandy ground." His presumption was that living things could be derived from nonliving matter—a presumption otherwise known as Aristotelian abiogenesis, i.e., spontaneous generation.

For two millennia, the theory of spontaneous generation challenged the beliefs and direct observations of Lucretius, Fracastoro and van Leeuwenhoek. But it was not until 1668 that the foundational principles of spontaneous generation would forever be challenged by the Italian physician, Francesco Redi (1626-1697). To refute one of the most fundamental ideologies of spontaneous generation, i.e., that decaying meat produced maggots spontaneously, Redi carried out a series of experiments. To begin, he placed meat into three containers, one uncovered, one covered with paper and the other covered with fine gauze. The paper and gauze excluded flies from contacting the decaying meat. Not surprisingly to those of our day, he found that maggots grew only on the meat of the uncovered container. Redi also noted that flies were attracted to the gauze-covered container and laid eggs on the gauze; the eggs later produced maggots.[2]

Redi's results indicated that decaying meat did not produce maggots spontaneously, but rather, the eggs of flies produced maggots. Redi's achievements appear to have been so revolutionary, that the history of Italian parasitology is now subdivided into two periods: pre-Redi and post-Redi.[4] But his, and others' experiments, only addressed the spontaneous generation of larger organisms. With the observation of van Leeuwenhoek's animalcules in 1676, the controversy renewed with some now proposing that microorganisms arose by spontaneous generation, while larger organisms did not.[2]

To support this notion, in 1748 John Needham (1713-1781), an English biologist and Roman Catholic priest, boiled mutton broth then tightly sealed the flasks. The flasks later became cloudy and contained microorganisms. Needham believed that a vital force within organic matter could offer to nonliving matter the properties of life. The controversy was tried once again when, two decades later, Italian biologist and naturalist Lazzaro Spallanzani expounded on Needham's experimental design.

Spallanzani sealed seeds and water in glass flasks then boiled them for ¾ of an hour. No growth occurred so long as the flasks remained sealed. When they were not sealed, growth occurred. His results led him to propose that germs were carried in the air to the medium. Supporters of spontaneous generation retaliated still, believing that by heating the air in the flasks, Spallanzani had limited the air's ability to donate life. The debate continued into the 1800s as Theodore Schwann (1810-1882) and others confirmed Spallanzani's findings whereas those who supported spontaneous generation found new hope in French naturalist, Felix Pouchet (1800-1872), who conclusively proved--so he believed--that microbial growth could occur without contaminating air.[2]

The prospontaneous generation claims, however, finally broke the proverbial camel's back and prompted a man by the name of Louis Pasteur (1822-1895), a French chemist turned microbiologist, to end the debate. Pasteur first filtered air through sterile cotton. He noted that plant spore-like particles gathered on the cotton and when placed into sterile broth, growth occurred. Pasteur then placed other nutrient broths in flasks, heated their necks with a flame and bent the necks into various configurations (similar to a p-trap) with the end of the neck remaining open to the air (Figure 1.2). Pasteur observed that dust and germs accumulated in the necks of the flasks, yet no growth

occurred in the broth. Once he broke the necks so as to allow the dust and germs to enter the broth, growth occurred straight away.

Pasteur's results seemed sufficient to shatter the claims of spontaneous generation, but what would have happened had Pasteur's experiments contained bacterial spores? If such were the case, the debate would have likely continued, but not for long. Within a matter of years following the work of Pasteur, the English physicist, John Tyndall (1820-1893), and the German botanist, Ferdinand Cohn (1828-1898), ultimately showed, respectively, that air free of dust did not cause growth in broth and that heat-resistant bacterial endospores do exist.[2]

The 60 years following Pasteur's work (from ~1857-1914) resulted in what is now considered The Golden Age of Microbiology.[5] During this era, Louis Pasteur, Robert Koch (1843-1910), Joseph Lister (1827-1912) and Ignaz Semmelweis (1818-1865) pioneered significant discoveries including the agents of infection, culture techniques, the role of immunity in disease, aseptic surgical technique, methods of microscopy and chemical activities of microorganisms. Notably, these discoveries would have a particular effect on the future of biomedical device development, which was in its infancy during the early 1900s.

The late 1800s and 1900s were considered The Golden Age of Microbiology, the early- to mid-1900s have been regarded as the Second Golden Age and it has recently been suggested that microbiological developments are now in a Third Golden Age.[5] This Age has included the discovery of nucleic acids and the impact of bacteria on medical device development. The latter development became particularly poignant following the discoveries of Claude E. Zobell, PhD (1904-1989)[6] and John William (Bill) Costerton,

PhD (1934-),[7] which indicated that bacteria in natural ecosystems predominantly dwell in polymicrobial communities of organisms and preferentially adhere to solid surfaces as opposed to existing as planktonic cells, or those that are defined as free-floating in a solution.

As will be seen in the following sections, these discoveries were so dramatic, that they literally altered decades-old misconceptions and provided important insights into the development of biomaterial devices. More specifically, these discoveries have provided investigators, clinicians, engineers, and companies an understanding of why there are difficult-to-treat infections that accompany the use of biomedical devices as well as the foundation for why the majority of patients with medical devices have been largely free of bacterial and biofilm contamination/infection for the past 30 years.

1.2 From Germ Theory to Biofilm Theory

Although the direct visual observations of van Leeuwenhoek may have arguably been sufficient evidence to suggest that viable, functional "animalcules" existed beyond the view of the human eye, a true understanding of what van Leeuwenhoek observed was not gained until nearly 300 years later.

In 1948, Dr. Zobell, a marine microbiologist working at the Scripps Institute of Oceanography, provided a previously undiscovered insight into the life of microorganisms. He also provided early on what is now known to be the rationale for why chronic infections that surround the use of medical implants are largely untreatable.

While collecting samples of sea water for microbiological analysis, Dr. Zobell observed that bacteria in the water preferentially adhered to the sides of bottles, as

opposed to floating freely as planktonic bacterial cells. He further outlined that an increase in the number of bacteria was seen on the surfaces of bottles with increasing surface area per volume of sea water. He concluded that "solid surfaces are beneficial to bacteria."[6]

Similar observations were made by civil engineers working with wastewater treatment processes in the 1960s. These engineers "Realized that most of the bacteria that removed organic molecules from sewage lived in sessile populations on surfaces, and they produced elegant models that predicted the efficiency of both biofilms and flocs in nutrient removal."[8]

In 1977, Gordon McFeters, PhD and Gill Geesey, PhD added to these observations by plating and culturing samples of water from icy streams in the Absorka and Bugaboo mountains of Canada. By culture, they were only able to quantify ±10 bacterial cells per milliliter (mL) of water, but "it soon became obvious that rocks in the streams were covered with slippery biofilms, and direct examination of these clear slime layers showed the presence of millions of bacterial cells encased in transparent matrices."[8,9]

By 1978, Costerton *et al.*[7] collated and coordinated these early findings into a general hypothesis that bacteria in natural ecosystems preferentially dwell in complex communities. Costerton later defined these communities as bacterial biofilms, which, according to Merriam Webster, are defined as "a thin usually resistant layer of microorganisms (as bacteria) that form on and coat various surfaces." Today, more than 30 years later, and with tens of thousands of publications on the topic, biofilm research has become one of the most noted fields of research with many new investigators

entering its ranks each year and Dr. Bill Costerton is considered by nearly all of those who work in this field as the father of biofilm discovery and research.

As will be shown throughout the remainder of this chapter, and dissertation as a whole, the work that has been performed by myriad investigators with biofilms to date has led to an in-depth understanding of biofilm morphology, characteristics, metabolic state and other intricate aspects. These findings have further helped investigators, clinicians and many others to understand why pathogenic biofilms comprise one of the most difficult-to-treat pathologies in the fields of biomaterial device development and medicine.[10]

1.3 Early Observation of Biofilm on a Medical Implant

Following the initial hypothesis of Costerton *et al*., the biofilm theory quickly gained wide acceptance by the medical and microbial research communities based on the significant amounts of data that began to support it.[11-16] One of the earliest and most compelling publications to support the biofilm theory came in 1982.[17] After treating a patient with a transvenous pacemaker, Thomas Marrie, MD, in collaboration with Dr. Costerton, published a case report that stated in part:

> A 56-year-old male was admitted to our hospital on August 28, 1981 with a 4-day history of anorexia, nausea, vomiting and shaking chills. Three weeks before admission, he had injured his left elbow and on two occasions he had expressed pus from it. He had undergone surgery for peptic ulcer disease, a history of ethanol abuse and syncopal attacks. In May 1975 a Medtronic bipolar transvenous pacemaker had been inserted when investigation of his syncopal attacks revealed prolongation of conduction through the atrioventricular node. Physical examination revealed a temperature of 39.2°C, a resolving indurated lesion on his left elbow, and tenderness in his

> right upper quadrant. Blood cultures grew *S. aureus*. He was treated with cloxacillin, 12 g/day i.v. for 4 weeks. During the third week in the hospital, his gall bladder was removed. One week after discharge he developed nausea, vomiting, fever and sweating. Blood cultures again grew *S. aureus*. He was treated for 6 weeks with cloxacillin, 12 g/day i.v., and rifampin, 600 mg/day orally. No signs of endocarditis were evident. There was no infection of the pacemaker pocket and serial echocardiograms showed normal cardiac values. He promptly responded to the antibiotic therapy, but was readmitted a third time 9 days after discharge with the same symptoms. Again, blood cultures grew *S. aureus*. On this occasion the entire pacing system was removed and replaced by an epicardial pacemaker. Intravenous cloxacillin was continued for 4 weeks after removal of the infected pacemaker lead. He has since remained well.[17]

As part of their investigation, Marrie *et al*. cut the distal 10 cm of the explanted pacemaker lead and confirmed the presence of bacteria residing in a biofilm on the surface of the lead using culture techniques and scanning electron microscopy (SEM). Their conclusion was that *Staphylococcus aureus* cells had contaminated the laceration on the elbow of the patient and hematogenously spread to the pacemaker lead. Once they colonized the lead, the cells developed a biofilm that served as a reservoir of infection in the patient. Thus, although antibiotics were able to eradicate septic bacteria residing in the planktonic state, the antibiotics were unable to completely eradicate those cells residing in the biofilm phenotype on the surface of the lead.

This early report of a biofilm implant-related infection represents a hallmark of biofilm implant-related infections. More specifically, multiple physicians began to document instances wherein patients, who had a biomaterial(s) either implanted long term or in transient use, would recover from infection with antibiotic treatment, but would then suffer from a recurring infection once the antibiotic treatment was removed.[16]

1.4 The Biofilm Theory Applied to Orthopaedics

One of the earliest reported instances of this sinusoidal recurrence of infection as it relates to orthopaedic implants occurred in 1984.[16] Once again in collaboration with Dr. Costerton, Anthony Gristina, MD, observed that two of his patients, one with a total hip replacement device and one with an intramedullary rod in the femoral canal, suffered from recurring infection that developed into osteomyelitis. The patient with the intramedullary rod received chronic antibiotic treatment for an astounding 7-year period until it was finally decided to remove the implant. Following explantation and a final long-term regimen of cephalothin, the patient no longer suffered.

In both case reports presented by Gristina and Costerton, biofilms were observed on the surface of the implants by SEM. In concluding their observations, they highlighted an important aspect of the clinical diagnosis of biofilm implant-related infection. Specifically, they stated that "Adherent bacteria can be efficiently recovered from tissues by homogenization and plating." In addition, "Direct observation of the colonized biomaterials and tissues, rather than standard sampling techniques, may also show morphological types compatible with the true pathogens."[16]

Many hundreds of clinical investigations have since confirmed these findings as well as observed that many pathogenic organisms in the biofilm phenotype, in particular those that colonize orthopaedic implants, are unculturable; meaning that these organisms will not grow on agar using standard plating techniques. Therefore, current data are now strongly suggesting that in addition to direct observation and culture techniques, molecular analysis of tissue samples may be required to give a proper clinical diagnosis.

1.5 Characteristics of Biofilms and Antibiotic Resistance

Despite the early indications that bacterial biofilms had a tremendous negative impact on the success of implanted devices, many of the defining characteristics that made biofilm infections difficult to treat were not well known until the mid-1980s and 1990s. For example, although there were clinical observations that biofilms appeared to have increased resistance to antibiotic therapy in patients suffering from biofilm-related infection, the degree and basis of that resistance was not well known.

1.5.1 Biofilms Can Be 1000x More Resistant to Antibiotics Than Planktonic Bacteria

Following what would become a lifelong pattern of being involved in every major advance of biofilm discovery and research, but also following a pattern of enthusiastic recognition for the contributions of others in this important field of research, in 1984 Dr. Costerton was the senior investigator of the research team of J. Curtis Nickel, MD to elucidate the concentration of antibiotic required to eradicate bacterial cells in the planktonic versus the biofilm phenotype. Their work began by growing biofilms of *Pseudomonas aeruginosa* in a modified Robbins Device.[18]

Nickel *et al*. used this device to grow biofilms on individual latex sections that modeled an artificial bladder/catheter system. After growing biofilms on the surfaces of the latex sections, they flowed broth that contained differing concentrations of tobramycin through the device. At various time points, they removed latex sections from the device to observe the biofilms directly with SEM or to quantify the number of

bacteria using standard culture techniques. A similar procedure was performed to test the efficacy of tobramycin against planktonic bacteria.

They published their results in 1985[18] and ultimately changed the field of biofilm research by showing that bacterial cells in the biofilm phenotype could be 1000x more resistant to tobramycin compared to the same species of bacteria in the planktonic phenotype. Since that time, numerous studies with many strains of bacteria and as many antibiotics have been performed with similar results–bacteria that reside in biofilms are typically more resistant to antibiotics than their planktonic counterparts.

Taken together, these data provided a strong rationale for why patients who suffered from biofilm implant-related infections may not have been effectively treated with antibiotic therapies: the infectious biofilms were likely more resistant to antibiotic treatment than planktonic bacteria that may have been present. But not only did Nickel *et al*., and additional investigators afterward,[19-22] show that biofilms have increased resistance to antibiotic therapy, their work also suggested that the concentration of antibiotic that would be required to eradicate biofilms in a patient would likely be an amount that could lead to toxicity in the body.

1.5.2 Biofilms Can Be Removed From Surfaces With Debridement

The fact that antibiotics may have reduced efficacy against bacterial biofilms has led to two important developments in recent years. 1) There is an ever growing need for investigators and clinicians to discover and employ novel antimicrobial compounds for the treatment of biofilm-related infections. This will be further discussed in Chapter 2. 2) Due to the limitations of antibiotics, physicians, such as Randy Wolcott, MD, who

specialize in treating patients with biofilm-related infections typically use a polytherapy approach including intense antimicrobial treatment in conjunction with surgical debridement.[20,21] Of these treatment methods, Wolcott *et al*. have suggested that debridement is a pivotal method of eradicating biofilms.[21] Debridement serves two purposes: it can immediately reduce the number of bacteria in a biofilm by several logs, which increases the potential for antibiotics to function more effectively, and it readily removes bacteria from the surfaces of a patient's skin, bone and/or implant surface if an implant is present.

1.5.3 Bacteria in Biofilms Have Strength in Numbers

In 1975, Gibbons *et al*. wrote a review article outlining the data that were available regarding the number and species of bacteria in the human mouth.[23] In their review, they reported that there were roughly 100 bacterial cells firmly attached to each epithelial cell on a human tongue. They further discussed that scrapings of human teeth contained ~10^{11} bacterial cells per gram of wet weight. Other work reviewed showed that the amount of bacteria in saliva fluctuated significantly throughout the day. Yet on average there were 10^9 bacterial cells per mL of saliva.

From these data, two points of interest can be made. 1) When Antony van Leeuwenhoek viewed scrapings from his own teeth, he arguably analyzed the best possible sample that was available to him for the detection of microbial cells. 2) It can easily be understood why bacterial biofilms need to be debrided on a regular basis from the surface of human teeth. If they aren't, they have greater potential to lead to gingivitis or dental carry formation.

Note that the data presented by Gibbons *et al*.[23] were collected and analyzed prior to the formalization of the biofilm theory by Costerton *et al*.[7] However, like Dr. Zobell, the investigators that pioneered these discoveries made similar observations about bacteria: they tended to adhere to solid surfaces, including those that exist in the human body, and they did so in incredibly large numbers. These and other early illustrations that billions of cells may be present in biofilms that contaminate human tissues and/or implant surfaces provided an important insight into why bacteria in biofilms have increased resistance to antibiotics; they have strength in numbers.

1.5.4 Biofilms Develop Into Three-Dimensional Structures

By 1991, another characteristic of biofilms was discovered that provided even deeper understanding into the architecture of biofilms, and once again, this discovery gave researchers and clinicians another rationale as to why biofilms have increased resistance to antibiotics.

Utilizing scanning confocal laser microscopy (SCLM), Lawrence *et al*. were the first group to observe that bacterial biofilms had the potential to develop into three-dimensional, polymicrobial communities that contained a variety of components (Figure 1.3).[24] More specifically, they observed that in addition to growing into vertical pillar-like formations upward of 100 μm in height, throughout the biofilm communities they observed many spaces, which created open channels (see Figure 1.3). Based on their observations of these channels, they were led to hypothesize that the biofilm architecture was not a random organization of cells, but rather an "optimal arrangement for influx of nutrients, transfer of wastes, and establishment of microenvironmental conditions, etc.,

subject to change as the biofilm progresses from initial to more established stages."[24] The work of Paul Stoodley, PhD, later supported this hypothesis by demonstrating, with real time videography, that these channels in biofilms were filled with water and thus could shuttle antibiotics throughout their community with limited interaction with cells.[25,26] Lawrence *et al*. also documented the presence of extracellular matrix components that appeared to act as a scaffold to which bacterial cells could attach within the biofilm, ultimately contributing to its three-dimensional architecture.

One of the most enlightening aspects of their work was the fact that by using SCLM, Lawrence *et al*. were able to circumvent the limitations that accompanied the use of SEM, which was the most common method of imaging biofilms up to that point. In short, SEM imaging always carried, and still carries, the limitation that it was performed under very high vacuum conditions, which had the potential of causing cells and the hydrated polysaccharide extracellular matrix (ECM) to collapse. Fixation protocols to prepare biofilms for SEM were also limited as they often failed to cross-link ECM components to the surface of a cell, which prevented investigators from observing the ECM components with SEM. Promisingly, Erlandsen *et al*.[27] and Williams *et al*.[28] have recently demonstrated how modified fixation and treatment protocols can cross-link ECM components more readily to cellular surfaces, thus providing a way to overcome one aspect of these previous limitations of imaging biofilm and their matrices with high resolution SEM.

Finally, in their conclusion, Lawrence *et al*. commented on the ability of small molecules that they used in their study to penetrate deep into the basal layers of a biofilm structure. This prompted them to state that their work corresponded to what Nichols *et*

al. had shown in 1988–that antibiotics had the ability to reach the deepest portions of a biofilm community in a matter of seconds.[29] These comments were noteworthy because they countered earlier notions that small molecules could not penetrate a biofilm due to the presence of ECM components, which were believed to act as a blockade of small molecule penetration.

1.5.5 Oxygen Gradients Discovered in Biofilm Communities

Although Nichols *et al*. demonstrated that antibiotics could penetrate the deepest interstices of a biofilm, they, and other researchers, were still left to wonder why these antibiotics had reduced efficacy against biofilms. Lawrence *et al*. had provided a partial answer by finding channels that shuttled antibiotics away from the bulk structure, but it was not until researchers discovered that the metabolic state of cells deep within a biofilm community was reduced, which contributed to why cells were resistant to antibiotic therapy despite the fact that antibiotics were able to come in direct contact with them.

To determine this, for example, Walters *et al*.[30] and Borriello *et al*.[31] examined the concentration of oxygen throughout biofilm communities of *P. aeruginosa*. In their studies, levels of oxygen and protein synthesis served as indicators of metabolic activity. In short, it was found that the concentration of oxygen in a biofilm was reduced as it was measured from the outer edges toward the inner most portions of a biofilm, creating an oxygen gradient. Thus, on the outer edges of a biofilm, an aerobic environment was observed and bacteria were readily killed, whereas there was a predominantly anaerobic environment in the center of a biofilm. The anaerobic environment resulted in a drastically decreased metabolic state of cells, which allowed cells to remain viable

despite the ability of antibiotics to completely penetrate the biofilm communities and interact with them. Borriello *et al*. confirmed that these results were similar after growing biofilms under anaerobic conditions: in a reduced oxygen environment wherein fermentation or denitrification served as metabolic pathways, antibiotics had reduced efficacy.

Reduced metabolic activity provided one of the most concrete rationales for why antibiotics had reduced efficacy against bacteria in biofilms. It hinged on the fact that for antibiotics to function properly, cells must be in a high or active state of metabolism.[32,33] In microbiological terms, this state of high metabolic activity is referred to as log phase growth. Thus, because bacterial cells that resided deep in a biofilm community, where oxygen was scant and nutrients less available, were found to be in a lower metabolic state compared to other cells in the community, they were largely immune to antibiotic therapy.

Additional work has shown that biofilms also contain persister cells that are present in reduced oxygen environments.[34,35] These are cells within a biofilm that are largely unaffected by antibiotic therapy and thus "persist" in a biofilm community while others are killed.

1.5.6 Plasmid Gene Transfer Occurs at a Higher Rate in Biofilms Than in Planktonic Bacteria

As a final note on biofilms and antibiotic resistance, one more discovery will be mentioned in this section. This discovery was made in 1999 by Martina Hausner, PhD and Stefan Wuertz, PhD.[36] Prior to their work, it was well known that small segments of

deoxyribonucleicacid (DNA), called plasmids, could be transferred from one bacterium to another via pili appendages.[37,38] More specifically, it was known that plasmids carried genetic coding that could ultimately result in the translation of protein(s) that specifically interact with, and even quench the activity of antibiotic compounds. In addition to random genetic mutation, plasmid transfer was an important method by which planktonic bacterial cells could obtain resistance to antibiotics.[37]

However, the rate of genetic transfer was not well known within bacterial biofilms. Thus, using quantitative *in situ* fluorescence methods in conjunction with SCLM, Hausner and Wuertz were able to show that in biofilms of *P. aeruginosa*, plasmids could be transferred at a rate 1,000 times faster than in cultures of planktonic bacteria. They concluded that the high rates of genetic transfer were likely due to the biofilm structure, the proximity of cells to one another as well as the presence of water channels that could shuttle molecules from one area of a biofilm to another.

1.5.7 Summary of Biofilm Characteristics

In summary, four major characteristics of biofilms have been outlined in this section, which specifically suggest why they have increased resistance to antibiotic therapy. First, bacterial biofilms may have millions or billions of cells that are packed into an extremely small volume; thus, they have strength in numbers and an extremely high local dose of antimicrobial may be necessary to have any significant effect on them. Importantly, there is no environmental or physiological requirement that bacterial biofilms must be comprised of millions or billions of cells. In fact, direct observations of biofilms from human skin have suggested that biofilms may consist of as few as 100 or

1,000 cells.[39] Yet to date, there has not been antibiotic resistance data obtained on biofilms that have less than a few million cells and this is one area that needs future investigation in order to understand the effect of small number biofilms on human health, particularly in the field of aseptic surgery (this will be discussed in more detail in Chapter 3).

Second, biofilm structure itself provides an ability to shuttle antibiotic or other antimicrobial compounds away from the bulk structure as well as individual cells within its community. This is done via water channels that develop within a biofilm. Notably, water channel formation in biofilm forming species of bacteria was likely a beneficial result of natural selection during the evolutionary process because not only can water channels shuttle antimicrobial compounds throughout a biofilm–which may also be considered a defense mechanism of biofilms–but toxic waste products and nutrients can also be diffused throughout the system. Similarly, natural selection likely also had a beneficial role for biofilms that produced ECM material, as the ECM has been shown to store nutrients that can be made available when nutrients become less available in the environment.[8]

Third, a gradient of oxygen, which goes from higher to lower levels as a function of biofilm depth, appears to influence the metabolic state of cells within a biofilm community. As a result, bacterial cells that reside on the outer edges of a biofilm, where oxygen and nutrients are readily available, may be much more susceptible to antibiotics than those residing in the inner most portions of a biofilm where oxygen and nutrients may be less available.

Fourth, bacteria in a biofilm have been shown to transfer plasmids at a much higher rate than their planktonic counterparts. In effect, this may provide cells in a biofilm the ability to upregulate their defense mechanisms at a much faster pace when exposed to antibiotic perturbations compared to cells in a broth culture. Similar to what was said about water channel formation, this aspect of genetic transfer in biofilms was likely also a beneficial outcome of natural selection during the evolutionary process, as was the biofilm structure as a whole.

In Figure 1.4, several diagrams and two SEM images are provided to present a visual understanding of each of the four major structural characteristics outlined above. These diagrams demonstrate what mature biofilms look like, the three-dimensional conformations they may take on as they mature, their life cycle and the extensive ECM products that they produce. The original diagrams shown in Figure 1.4 are used with permission from the Center for Biofilm Engineering at Montana State University (http://www.biofilm.montana.edu/resources/images?page=5), as well as in the published manuscripts of the author.[28,40]

Other aspects of bacteria that provide them with antibiotic resistance, including protein pumps in a bacterium's cell membrane that can quickly remove antibiotics from its cytoplasm,[41] cell wall thickness,[42] cell-to-cell (quorum sensing) communication,[43] geographical/anatomical location and an ability to grow in extreme environments,[44] have not been discussed in this dissertation, but each of these also has the potential to contribute to bacterial cells' resistance to environmental perturbations, including antibiotic therapies. Instead, this section has focused on just a few of the major aspects of antibiotic resistance as they apply to biofilms in clinical settings, specifically those that

apply to biofilm implant-related infections that are treated with antibiotics. Nevertheless, the fact that biofilms continue to develop resistance to all known types of antibiotics and other antimicrobials, and with recent data suggesting that bacteria can metabolize antibiotics as an energy source,[45] the astounding pace of development has led to what the author considers to be an antibiotic resistance era.

1.6 The Rise of an Antibiotic Resistance Era

Within months after discovering penicillin in 1928,[46] Alexander Fleming noted, perhaps with a measurable amount of concern, that *S. aureus* cells in laboratory cultures were already showing signs of resistance to the compound.[47] Specifically, he found that when penicillin was used in too low of concentrations, or when it was not used long enough, *S. aureus* could become resistant to it. Notably, this finding highlights the fact that bacteria in the planktonic phenotype can also develop resistance against antibiotics, albeit at a slower pace than cells that reside in the biofilm phenotype. Nevertheless, as Fleming spoke to audiences across the world, he warned, along with Almroth Wright, that the overuse of the penicillin antibiotic could lead to resistance and thus lose its efficacy.[48]

Despite these warnings, once it was put into mass production in the Spring of 1944, penicillin was heavily overused throughout the world, particularly during World War II. Although hindsight has perfect vision, it was likely difficult for those who overused penicillin to limit its use as it saved many thousands of soldiers' lives during the war and millions of civilian patients thereafter. In fact, there are currently a number of

illnesses that can still be treated with penicillin or other β-lactam antibiotics, including strep throat and sinus infections.

Nevertheless, antibiotic resistance is now one of the greatest concerns among healthcare officials in civilian and military settings across the world.[49-51] As stated by Clinton Murray, MD, "One of the most disconcerting facts about the bacteria complicating combat casualties is their increasing antimicrobial resistance."[50] Similarly, greater than 90% of clinical *S. aureus* isolates in the U.S. are now resistant to penicillin and 40% of *S. aureus* isolates cultured from hospitals are resistant to methicillin.[52] The concern of resistant organisms is now also becoming commonplace in national headlines. For example, TIME magazine recently ran a headline that stated, "Drug-Resistant Superbug Shows Up in Three U.S. States."[53] Fox News recently reported, "Europe in the Grip of Drug-Resistant Superbugs."[54] Alas, studies have suggested that the trend of emerging antibiotic resistance has not yet been addressed effectively.[55,56]

With an era of antibiotic resistance that appears to threaten healthcare systems across the world, in combination with the fact that bacterial biofilms are known to thrive on hard surfaces,[6,7] there are ever increasing rates and concerns of biofilm implant-related infections that accompany the use of biomedical devices. Government agencies and healthcare facilities across the world have also come to recognize this problem.[57,58] Thus, aside from the exponential growth of regulations that affect medical device development, biofilm implant-related infections threaten to make the future of development a difficult and complex challenge.[10,16,59]

1.7 The Current Impact of Biofilms on Biomedical Devices

As has been alluded to in this chapter and as will be evident throughout the remainder of this dissertation, the literature regarding biofilm-related infections and their adverse effects on human health, particularly in instances of biomedical device implantation, is growing at a steady pace. All reports of biofilm-related infections and studies that the author has read to date carry a similar theme: biofilm implant-related infections are becoming a tremendous concern to researchers and clinicians, these infections cost healthcare systems across the world billions of dollars each year, antibiotic resistance is the most disconcerting aspect of biofilm-related infections and the number of effective antimicrobial agents against biofilms are becoming less and less each year.[10,16,50,59,60] Yet companies are currently hesitant to produce novel agents due to the high cost of development, regulatory requirements and the rapid development of bacterial resistance.

According to a review by Rabih Darouiche, MD,[10] each year more than $3 billion dollars are spent in the U.S. to treat nine of the most frequent implant-related infections (see Table 1.1). Notably, the numbers he provided did not include infections that develop as a result of revision surgeries, which are accompanied by higher rates of infection.

In outlining the general principles of treating patients who suffer from biofilm implant-related infections, Darouiche noted that "The essential factor in the evolution and persistence of infection is the formation of biofilm around implanted devices. Soon after insertion, a conditioning layer composed of host-derived adhesins (including fibrinogen, fibronectin, and collagen) forms on the surface of the implant and invites adherence of" organisms, which ultimately leads to "A three-dimensional structure of biofilm . . . that

contains complex communities of tightly attached (sessile) bacteria. These bacteria display cell-to-cell signaling and exist within a polymer matrix containing fluid channels that allow for the flow of nutrients and waste."[10]

Granting agencies are also becoming aware of the adverse impact that biofilms have on human health. In a recent announcement, the National Institutes of Health (NIH) stated that over 80% of infections in the human body are biofilm related (see announcement PA-07-288). The Centers for Disease Control (CDC) placed that estimate at 65%.[58] In the case of implanted devices, Hetrick and Schoenfisch have stated that "When considering all indwelling devices, the number of implant-associated infections approaches approximately 1 million per year."[61] Chronic wounds are now considered by many investigators to be the result of acute infection that begins with biofilm contamination as opposed to a nonhealing wound that is later contaminated and suffers from biofilm formation/infection.[57,62-64]

From the literature it can be seen that open fracture wounds demonstrate one of the wound types that are most susceptible to the development of chronic biofilm-related infection.[50,65-69] This is due to the fact that open fractures are often contracted in a traumatic fashion, wherein the risk of contamination with bacteria from natural ecosystems is very high. The potential for bacterial contamination in open fractures may be highlighted by the work of Torsvik *et al.*[70] and Bakken.[71] Their work has demonstrated, on an independent basis, that tens of millions to tens of billions of bacterial cells may reside in a single gram of soil. In addition, based on the work of Geesey *et al.*,[9] Costerton *et al.*[8] and Wimpenny *et al.*[72] it has been estimated that greater than 99.9% of bacteria recovered from natural ecosystems such as dirt, human skin, plants and water

sources, reside in the biofilm phenotype. Thus, it could be argued that open fracture wounds that are contaminated with bacteria from natural ecosystems are at significant risk of being contaminated with bacteria that reside in the biofilm phenotype as opposed to the planktonic phenotype. This topic of biofilms contaminating wound sites initially as opposed to planktonic bacterial cells will be discussed in detail in Chapter 3.

Based on the fact that open fracture wounds have such a significant risk of being contaminated with bacteria that reside in biofilms, and because they result in unacceptably high rates of biofilm implant-related infection, with minimally efficacious methods of treatment to date, a model of a highly contaminated open fracture wound was the basis for this dissertation with the understanding that if a novel antimicrobial treatment could reduce rates of biofilm implant-related infection in this model, the antimicrobial strategy could then be applied to additional models in the future. To demonstrate just how high the rates of open fracture infections are as well as outline the prevalence of open fracture formation, the next section will focus on these data.

1.8 Prevalence of Open Fractures and Rates of Infection

According to the CDC, fractures are the leading cause of injury hospitalization in the United States.[73] Each year in America, there are between 3 and 6 million patients who suffer from bone fractures.[69,73,74] Of those patients, 3%-4% have open fractures.[69,75] Rates of infection that accompany these open fractures range between 5% and 50%.[50,65,66,75-78] This range of infection corresponds to the severity of an open fracture type. The most common classification system of open fracture severity, and correlatively the rates of associated infection, was first developed by Gustilo and Anderson in 1976.[78]

Using a retrospective analysis of long bone open fractures treated from 1955 to 1968 at the Hennepin County Medical Center, Minneapolis, Minnesota, Gustilo and Anderson classified fractures into three levels of severity. A Type I fracture was defined as an open fracture with a wound that was less than 1 cm and clean. A Type II fracture was one that had a laceration that was larger than 1 cm long without extensive soft-tissue damage, flaps, or avulsions. A Type III fracture was either an open segmental fracture, an open fracture with extensive soft-tissue damage, or a traumatic amputation. Special categories in Type III were gunshot injuries, any open fracture caused by a farm injury, and any open fracture with accompanying vascular injury requiring repair.

By 1984, Gustilo *et al*. once again performed retrospective analysis on open fractures that were treated from 1976-1979 and recognized that due to "Varied severity and prognosis . . . the current designation of Type III open fracture is too inclusive."[66] Therefore, they recommended "That Type III open fractures be divided, in order of worsening prognosis, into three subtypes."[66] They then defined these three subtypes as Type IIIA, Type IIIB, and Type IIIC. Specifically, these were defined as:

> Type IIIA–Adequate soft-tissue coverage, of a fractured bone despite extensive soft-tissue laceration or flaps, or high-energy trauma irrespective of the size of the wound.
>
> Type IIIB–Extensive soft-tissue injury loss with periosteal stripping and bone exposure. This is usually associated with massive contamination.
>
> Type IIIC–Open fracture associated with arterial injury requiring repair.

Gustilo *et al*. also provided the infection data that accompanied each of the Type III fractures. In doing so, they noted that Type IIIB open fractures had the highest rates

of infection, which were reported to be 52%. They also showed the amputation rates among patients with Type III fractures. Of those with Type IIIA fractures, 0% were amputated. Of those with Type IIIB fractures, 16% were amputated and of those with Type IIIC open factures, 42% were amputated. Amputations were primarily the result of the complications of infection and non-union.

Notably, these data were consistent with the personal experience of J. Peter Beck, MD, a collaborator on this project, who is a board certified orthopaedic surgeon with 40 years of clinical experience. In a personal conversation with Dr. Beck, he noted that in his clinical experience, the reason that it is common to see Type IIIC open fractures treated with amputation is due to the tremendous damage that has occurred to a patient's limb and the limited ability for their tissues to heal.

In the military theater, rates of open fracture formation are much higher compared to the civilian population. In a recent report by Owens *et al.*,[51] wherein all injuries in soldiers from October 2001 through January 2005 were considered, data from the Joint Theater Trauma Registry were obtained for U.S. soldiers who were being treated for wounds sustained in Operation Iraqi Freedom (OIF) and Operation Enduring Freedom (OEF). This report indicated that 26% of all injuries (915 out of 3,575) in soldiers were fractures. Of those fractures, 82% were open with rates of infection that reached as high as 60% in at least one instance.[79] Additional data collected from Brook Army Medical Center showed that 40% of injured soldiers treated, 26% of which had orthopaedic trauma, from January to June of 2006 received courses of antibiotics.[50]

Data that have been collected from military and civilian populations have suggested that Type IIIB open fractures of the tibia are extremely susceptible to bacterial

contamination, which leads to high rates of non-unions.[50] Johnson *et al.*[67] found that in a group of 35 soldiers who suffered from Type IIIB open fractures of the tibia, 77% of their wounds had bacteria present. Thirteen of these soldiers had non-unions after >9 months of treatment, which was the result of infection. Due to complications of infection, four of these were amputated. As was shown in the work of Gustilo *et al.*, similar results have been seen in the civilian population and high rates of infection with Type IIIB open fractures continue to be reported today.[65,66,75,77,78]

1.9 Rationale for Study Design and Dissertation Outline

Taken together, the infection data surrounding Type IIIB open fractures represent a class of fracture, and injuries in general, that are difficult to treat due to massive amounts of contamination with rates of infection that reach as high as 50% even after prophylactic antibiotic treatment and surgical reduction with fracture fixation devices. These high rates of infections have led to three major concerns. The first is due to the limited efficacy of current antibiotic therapies. Infections that accompany highly contaminated Type IIIB open fractures have the potential to develop into chronic osteomyelitis despite antibiotic therapy. The second concern is that there are currently a limited number of alternative antimicrobial strategies in clinical use that have been shown to effectively circumvent the problem of antibiotic resistance. The third concern is based on the fact that all animal models of infection that have been developed to date have utilized planktonic bacterial cells as opposed to bacteria that reside in well-established biofilms.[80-102] This is a concern since 99.9% of bacteria in natural ecosystems appear to

reside in the biofilm phenotype,[7,9,72] in addition to the fact that planktonic bacteria are much more susceptible to antibiotics than bacteria in a biofilm.[18,21]

Thus, the overall goal of the work presented in this dissertation was to employ a novel antimicrobial compound, known as cationic steroid antimicrobial-13 (CSA-13), which has been shown to be a very promising antimicrobial compound with broad spectrum activity against both Gram negative and Gram positive bacteria in the planktonic and biofilm phenotype,[103-109] as an alternative to traditional antibiotics to prevent biofilm implant-related osteomyelitis.

To demonstrate the exact method of how this work was performed, Chapter 2 of this dissertation will first outline a few of the most recent developments in alternative antimicrobial compounds and strategies to treat biofilm-related infections with a specific emphasis on why CSA-13 was chosen for this project. Chapter 3 will then outline the current limitations of animal models of biofilm-related infections in general. Specifically, this chapter will address the issue of using planktonic bacterial cells as opposed to bacterial biofilms as initial inocula in animal models of infection. Importantly, the concept of using biofilms as initial inocula in Chapter 3 cannot be overstated since, after a careful literature review, it provided the first proposal in the literature to use bacteria as they exist in natural ecosystems, i.e., biofilms, as initial inocula in animal models as opposed to planktonic bacteria.[57] Chapter 4 will outline the development of a membrane biofilm reactor that was machined with ultrahighmolecularweightpolyethylene (UHMWPE). This reactor was developed for this study to grow well-established biofilms of methicillin-resistant *Staphylococcus aureus* (MRSA) such that they could be used as initial inocula for *in vitro* and *in vivo*

testing.[40,110] The criterion for the successful development of this reactor was that it needed to grow biofilms with similar cellular number on the surface of polymeric membranes over various runs. If this reactor could not grow biofilms in a repeatable, consistent fashion, then the *in vitro* results would have been untrustworthy and the initial inoculum of bacteria in the *in vivo* portion of the study would have been inconsistent. Chapter 5 is then aimed at demonstrating how CSA-13 was used as an active release agent from a device coating against MRSA biofilms in an *in vitro* system. Chapter 6 will then add onto the work outlined in Chapter 5 by providing a specific characterization of the active release coating that was developed to elute CSA-13 away from its surface. Chapter 7 provides data obtained from pilot work that was performed in sheep in order to establish the experimental animal model of osteomyelitis using biofilms as initial inocula. The importance of this chapter, and the publication of this work, lies in the fact that this animal model demonstrated, for the first time, that when bacteria residing in a well-established biofilms grown under fluid sheer forces are used as initial inocula in an animal model, they have the potential to lead to a persistent, chronic and slow-developing osteomyelitis infection. Chapter 8 will then focus on the definitive animal study that was undertaken to test the efficacy of CSA-13 against biofilms in the animal model that was established in Chapter 7. Chapter 9 will then summarize the results, provide a discussion and outline the direction for future work that can be performed to validate the results of the work performed in this dissertation.

At the end of this dissertation, five appendices--Appendix A, Appendix B, Appendix C, Appendix D and Appendix E--will also be attached to provide the reader with a copy of the manuscripts that were published prior to the completion of this

dissertation work.[28,57,110] Three additional manuscripts will also be published as a result of this work and will be based on the work presented in Chapters 5, 6, and 8.

Taken together, this work, in addition to future work that will be performed, will be used to establish the principles for developing combination products for Food and Drug Administration (FDA) submission. The ultimate goal is to have CSA-13 approved as an active release agent of biomaterial device coating(s) that can be used clinically to prevent biofilm implant-related infections in human patients.

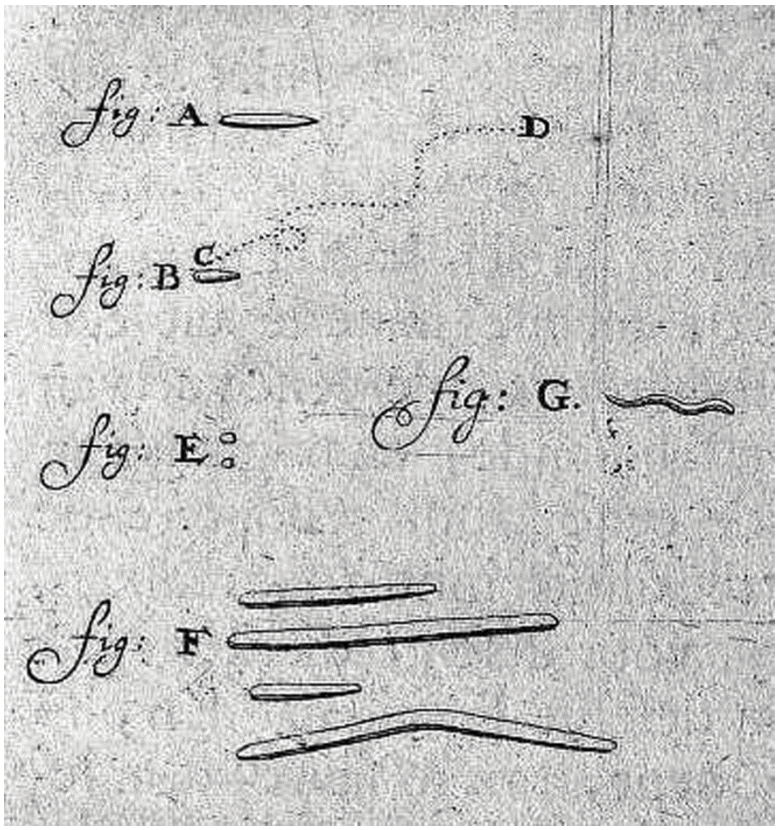

Figure 1.1: Hand drawn pictures of the "animalcules" that Antony van Leeuwenhoek observed as he analyzed the scrapings from his own teeth. These drawings are now known to represent the various shapes of bacterial cells including rods (fig: A and F), cocci (fig: E) and spirochetes (fig: G). It is important to note that van Leeuwenhoek observed organisms move as indicated in fig: B, which further suggested to him that these were viable, functioning organisms. Figure is available for use by the general public.

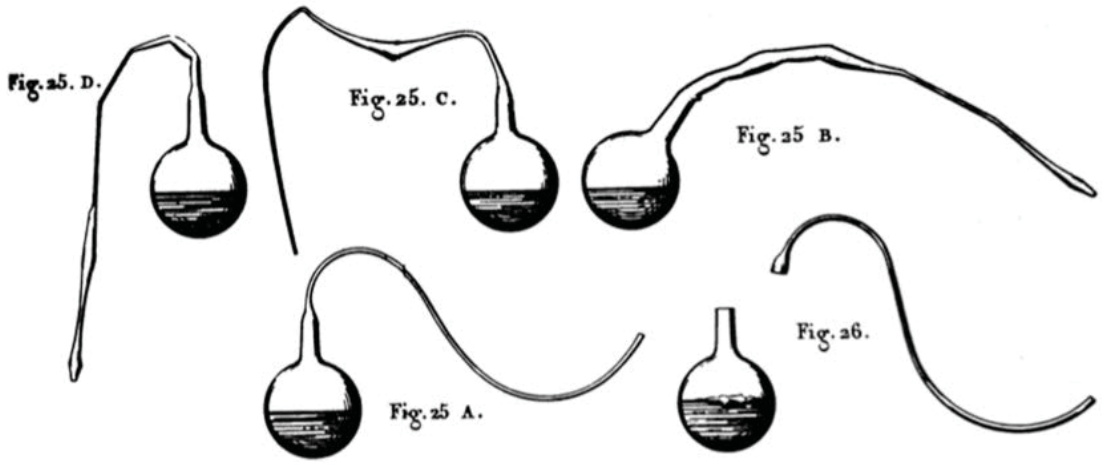

Figure 1.2: Hand drawn pictures of the flasks that Louis Pasteur used to disprove the theory of spontaneous generation. Note the p-trap appearance of the necks which led without blockage to the bulb portion of the flasks that held growth media. Figure is available for use by the general public.

Figure 1.3: The first three-dimensional reconstruction of a biofilm using SCLM. This image was created from a biofilm of *Vibrio parahaemolyticus* and was published by Lawrence *et al*.[24] Figure used with permission.

Figure 1.4: The various cartoons and images in the following figure provide an indication of the morphology, functionality and life cycle of bacterial biofilms. (A) Diagram outlining at least two conformations that a mature biofilm may take on as it grows to maturity. These conformations include mushroom-like formations or pillar-like structures. This diagram also shows that as a bulk fluid flows across a biofilm, it may pass through channels, similar to those that Lawrence *et al*. discovered. It is not uncommon for portions, or streamers, of a biofilm to detach from the main body of the biofilm as shown here. In a clinical setting, these streamers may detach and relocate to a distal site, causing additional biofilms to form in multiple areas of a patient's body. (B) As shown in this diagram, biofilm structures are dynamic. Their structure may be influenced by flow rates and a variety of other factors. Biofilms may even roll along a surface if turbulent flow is present. (C) Streamers that detach from the main body of a biofilm, as indicated in (A) and (B), may contain planktonic bacteria. The natural tendency of planktonic bacteria, as was outlined by Zobell, is to attach to a surface and subsequently colonize that surface by developing into a biofilm. This diagram provides a schematic of the life cycle of a biofilm showing how planktonic bacteria may colonize a surface, develop into a biofilm, and then planktonic bacteria detach again to colonize a distal location. This cycle has been followed using live imaging techniques and this is shown below the diagram. (D) SEM image of a biofilm of *Staphylococcus epidermidis* that was grown on the surface of titanium. Note that the biofilm structure has a mushroom-like appearance with the top of the mushroom extending toward the reader. (E) SEM image of a biofilm of *S. aureus* that was grown on a polymeric membrane. This biofilm demonstrated that an extensive ECM network can develop in a mature biofilm. (A), (B) and (C) used with permission from the Center for Biofilm Engineering at Montana State University (http://www.biofilm.montana.edu/resources/images?page=5).

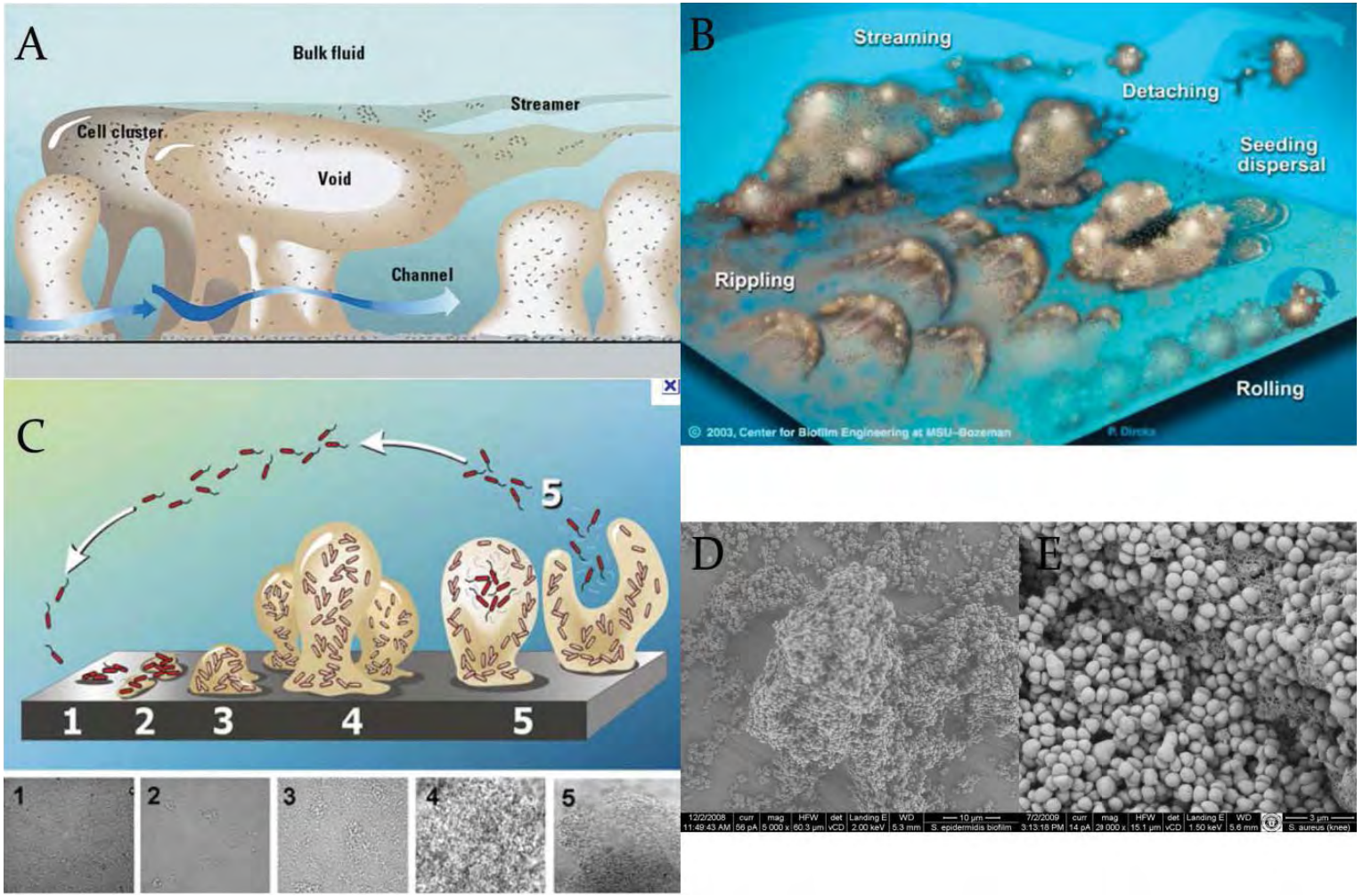
A
Bulk fluid
Streamer
Cell cluster
Void
Channel
B
Streaming
Detaching
Seeding
dispersal
Rippling
Rolling
© 2003, Center for Biofilm Engineering at MSU–Bozeman
C
5
1
2
3
4
5
1
2
3
4
5
D
E

Table 1.1: Estimated occurrences and rates of infections in the U.S. population that accompany a select number of implanted devices. The associated cost to treat each infection type is also given. Table used with permission and previously published by Darouiche.[10]

Implant	Implants Inserted in the U.S. Annually	Projected Infections of Implants Annually	Average Rate of Infection†	Preferred Practice of Surgical Replacement	Estimated Average Cost of Combined Medical and Surgical Treatment
	no.		%	*no. of stages*	*U.S. $*
Cardiovascular					
Mechanical heart valve	85,000	3,400	4	1	50,000
Vascular graft‡	450,000	16,000	4	1 or 2	40,000
Pacemaker–defibrillator	300,000	12,000	4	2	35,000§
Ventricular assist device	700	280	40	1	50,000
Orthopedic					
Joint prosthesis	600,000	12,000	2	2	30,000
Fracture-fixation device¶	2,000,000	100,000	5	1 or 2	15,000
Neurosurgical — ventricular shunt	40,000	2,400	6	2	50,000
Plastic — mammary implant (pair)	130,000	2,600	2	2	20,000
Urologic — inflatable penile implant	15,000	450	3	2	35,000

CHAPTER 2

PREANTIBIOTIC THERAPIES, THE DEVELOPMENT OF NOVEL ANTIMICROBIAL COMPOUNDS, AND ACTIVE RELEASE COATINGS

2.1 Methods of Treating Infection Prior to the Discovery of Antibiotics

By no means will this chapter have the capacity or necessity to cover all of the antimicrobial strategies that existed prior to the development of antibiotics. It will hopefully, however, provide information regarding a few of the most prominent advancements that have been made in antimicrobial treatments.

Prior to the mass production and optimization of antibiotic therapy(ies), the word "surgery" was synonymous with death. Indeed, surgical procedures, which were largely optimized on the battlefield, were often accompanied by mortality rates of 80% to 90% largely in part because of infection.[111] From the 1300s to the 1800s, the most widely adopted treatment to prevent infection of a wounded limb was amputation. A particular advocate of early amputation was Napoleon's physician, Baron Dominique Jean Larrey. In 1812, during the Battle of Borodino, Larrey was documented to have performed more than 300 amputations in a 24-hour period. The basis by which he amputated so readily was founded in the fact that early amputation "Reduced morbidity, mortality, the likelihood of tetanus, and the suffering of the soldier."[111]

Similarly, during those preantibiotic years, the general public was wary of maternity wards, wherein physicians such as Ignaz Semmelweis delivered babies in the mid-19th century.[112] Prior to the controversial implementation of hand washing by Semmelweis in 1847, which he did with an antiseptic chlorinated lime solution, mortality rates of childbirth ranged between 5% and 30% due mostly to infection. Though Semmelweis' hand washing procedure reduced rates of mortality to less than 2%, his work was not widely accepted and hospitals continued to perform surgeries using unsterile conditions, believing instead that a poisonous miasma in the air was the cause of infection.[112-114] However, adding onto the findings that were part of the Golden Age of Microbiology, the work of Joseph Lister, whom many consider to be the father of modern surgery, fundamentally changed this mentality after he demonstrated in 1865 that by washing surgical instruments and wounds with carbolic acid (also known as phenol), rates of surgical site infections could be drastically reduced.[115]

By World War I, Henry Drysdale Dakin had collaborated with Alexis Carrel to produce an irrigating solution, which consisted of 0.4% - 0.5% sodium hypochlorite and 4% boric acid.[116-118] This "Dakin's solution," as it came to be called, was used to irrigate the wounds of soldiers, and drastically reduced rates of battle wound infections. There are indications to suggest that Dakin's solution is toxic, but it appears that when used in applications wherein necrotic tissue is present and in concentrations at or lower than 0.025% sodium hypochlorite, toxicity may be limited.[116-120] From personal conversations of the author with practicing physicians, it appears that Dakin's solution is still in clinical use to either soak gauze and apply to the surface of an incision site or wound bed, or as an irrigating solution.

Notably, in the late-19th century, another method of treating infections had been discovered. In 1896, Ernest Hanbury Hankin noted that water from the Ganges and Yamuna rivers in India had antibacterial properties against cholera.[121] By 1915 Frederick Twort had discovered a small agent in these waters that he believed could be a virus. His belief became reality when, in 1917, Félix d'Hérelle, who worked at the Pasteur Institute in Paris, discovered an invisible, antagonistic microbe of the dysentery bacillus. He "knew" that it was a parasitic virus, and in 1923 the Eliava Institute was opened in Tblisi, Georgia to research this newly discovered organism and put it into practice.[121] These organisms are now well documented as bacteriophages, i.e., small viruses that have the potential to specifically infiltrate and kill bacterial cells (Figure 2.1). To date, many thousands of these organisms have been sequenced, characterized, documented and put into bacteriophage libraries across the world. In the mid-1940s bacteriophage research took a backseat to the much more reliable and potent action of antibiotics.[121]

Other inorganic compounds have also been used for many centuries. These include silver, copper, gold and platinum.[122-125] The Phoenicians were known to store water, wine and vinegar in silver bottles because it helped prevent spoilage.[126] During the 1800s, Western Pioneers placed coins such as pennies in their drinking water to help reduce spoilage.[127,128] Galen was the first to make reference to sutures made of gold[129] and physicians in the 1800s used sutures made of silver because they were known to have a reduced risk of infection.[130,131] As will be discussed below, many investigators today continue to apply these metallic molecules in device coatings.

Also deserving of mention are natural products, such as plants, herbs, spices and food, that have been used for centuries to fight infections in rural settings, Native

American tribes, amongst the pilgrims, aborigines, pioneers, and those who currently practice and advocate holistic medicine.[132,133] For example, honey has been used to treat wounds throughout the ages, but until recently its antimicrobial properties were not well known.[134] Traditional Chinese medicine has also been in use for centuries, but has had variable strength in clinical settings.[135] The antimicrobial activity of cinnamon, clove and cumin have also been tested recently[136] and the author has likewise tested the antimicrobial efficacy of cinnamon, plant leaf extracts, garlic, sugar and a variety of other natural compounds. In short, natural compounds and holistic therapies may display antimicrobial activity, but they have not been widely accepted as being clinically efficacious.

Importantly, there are several reasons why antiseptics, bacteriophages and holistic medicines have been limited in their ability to fight infections within the human body. First, the majority of antiseptic solutions cannot be taken orally due to their toxic nature. This toxicity further extends to use on human skin, where it may result in adverse side effects such as rashes, blisters, or irritation. For example, sodium hypochlorite (bleach) has remarkable antimicrobial potential,[137] yet it is well known to burn and irritate the skin and tissues of humans when used at high concentrations. As is commonly the case with antiseptics and virtually every other form of medicine, these adverse reactions are concentration dependent and vary from patient to patient. Similarly, chlorhexidine gluconate, a common skin prep agent for surgical procedures, was shown to cause anaphylactic shock in a select number of patients when it was used topically[138] or as part of a device coating.[139] Typically, the fact that antiseptics are limited in their ability to be taken orally limits their usefulness to skin prep solutions and small wound treatments.

With respect to bacteriophages, aside from the difficulty of convincing the FDA to approve the use of a biological agent, i.e., a virus, in human patients to treat wound and/or other infections, bacteriophages have been significantly limited in that the administration of a single bacteriophage or a cocktail of bacteriophages has been shown to be extremely delicate and dependent on the time of bacterial contamination as well as the stage of infection in a patient.[140] In addition, there is concern with the fact that bacteriophages can have one of two forms: they can be lytic, meaning after they replicate in a bacterial cell, they can cause it to lyse; or they can become lysogenic, which means the DNA of a bacteriophage can incorporate itself into the DNA of the host bacterium. This is a concern for human patients since the DNA of a virus may potentially incorporate itself into the DNA of the patient, leading to unknown, perhaps adverse results. At this time it appears that the main role of bacteriophages in nature is to keep bacterial numbers "in check," meaning as opposed to completely eliminating all bacteria with which they come in contact, they eradicate only a portion of them. After bacterial numbers decrease, the amount of bacteriophage decreases as well, resulting in a cyclical pattern of existence for bacteriophages and the bacteria they affect in nature.

Traditional Chinese medicines, holistic therapies, natural compounds and inorganic metals have all had variable clinical results.[135,138,139,141] Metal ions in particular have been hampered by their ability to elicit allergic reactions,[142] the lack of infection prevention in clinical trials in patients and their reduced efficacy against bacteria residing in the biofilm phenotype.[137,141,143] The variable clinical results that have been seen with holistic medicines may be due to a lack of regulated extraction protocols, varying concentrations of active compounds in plant products, unknown dosages that should be

given, and so forth. Nevertheless, as a result of the variable outcomes, these medicines have been viewed with at least some skepticism by western academic medicine and will require hypothesis driven, scientific testing and evidence-based clinical studies before they can be deemed as efficacious. At this time, they are considered alternative or complementary medicines.

As a result of the discoveries that have been made and the research that has been performed over the centuries, in clinical settings today and within the general public, the most efficacious method of fighting infection is to prevent infection. This is primarily done in hospitals and in the home by combining the power of antiseptics with antibiotics, i.e., using a polytherapy approach to kill microorganisms. For example, this is done by wiping surfaces with disinfectants or antiseptics, using scrupulous methods of cleaning clothing, bedding and other materials, along with frequent hand washing. Although there are concerns that the overuse of disinfectant solutions and the overuse of triclosan antibiotic in hand soaps run the risk of engendering bacterial resistance and weakening the human immune system,[144] these methods are still largely effective in reducing rates of infection and illness in general. Moreover, in surgical settings today, prepping a patient's skin with antiseptics, such as betadine, isopropanol or chlorhexidine solution, prior to surgery is common practice. Similarly, patients in America who undergo surgery are given prophylactic doses of antibiotic before surgery, after surgery or both, depending on the physician.

In summary, antibiotics have largely overcome the limitations of antiseptics, metals and bacteriophages due to the fact that they have lower toxicity comparatively, they can be administered orally and are well tolerated by the majority of patients, and

their obvious success to treat infections has been overwhelming for more than 50 years. Yet, as discussed in Chapter 1, the most concerning limitation of antibiotics is that many bacteria themselves produce them, and they can quickly "learn," evolutionarily and via mutation, how to refuse them. This makes the outlook for antibiotic use grim and strongly suggests that alternative molecules need to be developed and/or discovered to address the current trends of antibiotic resistance.

2.2 A Novel Class of Antimicrobial Compounds Discovered

In 1981, Michael Zasloff, MD PhD, discovered, somewhat serendipitously, a unique class of antimicrobial compounds that showed tremendous promise to overcome the limitations of antiseptics, bacteriophages and antibiotics.[145] While working for the National Institutes of Health in the field of molecular biology, Dr. Zasloff noted that after performing surgeries on African clawed frogs (*Xenopus laevis*), their suture sites healed without infection, inflammation or scarring despite the fact that the frogs were placed into tanks of water that contained high quantities of bacteria. Curious as to why that was the case, he extracted peptides from the skin of these frogs, which he found to have significant antimicrobial activity against Gram negative and Gram positive bacteria, protozoa, fungi and viruses. He classified these compounds as antimicrobial peptides (AMPs), and called the AMPs from African frogs magainins (magainin means "shield" in Hebrew). It was found that magainins were part of the innate immune system of the African frogs.

Since Dr. Zasloff's initial discovery, thousands of AMPs have been discovered as part of the innate immune system in nearly all life forms including plants, insects,

mammals and amphibians.[146-148] Over time, it has been found that nearly all AMPs that display antimicrobial activity have very similar characteristics.[146-150] Typically, AMPs have a predominantly net positive charge due to significant amounts of arginine and/or lysine residues, they commonly contain multiple cysteine bonds and they also commonly comprise an α-helical structure with amphipathic properties, meaning that one face of the alpha helix is charged and the other is hydrophobic.[147,151] The fact that these peptides carry a net positive charge makes them prime candidates to adhere to the negatively charged components of bacterial cell membranes. As a side note, eukaryotic cells are largely unaffected by antimicrobial peptides due to the fact that they are predominantly zwitterionic, or have a net positive charge and they contain cholesterols.[147] Nevertheless, because erythrocytes typically have a net negative charge, hemolysis is a known effect of AMPs.[147]

When AMPs were first discovered, one of their most promising aspects was immediately apparent: they had an inherently reduced risk of engendering resistance in bacteria. There are three main reasons why this is so. The first reason relates to the fact that AMPs have been in existence for millions of years and continue to display significant antimicrobial activity against bacteria.[146] The second reason has recently been highlighted by the work of Fantner *et al*.[152]

Using novel high-speed, high-resolution atomic force microscopy (AFM) in conjunction with live/dead staining and fluorescence microscopy, this group tested a naturally occurring AMP, called CM15, against cells of *Escherichia coli*. The purpose of their work was to determine the rate at which an AMP might have a bactericidal effect against individual bacterial cells as well as determine the morphological changes that

occur in a cell after it has been exposed to an AMP. The AFM results showed that CM15 caused cells to display a corrugated surface within ~80 seconds of exposure. Fluorescence imaging results indicated that the corrugation was related to cell death. Thus, Fantner *et al*. were able to demonstrate that the second reason AMPs carry reduced risk of engendering bacterial resistance is due to the rapidity with which they act on bacterial cells.

The third reason relates to the nonspecific method of action that these molecules use to attack a bacterial cell.[151] More specifically, in a manner that is still not well known, many thousands of AMP molecules adhere to the cell membrane of a bacterium. In doing so, the molecules can cause the membrane to depolarize.[151] This depolarization is believed to lead to the formation of nanosized holes in the cell membrane, which subsequently leads to the corrugated appearance of the cell, as demonstrated by Fantner *et al*. In the end, membrane depolarization and corrugation lead to full or partial lysis of a bacterium, which equates to cellular death.

Notably, this nonspecific method of attack by AMPs is in stark contrast to the method of action of antibiotics. The method of action of antibiotics was alluded to in Chapter 1, section 1.5 above. However, to reiterate, the large majority of antibiotics that are clinically approved have a very specific method of action against a single type of molecule, protein or enzyme in a metabolic pathway of bacteria. For example, penicillin specifically targets DD-transpeptidase enzymes, which play an integral role in the cross-linkage of peptidoglycan units in the cell wall of bacteria.[153] The speed of function, then, of penicillin correlates with the speed of the components that are deployed to build the cell wall. Yet without cross-linkage, osmotic pressure becomes too much for a cell and it

begins to lyse. To combat the effects of penicillin, which is a β-lactam based molecule, bacteria can produce β-lactamase enzymes to break down penicillin enzymatically.[154] This is one example of how bacteria have evolved in the presence of antibiotics and antibiotic-like compounds and have "learned" how to circumvent their specific method of action. Thus, antibacterial molecules such as AMPs that have a nonspecific method of action and which act quickly on bacteria prevent them from being able to upregulate their defense mechanisms.[146-148]

Several models have been proposed for how AMPs act on a bacterium's cell membrane. These have been well reviewed by van 't Hof *et al*.[151] In short, there are three main models.[150,151] The first is described as the barrel-stave model. In this model, the nonpolar side chains of an α-helix "Face the hydrophobic fatty acid tails at the inside of the phospholipid bilayer and the hydrophilic side-chains are pointed inward into the water-filled pore. Progressive recruitment of additional peptide monomers leads to a steadily increasing pore size."[151] A diagram of this model, as published in van 't Hof's review, can be seen in Figure 2.2A. The second model is the carpet model. In this model, "The microbial cell membrane is fully covered by a carpet-like cluster of peptides. When a critical concentration is reached, the membrane collapses, and in a short span of time, worm holes are formed all over the membrane, leading to lysis of the microbial cell."[151] A diagram of this model is shown in Figure 2.2B. Notably, this model was specifically developed to describe what was believed to be the function of magainins. Finally, the third model is the aggregate model. In this model, "The peptides insert into the membrane and then cluster into unstructured aggregates that span the membrane. The water molecules associated with the aggregated peptides would provide channels through

which ions and larger molecules could leak."[151] Again, a diagram of this model is shown in Figure 2.2C.

Although AMPs entail a very promising class of alternative compounds to antibiotics, there are three major limitations that have prevented them from being put into clinical use.[147] First, AMPs are prohibitively expensive to manufacture on a commercial scale. According to a personal conversation of the author with one of the world leaders in the field of AMP research, Bob Hancock, PhD, it costs several thousand dollars to produce a few milligrams (mg) of AMPs using recombinant DNA technology. Since hundreds of mg of compound may be required clinically to have bactericidal effects, these costs are currently not feasible for clinical use. Second, because they are natural peptide products, AMPs are direct targets for proteases in the human body. As such, multiple doses have been needed in *in vivo* studies to have even minimal effects against infection. Third, AMPs have limited stability outside of their natural environments. Thus, their shelf life and ability to be sterilized are not always conducive to the clinical requirements of an antimicrobial product.

For these reasons, multiple investigators have engaged in the development of antimicrobial peptoid oligomers,[155] peptide mimetics[156] and synthetic analogs of AMPs.[109] Of these, there is a particularly promising class of compounds. These compounds have been shown to have significant, broad spectrum antimicrobial activity against Gram positive and Gram negative bacteria in the planktonic and biofilm phenotype, they are stable *in vivo* since they are not targets for proteases, they can be sterilized by gamma radiation, autoclaving and ethylene oxide treatment, they can be

manufactured on the kilogram scale for hundreds of dollars, and many of them have a shelf life of several years. These compounds are called ceragenins.

2.3 CSA-13 Ceragenin: A Novel Synthetic Analog of AMPs

Ceragenins are synthetic analogs of AMPs. They were developed in the late 1990s by Paul Savage, PhD.[109] Using cholic acid (Figure 2.3), a bile salt from humans, as the backbone molecule, Dr. Savage developed a method of attaching alkane chains with varying lengths to hydroxide groups that are an integral part of cholic acid's sterol backbone.[107] These alkane chains can be further modified to contain positively charged primary or secondary ammonium salts. These positively charged salts, in combination with the hydrophobic sterol backbone, result in the formation of a facially amphipathic molecule, one that has a positively charged face and a hydrophobic backbone.[109] In this study, of the many ceragenin compounds that could have been used, CSA-13 (Figure 2.4) was chosen due to the fact that it has displayed significant activity against prokaryotes, fungi, and viruses with limited toxic effects to human eukaryotic cells. CSA-13 has also been shown to have superior activity compared to other CSA molecules and AMPs.[106] In addition, CSA-13 is highly stable in a variety of environments including *in vivo* environments, broth solutions, aqueous solutions and organic solvents.

To date, Dr. Savage and others have published several dozen papers outlining the broad spectrum efficacy of CSA-13.[103,104,106-108,157-161] As will be seen in Chapters 5 and 8 of this dissertation, the author will also show that CSA-13 has the ability to kill very high inocula of bacteria residing in the biofilm phenotype in *in vitro* and *in vivo* settings. From Dr. Savage's lab it has been shown that in head to head comparisons with

antibiotics, CSA-13 has superior antimicrobial activity.[104] Furthermore, CSA-13 was shown to act synergistically with antibiotics,[160] suggesting that the minimum inhibitory concentration (MIC) of an antibiotic can be reduced with the help of CSA-13 (a more detailed discussion of what an MIC is will be provided in Chapter 3). Epand *et al*.[106] also recently published a manuscript that elucidated, at least in part, the method of action of CSA-13.

This method of action was elucidated by analyzing the ability of several ceragenin molecules (CSA-8, CSA-13 and CSA-54) to permeabilize the outer *and* inner membranes of Gram negative *E. coli* cells as well as the membrane of Gram positive cells. Permeabilization of *E. coli* was monitored through the use of two chromogenic reporter molecules, nitrocefin and *o*-nitrophenyl-3-D-galactoside, that were cleaved once they crossed the outer and inner membrane, respectively. Permeabilization of Gram positive membranes was monitored with 3,3'-diethylthiadicarbocyanine iodide. Once cleaved, each molecule had a color change that was detected spectrophotometrically. Importantly, the *E. coli* isolate used in this study was genetically tailored to cleave these molecules only after they traversed a permeabilized membrane. Results indicated that CSA-13 was the only ceragenin to permeabilize both the outer and inner membrane of *E. coli*. CSA-13 was also shown to permeabilize the membrane of all Gram positives that were tested. (*S. aureus, Enterococcus faecalis, Bacillus cereus*) within minutes after being added to a solution. CSA-8 and CSA-54 permeabilized the outer membrane, but they failed to permeabilize the inner membrane of *E. coli*. As such, this study not only indicated that CSA-13 had greater antimicrobial potential than CSA-8 and CSA-54, but that the method

of antimicrobial action of CSA-13 was based on its ability to permeabilize the cell membranes of bacteria.

To corroborate these findings, Bucki *et al.*[103] compared the efficacy of naturally occurring AMPs to CSA-13 and showed that CSA-13 was more effective in killing bacteria. They also showed by AFM, similar to Fantner *et al.*,[152] that CSA-13 caused bacterial cells to become corrugated after they had been exposed to CSA-13. Taken together, the studies undertaken by Epand *et al*. and Bucki *et al*. have indicated that CSA-13 has a similar, if not equivalent method of action against bacteria as naturally occurring AMPs. In clear terms, the method of action of CSA-13 is to adhere nonspecifically to the negatively charged cell membrane of bacteria, cause the membrane to depolarize, then take on a corrugated appearance, which provides an indication that its cytoplasmic components have leaked out and the cell has died or soon will die.

One of the most important aspects of all the work that has been done with CSA-13 is that the MIC levels of CSA-13 have ranged from 0.4 μg/mL to 3 μg/mL for Gram positive cells and 2 μg/mL to 3 μg/mL for Gram negatives.[104,107] Furthermore, minimum bactericidal concentrations (MBC) have been shown to range between 1 μg/mL - 5.5 μg/mL.[106] This is significant in the context of the MICs and MBCs of traditional antibiotics, which can be one or two orders of magnitude greater.[104]

2.4 General Hypothesis of Dissertation and Specific Aims

In 2005, the author was hired by a company specifically to investigate alternative antimicrobial therapies to prevent infections that have the potential to accompany the use of a novel orthopaedic implant known as an osseointegrated implant. This work was

headed by Roy Bloebaum, PhD. As that work was taking place, the author came across a Press Release indicating that Ceragenix, a company that previously licensed CSA-13, had received permission from the FDA for an expedited review of CSA-13 for medical device applications. Following the reading of this Press Release, the author emailed Dr. Savage and a collaboration ensued to test its efficacy independently. Following a series of pilot experiments, CSA-13 showed tremendous efficacy against a variety of bacteria in broth solutions including when it was used as the active release agent of an antimicrobial coating on metal implants.

Three years later, the author and Dr. Roy Bloebaum gathered together a team of researchers and collaborators, including Dr. Paul Savage and Dr. Bill Costerton, to test the efficacy of CSA-13 in an animal model that had never before been established. Together, this team, with the current author being the lead author, wrote a NIH R01 grant. The **general hypothesis of the grant was that when CSA-13 was used as an active release agent of a medical device coating, it would prevent biofilm implant-related infection in an *in vivo* animal model of Type IIIB open fractures**. Three Specific Aims were used to test this hypothesis:

Aim 1: Develop a membrane biofilm reactor to grow biofilms of MRSA on the surface of polymeric membranes in a repeatable fashion.

Aim 2a: Confirm the efficacy of CSA-13 to eradicate biofilms of MRSA *in vitro*.

Aim 2b: Determine the elution profile of CSA-13 out of the device coating.

Aim 2c: Characterize the novel active release coating.

Aim 3: Confirm the efficacy of CSA-13 to prevent biofilm implant-related infection in an *in vivo* animal model of Type IIIB open fractures.

The grant outlining this work was funded in April of 2009 and the work presented herein shows the results of each Specific Aim as well as how these results helped to support the general hypothesis. More specifically, Chapter 4 addresses Aim 1, Chapters 5 and 6 address Aim 2 and Chapters 7 and 8 address Aim 3.

Importantly, the method of delivering CSA-13 in this work was to use it as an active release agent in a device coating. The development and method of producing this coating is outlined in detail in Chapters 5 and 6 of this dissertation, but it is important to understand the rationale for why CSA-13 was delivered as a local, active release agent in a coating as opposed to being administered systemically as is the common method of administering antibiotics to a patient in the clinic. It is also important to address the rationale for why silicone was chosen as the carrier polymer in this work over other polymer types. Thus, the next section (2.5) will provide a review of active release coatings, their advantages and disadvantages, and the advantages and disadvantages of systemic antimicrobial therapy. Section 2.6 will then provide the rationale for why silicone was chosen for this work.

2.5 A Practical Approach to Delivering Antimicrobials: Active Release Coatings

2.5.1 Advantages of Active Release Coatings

In 2005, Dr. Bill Costerton suggested in a review article of the biofilm theory that "One of the most practical strategies for the prevention of colonization and consequent biofilm formation on biomaterials is the use of materials and coatings that release conventional antibiotics into the surrounding tissues and fluids."[60] Coatings on

biomedical devices that are specifically designed to incorporate and release agents into the surrounding tissues and fluids are known as active release coatings.

As suggested by Hetrick and Schoenfisch, "The primary advantage of delivering antibiotics directly at the site of implantation is that high local doses can be administered without exceeding the systemic toxicity level of the drug. In this fashion, enhanced efficacy can be achieved at the implant site. Localized administration also allows for the tailored selection of antibiotics toward specific pathogens associated with implant infections, circumventing potentially harmful side reactions in other parts of the body. Such delivery also enables long-term antibiotic administration and presumably avoids fostering resistance."[61]

Although Costerton, and Hetrick and Schoenfisch suggested that antibiotics can be used as active release agents, it will be clear to the reader after Chapter 1 of this dissertation that antibiotics may not always be the most effective agent to use. Nevertheless, the most common method found in the literature and which is used clinically for delivering active release agents as part of a device coating is to incorporate them with carrier polymers. To do so, an antimicrobial agent is typically mixed with a prepolymerized solution or dispersion at a particular concentration that is determined by the investigator or clinician. This solution is then used, for example, to dip coat, spray coat, electrospin or brush coat onto a device.

2.5.2 Active Release Strategies Apply to Multiple Material Types

As a brief side note, there are active release systems that may not be used as coatings. For example, the addition of antibiotics into bone cement in the 1970s was in

fact the first documented instance of eluting antibiotics out of a polymer carrier system into the surrounding tissues and fluids of a patient.[162,163] Bone cements are methylmethacrylate based and were developed clinically to increase the stability of total joint replacement devices when they are inserted into the body. In this instance, an antibiotic is mixed with a bone cement that is not yet polymerized and placed by a surgeon into the medullary canal of a long bone prior to the insertion of a replacement device with the intent to prevent perioperative infection. As the methylmethacrylate polymerizes, it hardens and holds the device in place while also providing the ability to elute antibiotic based on diffusion out of the polymer as the fluids of a patient penetrate the polymerized polymer.

By the 1980s, this technique of incorporating antibiotics into a polymer system was adopted and applied to device coatings.[164] Since that time, investigators and clinicians have tested a variety of polymer types. These have included, but are not limited to, polyurethanes (PUs),[165] polymethylmethacrylates (PMMAs),[166-168] polyhydroxyethylmethacrylates (PHEMAs),[169] hydroxyapatite (HA),[170,171] silicones (which are also known as polydimethylsiloxane, or PDMS),[164,172] polylactic acids (PLLAs),[94,173,174] polylactide-*co*-glycolide acids (PLGAs),[175] etc. As will be discussed in section 2.5, the choice of polymer is application dependent.

2.5.3 Limitations of Previous Active Coating Investigations

As a preface to discussing the development of active release coatings, the author would like the reader to keep in mind three limiting factors that almost all investigators, companies and clinicians have failed to address during the development of active release

coatings that have been intended for medical devices. It is believed by the author that these three limitations are the primary contributing factors that have prevented the development of a greater number of effective active release coatings on medical devices for clinical use. Indeed, as a result of these limitations, which are evident from a careful literature review, at this time there are only a handful of approved medical devices that contain active release agents.[141,143,176-185] These include triclosan coated vicryl sutures (for example the Coated Vicryl Plus suture by Ethicon)[176,177] and silver/platinum coated catheters (for example the Vantex Central Venous Catheter by Edwards Lifesciences).[141,143,178,180,186] Synthes has also recently undertaken the development of an intramedullary nail (the Expert Tibial Nail PROtect) for fracture fixation of the tibia.[187]

To address the three limitations that are found in the literature, the first limiting factor, which will be discussed in more detail in Chapter 3, is that investigators have often trusted in MIC values of an antibiotic, which are completely based on the efficacy of an antibiotic against planktonic bacteria, without considering that higher concentrations of antibiotic may be needed to prevent or treat biofilm implant-related infection.[84,173] As such, antibiotic coatings have been designed to release just enough antibiotic to kill bacteria residing in the planktonic phenotype, which carries the risk of making a coating that is ineffective against bacteria in the biofilm phenotype. The second limitation has been the lack of translatability of experiments from *in vitro* testing to the *in vivo* paradigm.[57,165,174,175,188] Specifically, essentially all of the *in vitro* testing that has been performed with active release coatings has employed with the use of stagnant broth solutions and/or Kirby-Bauer-like agar diffusion testing to monitor zones of bacterial inhibition that develop when a coated device is placed on top of a "lawn" of

bacteria. The problem with these tests is that in the body, physiological fluids have flow. Stagnant broth solutions and agar surfaces do not model the flow of fluids in a body and the efficacy of these tests may not necessarily correlate with the efficacy of an antibiotic *in vivo*. If an antimicrobial coated device is placed into a stagnant broth solution, the active release agent will be released into the surrounding broth solution and ultimately reach concentrations that may be well above those that would be reached physiologically. Thus, if stagnant broth or hard surface agar systems are used to test the antimicrobial efficacy of a coated device, data interpretation may be severely skewed. Finally, the third limitation of testing antimicrobial coated devices is the common use of planktonic bacteria in *in vitro* and *in vivo* settings.[80-102] Once again, this problem of using planktonic bacteria as initial inocula will be discussed in detail in Chapter 3.

As will be seen in Chapters 5, 7, and 8, the work in this dissertation addressed each of these limitations by developing a flow cell system that could be used for *in vitro* testing to model the flow of fluid in a physiological environment instead of trusting in MIC values that are obtained with stagnant broth, and by using well-established biofilms as initial inocula for the *in vivo* work to model the phenotype of bacteria as they exist in natural ecosystems.

2.5.4 Earliest Use and More Recent Developments of Active Release Coatings

To provide an example of the earliest use of a device coating as well as more recent investigations that have been undertaken, in the early-1980s, Rushton *et al.*[164] performed work showing the efficacy of incorporating fusidic acid and gentamicin into a

one part room temperature vulcanizing (RTV-1) PDMS dispersion, then brush coating the surface of electrical stimulator devices. The PDMS was allowed to cure for a several day period and sterilized by ethylene oxide (ETO) treatment. These devices were tested *in vitro* on hard agar surfaces and then *in vivo* in human patients. Using their active release coating, they reported that they were able to reduce rates of infection that typically accompanied these devices, to less than 1%. This rate of infection was more than 10-fold less than patients who received the same implant without an antibiotic coating, but who received systemic antibiotic treatment instead. Thus, this provided one of the first indications that an antibiotic-loaded polymer system could reduce rates of implant-related infection.

As will be seen in the following paragraphs, not all coatings have had the *in vivo* success that Rushton *et al*. had, but the work of Rushton *et al*. may be criticized for four reasons. First, their *in vitro* work was performed by placing their device on a "lawn" of bacteria on hard agar surface. Second, their work did not display strong scientific, hypothesis driven research. Many patients that received one of their coated devices also received postsurgical antibiotics and some on multiple occasions confusing the interpretations of the findings. In doing so, their work was not randomized, and it is difficult to know whether the active components of the coating itself prevented infection or if the systemic antibiotics did so. The possibility existed that the systemic antibiotics worked in a synergistic fashion with the coating. Nevertheless, a careful review leaves one to wonder what the effect of the coating alone would have been. This might have been elucidated in a hypothesis-driven, scientific, randomized animal study prior to human testing. Third, when Rushton *et al*. performed their work nearly 20 years ago,

they were specifically concerned about *S. aureus* bacteria and they used two active release agents, fusidic acid and gentamicin, that are now well known to develop bacterial resistance and their coating may not have the same efficacy today as it had then. In addition, they had limited if any knowledge of the pending problems with *S. aureus* biofilm formation on implanted devices. Fourth, the amount of antibiotic they used (~40mg/implant) may have been in a toxic range, and is likely the reason their coating did show efficacy, yet at such high amounts the mechanical stability of their PDMS likely suffered and there may have been unreported issues of toxicity. Unfortunately, they did not publish any results of mechanical testing, histology of interface or regional tissues near the coated device, and they put these into humans without any mention of what regulatory guidance they had to perform the study. Granted, the development of active release coatings was in its infancy at the time and these issues are apparent in hindsight.

Since the work of Rushton *et al*. was undertaken, there have been relatively few human studies performed with active release coatings. In at least one human study that *has* been performed to test the efficacy of a pseudo antibiotic coating on penile prostheses, the number of patients in the two study groups was variable (there were more than 2,200 patients in the group that received a coated implant and 400 in the other), and although there was statistical significance between the two groups (1.06% vs. 2.07% infection), it is difficult to know if this difference would have remained significant with equal numbers of patients.[189]

Due to the fact that human studies with coated devices have often not been able to be performed in a randomized, blinded fashion, in addition to the variable outcomes that have been seen, and because of the concerns of bacterial resistance to antibiotics, the

FDA has pushed investigators toward generating more translatable data with greater emphasis on performing *in vitro* work first, then *in vivo* animal model studies prior to testing in humans. As a result, there is now a plethora of *in vitro* experiments and *in vivo* animal studies in the literature that have undertaken to develop antimicrobial coated devices. But once again, as was mentioned, these studies are limited in three main areas of testing.

To provide a few examples of what is currently found in the literature with regard to the development of antimicrobial coated devices, particularly for orthopaedic applications, and how they have failed in the three aforementioned areas, the work of Darouiche *et al*. will be examined first.

Dr. Rabih Darouiche has been involved with more than a dozen published papers investigating the efficacy of various antimicrobial coated devices with a variety of antiseptics and antibiotics as active release agents.[83-85,172,188,190-192] For example, in the late 1990s, he and his group coated simulated intramedullary nails with chlorhexidine and chloroxylenol using a proprietary dip coat method.[83,188] These nails were used in rabbits to test their efficacy to prevent biofilm implant-related infection. After creating an osteotomized tibial fracture, the medullary canals of rabbits were inoculated with 10^6 planktonic bacteria followed by reduction with a coated or uncoated nail, depending on the rabbit group.

Notably, in their study design, they administered antibiotics prophylactically in a systemic fashion, which is consistent with what would be used in a clinical setting, but the use of prophylactic antibiotics has the potential to compromise an experiment to determine the ability of an active release coating alone to prevent localized infection.

Nevertheless, their outcomes showed that 9% of rabbits became infected despite receiving an implant that was coated, whereas 62% of rabbits became infected that received implants that were not coated. These results suggested that in their particular animal model, systemic antibiotics were able to reduce rates of infection by roughly 40%, but systemic antibiotics in combination with a coated device reduced infection to 9%. It may be considered by some that a 9% rate of infection would be clinically unacceptable, making these results promising, but potentially unsatisfactory.

Importantly, Darouiche *et al*. did test the efficacy of chlorhexidine and chloroxylenol coated devices *in vitro* prior to using them *in vivo* and they published this work separately.[83] However, in accordance with the limitations outlined above, their *in vitro* tests were performed against planktonic bacteria using zones of inhibition on agar surfaces, which, in the case of a coated device, has limited ability to translate to clinical applications.

Price *et al*.[175] was another group to perform *in vitro* work that was potentially limited in two areas. In their study, they incorporated gentamicin antibiotic with PLGA polymer and coated sections of narrow fracture fixation plates using a coating method that they failed to outline in their paper. The coated sections were placed in 10 mL of stagnant broth that contained 10^6 *S. aureus* cells in order to test the ability of gentamicin to eradicate the bacteria as it was released over a 24-hour period. Their results indicated that they were able to reduce the number of cells to less than 10^1/mL of broth. However, their data interpretation may have been skewed by two factors. First, they used stagnant broth solution for their testing, which allowed the concentrations of antibiotic to reach levels that likely would not be present in the body. Second, they suggested that because

the levels of gentamicin in the broth were above its MIC value, such was an indicator that their coating would be effective against biofilm implant-related infection.

In another study published in 2006, Kalicke *et al.*[174] tested the efficacy of antibiotic compounds and antiseptics incorporated into bioresorbable PLLA coatings. In this study, using a solvent casting technique, pieces of manufactured fracture fixation plates were coated with either Rifampicin and fusidic acid antibiotics, or Octinidin and Irgasan antiseptics. These coatings were tested *in vitro* using stagnant broth solution against planktonic bacteria prior to being tested *in vivo*. For the animal model portion of their study, they used four groups of animals with n=12 animals per group. The groups were arranged in this manner:

Group I: Six-hole AO DC minifragment titanium plate without PLLA

Group II: Six-hole AO DC minifragment titanium plate with PLLA without antibiotics/antiseptics

Group III: Six-hole AO DC minifragment titanium plate with PLLA + 3% Rifampicin and 7% fusidic acid

Group IV: Six-hole AO DC minifragment titanium plate with PLLA + 2% Octenidin and 8% Irgasan.

In contrast to the work of Dariouche *et al*., Kalicke *et al*. did not administer prophylactic antibiotics to their rabbits and they also did not create an osteotomized fracture in rabbit tibiae. To perform their surgeries, they created an incision in the anteromedial margin of the left tibia, secured a minifragment plate (coated with antibiotics or antiseptics as outlined above) to the bone, inserted a sterile puncture needle at the proximal margin of the plate, closed the wound and lastly inoculated the plate bed through the opening that was made with the puncture needle using a range of *S. aureus* bacteria from 2×10^5 to 2×10^8 per 100 μL. Results from their work indicated that in

both of the rabbit groups that received a coated device (Groups III and IV), 17% became infected, whereas 83% of rabbits without a coated device (Groups I and II) became infected. Similar to the outcomes of Darouiche *et al*., a 17% rate of infection may be considered clinically unacceptable and once again, although these coating types were promising, they may be unsatisfactory in the end. Notably, neither Darouiche *et al*. nor Kalicke *et al*. used negative control groups (i.e., an implant only and no bacteria) in their studies.

Another important observation can be made from the work of Kalicke *et al*. and that is without systemic antibiotic treatment, they were only able to cause infection in 83% of the animals in their positive control groups (Group I and II). The fact that they did not infect 100% of animals foreshadows the discussion and the work that will be shown in Chapters 3, 7 and 8 of this dissertation. As a preface, the use of planktonic bacteria in animal models of biofilm implant-related infection has been limiting in that there are times when investigators have seen 40% of positive control animals become infected and there are times when investigators have seen 100% of animals become infected. Gaudin *et al*.[193] have noted that this variability in infection outcomes is one of the most difficult aspects of developing animal models of infection. Based on this understanding, the goal of the work in this dissertation was to develop an animal model of infection wherein 100% of positive control animals would become infected and 0% of animals treated with an antimicrobial coated implant would become infected, thus providing strong evidence that infection could be developed in positive controls and prevented in treated animals.

Similar to the studies outlined above, the trends and principles of trusting in MIC values, using stagnant broth solutions and/or hard agar surfaces, and the use of planktonic bacteria for all *in vitro* and *in vivo* predominate in the literature. It is proposed that these limitations are what have led to a paucity of antimicrobial coatings that have shown *in vivo* and clinical efficacy. Promisingly, researchers, including the current author, have begun to incorporate the use of flow cell systems to model the flow of physiological fluids in an application dependent manner with the intent to more closely model the clinical use of biomedical devices and antimicrobial therapies.[194]

2.5.5 Potential Limitations of Active Release Coatings

Although active release coatings provide a promising method of fighting local biofilm implant-related infections, there are at least three major limitations that may accompany the use of these coatings. First, due to the fact that there are classes of antibiotics that are effective against Gram positive bacteria and classes of antibiotics that are active against Gram negatives, the incorporation of two antibiotics may be necessary in a coating if antibiotics are the active agent of choice in order for the coating to have broad-spectrum capacity. Some of the difficulties that may be associated with using more than one active release agent include a difference in solubility between two molecules, toxicity, poor mechanical properties of a polymer, if the molecules are incorporated as particles their particle size may differ, which may affect pore size in the polymer system and elution kinetics. As such, the use of a single, broad spectrum antimicrobial agent may reduce these complexities.

Second, active release coatings tend to release active agents for a temporary period of time, typically meaning days or weeks.[162] Thus, after the active agent in a coating is completely released away from an implant surface, an implant that is intended to be present in the body for an extended period of time may be colonized by bacteria that are hematogenously spread in the body. The risk of infection is significantly decreased, however, if bacteria are eliminated at the time of implantation. There are also concerns with developing a coating that releases or is comprised of an agent that is constantly present. For example, the long-term presence of an active agent may result in toxicity or may be carcinogenic. Thus, the use of a transient or long-term coating is application dependent. In the context of this dissertation, the goal was to develop a transient release coating that could release CSA-13 for greater than 10 days, but less than 30 days to prevent perioperative device-related infection from developing when high inocula of bacteria are known to have contaminated a wound site.

Third, since it is the inherent nature of an active release agent to kill bacteria in the surrounding tissues and fluids of a patient, bacteria that are killed carry the risk of releasing toxic byproducts into the surrounding tissues and fluids.[195,196]

Other considerations that should be taken into account by investigators or clinicians who are undertaking to develop active release coating(s) include, but are not limited to, the rate at which an active agent is released; the amount of agent that needs to be released so as to kill bacteria without engendering bacterial resistance; the rapidity with which bacteria develop resistance to a compound; the duration of active agent release; the toxicity of an active release agent; the thickness of a coating and how that

may affect clinical applications; the mechanical and chemical stability of a coating after the agent, or additive, is incorporated.

2.5.6 Passive Coatings

The most obvious alternative to active release coatings are coatings that consist of molecules that are covalently bound to an implant surface.[61,162,197] These types of coatings do not release an active agent into the surrounding tissues and fluids of a patient and they are referred to as passive coatings. The intent of these coatings is to achieve one of two things: to either prevent the adhesion of bacteria to the surface of an implant, as is the case with polyethyleneglycol (PEG),[198] or to kill bacteria that come in contact with the surface of an implant, as is the case with covalently bound antibiotics such as vancomycin.[199]

Although passive coatings may last on the surface of an implant for an extended, if not life-long period of time, there are several drawbacks to using them. For instance, if bacteria reside even a few millimeters (mm) away from the surface of an implant that has a covalent coating, the antimicrobial agent will not kill the bacteria. In addition, within seconds after a medical device is implanted into the body, a conditioning film of lipids, proteins, electrolytes, nucleic acids and carbohydrates forms on its surface.[200,201] This conditioning film has the potential to mask and prevent the interaction of covalently bonded antimicrobial molecules with bacteria that may come in contact with the implant. Taken together, although passive coatings may have the ability to prevent biofilm growth/formation on the surface of an implant, they do not have the ability to kill bacteria

that may be in the surrounding tissue regions and even this ability may be drastically reduced by the formation of a conditioning film on an implant.

2.5.7 Advantages and Disadvantages of Systemic Antibiotic Treatment

At this time, the most common (and FDA approved) method of administering antibiotics to a patient is to administer them systemically. This can be done by administering antibiotics orally or by injection. The intent of systemic delivery is to have the antibiotics circulate throughout the organs/tissues of a patient's body. The advantage in doing so is that they have the potential to interact with bacteria wherever they may be located in the body. This may be beneficial in particular in a patient who may be suffering from infections that are present in multiple areas of their body. The drawback, however, in doing so is that in addition to killing unwanted bacteria that are causing infection, normal flora bacteria are likewise killed. The problem with killing normal flora bacteria is that they provide protection to the host and they also help maintain homeostasis.[202] Moreover, systemic therapy also carries the risk of being toxic to a patient's organs.[203,204] For these reasons, it may be beneficial to deliver antimicrobial agents in a local, high dose fashion as is the case with active release antimicrobial coatings.

2.6 The Selection of Polymer for an Active Release Coating

There are several factors that influence the type of polymer that could be used for active coating applications. As mentioned previously, in the literature the most

common polymers that are used as carrier polymers for active release coatings include PU, PDMS, HA, PMMA and bioresorbable polymers such as PLGA, PLLA and polycaprolactone. There are a variety of others as well, but only a few principles will be reviewed. Each polymer type has its advantages and disadvantages. For example, for this dissertation, a bioresorbable polymer was specifically not chosen based on previous work published by Uhthoff *et al*.[205] In a study they undertook, they showed that when PLA was used on a fracture fixation plate, as the polymer degraded it led to micromotion of the implant, which subsequently led to implant failure. Specifically, this was due to the fact that as the polymer resorbed, a gap was left between the plate, screws and the bone surface, which allowed the implant to move and ultimately come loose resulting in implant failure.

2.6.1 Dissolved Material vs. Particles and Particle Aggregates in Polymer Dispersions

Another important criterion for polymer selection is the solvent in which a pre-polymerized dispersion or mixture is suspended. This is a particularly important aspect of polymer selection for CSA-13. For example, prior to polymerization, PDMS is dispersed in organic solvents such as xylene or naphtha that are very hydrophobic and in which CSA-13 is minimally dissolved. Because CSA-13 does not dissolve well in these organic solvents as it is stirred in them, it remains as particles in the solvent that are nanometer (nm) in size or it creates particle aggregates that are micrometer (μm) sized as opposed to dissolving to individual molecules as it would in a solvent that was, for example, water or alcohol-based. As a result, when CSA-13 is mixed with a PDMS

dispersion, the particles of CSA-13 cause pores to form in the PDMS polymer as it cures over time. These pores allow water to penetrate the PDMS network and release CSA-13 as an active agent. Data will be provided in Chapter 6 to demonstrate what these pores look like, their size, as well as show that CSA-13 particles are in fact what cause them to form.

It is difficult to overstate the importance of the concept of an antimicrobial compound residing in particles or particle aggregates or having it dissolve completely into a solvent. For example, during the developmental phase of CSA-13 as an active release agent, the author worked with Dr. Savage's group to incorporate CSA-13 into PU polymers. To do so, CSA-13 was mixed with a solvent that contained methanol. Notably, CSA-13 is very soluble in alcohol-based solvents such as methanol. Thus, in this instance, as opposed to residing as particles or particle aggregates, CSA-13 was dissolved into the solvent prior to mixing it with a prepolymerized PU mixture. When this mixture was used to dip coat various materials, we found that we had to add CSA-13 at a concentration of 33% weight-to-weight (w/w) in order to achieve bactericidal levels. We also found that only 7% of the total CSA-13 that was added to the coating was actually released, which indicated why such a high amount (33% w/w) had to be added initially. Furthermore, we were only able to confirm antimicrobial activity of CSA-13 with a PU coating for 3-4 days as opposed to greater than 10 days with PDMS as will be shown in Chapter 7 of this dissertation.

As we examined the PU coatings with SEM, we noted that the PU network was largely aporous, which was in stark contrast to the results of CSA-13 being incorporated into PDMS polymer wherein the PDMS network was highly porous. In comparing these

results, it was concluded that the reason only 7% of CSA-13 had been released from the PU network was that the PU crosslinked to such a degree that water was unable to penetrate the deep layers of its network and likely only caused CSA-13 to be released from the outer most layers. Importantly, as will be shown in Chapter 6, we were able to confirm that by our detectable limits, all of the detectable CSA-13 added to the PDMS product that was used in this dissertation was released by 30 days of exposure to aqueous solution.

These findings may help investigators and clinicians understand why it is that in many instances, not all of an antibiotic or other antimicrobial product is released from a polymer network. This is particularly apparent for PMMA bone cements wherein it is well known that not all of an antibiotic is released when it is incorporated into PMMA.[162,206,207] In short, if an antibiotic or antimicrobial is dissolved completely in a solvent or if it resides as particles or particle aggregates, it may have a different effect on the physical properties of a crosslinked polymer, such as porosity, and it may also affect release kinetics.

2.6.2 Additional Factors to Consider

There are many other factors to consider when selecting a polymer for active release coating applications. These include the stability of a polymer *in vivo*, tensile strength, shear strength, adhesive strength, degradability, toxicity, cure time, cure temperature, pore size and so forth. For this particular dissertation, PDMS was selected for several reasons. It was able to release CSA-13 and display antimicrobial activity over a minimum of a 10-day period (as will be shown in Chapter 5). Using SEM techniques,

all of the detectable CSA-13 was found to be released from the polymer by 30 days of elution. PDMS is also well known for its biocompatibility in the human body. The particular PDMS selected for this work was found to be compatible, i.e., cross-link well in the presence of CSA-13, which has not been the case with PU polymer or other types of PDMS polymers. Another advantage was that the PDMS was found to be mechanically and thermally stable (see Chapter 6). Finally, the PDMS used for this dissertation cured at room temperature, which was an important requirement for CSA-13 to remain as particles or particle aggregates because it has a melt point of approximately 81° C and begins to oxidize at high temperatures (above ~150° C). Various polymers are heat curing polymers that require temperatures greater than 150° C to cure.

Based on the above material, chemical properties and rationale, an active release coating which incorporated CSA-13 as the active release agent of a PDMS polymer network was developed for this project and applied in a translational manner by testing its ability to eradicate biofilms of MRSA *in vitro* followed by testing its efficacy to prevent biofilm implant-related infection in an *in vivo* animal model of a Type IIIB open fracture. This animal model is the first model in the literature to utilize well-established biofilms of MRSA that were grown under fluid sheer forces to cause infection. The importance of this model will be discussed in the next chapter.

Notably, at roughly the same time that the work from this dissertation was being performed, Zhao *et al.*[208] had undertaken a study wherein polycarbonate filters were placed on the surface of lysogeny broth agar plates that were plated with *P. aeruginosa*. Though bacteria grew on the surface of the filters prior to being placed in mice, and thus it was assumed that biofilms had formed on them, these biofilms were not well

characterized, the method for producing the biofilms was not tested for repeatability and they were not grown under fluid sheer conditions. Nevertheless, the important aspect of the work performed by Zhao *et al.* and the work of this dissertation is that the concept of using biofilms as initial inocula is currently being introduced in the fields of biofilm research. The work presented in this dissertation constitutes the first study to use biofilms of MRSA that were grown under fluid sheer conditions in a biofilm reactor.

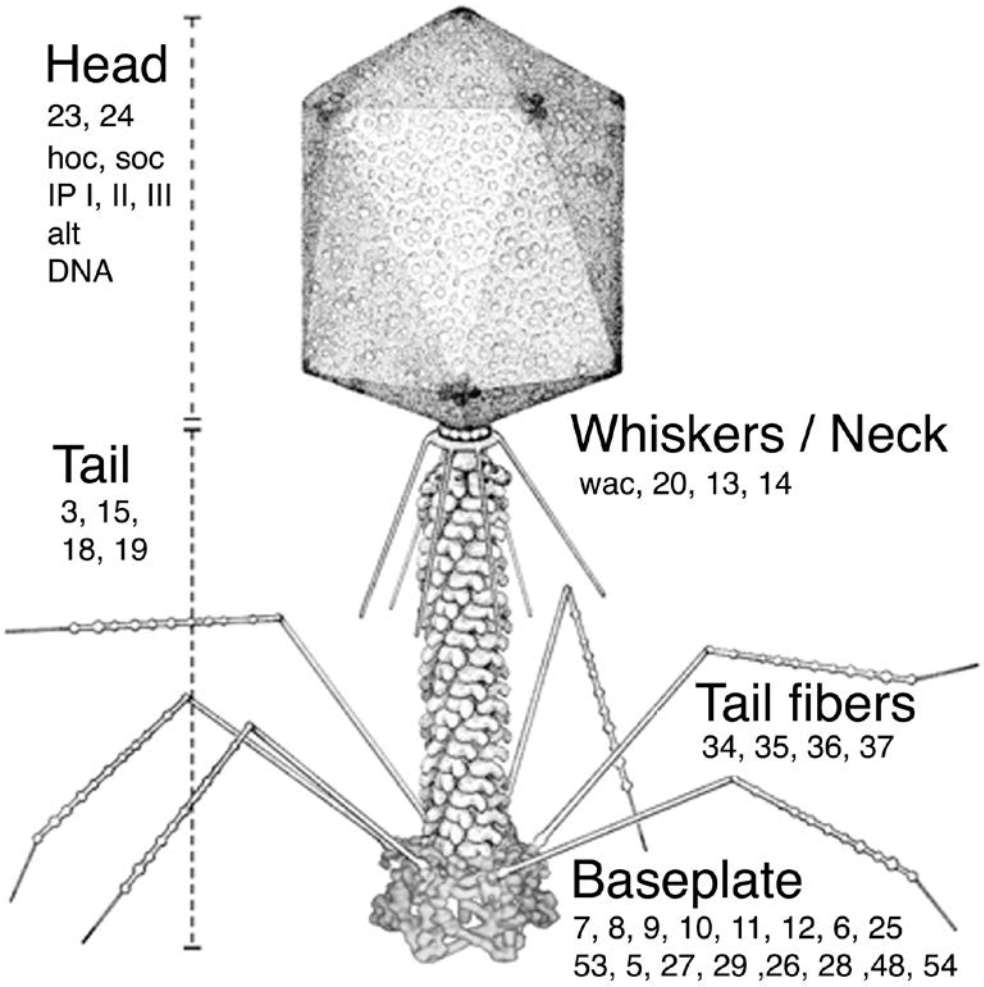

Figure 2.1: Schematic of a T4 bacteriophage. This particular bacteriophage displays antimicrobial activity against *E. coli* cells. Note the prolate icosahedral head shape, the neck, tail fibers and baseplate. As this bacteriophage "docks" with an *E. coli* cell via its tail fibers and baseplate, it contracts at the neck and injects its DNA into the cell. In doing so, it provides the genetic information required to replicate within the bacterial cell and ultimately lyse the cell, which leads to its death. For a detailed description of the various numbers associated with the viral components, refer to the review article of Miller *et al*.[209] Figure used with permission.

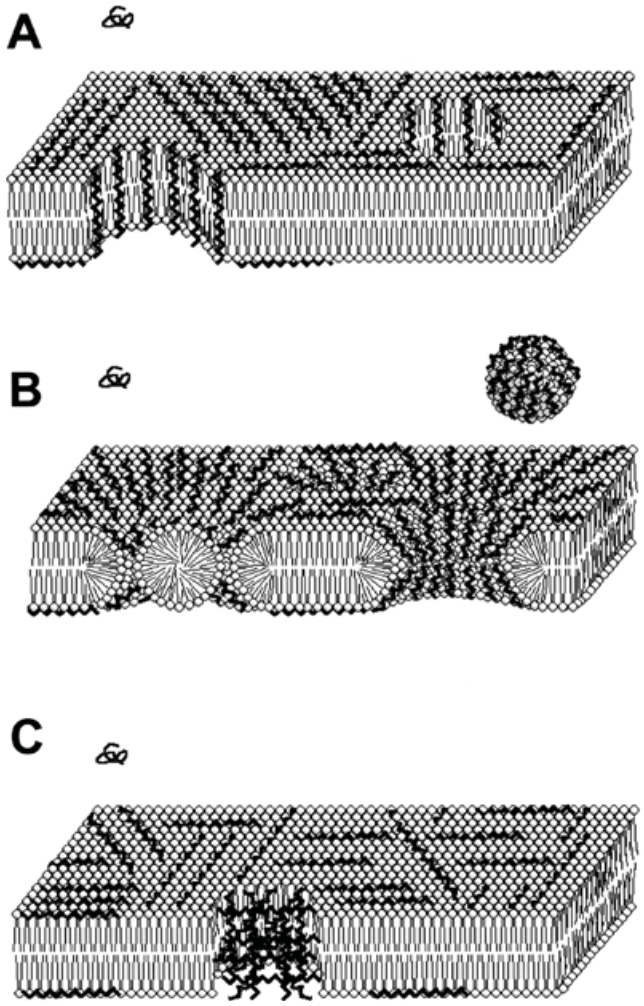

Figure 2.2: Possible methods of action for AMPs. (A) Diagram of the barrel-stave model of AMP action against a lipid bilayer of a bacterial cell membrane. (B) Diagram of the carpet model of AMP action on a cell membrane. (C) Diagram of the aggregate model of AMPs acting on a bacterial cell membrane. Figure used with permission and originally published by Hoff *et al.*[151]

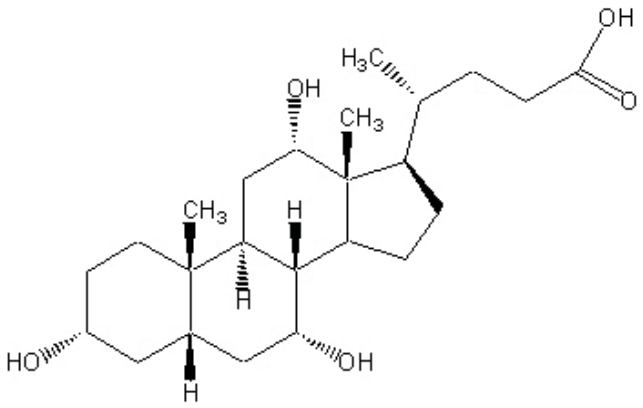

Figure 2.3: Schematic diagram of the chemical composition of cholic acid. Note the hydroxyl groups that are attached to various portions of the steroid backbone. It is to these hydroxyl groups that alkane chains and their accompanying ammonium salts can be attached to produce ceragenin molecules.

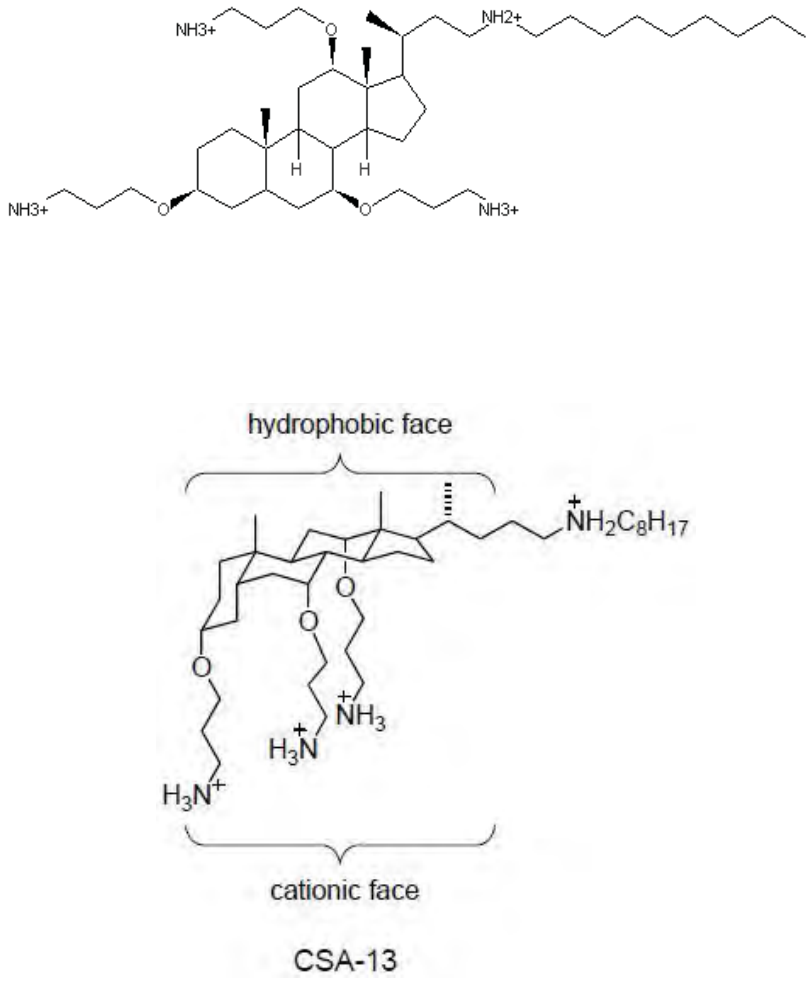

Figure 2.4: Schematic diagrams of the CSA-13 molecule. The top diagram is a depiction of CSA-13 in two dimensions. The bottom diagram is what CSA-13 may look like in three dimensions. In these diagrams, alkane chains can be seen attached to oxygen atoms that comprised the hydroxyl groups on the cholic acid sterol backbone. In addition, positively charged ammonium salts can be seen attached to the alkane chains. The steroid group creates a hydrophobic backbone and the ammonium salts create a polycationic face, the combination of which results in an amphipathic molecule.

CHAPTER 3

USING BIOFILMS AS INITIAL INOCULA IN ANIMAL MODELS OF BIOFILM-RELATED INFECTIONS

3.1 The Use of Planktonic Cells in Animal Models

The information presented in this chapter is based on a review article that was written and published by the author and Dr. Bill Costerton.[57] For the reader's reference, a copy of the published review article is provided as Appendix A at the end of this dissertation.

As has been the theme of this dissertation so far, combination biomaterials and coatings are being developed for the treatment and prevention of biofilm implant-related infections. The majority of animal studies that are used to model infections related to these materials primarily involve the use of an initial inoculum of planktonic bacterial cells from batch cultures.[80-102] The expectation has been that these planktonic cells would attach to the surface of a biomaterial, medical device or surrounding tissue and subsequently form a biofilm. Although valuable, data that have been derived from these experiments may not provide clinicians and biomaterials scientists additional clinical insight into how bacteria that reside in well-established, mature biofilms impact device-related and other human infections when they initially contaminate an implant site.

The history of biofilm discovery was outlined in Chapter 1 and in the context of this dissertation the importance of the discoveries that have been made may be

summarized to state that bacteria in natural ecosystems preferentially reside in the biofilm phenotype on solid surfaces. Based on this information, it is important to consider that when bacteria come in contact with wound sites, biomaterials or portals of entry in humans, i.e., inoculate patients, there is strong evidence to suggest that the majority of these bacteria are inherently residing in well-established, mature biofilms. A specific example of this scenario was also provided in Chapter 1 and is that of a patient who suffers from a Type IIIB open fracture, which is reduced with a fracture fixation device. To reiterate, these fractures have high rates of infection due the potential that they have to be contaminated with many millions or billions of bacteria that are ubiquitous in soil and other natural environments. The biofilms that contaminate these wound sites have the potential to colonize and cause infection near a fracture fixation device that has been implanted.

However, in all animal models of open fracture infections and other device-related infections to date, planktonic bacteria have been used as initial inocula. The same is true for other animal models of biofilm device-related infections. [80-102]

3.2 Limitations of Using Planktonic Cells as Initial Inocula

At least three proposed rationales can be given for why the use of planktonic cells has potentially limited investigators' abilities to detect clinically relevant outcomes of device biofilm-related infections. 1) Planktonic cells are more readily cleared by the immune system than cells residing in a biofilm.[210-212] Furthermore, animals typically have immune systems that are inherently advantaged compared to those of humans. Thus, when planktonic cells are used in *in vivo* models, it may be that the majority are

eradicated before they can form biofilms. This may contribute to the low reproducibility for the induction of osteomyelitis, which has been suggested by Gaudin *et al.*[193] as a common problem with animal models of osteomyelitis. 2) It is well documented that planktonic bacterial cells are more susceptible to antibiotics than those residing in a biofilm.[18,213] Therefore, if antibiotics are administered immediately following inoculation, they may affect planktonic cells more effectively than they would biofilm cells. 3) When planktonic cells are added to an *in vivo* system, the possibility exists that they may be dispersed rapidly away from the site of initial inoculation, which would dilute the concentration of bacteria per given area—potentially making it easier for the body to handle the bacterial load[214] and prevent attachment to a medical device.

In addition to these limitations that may accompany the use of planktonic cells as initial inocula, investigators have depended heavily on MIC values to determine the dose of antimicrobial that should be delivered, either from a device coating or intravenously, to prevent and/or treat biofilm-related infections.[84,173] The limitation of the MIC value in this specific instance is that it is based on data derived from planktonic cells from batch culture. Specifically, a MIC is defined by the Clinical and Laboratory Standards Institute (CLSI) as the dose of antimicrobial that is needed to result in a three $\log_{10}$ reduction ($10^5 \rightarrow 10^2$) of planktonic bacteria over a 24-hour period (see CLSI standard M26-A). Antimicrobial efficacy tests as standardized by the Environmental Protection Agency (e.g. standard operating procedure (SOP) Number: MB-09-04 and SOP Number: MB-06-05) are also based on planktonic bacterial responses. At least one standard of the American Society for Testing and Materials (ASTM E645-07) was found to recommend that microbicides be tested against biofilms. Citing these planktonic cell-based standards,

Ceri *et al*.[215] suggest that additional standards must be developed to treat and/or prevent recurring and untreatable infections that are the result of biofilm contamination and/or subsequent biofilm formation on medical devices.

3.3 Number of Bacteria in a Biofilm That May Be Used as Initial Inocula

It does not appear that all biofilms carry the same infectious potential and the author has proposed that most have minimal pathogenicity. If the opposite were true, it is likely that many more people would suffer from infections including gingivitis, periodontitis, sinusitis, conjunctivitis, cellulitis, gastroenteritis, vaginitis and/or colitis. Each human being is colonized with billions to trillions of bacteria, the majority of which appear to reside in well-established biofilms.[216] As such, infection may be considered an anomaly that extends beyond the normal host/bacterial relationship. Infection may also occur as humans are exposed to well-known pathogens that reside in biofilms from soil samples, on grocery carts, in food, within the human microbiome, on office desks, in shower heads, women's purses, grocery bags, and a plethora of other locations all over the world.

The number of bacteria that should be used as initial inocula in animal models is application dependent. Conditions may be considerably different in an animal that is intended to model a patient of total joint replacement, or some other elective surgery. Elective surgeries are performed under scrupulously aseptic conditions, yet despite these efforts, rates of infection still range from 1% - 4% and at times higher.[50,51,217-222] If an animal model were used to replicate an elective surgery scenario for biomaterial

development, it may be more appropriate to use a low number biofilm as the initial inoculum than what might be used for a massively contaminated open fracture model. Additional consideration would also need to be taken for the inclusion of organisms associated with human skin. Similarly, the use of planktonic or biofilm bacteria is application dependent.

When biofilms are grown in the laboratory, it is common to see them reach incredibly high numbers—on the order of 10^7 or 10^{10} cells/given area.[18,21,25,40] Biofilms that contain high numbers of cells can also be found in nature.[6,7,9,70,71] Similarly, bacterial cells that have been directly observed on and in the human body have been shown to reside in the biofilm phenotype.[216,223] Biopsy punches of human skin have been estimated to contain ~10^6 cells/cm^3 and it is well documented that the hardy biofilm former, *Staphylococcus epidermidis*, comprises a large portion of these resident commensal bacteria.[216,224,225] In the large intestine, several hundred grams of bacteria can be found with numbers reaching an astounding 10^{11} or 10^{12} cells/gram of tissue comprised of hundreds of species.[202,216,226] Notably, 60% of fecal solids have been shown to be comprised of bacteria.[227]

Although biofilms are ubiquitous and they tend to dwell in communities that can have very high numbers of cells, it may nevertheless be incorrect to assume that wound sites or surgical sites only become infected when they are contaminated with high number biofilms. To the contrary, a biofilm, or a portion of biofilm that has broken off, that contaminates a wound site may consist of as few as 10^2 or 10^4 cells, if not fewer.

Consider the paradigm of a patient who undergoes elective surgery, such as total joint replacement. After the patient's skin is prepped, 10^6 cells/cm^3 of normal flora may

be reduced in number to less than 10^3 cells/cm^3 (a 99.9% reduction, which is the most common claim of antiseptics). Note that the majority of these have been shown to reside in the biofilm phenotype. Importantly, groups have shown that even following antiseptic treatment, viable cells continue to reside several layers deep in skin,[228,229] and Dr. Costerton has observed matrix-enclosed bacterial biofilms between stratified squamous cells in the distal 5 – 7 layers of human prepped skin (unpublished observations). During surgery, these cells would have direct access to tissue throughout a patient's integument, while an incision is made, and they would also have direct access to the surfaces of transcutaneous or other implanted biomaterials. As there are no data in the literature that involve small number biofilms contaminating wound and/or surgical sites, surgeons and investigators are left to wonder what effect these might have on the development of infection in these scenarios.

There are myriad other paradigms that could be considered with similar scenarios of low numbers of cells within a biofilm contaminating wound and/or surgical sites. What remains is the fact that hypothesis driven research needs to be undertaken to determine the impact that low number biofilms have on human health as they attach to and form on the surface of biomaterial devices. Furthermore, the author has found no comparative study in the literature to determine the effect that fewer versus higher numbers of cells in a biofilm, which derive from the same bacterial strain(s), have on the formation of biofilms on or near biomaterials. For now, the understanding of critical doses required to cause infection are based solely on concentrations of planktonic bacteria.

3.4 The 10^5 Rule May Not Apply to Biofilm

Studies have shown that to prevent infection, bacterial loads must be kept below 10^5 cells per gram of tissue and this is the rule of thumb used by various clinicians as an indicator of infection.[214,228,230-232] However, this number is strain dependent and is based on planktonic bacterial cell counts. Citing Bowler,[233] Edwards and Harding have stated that, "The clinical relevance of the theory that bacterial counts of over 10^5 represent clinical infection has been questioned."[230] The work of Smeltzer *et al.*[234] has helped to validate this question. In a rabbit model of osteomyelitis, they demonstrated that a particular strain of *S. aureus* was able to cause osteomyelitis in 75% of animals at concentrations of 2×10^3 whereas a different strain of *S. aureus* was unable to cause infection even at a concentration of 2×10^6. In addition, it may be that smaller numbers of cells are required to cause infection if they reside in the biofilm phenotype. Indeed, the ability of low number, mature biofilms to resist antimicrobial treatment may enhance our understanding of how bacteria cause infection when initial inocula are on the order of thousands or tens of thousands of cells as opposed to the hundreds of thousands or hundreds of millions in planktonic form that are commonly used for *in vivo* studies.

Wolcott *et al.*[21] have recently undertaken a study wherein they showed that in the early stages of development, biofilms were more sensitive to antimicrobials when compared to biofilms that had matured for more than 24 or 48 hours. Their data further suggested that even if similar numbers of cells were present, the maturity, and not so much the number of cells within the biofilm, had a significant influence on its ability to resist antimicrobial perturbations. Their work was designed to model a specific clinical application and effectively addressed those scenarios. Importantly, however, this work

also followed the predominant pattern of biofilm research wherein enormous numbers of cells accumulated over time within the biofilm growth system.

Yet, as mentioned, it may not always be accurate to analyze biofilms as they undergo an increase in their number of cells. Though dynamic, biofilms in real life systems typically do not display the same growth rates as those generated under optimal conditions in the laboratory. Rather, in natural systems biofilms increase in cellular number over a longer period of time, mature to a level of equilibrium and when challenged by modifications in their environment, they respond appropriately. The hypothesis is that these equilibrated, matured, slow growing biofilms are what primarily contaminate wound sites, parenteral routes and medical devices within humans. Thus, to model contamination of a wound site with matured, equilibrated biofilms, similar to how they are found in nature, studies such as outlined in this dissertation may benefit from growing biofilms to threshold levels, allowing them to mature, and then exposing them to wound sites, antibiotics or other antimicrobial agents in *in vitro* and/or *in vivo* systems.

3.5 Future Methods of Growing Biofilm for Use as Initial Inocula

Connell *et al.*[235] have recently developed a remarkable method of growing biofilms in small numbers using micron sized "lobster traps." Although countless possibilities exist for *in vitro* experimentation with these traps, they are currently limited in that they are adhered to a solid surface. However, modifications to the substrate could make it possible for them to be used as initial inocula in an *in vivo* model.

In this dissertation, the development of a membrane biofilm reactor system will be shown in Chapter 4. This reactor was developed to grow biofilms on the surface of

polyetheretherketone (PEEK) membranes.[40,110] As will be seen in Chapter 4, biofilms of MRSA were shown to develop into three-dimensional pillar like structures on the surface of these membranes. Appendix B and Appendix C are also provided at the end of this dissertation to provide the reader with two manuscripts that have been published to date demonstrating the development and repeatability of this reactor. This reactor is the first to be developed specifically for growing well-established biofilms that can be used specifically as initial inocula in an *in vivo* animal model.

At this time, with the variety of biofilm reactor devices that are currently available, such as the CDC biofilm reactor, the membrane biofilm reactor developed in this dissertation, the Drip Flow Biofilm Reactor, and "lobster traps," the outlook is promising for a transition in biofilm investigation to occur from the *in vitro* paradigm to the *in vivo* setting.

3.6 Concluding Discussion

During the design process of an animal study, in particular an infection model, investigators often take careful consideration to select animals that have not been influenced by antibiotic feed, those that have not been specially treated in some manner at a housing facility, and, depending on the study design, those that have not been genetically modified or otherwise altered to influence the outcomes of a study. In contrast, investigators tend to select animals that come from natural environments so as to select a group that will model an uninfluenced, random sample. A similar process should be used when selecting bacterial isolates. These should be derived, as closely as possible,

from natural systems and grown under conditions that are conducive to their environment and phenotype. This may be the biofilm phenotype and in other cases, the planktonic.

In summary, as an isolate(s) is selected for application in an animal model of infection, or as one is selected for specific *in vitro* testing, such as an antimicrobial eluting biomaterial, the author recommends that, depending on the specific application, 1) the isolate be derived from a primary culture, either from a patient or natural environment, that has not been passaged numerous times, 2) that it be grown under conditions that will promote biofilm formation to the nearest possible extent as they are found in their natural environment and, 3) that biofilms be applied in numbers that, as closely as possible, model clinical and/or environmental scenarios to which biomaterials may be exposed.

The impact of biofilm-dwelling bacteria on human health is becoming ever more apparent. Chronic wounds are now considered to be the result of acute infection that begins with biofilm contamination as opposed to a nonhealing wound that is later contaminated and suffers from biofilm formation/infection.[62-64,236] Heart disease is now indicated to be compounded by biofilm dwelling bacteria from oral plaque that enter the vasculature.[237,238] Overall human health is believed to be significantly influenced by an intricate balance of biofilm dwelling bacteria in gut flora.[202] In short, it is difficult to overestimate the impact of biofilms on human well-being and disease.

Looking to the future of biofilm and biomaterials research, additional approaches for *in vitro* analyses and design modifications to *in vivo* models that encompass the use of preformed, well-established, sessile communities of mature biofilms that model those found in nature, in patients and within the environment, can be envisioned. As future

studies are undertaken to analyze the impact of low number biofilms on infection outcomes, results may indicate that less than 10^5 cells will be required to cause infection.

If the efficacy of antimicrobials is tested against high and low number biofilms, those on the order of 10^7 to 10^9 cells and 10^2 to 10^4, respectively, it may uncover deeper insights into the concentrations of antimicrobial in, for example, antimicrobial eluting biomaterials, that are needed to prevent and eradicate biofilm-related infections from developing. We can only wonder at this time how many antimicrobials and antimicrobial eluting biomaterials have been prevented from progressing to clinical, home, industrial and/or environmental use based on the fact that MIC values, which are primarily the result of planktonic cellular response, have been used to determine the amount that was needed to eradicate bacteria residing in well-established biofilms.

The opposite may be true as well. There is no indication that antibiotics that have been put into clinical use have shown efficacy against low and/or high number biofilms on implants. Although this trend may change as an understanding of the role of biofilm increases, this paradigm has potentially been a contributing factor to the development of antibiotic resistance. More specifically, in various systems, bacteria residing in biofilms may have been exposed to lower concentrations than are needed to prevent their growth and eradicate them within *in vitro* and *in vivo* systems. However, a cavalier approach of simply increasing dosages of antimicrobials alone or used in eluting biomaterials could potentially lead to toxic effects *in vivo* and cause additional problems. Thus, future work will be needed to elucidate the efficacy and toxicity of antimicrobials used alone or in eluting biomaterials against biofilms in translational and clinical studies.

In summary, the impact that low number biofilms have on human infection as well as using well-established, mature biofilms as initial inocula for *in vitro* and *in vivo* models may help further the optimization of antimicrobial treatments, such as those used in coatings on biomaterials. In addition, the understanding of the impact that biofilms from natural systems have as initial contaminants of wounds may also be increased. Most importantly, a shift in the use of biofilms for inoculation methods and analytical techniques may help biomaterial researchers take a step forward, and thus obtain the advantage in the battle against biofilm implant-related infections.

The work that was performed in this dissertation directly addressed these issues by using well-established biofilms as initial inocula, optimizing the dosage of a novel antimicrobial compound against these biofilms in a translational manner by performing *in vitro* then *in vivo* work, as well as establishing an animal model of osteomyelitis to demonstrate that using biofilms as initial inocula may have the ability to simulate biofilm implant-related infections that are seen clinically.

CHAPTER 4

A MEMBRANE BIOFILM REACTOR TO PRODUCE MATURE BIOFILMS ON THE SURFACE OF PEEK MEMBRANES FOR THE *IN VIVO* ANIMAL MODEL APPLICATION

4.1 Introduction

Information provided in this chapter is based off a published manuscript.[40] This manuscript is provided for the reader as Appendix B of this dissertation. Furthermore, the work outlined in this chapter relates directly to Specific Aim 1 outlined in Chapter 2, Section 2.4.

In this study, a modified CDC biofilm reactor,[239] referred to hereafter as the membrane biofilm reactor, was developed to grow well-established biofilms on the surface of PEEK membranes. The PEEK membranes were made of crisscrossing threads of 200 μm diameter with 300 μm openings. It was intended that these biofilm-ridden membranes be used for the *in vitro* and *in vivo* testing that will be outlined in Chapters 5, 7 and 8. However, prior to using these biofilms for those applications, the repeatability of this reactor needed to be confirmed.

The rationale for modifying the original CDC biofilm reactor to grow biofilms on the surface of PEEK membranes was two-fold. First, the original CDC biofilm reactor was designed to grow biofilms on the surface of circular metal discs (1/8" thickness x 1/2" diameter; referred to as coupons by Biosurface Technologies, Bozeman, MT). These coupons can be made of nearly any desired material. However, they are relatively large and may be cumbersome to use in an *in vivo* model, and they are difficult to remove from the CDC biofilm reactor without disturbing the biofilms. Second, our animal model was designed to test the ability of CSA-13 to eradicate biofilms by placing them in apposition to an antimicrobial coated orthopaedic device. It was therefore found that if the coupons were used in the intended study design, the coupon(s) may not have allowed for effective diffusion of the antimicrobial throughout the biofilm community.

Thus, the CDC biofilm reactor was modified to grow biofilms on the surface of PEEK membranes to address these above limitations. More specifically, the advantages of using the membranes included 1) a high surface area material that allowed for significant and consistent biofilm growth. As mentioned, open fractures and other open wounds have significant potential to be contaminated with very high inocula of bacteria. 2) The PEEK membrane used for this study was a thin material that could be placed easily between bone and a metal orthopaedic device. 3) The PEEK membrane would allow for diffusion of an eluting antimicrobial through the pores of the membrane and throughout the biofilm community.

The hypothesis of this study was that mature biofilms of MRSA would develop on the surface of PEEK membranes in a repeatable fashion over several runs of the reactor.

4.2 Materials and Methods

4.2.1 Isolate Selection

A freshly cultured, clinical isolate of MRSA was collected from a patient and used for this study. More specifically, a patient who underwent knee surgery developed infection and an aspirate was sent to ARUP Laboratories, Salt Lake City, UT for characterization and susceptibility testing. The isolate was characterized as MRSA based on resistance to penicillin and oxacillin using the Kirby Bauer disc diffusion technique. Preliminary work indicated that the isolate was a biofilm former following black colony formation on Congo Red agar and detection of the *icaADBC* gene cluster.

4.2.2 Modified Design of the CDC Biofilm Reactor

The CDC biofilm reactor was purchased from Biosurface Technologies (Bozeman, MT). The original design of the reactor is provided in Figure 4.1A. A modified lid was designed and machined using the University of Utah Chemistry machine shop. The modified lid contained four slots into which guillotine-like holders (20 centimeters (cm) in length with a 3mm groove down the middle of the interior portion) made of ultra-UHMWPE were inserted (Figure 4.1B). Into the guillotine holders were placed PEEK membranes that were held in place between two 316L stainless steel plates with a 0.64cm^2 opening (Figure 4.1B). A photograph of the membrane reactor is provided in Figure 4.1C. All other aspects of the reactor were the same as the original CDC biofilm reactor.

Notably, during the developmental phase of this membrane reactor, Delrin plastic was used to machine the various components of the lid and guillotine holders. However,

following multiple autoclave cycles, Delrin was found to decompose into its monomeric components of formaldehyde. The formaldehyde subsequently killed the bacteria in the reactor and prevented biofilm formation. A technical note was published[110] describing this problem and is provided as Appendix C at the end of this dissertation.

4.2.3 Biofilm Growth in Reactor

The membrane reactor held eight PEEK membranes with two membranes in each of the four guillotine holders (see Figure 4.1). PEEK membranes were first sonicated for 10 minutes in detergent, rinsed under running reverse osmosis water for 10 minutes, and sonicated in reverse osmosis water for 10 minutes and rinsed once again using 70% ethanol. The reactor was then assembled and all components autoclaved prior to use.

Following ASTM standard E2562-07, the membrane reactor was run under the following conditions: approximately 1.5×10^7 bacterial cells were inoculated into 500 mL of brain heart infusion (BHI) broth (modified; catalog # B99070, Fisher Scientific) in the biofilm reactor. The rotator was stirred at 130 rpm and the unit was placed in an incubator set at 28.5° Celsius (C) for 24 hours. A 10% BHI broth (modified) solution was then flowed through the reactor at 6.944 mL/min for 24 hours (for a total of 10 L).

4.2.4 Sample Fixation, Dehydration and Imaging

Importantly, the fixation and imaging protocol used for this portion of the study was modified from a published protocol that the author published with Dr. Bloebaum previously.[28] This publication is provided for the reader as Appendix D at the end of the dissertation. Since glutaraldehyde was found in this published study to be a superior

fixative for imaging the ECM components of a bacterial biofilm, it was used for this study.

To qualitatively observe the biofilms that had developed, 8 membranes were fixed, then imaged using SEM. For imaging preparation, membranes were removed from the reactor, placed in 2.5% glutaraldehyde for 24 hours then dehydrated using ascending grades of ethanol with 3 x 20 minute exchanges of each up to 100%. Samples were dried in a desiccator overnight, sputter coated with ~3 nm of gold, and imaged using a FEI NOVANano SEM 600.

4.2.5 Bacterial Quantification

In order to determine uniformity, following eight separate runs of the membrane biofilm reactor, a total of 64 PEEK membranes were used to quantify the number of bacteria that grew on the surface of each membrane. The membranes from each run were randomly assigned to one of two treatment groups (i.e., with 4 membranes per group).

Following growth in the reactor, the 4 membranes in Group 1 were removed from the guillotine holders, rinsed 3x in 6 mL of saline, placed on a shaker at 100 rpm for 20 minutes and allowed to remain stationary for 1.5 hours. The membranes were then vortexed for 1 minute, sonicated at 42k hertz (Hz) for 10 minutes, allowed to recover from sonication for 20 minutes and then enumerated using a 10-fold dilution series. One hundred microliters (µL) of each dilution (1:10-1:10,000,000) was plated onto Columbia blood agar in duplicate and incubated overnight at 37° C. The following day, the colony forming units (CFU) were counted to determine the number of bacteria per membrane

(CFU/membrane). Fifteen randomly selected membranes were imaged by SEM to confirm that bacteria had been removed from the surface.

The rationale for shaking the membranes at 100 rpm for 20 minutes was to model the car ride that they would be exposed to when they were transported from the lab to the site of animal surgery. Furthermore, the 4 membranes in Group 1 were allowed to remain stationary for 1.5 hours in order to model the time that they would be stationary while at the surgical facility and animals were prepped for surgery prior to inoculation. Group 2 membranes were treated in the same manner as those in Group 1 with the exception that they were allowed to remain stationary for 3 hours as opposed to 1.5 hours so as to model the time that they would remain stationary during the first surgery of the future animal model.

The density of bacteria in CFU/membrane was recorded for each PEEK membrane and then $\log_{10}$ transformed. For each of the two treatment groups separately, an Analysis of Variance (ANOVA) was fit, with run as a random effect, to calculate the mean and repeatability standard deviation (SD) of the log densities on the PEEK membranes over the eight reactor runs. Another ANOVA, with group as a fixed effect and run as a random effect, was used to compare the group means and to calculate the repeatability SD for both groups pooled together. These statistics were used to determine if any difference in bacterial response could be seen between membranes that were allowed to remain in a dilute broth solution for varying periods of time. The analyses also showed the percentage of the repeatability variance attributable to within-run sources and between-run sources.

4.3 Results

4.3.1 Growth on PEEK Membranes Within the Biofilm Reactor

Images collected of the PEEK membranes following growth, sample fixation and dehydration indicated that copious amounts of biofilm formed on the membrane surfaces (Figure 4.2A). Furthermore, each of the three indicators[240] that a mature biofilm had developed were detected, i.e., significant ECM production (Figure 4.2A and B), three-dimensional structures of mushroom- or pillar-like formations (Figure 4.2C) and possible water channel development (Figure 4.2D) were observed upon SEM analysis. In addition, the ECM appeared to act as a scaffold to which the bacteria attached to create a "bridge" that connected cells of the biofilm from one strand of the PEEK membrane to another (Figure 4.2B). These results indicated that mature, viable biofilms did form on the surface of PEEK membranes when grown within the modified membrane reactor.

Notably, although the temperature of the incubator was set at 28.5° C, the recorded temperature of the broth after the first 24 hours of each run was 28.1° ± 1.2° C. After 48 hours of growth, the broth temperature from each run was 29.8° ± 0.5° C.

4.3.2 Bacterial Quantification

The number of bacteria on each PEEK membrane was quantified following eight separate runs of the reactor, with 8 membranes per run, and four membranes randomly assigned to each of two treatment groups to confirm uniformity. The data are shown in Figure 4.3.

Mean log densities and repeatability SDs for each of the two groups individually and also for all 64 membranes pooled together are given in Table 4.1. The table

corroborates what is evident in Figure 4.3: the two groups had similar means and repeatability SDs. A 90% confidence interval for the difference of the Group 1 mean log density subtracted from the Group 2 mean log density was found to be (0.06, 0.19), which indicated statistical equivalence between the two group means at a significance level of 5% as long as mean differences up to 0.19 are considered to be negligible.

Taken together, these results show that copious amounts of *S. aureus* biofilm formed on the surface of each PEEK membrane within the reactor and that the mean log densities for the two treatment groups were statistically equivalent. Furthermore, the biofilm log density exhibited acceptable repeatability from run to run under the conditions described.

SEM images of the PEEK membranes that were collected after the quantification process indicated that only sparse microcolonies of bacteria remained on the surface. As such, the number of bacteria in the microcolonies was inconsequential with respect to the billions of cells that were enumerated (SEM images not shown).

4.4 Discussion

An increased understanding of the important role of biofilms in device-related and chronic infections suggests that *in vitro* and *in vivo* studies may be strengthened with the use of mature biofilms as opposed to the application of planktonic bacteria alone. This study highlighted the ability of the CDC biofilm reactor to be modified in such a way that mature biofilms could be grown on a polymer surface that could later be applied toward the *in vitro* and *in vivo* experiments that were performed in this dissertation. Taken

together, the hypothesis that mature biofilms would develop on the surface of PEEK membranes in a repeatable fashion was supported.

Interestingly, during the optimization of the modified reactor, it was found that when the unit was placed in an incubator set at 37° C, which resulted in a broth temperature of ~38° C, biofilms did not form as well as when they were grown at 28.5° C. More specifically, when grown at 37° C, there was no biofilm growth on the PEEK membranes by visual observation, whereas at 28.5° C, copious amounts of biofilm could be seen. Since our group was interested in having ~10^9 cells/membrane, no further runs at 37° C were performed. Nevertheless, this finding was similar to that of Rode *et al.*[241] They found that several clinical and food-related isolates of *S. aureus* produced biofilms optimally near 30° C, but not at 37° C.

It is important to note that the sonication level of 42k Hz that was used to break the cells apart in this study were well below lethal levels of sonication when compared to what has been reported in the literature. Previous work by Bill Pitt, PhD has shown that sonication above 100k Hz can in fact kill bacterial cells, whereas levels below 100k Hz are not detrimental to bacterial biofilms, and can even enhance their ability to develop over a 24-hour period.[242]

The overall mean bacterial log density was 9.51 log CFU/membrane and the repeatability SD was 0.213. As a comparison, in the 13 experiments described by Buckingham-Meyer *et al.*,[243] *S. aureus* ATCC 6538 biofilm grown in the CDC reactor on glass coupons exhibited a mean of 8.3 log (CFU/cm^2) and a repeatability SD of 0.224 (based on 2 coupons). In a different set of 12 experiments, Buckingham-Meyer *et al.*[243] grew *P. aeruginosa* biofilms in the CDC reactor on glass coupons, with a mean of 8.5 log

(CFU/cm^2) and a repeatability SD of 0.211. Goeres *et al.*[239] grew *P. aeruginosa* biofilm in the CDC reactor on polycarbonate coupons over 9 experiments and reported a mean of 7.06 log (CFU/cm^2) and a repeatability SD of 0.510 (based on 2 coupons per experiments). Thus, the biofilm bacteria grown on PEEK membranes in the membrane reactor exhibited acceptable run to run repeatabiliy in this study. At the time that this dissertation was written, the membrane biofilm reactor had been run more than 60 times with statistically equivalent numbers of cells each time.

In summary, demonstrating that biofilm growth on PEEK membranes was repeatable from run to run was an important aspect of this project. It was important that the *in vitro* testing portion of this work was performed with biofilms that had similar numbers of cells. Furthermore, it would be highly important that individual animals received equivalent biofilm challenges. Therefore, the statistical equivalence of the biofilms grown on membranes in each of the treatment groups suggested that if these biofilms were used, they would be used reliably and in a repeatable fashion during our *in vitro* and *in vivo* portions of the study.

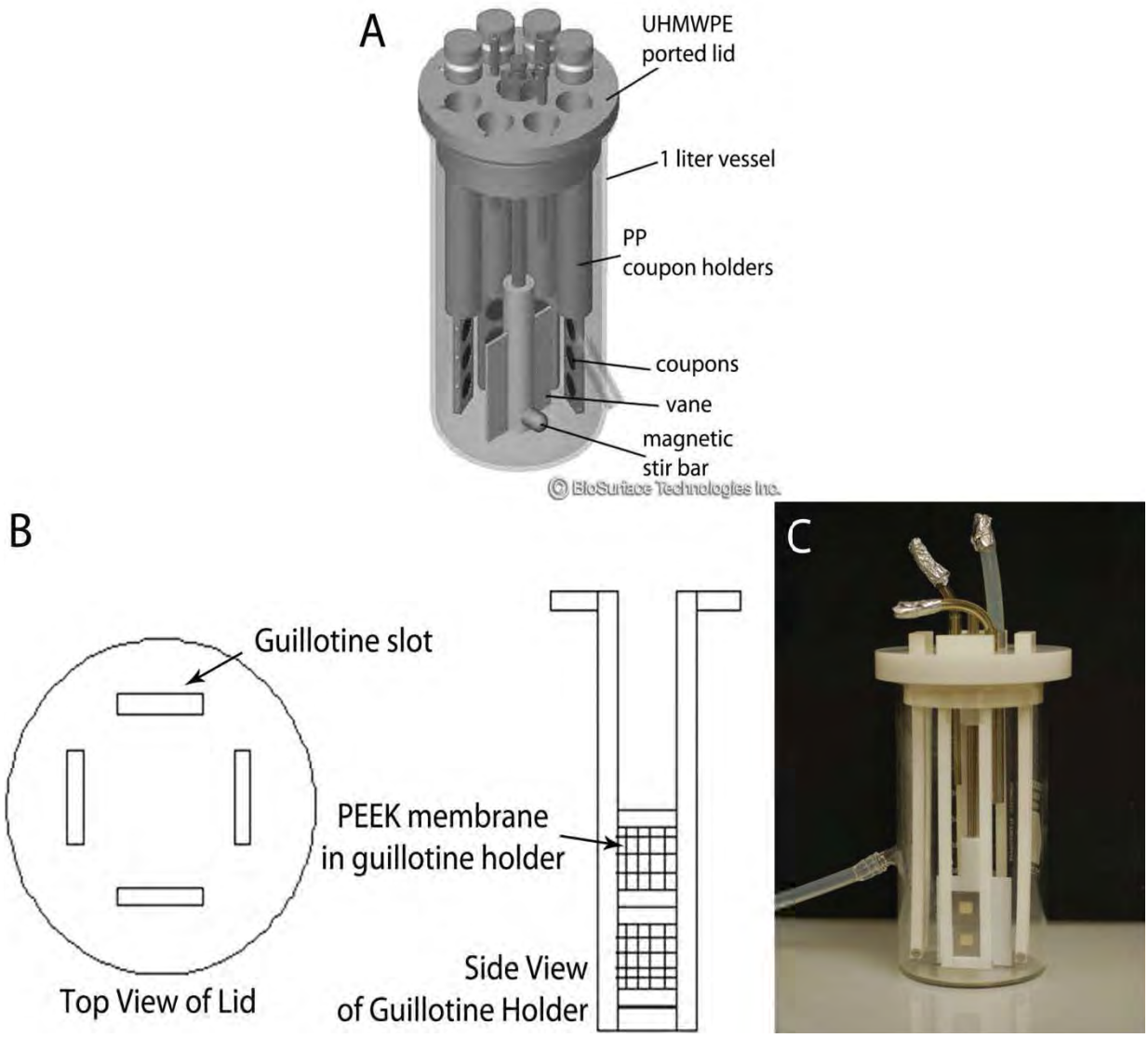

Figure 4.1: Diagrams and photo of the CDC biofilm reactor and membrane biofilm reactor. (A) Schematic diagram of the CDC biofilm reactor. The swirling paddle in the base of the reactor causes shear forces to be generated as broth circulates in the reactor. Shear forces help to increase the mechanical strength of biofilms. (B) Schematic diagram of the membrane biofilm reactor lid and guillotine-like holder. Biofilms grow on the surface of PEEK membranes that are held between two metal plates that slide in the guillotine-like holders. (C) Photograph of the completed membrane biofilm reactor.

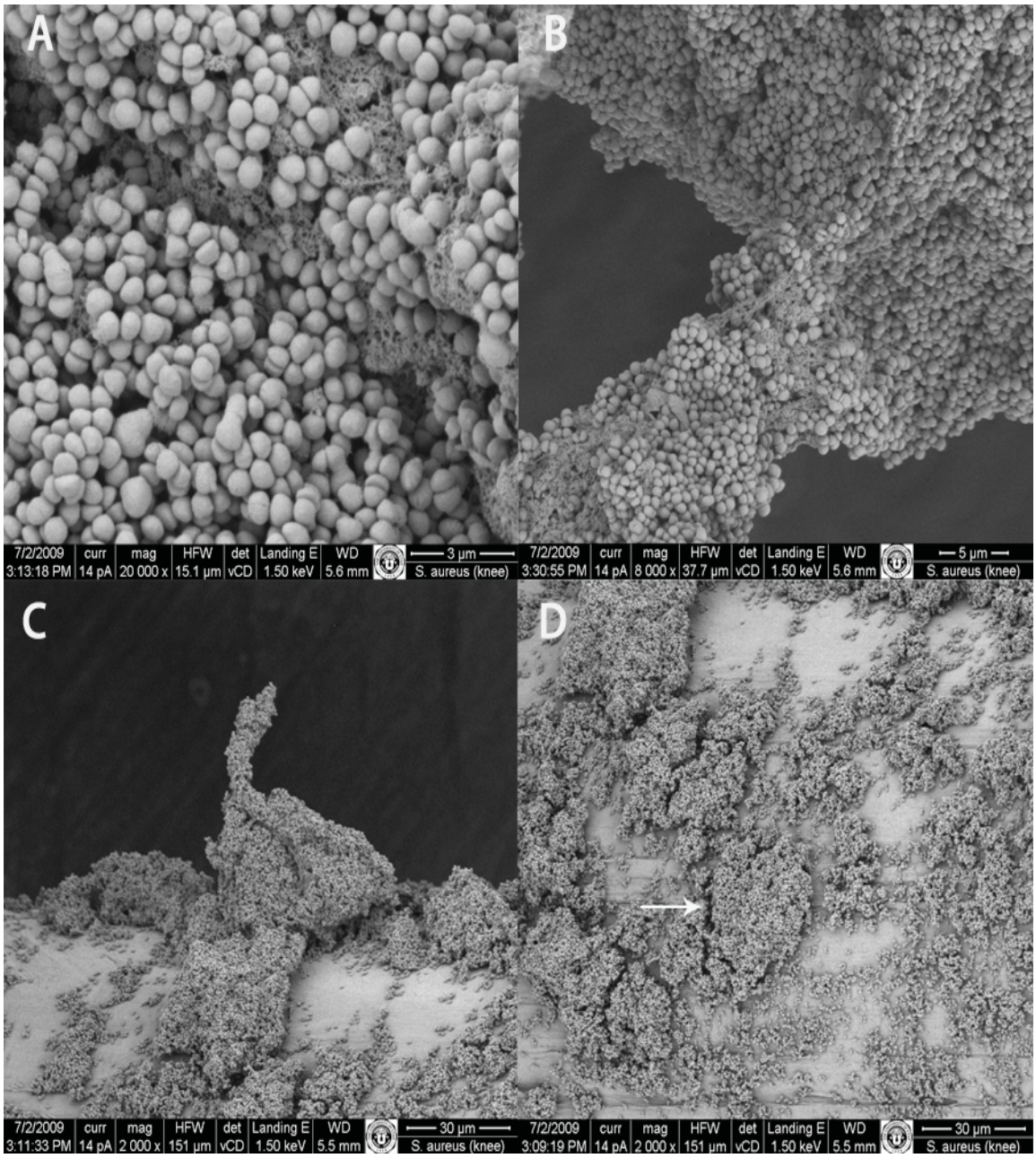

Figure 4.2: Images of biofilms in the following Figure were grown on the surface of PEEK membranes. (A) Representative SEM image of the *S. aureus* biofilm showing strands of the EPS network. (B) Additional image of the EPS providing a scaffold for bacterial cells within the biofilm to create a bridge from one surface of the PEEK membrane to another. (C) Representative image showing a three-dimensional structure of biofilm extending vertically from the surface of the PEEK membrane. (D) Representative image showing possible water channels within the biofilm structure (arrow).

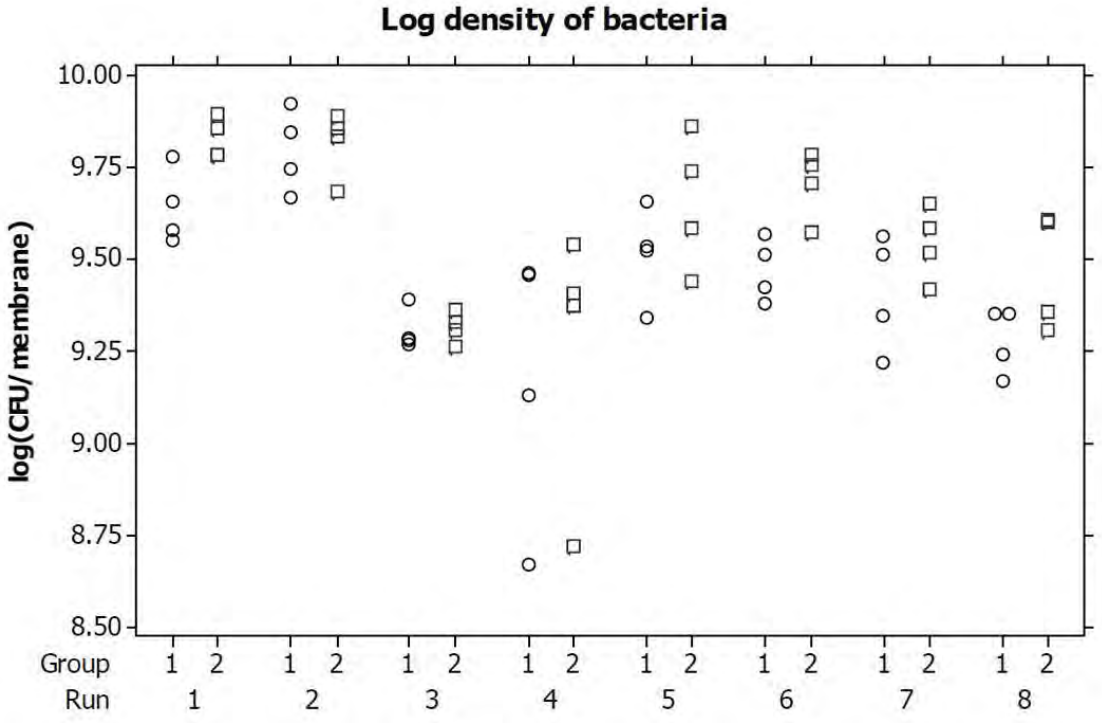

Figure 4.3: An individual value plot of the log density of bacteria per PEEK membrane. Group 1 (O) membranes were those that were allowed to remain stationary for 1.5 hours prior to quantification. Group 2 (□) membranes were those that were allowed to remain stationary for 3 hours prior to quantification. Each point represents 1 membrane.

Table 4.1: Statistical characteristics for each of the two treatment groups, and both groups pooled together. The standard error (SE) of the mean and the repeatability SD are based on 4 membranes per run. These data were derived from the raw data shown in Figure 4.3.

Group	**Mean Log_{10} Transformed CFU/Membrane**	**SE**	**Repeatability SD**	**Percentage Contribution**	
				Within Run	**Between Run**
1	9.45	0.0296	0.2020	17%	83%
2	9.58	0.0297	0.2162	15%	85%
Both 1 and 2	9.51	0.0203	0.2130	14%	86%

CHAPTER 5

IN VITRO ANALYSIS OF THE CSA-13 ACTIVE RELEASE COATING TO ERADICATE BIOFILMS OF MRSA

5.1 Introduction

In this portion of the dissertation work, the goal was to test the ability of CSA-13 to elute out of a PDMS polymer as an active release agent and eradicate biofilms of MRSA in an *in vitro* system. As such, this study addressed Specific Aim 2a and 2b as outlined in Chapter 2, Section 2.4. The *in vitro* system was designed specifically to model a clinically relevant scenario. In other words, it was designed to translate to the animal model of a massively contaminated Type IIIB Gustilo open fracture, and ultimately to translate to the clinical paradigm. The hypothesis was that as CSA-13 eluted from the PDMS polymer, it would reduce MRSA cells within the biofilm to a level that would be clinically acceptable (this acceptable level will be discussed in the Methods section below).

As was discussed in Chapter 2, numerous *in vitro* experiments have been designed to test the efficacy of active release coatings with the intent to model clinically relevant paradigms of biofilm implant-related infection. The limitations of these previous tests have been discussed in Chapter 2.

The flow cell that was designed was machined in such a way that stainless steel (SS) plates, coated with a PDMS/CSA-13 conjugate polymer, could be placed in a chamber that had a flow of broth running through it at a rate that modeled the flow of interstitial fluid in the proximal medial aspect of a sheep tibia,[244] which is the anatomical location that these coated plates and biofilms were to be tested in the animal model. This provided the ability to test the efficacy of CSA-13 to reduce biofilms of MRSA under more physiologically and clinically relevant conditions.

In summary, this study used an optimized dip method and concentration of CSA-13 to reduce biofilms of MRSA *in vitro* to a level that may prevent biofilm implant-related infection from developing in a future animal model.

5.2 Material and Methods

5.2.1 Stainless Steel Plates

For this study, 316L SS was used to machine plates that were 2 cm x 2 cm with 2.7 mm screw holes drilled in each corner. Each plate had a consistent thickness of 1.85 ± 0.01 mm. On the underside of each plate, a well with a depth of 300 μm and 1.2 cm width x 1.2 cm length was machined such that a 1 cm width x 1 cm length PEEK membrane could be placed in the well (Figure 5.1).

Prior to dip coating, each plate was grit blasted at 90 psi using fine silica beads in a dry blast cabinet to enhance the attachment of PDMS primer and polymer to the metal surface. After grit blasting, the plates were cleaned and passivated following ASTM standard F86-04. In short, this passivation process involved cleaning and sonicating the plates in detergent, exposing them to a 35% nitric acid solution for 30-60 minutes and

rinsing/sonicating them in water for 20 additional minutes. Each plate was allowed to air dry prior to dipping.

5.2.2 PDMS (Silicone)

The PDMS polymer that was used for this study was purchased from NuSil Technologies (catalog # MED-6607, Carpenteria, CA). This PDMS is on master file with the FDA for use in approved medical devices. In addition to the reasons described in Chapter 2, section 2.6 previously, the rationale for using this specific PDMS was based upon several months of testing other PDMS products, other polymer types and various dipping methods. Due to the nature of CSA-13, PDMS polymers that utilized platinum catalysts as a catalytic agent for cross linkage could not be used as the platinum was poisoned by the nitrogen compounds in the CSA-13. Furthermore, as was mentioned, high temperature vulcanizing PDMS could not be used since CSA-13 melts at ~80°C and begins to degrade over time at temperatures above ~150° C. As was also previously discussed, CSA-13 was found to have undesirable release profiles from PU.

Importantly, there have been two provisional patents filed following the development of this PDMS coating with CSA-13 incorporated in it and the author is the primary inventor on both of these patents.

5.2.3 PDMS Suspension/Concentration of CSA-13

Over a several month period, varying ratios of PDMS to naphtha (e.g., 0.5:1, 1:1, 2:1) as well as varying amounts of CSA-13 (from 2% – 20% w/w) were tested in PDMS dispersions to develop an optimized formula that would result in a uniform coating as

well as reduce the amount of bacteria in MRSA biofilms from greater than 10^9 CFU to less than 10^2 CFU in a 24-hour period.

The rationale for using biofilms that contained ~10^9 CFU was to model the number of bacteria that may be present clinically in a Type IIIB open fracture wound that is contaminated with roughly 1/3 of a gram of soil. Recall from Chapter 1 that one gram of soil has been shown by Bakken[71] and Torsvik *et al.*[70] to contain between 10^7 and 10^{10} bacterial cells, the majority of which may reside in the biofilm phenotype. Obviously, ~10^9 bacteria in an open wound might represent a worst case clinical scenario, wherein significant amounts of soil and/or bacteria would be present, many of which may be compressed between a fraction fixation plate and the bone of a patient. Modeling a worst case scenario was important so that the amount of CSA-13 needed would not be underestimated.

Furthermore, the rationale for wanting to reduce biofilms from 10^9 to less than 10^2 as an indicator that CSA-13 was effective was based on the CLSI guideline M26-A, which suggests that to demonstrate the efficacy, i.e., MIC, of an antimicrobial, it should result in a reduction of 10^5 to 10^2 CFU within a 24-hour period. However, these guidelines are optimized for planktonic bacteria, which are much more susceptible to antimicrobial treatment than those residing in a biofilm.[18,21] Since this study intended to develop an antimicrobial coating that would eradicate bacteria in the biofilm phenotype, the author and technicians optimized the coating to reduce the number of bacteria to below the 10^2 CFU requirement outlined by the CLSI.

Taking these considerations into account the final formula, which was found to meet these outlined criteria and which resulted in a consistently uniform coating on the

SS plates, was comprised of a 1:1 PDMS:naphtha ratio with an 18% w/w CSA-13 concentration. In all cases, an 18% w/w concentration of CSA-13 was the only concentration that proved to have the desired antimicrobial efficacy. Counter intuitively, a 20% w/w ratio had lower antimicrobial activity than 18%. The 20% w/w ratio also resulted in poor mechanical properties of the PDMS material. More specifically, the polymer did not cross-link well, it became too pasty to dip into and the PDMS surface tended to wrinkle when multiple dips were performed. In addition, a 1:1 ratio of PDMS:naphtha was deemed to result in the most uniform coating with sufficient amounts of CSA-13 on the SS plates.

Naphtha (VM&P) was purchased from Fisher Scientific and CSA-13 was manufactured by Dr. Paul Savage's group at Brigham Young University. To produce a CSA-13/PDMS dispersion, jet mill micronized CSA-13 (50-200 nm particle size) was added to 10 mL of naphtha solvent and stirred for a minimum of 45 minutes. Ten mL of PDMS dispersion were then added to the suspension for a final 1:1 PDMS:naphtha ratio and 18% w/w CSA-13 concentration. The equation below shows the calculation that was used to determine the amount of CSA-13 that was needed to add to a solution for a final 18% w/w concentration:

$$x = (0.18\,(y + x))/0.825$$

where x equals the amount of CSA-13 in mg/mL and y equals the solids content of PDMS in mg/mL. The sum of y+x represented the total solids content of the mixture. The number 0.825 was used to take into account the salt content of the CSA-13 powder.

Importantly, *y* was a known amount that was calculated after taking into account the dilution of PDMS after it was added to the naphtha solvent. Since the naphtha in which the PDMS was initially suspended and which was added to the mixture evaporated away from the system during the curing process, its presence was considered negligible to the final w/w concentration. In addition, the evaporation of the methylethylketoxime byproduct of the condensation cure reaction was considered negligible to the final w/w concentration.

After PDMS had been added to the CSA-13:naphtha suspension, it was stirred for a minimum of 3 hours. For those plates that were coated with PDMS only, the PDMS and naphtha were stirred alone at a 1:1 ratio for a minimum of 3 hours. The dispersions were degassed at ~25 inches of mercury (inHg) to remove any air bubbles.

5.2.4 Dip Coating Procedure

Following passivation, SS plates were first hand dipped into MED-160 primer (NuSil Technologies) and allowed to dry for 45 minutes in ambient air and temperature on a rotating wheel set at 5 rpm. The rotating wheel was custom made to hold each plate on two prongs that were perpendicular to the face of the wheel. By rotating the wheel at 5 rpm, the primer spread across the plate in a uniform manner.

After priming, SS plates were dipped by hand into a dispersion of PDMS only or PDMS with CSA-13. Plates were placed onto the rotating wheel set at 5 rpm. This process was repeated two more times for a total of three dipped layers on each plate. There was a 10-minute interval between each of the dips, which was within the recommendations of the manufacturer if multiple dips were to be performed.

Importantly, the same person dipped each of the plates under similar room conditions in an attempt to reduce lot to lot variability. After dipping, each SS plate was left on the rotating wheel at 5 rpm for 7 days (as per manufacturers recommendation) in a hood under ambient conditions. Uniformity of the coating was determined by measuring the thickness of the coating in three different areas of the plate using calipers with a measuring capacity to 10 μm: the thickness was further confirmed by cutting the coating of n=10 plates with a razor blade perpendicular to the plate surface, then measuring the thickness with a JEOL-6100 scanning electron microscope. The amount of CSA-13 per plate was calculated by weighing each plate before and after it was dipped, subtracting the weight of the plate, then multiplying the final coating weight by 0.18 since it was added at an 18% w/w concentration.

5.2.5 Flow Cell

A flow cell unit was designed by the author and machined by Biosurface Technologies (Bozeman, MT). The unit consisted of 6 individual chambers, each having a 4 cm width x 4 cm length x 2 cm height (Figure 5.2A and 5.2B). A 1/16 inch inlet was machined in the center of each lid that covered each chamber. A barbed connection was used to connect each inlet to 1.42 mm inner diameter Tygon tubing (catalog # EW-96429-34, Cole Parmer). One end of the tubing was connected to this barb, the middle portion of the tubing passed through a peristaltic pump (Masterflex L/S, catalog # 07523-80, Cole Parmer), and the other end of the tubing was placed into 10% BHI broth (modified). As such, the broth could be pulled through the tubing to a chamber of the flow cell unit.

One side of each chamber was further drilled to have a 1/4" outlet hole (see Figure 5.2A). The bottom of the hole was exactly 1 cm up from the bottom of each chamber. A barbed connection was used to connect 1/4" inner diameter silicone tubing to an effluent bottle (Figure 5.2C).

5.2.6 Biofilm Growth

Biofilms of MRSA were grown on the surface of PEEK membranes using the membrane biofilm reactor.

5.2.7 Quantification of MRSA Cells in the Biofilms

The quantitative and qualitative experiments to determine the repeatability, number of bacteria and maturity of biofilms on PEEK membranes that were grown with the membrane biofilm reactor were discussed in Chapter 4. However, to confirm that the published numbers were consistent in this portion of the study, as well as to obtain a baseline of the number of CFU that grew on each membrane, two PEEK membranes were removed for quantification following each run of the reactor. The remaining six membranes were used in the actual experiment.

To quantify the CFU per membrane, the same procedure was used as described in Chapter 4, section 4.2.5.

5.2.8 Flow Cell Setup/Efficacy of CSA-13 in Thin Films

Following the 48-hour growth period of the biofilm reactor, a PEEK membrane was aseptically removed and placed into a well on the underside of a SS plate. The plate

was then secured to an autoclaved piece of bone using sterile cortical bone screws (Figure 5.2D). The bone/SS plate/PEEK membrane construct was then placed into a chamber of the flow cell unit (see Figure 5.2B). This procedure was repeated for all six chambers of the flow cell. Each chamber was then filled with 20 mL of 10% BHI broth (modified) in order to cover the entire bone/PEEK/SS plate construct. To model the body temperature of sheep, the incubator was set at 39° C. Importantly, CSA-13 has the same activity at 39° C as it has at 37° C.

Over a 24-hour period, a 10% BHI broth solution was flowed through the flow cell at a rate of 4.5 mL/hr. This flow rate was chosen based on the work of Smith *et al*.,[244] which indicated that the rate of interstitial fluid flow in the hind limb of sheep can be between 1 mL/hr and 8 mL/hr. Moreover, the use of BHI broth (modified) was important as BHI (modified) is derived from boiled animal tissues. This broth was chosen to more closely model the environment that bacteria and CSA-13 would be exposed to in the future *in vivo* paradigm.

At 4-, 8- and 24-hour time points, a bone/SS plate/PEEK membrane construct was aseptically removed from a chamber of the flow cell. The cortical bone screws were aseptically removed. The bone piece was placed into 20 mL of Dey Engley (D/E) broth (catalog #DF0819-17-2, Fisher Scientific), the SS plate was placed into 10 mL of D/E broth and the PEEK membrane was placed into 5 mL of D/E broth. The rationale for using D/E broth was that it contained lecithin, which is known to deactivate nitrogen containing antimicrobial compounds. In this case, the CSA-13 was deactivated so that it did not have residual kill against bacteria during the quantification process. The different

volumes of D/E broth were used to cover the entire surface of each of the different components.

Each bone piece, SS plate and PEEK membrane was vortexed for 1 minute, sonicated for 10 minutes and allowed to recover for 20 minutes prior to performing a 10-fold dilution series to quantify the number of CFU. Results were calculated to show the number of CFU/gram of tissue for the bone samples, CFU/SS plate and CFU/PEEK membrane. In addition, a 100 µL sample of broth was collected from each chamber and each effluent bottle to determine the CFU/mL of broth in each. Since six PEEK membranes were present in each flow cell, an n=2 experiments (an n=1 experiment comprised of a 4-, 8- and 24-hour time point) could be performed per run of the flow cell.

In total, n=27 experiments were performed. This included n=9 experiments with CSA-13-coated plates tested against MRSA biofilms (test group), n=9 experiments that involved PDMS only coated plates with biofilms (positive control group), and n=9 that involved PDMS only coated plates with no biofilm on the PEEK membranes (negative control group). The rationale for performing these experiments in groups of 9 was to model the number of sheep that would be used in the animal study, wherein 9 sheep would be treated in a similar manner as each of the three treatment groups outlined. As such, this study included the proper controls to ensure that PDMS itself did not have an antimicrobial effect on the biofilms (positive control group) and that the experiment was performed aseptically (negative control group).

5.2.9 Short Term Elution Kinetics

At each collection time point of 4, 8 and 24 hours, the broth from the chamber and from the effluent bottle was collected and analyzed using high pressure liquid chromatography/time of flight mass spectrometry (LC/MS) with a reverse phase C_{18} column to determine the amount of CSA-13 that had eluted out of the coating. More specifically, a 50 µL sample of broth was spiked with 50 µL of a known amount of deuterated CSA-13 (dCSA-13), which was mixed with NaOH to remove the positive charge from both CSA-13 compounds. The mixture was resuspended in dichloromethane to separate the phases, then allowed to dry in order to be resuspended in 60% acetonitrile. A 5 µL sample was then injected into the LC/MS instrument and pushed through the column over 3 ½ minutes while the acetonitrile concentration was increased from 60% to 100%. The ratio of counts from the CSA-13 and dCSA-13 was used to calculate the concentration of CSA-13/mL that was present in the original broth sample.

5.2.10 Long Term Elution Kinetics/Residual Antimicrobial Kill

Five CSA-13-coated SS plates were used to determine the amount of CSA-13 that eluted out of the PDMS polymer over a 30-day period. To do so, these five plates were placed in five separate chambers of the flow cell. A 10% BHI broth (modified) solution was flowed through the chambers for 30 days. At 24-hour intervals, the broth was collected from the effluent bottles and analyzed using the same LC/MS technique as before.

In addition to collecting broth for elution kinetics data, each of the broth samples was also used to determine the efficacy of the eluted CSA-13 against planktonic bacterial

cells in order to determine the duration of antimicrobial kill that the active release agent provided. This was done by pipetting 990 µL of a broth sample from each of the six plates that had eluted over a 15-day period into a test tube followed by 10 µL of water that had been adjusted to a 0.5 McFarland. The final concentration of bacteria was ~5 x 10^5 cell/mL. The rationale for using this amount of bacteria was to coincide with the recommendations of CLSI standard M26-A. Each broth sample was incubated overnight at 39° C to model the temperature of a sheep's body. A 10-fold dilution series was used to quantify the number of bacteria that remained in each broth sample.

5.2.11 Statistical Analysis

To compare the number of CFU that were present in the various samples of the CSA-13 (treatment) group and the PDMS only (positive control) group, an independent sample *t* test was used. This was used based on the fact that in each case, the data sets from all samples in the two groups were normally distributed, the data were sampled independently, and Levene's test of equality was statistically insignificant, suggesting that there was not a statistically significant difference in the variance of the two groups.

5.3 Results

5.3.1 Dip Coating

Plates that were coated with PDMS only (Figure 5.3A) had a final coating weight of 71.4 ± 14.6 mg and a thickness of 97 ± 18 µm. In contrast, plates that were coated with Si/CSA-13 (Figure 5.3B) had a coating thickness of 113 ± 22 µm and a final coating weight of 96.3 ± 9.7. The amount of CSA-13 per plate was calculated to be 17.2 ± 0.61

mg. Notably, the increase in coating thickness of plates that were dipped in the PDMS/CSA-13 suspension compared to those that were dipped in the PDMS only suspension was believed to be due to the fact that the PDMS/CSA-13 suspension was thicker (more viscous) with the CSA-13 added to it, which appeared to have led to a slight increase in the amount of solution adhering to the plates.

5.3.2 Biofilm Quantification

A total of n=36 PEEK membranes from 18 different runs of the biofilm reactor were used to quantify the CFU/PEEK membrane in order to obtain a baseline of cells on each membrane. Results showed that, similar to previously published data,[40] there were 9.41 ± 0.35 $\log_{10}$ CFU/PEEK membrane.

5.3.3 Efficacy of CSA-13 in Thin Films

Over the 24-hour period that the 10% BHI broth (modified) was flowed through the flow cells, there were 107 ± 6 mL of broth that flowed through each of the chambers.

Results from the samples that were in chambers with PDMS only coated plates (positive control group) showed that there was a slight decrease in the number of CFU/PEEK membrane compared to the number of CFU/PEEK membrane that were quantified immediately after the 48 hour growth period in the biofilm reactor (Figure 5.4A). More specifically, there were 7.75 ± 0.75 $\log_{10}$ CFU/PEEK membrane that were quantified on membranes after 24 hours of exposure to PDMS coated plates (Figure 5.4A). This difference was statistically significant ($p<0.05$).

The broth samples from the chambers and bottles that were collected with the PDMS only coated plates had an increase in the number of CFU/mL of broth at each time point (Figure 5.4A). By 24 hours, there were 8.19 ± 0.20 $\log_{10}$ CFU/mL of chamber broth and 6.46 ± 1.89 $\log_{10}$ CFU/mL of bottle broth.

Results indicated that those biofilms on PEEK membranes which were placed in chambers with CSA-13 coated plates (treatment group) had greater than an 8 $\log_{10}$ reduction of bacteria on the surface over a 24-hour period (Figure 5.4B). More specifically, there were 0.50 ± 0.75 $\log_{10}$ CFU/PEEK membrane after 24 hours. When compared to the number of bacteria that were on the PEEK membranes used for quantification, the difference was statistically significant ($p<<0.05$). The broth samples collected from chambers that had CSA-13 coated plates had no detectable amounts of bacteria after 24 hours in the broth from the chamber or from the bottles (Figure 5.4B). There were 0.22 ± 0.67 $\log_{10}$ CFU/SS plate detected.

Interestingly, the number of bacteria in the bone samples exposed to CSA-13 increased over the 24-hour period, with 3.49 ± 1.42 $\log_{10}$ CFU/gram of tissue being detected in the first 4 hours and 5.27 ± 1.52 $\log_{10}$ CFU/g of tissue being detected after 24 hours (Figure 5.4B). This was believed to be due to an interaction of the positively charged CSA-13 with the negatively charged components of the bone. This suggested that CSA-13 may have reduced efficacy to kill bacteria that are present in nonviable bone samples.

However, there were ~3 $\log_{10}$ more CFU in the bone samples from chambers with PDMS only coated plates compared to those bone samples that were in the chambers with CSA-13 coated plates. Specifically, after 24 hours, there were 8.41 ± 1.08 $\log_{10}$

CFU/gram of bone in the PDMS only group, versus 5.27 ± 1.52 $\log_{10}$ CFU/gram of bone in the CSA-13 treated samples. This difference suggested that although CSA-13 appeared to have reduced efficacy in bone, it did have greater efficacy than no CSA-13 at all. Furthermore, this difference was statistically significant ($p<0.05$), as were all of the differences in bacterial numbers between each of the samples in the positive control group and the treatment group when compared with an independent sample *t* test.

There was no growth in any of the samples from the third group (negative control) of testing, wherein no bacteria were added to chambers. This confirmed that the process could be performed aseptically.

5.3.4 Short Term Elution Kinetics

Elution kinetics results indicated that although there was a reduction in the overall μg/mL of CSA-13 from 4 hours to 24 hours in the chamber broth and in the bottle broth, there was no significant difference in the overall % release of CSA-13 (see Table 5.1), which was indicative of zero-order release. This was likely due to the fact that CSA-13 was saturated in the solution during that time. In addition, over time, it appeared that CSA-13 molecules may have accumulated in the bone samples and the molecules were likely interacting with the bacterial cells that were present, which may explain the slightly lower overall % release at 24 hours compared to 4 hours and 8 hours. The overall % release was calculated using the total volume of broth that had flowed through the flow cell over 24 hours. By 24 hours, approximately 107 mL of broth had flowed through each of the chambers and into the effluent bottles and there were approximately 15 mL of

broth in the chambers. No CSA-13 was detected in the broth from those chambers that had PDMS only coated plates.

5.3.5 Long Term Elution Kinetics/Residual Antimicrobial Kill

Long term elution data indicated that the release of CSA-13 declined in a first-order fashion over the first five days (Figure 5.5). After five days, the detection limit of the particular LC/MS technique used in this study was surpassed as the broth samples contained less than 0.5 μg/mL of CSA-13. In this portion of the study, by 24 hours there were approximately 13 μg/mL of CSA-13 in the broth that was collected and by day 5 there were approximately 0.69 μg/mL.

Table 5.2 presents the data that were collected by testing the residual antimicrobial efficacy of the broth that was collected during the long term elution kinetics study. A reduction of greater than 3 $\log_{10}$ CFU/mL was seen out to day 10. By day 12, there was a notable increase in the number of CFU/mL indicating that the concentration of CSA-13 in the broth had dipped below bactericidal levels.

5.4 Discussion

In direct response to previous limitations of testing active release coatings, this work undertook to test the efficacy CSA-13 as an active release agent to eradicate well-established biofilms of MRSA *in vitro* in a flow cell system as opposed to stagnant broth solutions. This was further done by determining the optimum concentration of CSA-13, as opposed to relying on the MIC values of CSA-13 against planktonic bacteria. Thus, this work was designed to translate to the *in vivo* paradigm wherein coated SS plates and

biofilms were used in the animal model of biofilm-related infection that will be shown in Chapter 8.

The results from this work strongly indicated that the use of CSA-13 at an 18 % w/w concentration would be efficacious to reduce the number of bacteria in a biofilm to a clinically acceptable level. More specifically, within 24 hours, the number of CFU on the PEEK membranes were reduced to less than 1 $\log_{10}$ on average with minimal amounts of bacteria cultured from the other components of the flow cell. Although there were ~10^5 CFU/gram in the bone samples, it was recognized that this was dead bone that had no host immunity. Thus, when used *in vivo*, bacteria would also be attacked by host immune components. Furthermore, in a head-to-head *in vitro* comparison, vancomycin was used as the active release agent of the PDMS coating and performed more poorly with nearly 3 $\log_{10}$ more bacteria in the bone samples compared to CSA-13 (unpublished data).

The fact that the results were repeatable over an n=9 runs was very promising. This strongly suggested that the various lots of CSA-13/PDMS dispersions were made in a consistent manner, that the dip method was performed in a repeatable fashion and that CSA-13 eluted from the silicone of each coated plate. Furthermore, this suggested that when CSA-13 was used as an active release agent in the animal model of n=9 animals, it would perform in a repeatable fashion.

A potential limitation of this study was the variability in the amount of CSA-13 that was detected by LC/MS in the broth samples from the short term and long term elution kinetics. There were three possible reasons for this. 1) The broth that was used for this experiment was an undefined media that contained lipids, carbohydrates, electrolytes and other components derived from boiled brains, hearts and tissues of cattle.

It has been found that CSA-13 has a lower solubility in this broth (solubility of 35-40 μg/mL) compared to saline (solubility of 85-90 μg/mL) (unpublished data). Thus it appeared that due to its charge, CSA-13 may have had the potential to interact with the various components in the broth, which may have influenced the variability in concentrations. 2) Also due to its positive charge, CSA-13 likely interacted with the negatively charged components of bone. This interaction may have also influenced the variability in concentration. 3) Although a repeatable jet mill process was used to micronize the CSA-13 powder prior to use, CSA-13 had the tendency to create micron sized aggregates as the PDMS-based dispersion was being made. These aggregates resulted in varying pore sizes within the PDMS polymer (these pores sizes will be shown in Chapter 6). Thus, the rate of elution may have been influenced by the variation of pore sizes that were present. Future work would need to be undertaken to more thoroughly regulate the particle size of CSA-13, but for this project the important factor was that the antimicrobial efficacy of a 18% w/w concentration of CSA-13 was able to consistently eradicate MRSA biofilms.

In conclusion, when used as an active release agent in this *in vitro* study, CSA-13 supported the hypothesis that it would reduce biofilms of MRSA to a potentially clinically acceptable level. By reducing the amount of bacteria in MRSA biofilms from greater than 10^9 to less than 10^1 in 24 hours, this novel antimicrobial compound provides significant promise to translate to clinical use. These promising results became even more apparent after the animal work was performed, as will be shown in Chapter 8.

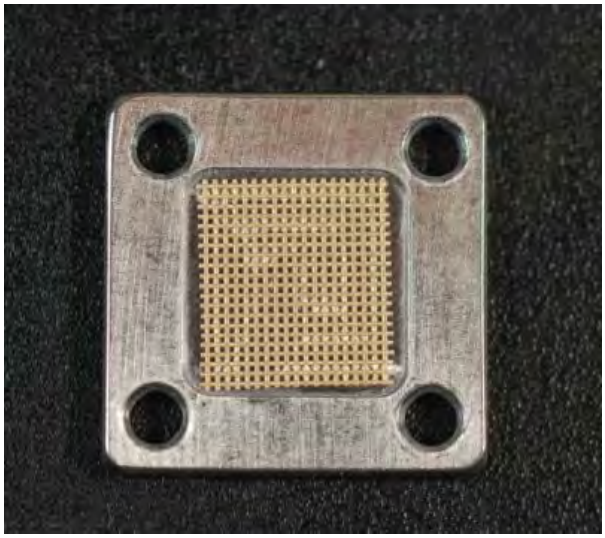

Figure 5.1: Image of a stainless steel plate that has a 1 cm x 1 cm PEEK membrane inserted into the well that was machined out of the underside of the plate.

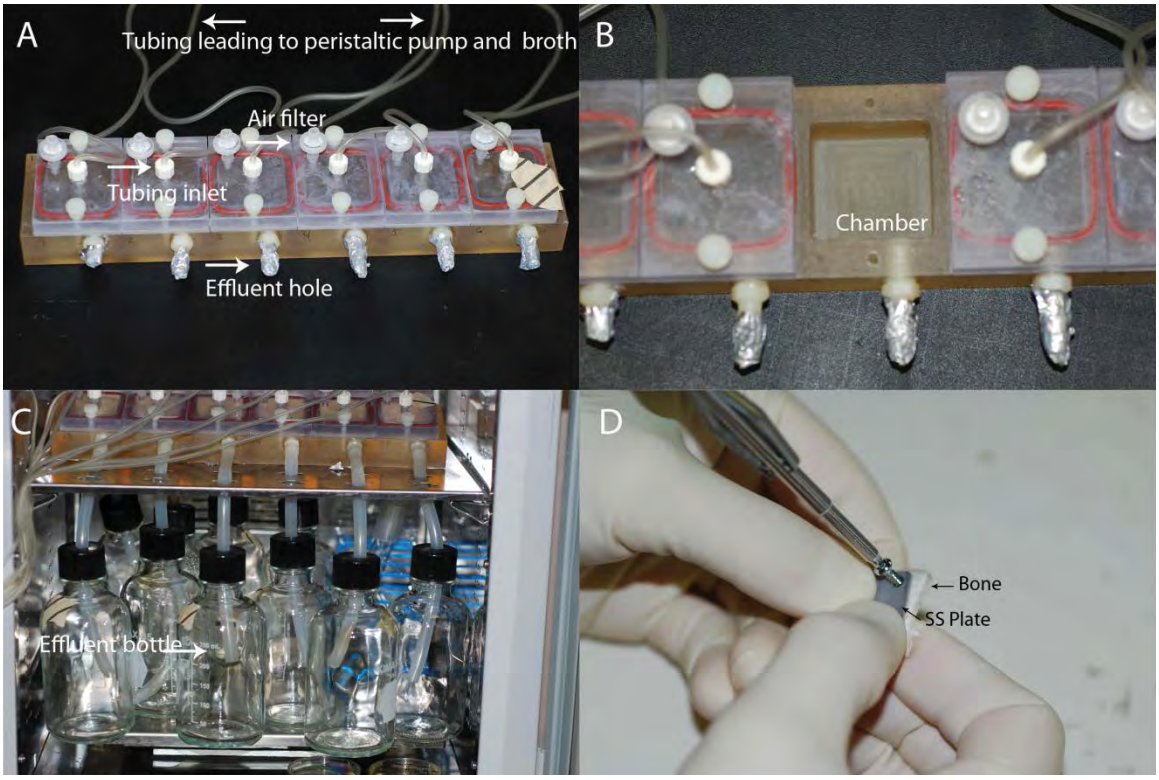

Figure 5.2: Images of the flow cell unit that was designed for *in vitro* testing. (A) Image of the flow cell unit. Arrows and descriptions indicate the different components of the flow cell. (B) Image of a single chamber of the flow cell. (C) Image of the effluent tubes and bottles in which broth was collected after it flowed through a flow cell chamber. (D) Image of how a SS plate, PEEK membrane and bone piece were constructed in order to place them in a chamber of the flow cell unit.

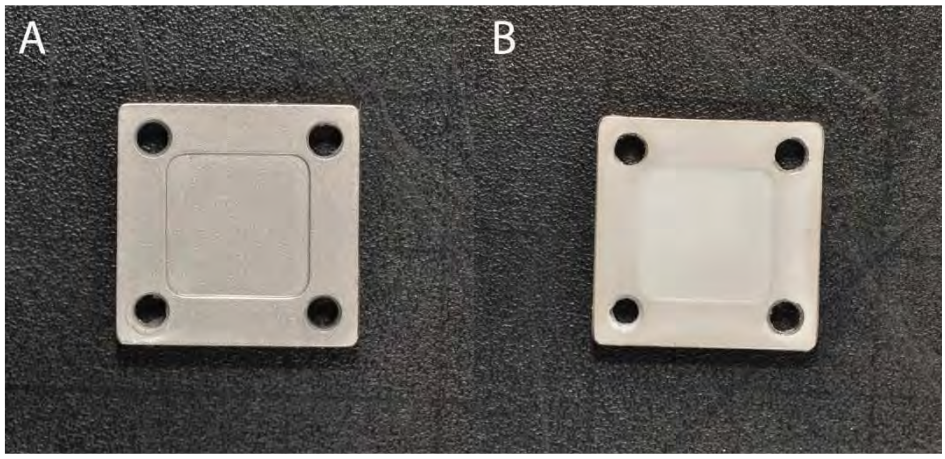

Figure 5.3: Photographs of SS plates that were coated with PDMS only or PDMS with CSA-13. (A) SS plate coated with PDMS only after being dipped in the 1:1 PDMS:naphtha dispersion, cured for 7 days and sterilized by ETO. (B) SS plate coated with the 1:1 PDMS:naphtha + 18% w/w CSA-13 dispersion, cured for 7 days and sterilized by ETO. The slight jaggedness that can be seen in the inner edges of the holes is due to the prongs that were used to hold the plates in place on the spinning wheel as they cure. These plates had a white tint to them due to the presence of CSA-13, which is a white powder.

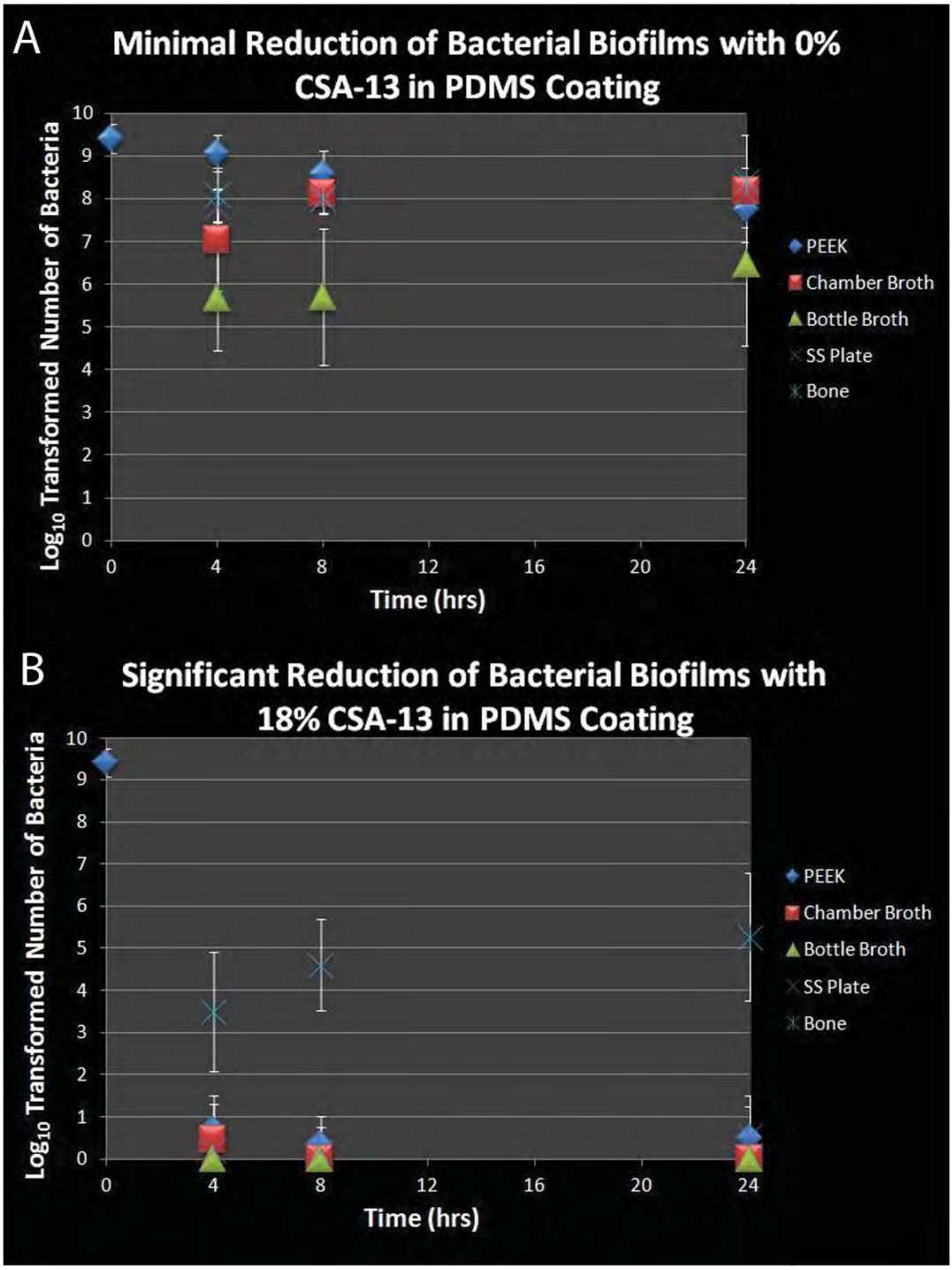

Figure 5.4: Graphs showing the results of exposing CSA-13 to biofilms of MRSA using the flow cell system. (A) Results from the quantification of bacteria that were exposed to SS plates coated with silicone only. These data are presented in $\log_{10}$ transformed numbers of CFU/PEEK membrane, CFU/mL of broth, CFU/SS plate and CFU/gram of bone tissue. (B) Results from the quantification of bacteria that were exposed to SS plates coated with PDMS/CSA-13.

Table 5.1: LC/MS data and overall % release calculated from each of the broth samples at 4, 8 and 24 hours of sample collection.

B**roth Sample**	**µg/mL**	**Overall % Release**
4 Hour Chamber	66.56 ± 32.4	8.8 ± 4.1
4 Hour Bottle	16.66 ± 12.48	
8 Hour Chamber	57.37 ± 36.89	8.5 ± 3.7
8 Hour Bottle	19.35 ± 12.62	
24 Hour Chamber	23.68 ± 18.86	8.1 ± 3.9
24 Hour Bottle	9.38 ± 5.25	

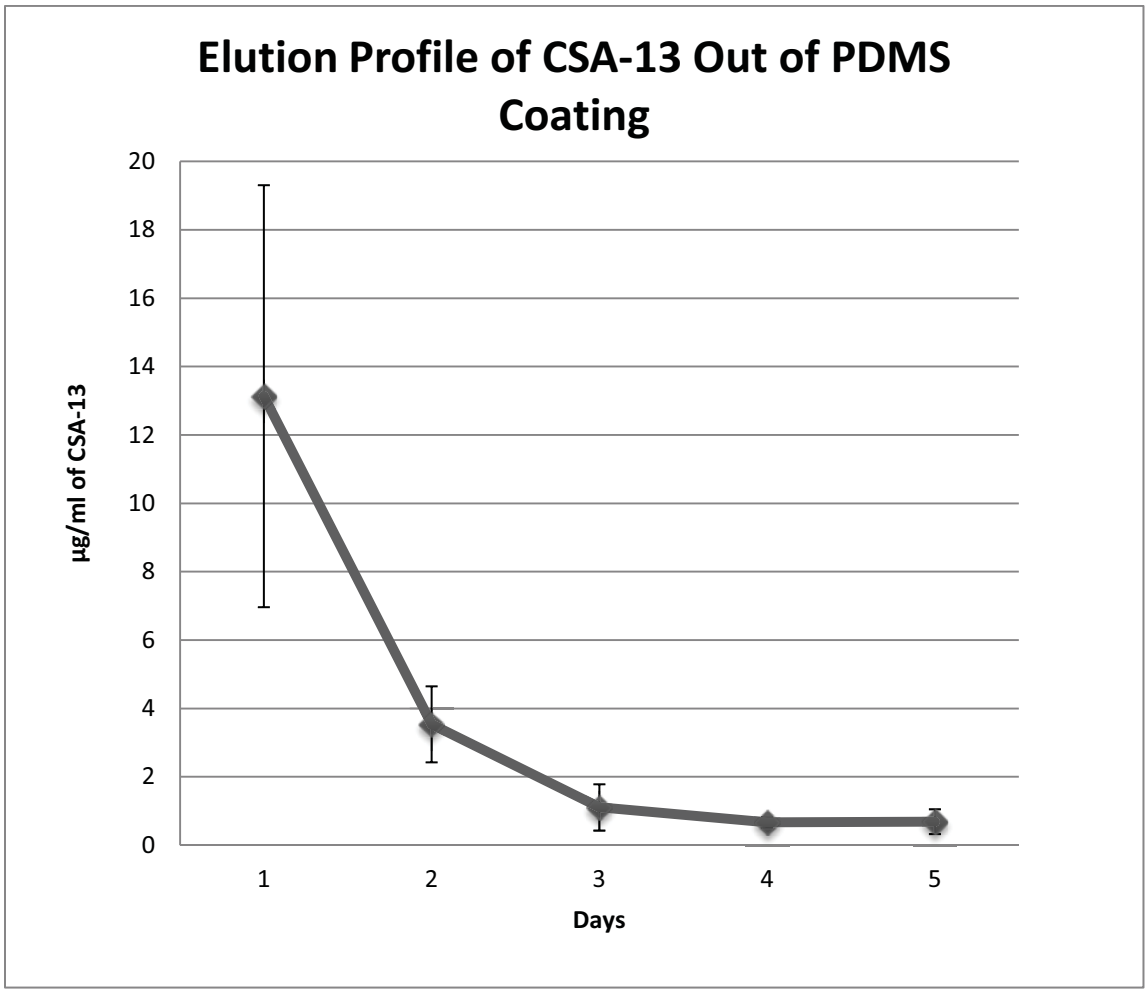

Figure 5.5**:** Release profile of CSA-13 out of the PDMS coating over a five-day period. By Day 2, the amount of CSA-13 released was less than half of what it was on Day 1. By Day 5, there were approximately 0.69 µg/mL of CSA-13.

Table 5.2: Data outlining the number of $\log_{10}$ transformed bacteria/mL that were present in the broth samples collected during the first 15 days of the long term elution study. These data suggested that for the first 10 days of release, the amount of CSA-13 in the broth samples was sufficient to reduce a 10^5 inoculum to less than 10^2 in a 24 hour period. By day 12, the number of bacteria increased to greater than ~10^6 cells/mL, suggesting that the levels of CSA-13 were below bactericidal concentrations. Each day of release represented an n=6 broth samples from the n=6 plates that were used for the long term elution study.

Day	**Average Log_{10} CFU/mL ± SD**
1	0 ± 0
2	0 ± 0
3	0 ± 0
4	0 ± 0
5	0.82 ± 1.21
6	0.92 ± 1.31
7	1.75 ± 1.88
8	0.22 ± 0.61
9	0.92 ± 1.31
10	1.79 ± 1.89
11	2.70 ± 3.09
12	6.52 ± 6.91
13	7.14 ± 6.97
14	6.18 ± 6.51
15	6.52 ± 6.91

CHAPTER 6

CHARACTERIZATION OF THE CSA-13 ACTIVE RELEASE COATING

6.1 Introduction

In this portion of the study, which directly addressed Specific Aim 2c as outlined in Chapter 2, section 2.4, the active release coating with CSA-13 was characterized using durometer measurements, scanning electron microscopy (SEM), attenuated total reflectance Fourier transformed infrared spectroscopy (ATR-FTIR), contact angle, tensile testing, thermal gravimetric analysis (TGA) and optical profilometry. The coating with PDMS only was also characterized using these techniques with the exception of optical profilometry. These techniques of characterization were performed in order to gain an understanding of the physical and chemical properties of the CSA-13/PDMS conjugate coating.

Characterizing the coating helped to understand its morphology, stability, how CSA-13 affected polymerization of the PDMS polymer, and how CSA-13 was released. It also helped to file the patent for this product.

6.2 Materials and Methods

6.2.1 Stainless Steel Plates/Coating Method

The same size and type of SS plates were used in this study as those used in Chapter 5. Furthermore, the same dip coating procedure was used to dip coat SS plates with dispersions that contained CSA-13 or PDMS only.

6.2.2 PDMS/Concentration of CSA-13

The same MED-6607 PDMS dispersion was used as that discussed in Chapter 5 and the same 18% w/w CSA-13 concentration was added to the dispersion. An important item of note is that more than 10 lots of dip coated plates (n=20 plates dipped per lot) were made to confirm that the dipping method showed repeatable outcomes.

6.2.3 Hardness (Durometer) Testing

To determine the hardness of the cured PDMS and PDMS with CSA-13, thin films were made from each formulation by pouring the dispersion into multiple 2 cm x 2 cm chase containers that had a depth of 2 mm. The dispersions were allowed to cure for a seven-day period (as per the manufacturer's recommendation), and then removed from the containers. Following ASTM standard D2240, multiple films were stacked one on top of the other to a height greater than 6 mm. An Asker XP-A Type A durometer was then used to determine the hardness of both material types.

6.2.4 Scanning Electron Microscopy

SEM analysis was used for three purposes. First, the surface of n=5 plates with PDMS only and n=5 plates with PDMS and CSA-13 from three different lots of the dip

coating procedure were imaged under secondary electron (SE) mode in an FEI NOVANano high resolution SEM. A total of 25 images per coating type were collected from five different areas of each plate to determine the surface morphology of the coating.

Second, backscatter electron (BSE) images (n=5 plates; 5 images per plate) were collected using a JEOL-6100 SEM. These images were subsequently used to measure the porosity and pore size distribution of each coating type. To measure the size of pores throughout the bulk of the polymer, a razor blade was used to cut through the polymer to the surface of the metal.

Third, using the JEOL-6100 SEM, energy dispersive X-ray (EDX) analysis was performed, again in five areas of n=5 plates coated with PDMS with and without CSA-13, for elemental mapping to determine particle distribution, particle sizes and particle aggregate sizes of CSA-13 throughout the coating. Again, a razor blade was used to cut the polymer and analyze the bulk of the material.

Importantly, an additional n=5 plates per coating type were placed in a solution of 10% BHI broth that flowed at a rate of 4.5 mL per hour to model the flow of fluid in the anatomical location of the animal model in which these plates were tested. This flow was continued for a 30-day period. This procedure was done to allow the CSA-13 to be eluted out of the coating completely. Although there was no CSA-13 in those plates coated with PDMS only, this experiment was also performed as a control. After the 30-day elution period, the coating on each plate was cut at a 45° angle with a razor blade to allow the polymer to be analyzed from the top of its surface down to the metal plate. In doing so, SE images were collected to determine the morphology of the coating following

elution and EDX analysis was performed to confirm that there was no residual CSA-13 in the top or bottom portions of the coating.

6.2.5 Attenuated Total Reflectance Fourier Transformed Infrared Spectroscopy

ATR-FTIR spectra were collected using a Thermo Scientific Nicolet 6700 FTIR spectrometer. Spectra were acquired using a single reflection ATR SmartOrbit accessory equipped with a single-bounce diamond crystal. The data were then analyzed using Omnic^{TM} software (Thermo Scientific). FTIR spectra were obtained first by collecting a baseline reading without any sample on the diamond crystal and followed by analyzing five areas per plate on a total of n=5 plates per coating type. Soxhlet extraction was performed with isopropanol for a 48-hour period after plates were analyzed initially. In doing so, the CSA-13 was eluted from the coating. Plates were then once again analyzed by ATR-FTIR to determine if the spectrum would return to the original PDMS only profile.

6.2.6 Contact Angle

Contact angle measurements were collected using a KSV Thetalite goniometer. A similar protocol as Hulterstrom *et al.*[245] was used wherein five different areas of a single plate were analyzed by placing a drop of millipore water on the surface. Each drop was allowed to sit for 10 seconds prior to reading a measurement. In total, there were n=5 plates analyzed for each of the two coating types for a total of 25 contact angle measurements of PDMS only and PDMS with CSA-13.

6.2.7 Tensile Testing

Tensile testing was performed following the ASTM standard D882-10 protocol at Nelson Laboratories of Salt Lake City, UT. Using this standard procedure, the tensile strength, percent elongation and modulus of thin plastic materials that have less than a 1 mm thickness could be determined. For this work, thin films of PDMS only or PDMS with CSA-13 were made by first mixing the dispersions as outlined in Chapter 5. Approximately 1.5 mL of each dispersion was poured into a Teflon chase container that had a width of 1/2" (1.27 cm) and a length of 5" (12.7 cm) as per the ASTM standard. After a 7 day curing period, films were conditioned as per the ASTM standard, i.e., at 23 ± 2° C at 50 ± 10% relative humidity for greater than 40 hours. After measuring the thickness, each film was uniaxially strained at a crosshead speed of 20 feet per minute until break using an Instron tensometer (model 5565, Instron Corp.). Ultimate force and elongation at break were noted. The tensile strength was calculated by dividing the ultimate force by the cross-sectional area of the thin film. Elastic modulus was calculated by dividing the stress by the strain using data points in the linear elastic region. Although the ASTM standard suggested that at least n=10 films to be used for testing, in this study an n=15 films were used per group.

6.2.8 Thermal Gravimetric Analysis

TGA was performed at Intertek Plastics Technology Laboratories following ASTM standard E1131-08. In short, three samples (7-10 mg) of each cured material type were subjected to TGA analysis using a Perkin Elmer Pyris 1 TGA (Perkin Elmer Inc.). The samples were initially purged for 5 minutes with nitrogen, then heated in air from

25° C to 850° C at a heating rate of 10° C/min. The flow of air through the furnace chamber was controlled at 35 mL/min.

6.2.9 Optical Profilometry

In order to determine the surface roughness and topography of the PDMS coating with CSA-13, an optical profilometer (Zygo NewView™ 5032) was used. The coating with PDMS only was unable to be analyzed by optical profilometry because of its translucent properties. Quantification of the 3D surface roughness parameters of the PDMS/CSA-13 coating was performed by Metropro™ metrology software (Zygo). Similar to the contact angle measurements, an n=5 plates were used from three different lots of coated plates, and five areas per plate were imaged at a 20x magnification to obtain a total of 25 measurements.

6.3 Results

6.3.1 Dip Coating

Plates that were coated with PDMS only (Figure 5.3) had a final coating weight of 75.2 ± 11.8 mg and a thickness of 83 ± 12 μm. In contrast, plates that were coated with PDMS/CSA-13 (Figure 5.3B) had a coating thickness of 112 ± 17 μm and a final coating weight of 96.4 ± 11.8 mg. The amount of CSA-13 per plate was calculated to be 17.2 ± 0.61mg. These results of dip coating were similar to those provided in Chapter 5, section 5.3.1.

6.3.2 Surface Analysis by SEM

SE micrographs of both coating types prior to eluting the CSA-13 out of the coating are given in Figure 6.1. These images indicated that those plates coated with the PDMS only formulation had micron sized concave "dimple-like" features on the outermost layer. The diameter of these dimples ranged from 1-2 μm. Notably, it was confirmed that the small dimple-like structures found on the surface of the PDMS only coated plates were not present throughout the bulk of the coating. This was done by cutting the coating with a razor blade and imaging the bulk of the polymer. The bulk area had no detectable porosity, but rather had a uniform structure. Overall, the PDMS only coating (Figure 6.1A) had a markedly smoother surface morphology compared to those that had CSA-13 in the coating. More specifically, it is believed that the presence of CSA-13 created a more porous surface with small particles of CSA-13 entrapped in pores on the outer most surface of the coating (Figure 6.1B). These small particles were further confirmed to be CSA-13 by EDX analysis (Figure 6.2).

The difference in the surface morphology of both coating types became even more apparent after the CSA-13 had been eluted out of the coating. The porosity of the PDMS/CSA-13 coating type profoundly increased (Figure 6.1C) after soaking in broth, whereas the PDMS only coating composition had no change in its surface morphology after being soaked in broth. These results indicated that the presence of CSA-13 in the dispersion caused various shapes and sizes of pores to form throughout the PDMS polymer coating as it cured. It is believed that immiscible CSA-13 particles in the PDMS dispersion were physically entrapped within the polymer matrix as it cured, and as a consequence, pores were formed. These pores then allowed water to penetrate the

coating and release CSA-13. Importantly, when multiple coatings were cut with a razor blade to analyze the cross-sectional morphology of the coatings, the SEM micrographs confirmed that the pores were present from the outer most level down to the metal surface.

BSE images that were used to calculate the porosity of the material indicated that the PDMS only coating had no detectable porosity (Figure 6.2, top row), whereas the coating with CSA-13 had 17% ± 3% porosity (Figure 6.2, middle row). The pore sizes ranged from ~0.5 μm to ~20 μm with an average pore size of 5 ± 8 μm.

Because the PDMS only coating had very similar chemical constitution to CSA-13, the only defining element that was different and detectable by EDX in the CSA-13 coating compared to the PDMS coating was chlorine (Cl). Tetra hydrogen chloride is the conjugate anion of the CSA-13 compound. Using EDX mapping with silicone and chlorine channels, the location and distribution of CSA-13 throughout the coating were determined. The EDX map for chlorine (Figure 6.2) showed that CSA-13 particles and/or particle aggregates were predominantly present within the pores of the PDMS film thereby supporting that CSA-13 particles were what caused the formation of pores in the PDMS film. These data also pointed out that the distribution of CSA-13 was uniform throughout the coating.

The fact that there was no detectable Cl in the top portions of the PDMS polymer or throughout the bulk of the polymer after soaking for 30 days in BHI (modified) broth indicated that all detectable amounts of CSA-13 had eluted out of the PDMS polymer matrix by this period (Figure 6.2, bottom row). Importantly, EDX analysis was performed on one plate that had been soaked in broth for just 24 hours to determine

whether Cl was still present. The data from this test indicated that Cl was present, albeit at reduced levels, suggesting that CSA-13 had begun to elute out of the coating. Moreover, the microbiological data that were shown in Chapter 5 correlated with this finding. More specifically, there were sufficient amounts of CSA-13 eluted from the coating to kill bacteria for 10-15 days. After 10-15 days, bacteria began to grow at increased levels in the broth suggesting that the amount of CSA-13 that was released decreased gradually until it was below bactericidal concentrations.

6.3.3 Attenuated Total Reflectance Fourier Transformed Infrared Spectroscopy

The rationale for performing ATR-FTIR was two-fold: first, to gain an understanding of IR active chemical bonds (functional groups) within the PDMS only and PDMS with CSA-13 coatings and second, to determine if any covalent linkage formed between CSA-13 and the PDMS polymer. The ATR-FTIR spectra of PDMS with and without CSA-13 are shown in Figure 6.3. The data showed that there were specific differences between the two coating types. The spectrum of PDMS/CSA-13 samples showed characteristic infrared scissoring absorptions of NH_2^+ and NH_3^+ at ~1450-1600 cm^{-1} [246] as well as asymmetrical and symmetrical stretching of $-CH_2$ at ~2940 cm^{-1} and ~2850 cm^{-1}, respectively.[246] These particular characteristic absorptions were not seen in samples that had PDMS only. Importantly, the fingerprint region (between ~500 cm^{-1} and ~1200 cm^{-1}) of both coating types was very consistent with what is found in the literature involving FTIR spectra of PDMS polymers.[246-250]

If any potential chemical reaction between PDMS and CSA-13 molecules had occurred, based on the known relativities of the functional groups of CSA-13 and PDMS,

one may have seen the formation of Si-N and/or N-O bonds in the resultant products. N-O bonds would have had characteristic infrared absorption bands centered at ~1300 cm^{-1}. If Si-N bonds were present, they may have shown in the 700-900 cm^{-1} range of the fingerprint region. As such, the Si-N bonds may have potentially been masked in the fingerprint region where Si-C absorption bands were predominant. For this reason Soxhlet extraction was performed in isopropanol for a 48-hour period to elute CSA-13 out of the coating. After extraction of CSA-13, ATR-FTIR was performed once again and the spectrum was found to be identical to the PDMS only IR spectrum, thus indicating that CSA-13 had not covalently bound to the PDMS material. The EDX analysis data further confirmed these results indicating that after CSA-13 was extracted from the PDMS material, it was no longer detectable. Taken together, these data suggested that CSA-13 particles and/or particle aggregates were physically suspended/present within the PDMS matrix as opposed to being chemically cross-linked.

6.3.4 Contact Angle

Contact angle data indicated that the coating with PDMS only had a hydrophobic surface compared to the coating that had CSA-13. Specifically, the PDMS only coating had a contact angle of 113.74° ± 4.14°. These data were consistent with what has been reported in the literature previously with respect to PDMS polymers.[245] The coating with PDMS/CSA-13 resulted in a reduced contact angle of 84.18° ± 6.33°. When compared using an independent samples *t* test, these differences were significant ($p<0.05$). This difference may be attributed to the presence of the positively charged CSA-13 that decreased the surface tension or it may have also been partially attributed to the increased

roughness of the surface.[251,252] Taken together, these data indicated that the coating with CSA-13 was more wettable, which may be a unique property that aids in the dissolution of the CSA-13 from the coating.

6.3.5 Tensile Testing

Table 6.1 provides the results from tensile testing. Results indicated that the coating with CSA-13 had a statistically significant reduction in tensile strength ($p<0.05$) as well as percent elongation ($p<0.05$; statistical analysis performed using an independent samples *t* test). Furthermore, there was an increase in the initial elastic modulus of the PDMS material with CSA-13, which was also significantly different ($p<0.05$). This increase suggested that the PDMS with CSA-13 was stiffer compared to the PDMS only films. This may be attributed to the filler effect of CSA-13 within the PDMS matrix of the polymer.

6.3.6 Thermal Gravimetric Analysis

The rationale for performing TGA was to determine the thermal stability of the PDMS only and PDMS with CSA-13 as well as determine if there were any volatile components that were released from each coating type. Each experiment was run from room temperature to 850° C, with close attention being given to the temperature range of 35° C - 41° C. This temperature range was chosen because it was within the body temperatures of interest for sheep (*in vivo* model) and humans (potential coating for clinical applications). Results from TGA testing indicated that both of the material types were heat stable up to greater than 100° C (Figure 6.4).

In both polymers, with and without CSA-13, the first significant onset of weight loss was seen at approximately 150° C. Nevertheless, in both cases, this weight loss was well above the temperature range of interest, suggesting that the material was thermally stable in the intended use range of 35° - 41° C.

6.3.7 Optical Profilometry

Roughness data measured using optical profilometry indicated that the average surface roughness of the PDMS with CSA-13 was 1.30 ± 0.87 μm. In Figure 6.5, a representative surface topography is shown that outlines the undulating, porous surface of the PDMS with CSA-13.

6.4 Discussion

There are many studies in the literature that have demonstrated the antimicrobial efficacy of active release coatings both *in vitro* and *in* vivo. However, aside from the limitations of protocols that have been employed to test these coatings, another limiting factor of these coatings has been that investigators often have not characterized the coating in order to understand their physical and chemical properties.

The goal of this work was to characterize the physical and chemical properties, as well as determine the reproducibility of the novel active release CSA-13 coating. Results showed that the incorporation of CSA-13 into the PDMS polymer did influence the physical and mechanical properties of the PDMS, but it did not appear that that influence was adverse to the desired material properties. No chemical reactivity was observed between CSA-13 and the particular PDMS material that was used. It was found that the

coating thickness and amount of CSA-13 in the device coating was consistent over multiple lots of dip coated plates. SEM data also showed that the coating morphology was consistent from lot-to-lot and that CSA-13 was distributed uniformly throughout the PDMS polymer.

The SEM data demonstrated that CSA-13 particles resided in the pores of the PDMS polymer and that the CSA-13 eluted out of the surface and bulk of the polymer after being soaked in broth for a 30-day period. Furthermore, SEM data indicated that the PDMS with CSA-13 was highly porous. The porosity of the material was reflected in the reduction in tensile strength of the material. More specifically, the pores likely served as points of stress that led to reduced elongation at break compared to the PDMS only films. In addition, the presence of the particles and particle aggregates seemed to influence the stiffness of the material, perhaps by acting as boundaries that interacted with polymer movement as the material was pulled under tension.[253,254] These particles and particle aggregates also appeared to influence the hardness of the material, as indicated by the durometer measurements.

Another point of interest was made with regard to the contact angle data that were collected. It has been previously suggested that bacterial cells tend to form biofilms more readily in patients that have an implanted device with a hydrophobic surface.[255] Counter intuitively, however, Sousa *et al*.[256] have shown that staphylococci cells grown on the surface of hydrophobic polymeric materials have a predominantly hydrophilic surface when measured with contact angle. Thus, although it is believed that bacteria adhere to surfaces primarily by the hydrophobic effect, in their conclusion, Sousa *et al*. suggest that other factors likely influence bacterial adhesion to hydrophobic surfaces.

Data from ATR-FTIR analysis strongly suggested that there were no other byproducts in the CSA-13 containing coating other than the CSA-13 additive when compared to the PDMS only coating. In the ATR-FTIR data, the absorption peaks that were present in the spectra corresponded to the bonds that were present in both coating types with important differences distinguishing the presence of CSA-13 from the PDMS only coating.

The results of this work indicated that the active release agent, CSA-13, was able to be incorporated homogeneously into a PDMS dispersion. After plates were dipped into the dispersion, CSA-13 particles caused the PDMS to become porous upon curing. The particle and/or particle aggregate sizes in the final cured product corresponded to the size of the pores that they formed in the PDMS polymer. Because the PDMS polymer was made porous, water was able to penetrate the pores and facilitate the dissolution and diffusion of CSA-13 from the surface and bulk of the coating. Importantly, although the presence of CSA-13 did appear to affect the physical properties of the polymer, the effect was not determined significant for this particular application. The desired mechanical properties of the material were maintained. Finally, the thermal stability of both materials as demonstrated by TGA analysis suggested that the materials would remain stable in the range of body temperatures of sheep and humans.

In conclusion, several key characteristics of this novel active release coating were identified in this study and in the *in vitro* study from Chapter 5. These include 1) the manner by which this coating functioned is based on the fact that particles of CSA-13 are uniformly distributed into a medical grade PDMS, and as the PDMS cures, these particles create pores in the polymer network. 2) As water penetrated the porous network, it

caused the dissolution and diffusion of CSA-13 out of the matrix. 3) As outlined in Chapter 5, this coating has displayed promising bactericidal activity *in vitro* and in Chapter 8 the *in vivo* efficacy of this coating will be shown. 4) Results showed that differences were seen between the PDMS only polymer and PDMS with CSA-13, but none of these differences suggested that they would have deleterious effects on the function or stability of the PDMS with CSA-13 *in vivo* for this particular application. If this coating were to be used in applications wherein shear forces might be present, further data would be needed to show its stability under those forces. Taken together, the thermal and mechanical stability, and antimicrobial activity of this novel active release coating provide significant promise for it to prevent biofilm implant-related infections from developing in orthopaedic and other biomaterial applications.

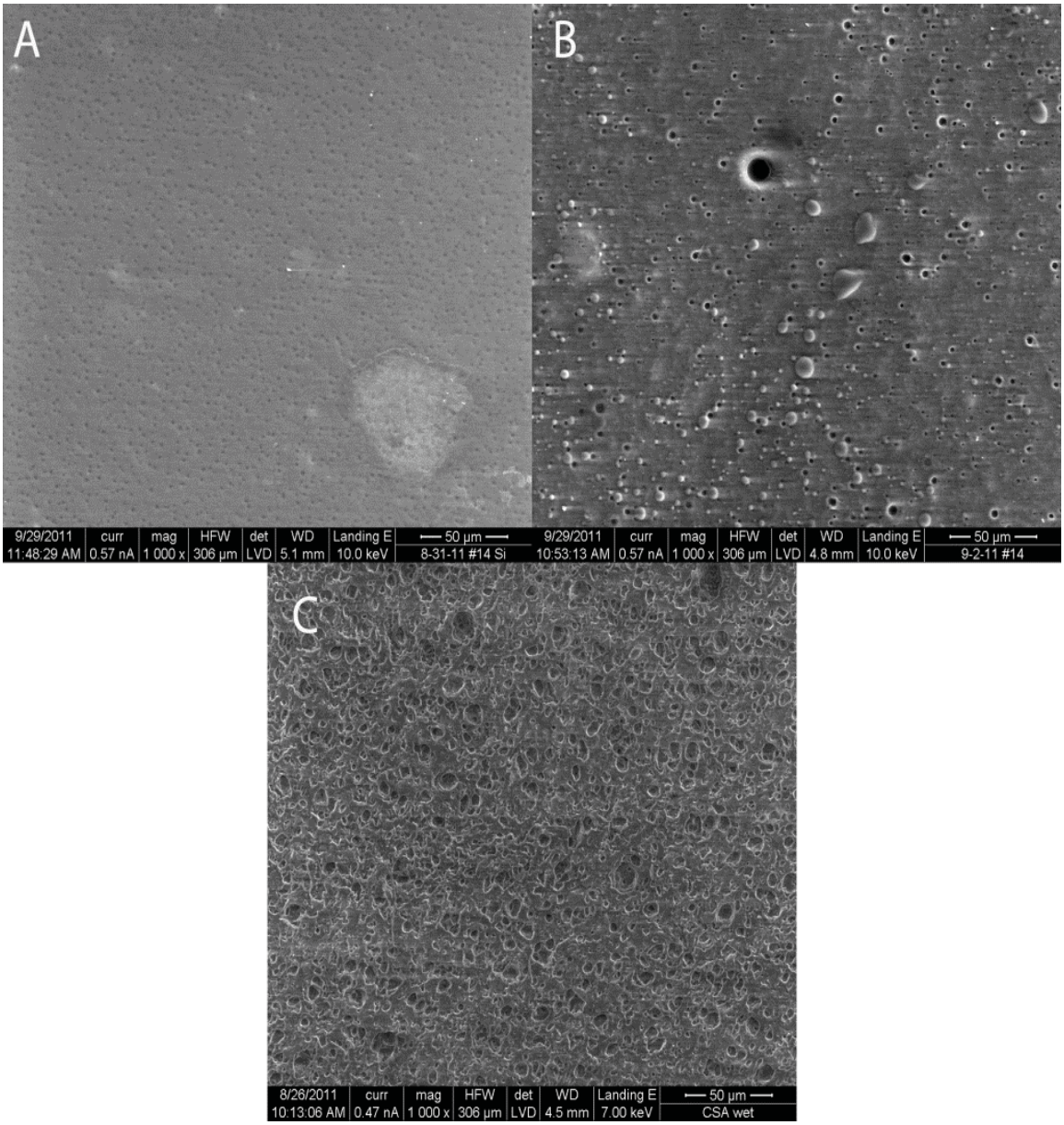

Figure 6.1: SEM images of PDMS only and PDMS with CSA-13. (A) Image of the PDMS only coating showing the surface morphology of the polymer without CSA-13. (B) Image of the coating that had CSA-13 in it. (C) Image of a coating after it was soaked in BHI broth (modified) for 12 weeks to allow CSA-13 to elute out of it. Note the extensive amount of pores that were visible after the CSA-13 had eluted out.

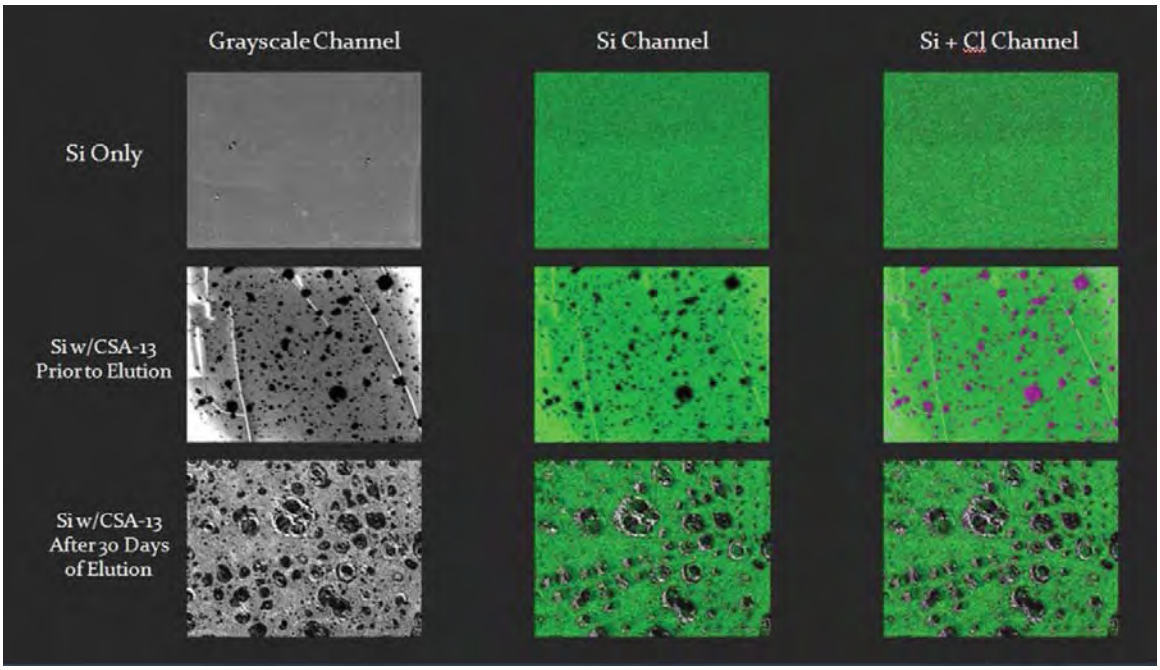

Figure 6.2: BSE and EDX images of the PDMS only and PDMS with CSA-13 coatings. (Top Row) BSE images (Grayscale Channel) and elemental maps from EDX analysis (Si Channel and Si + Cl Channel) of a PDMS only coating. Note the lack of porosity in the grayscale image as well as the lack of Cl in the Si + Cl channel. (Middle Row) Backscatter electron images of a Si coating with CSA-13. In the grayscale channel, pores can be seen. These pores were formed by the presence of CSA-13 particles as indicated by the presence of Cl precisely in the pores. (Bottom Row) Images of a coating that had CSA-13 in it prior to the 30 day elution in BHI broth. More than 30 areas on n=5 plates were analyzed by EDX including areas of coatings that were cut to the metal with razor blades to detect CSA-13 in the bottom regions of the polymer. No Cl was detected in any of the eluted samples.

Figure 6.3: FTIR spectra in the following graph showed the absorption peaks of radiant energy by organic molecules in the coating containing CSA-13 (top line) and PDMS polymer alone (bottom line). In the top left hand corner, images of CSA-13 and the PDMS are provided for the reader to see what bonds were present and how they correspond to the spectra. A detailed description of the bending/scissoring that occurred, as well as the major differences that were seen in absorption patterns in the spectra are provided.

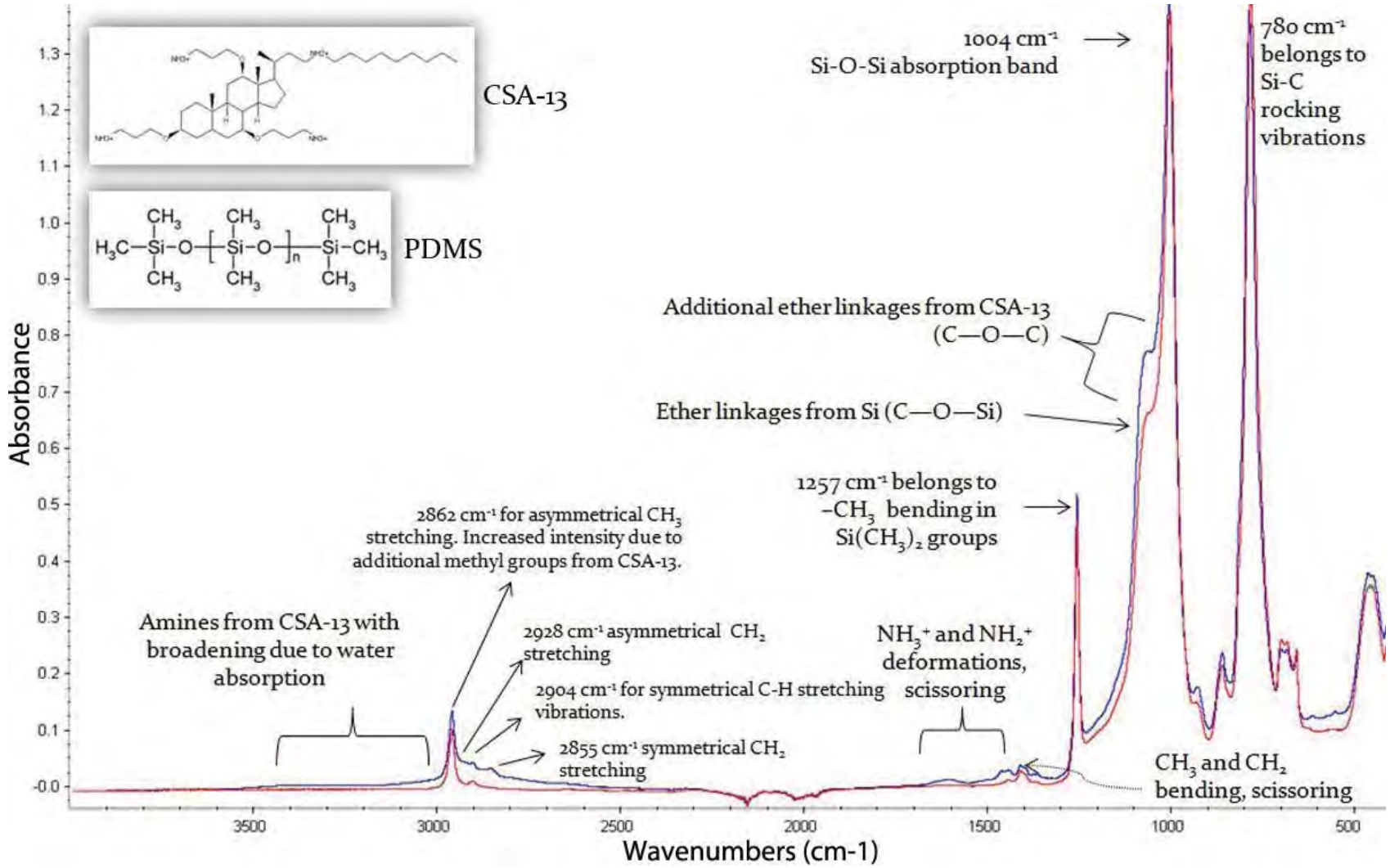
CSA-13
PDMS
1004 cm⁻¹
Si-O-Si absorption band
780 cm⁻¹
belongs to
Si-C
rocking
vibrations
Additional ether linkages from CSA-13
(C—O—C)
Ether linkages from Si (C—O—Si)
1257 cm⁻¹ belongs to
–CH3 bending in
Si(CH3)2 groups
2862 cm⁻¹ for asymmetrical CH3
stretching. Increased intensity due to
additional methyl groups from CSA-13.
Amines from CSA-13 with
broadening due to water
absorption
2928 cm⁻¹ asymmetrical CH2
stretching
2904 cm⁻¹ for symmetrical C-H stretching
vibrations.
2855 cm⁻¹ symmetrical CH2
stretching
NH3+ and NH2+
deformations,
scissoring
CH3 and CH2
bending, scissoring
Absorbance
Wavenumbers (cm-1)

Table 6.1: This table shows the data that were collected from tensile testing of the PDMS and PDMS + CSA-13 materials.

Material Type	Tensile Strength (MPa)	Tensile Strength at Break (MPa)	Elongation (%)	Elastic Modulus (MPa)
PDMS Only	2.26 ± 0.58	2.06 ± 0.62	327.72 ± 75.68	1.24 ± 0.69
PDMS with CSA-13	0.90 ± 0.33	0.79 ± 0.27	215.78 ± 39.01	3.20 ± 1.39

Figure 6.4: The following graphs were obtained after TGA was performed on the PDMS only and PDMS with CSA-13 materials. (A) Graph indicating the TGA curve of the material that had PDMS and CSA-13. Note that the material had no significant weight loss until approximately 300° C suggesting that the material was stable in the 35°- 41° C range. (B) Graph indicting the TGA curve of the PDMS only material. This material showed no signs of thermal degradation until approximately 380° C, also suggesting that it was stable in the 35°- 41° C range.

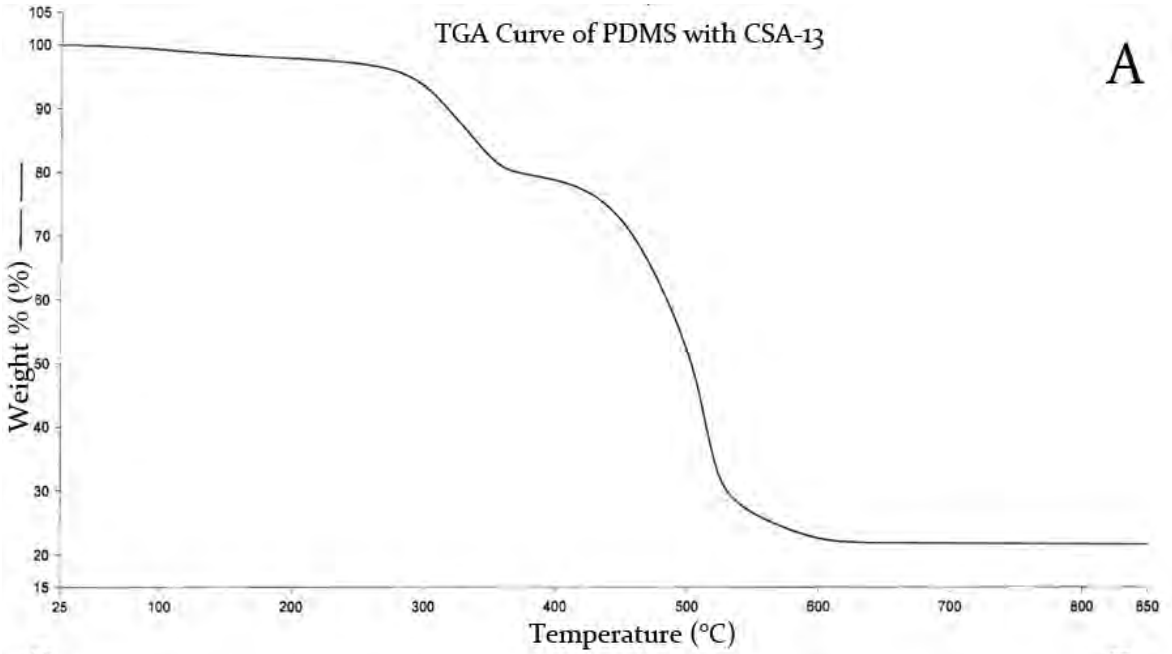
TGA Curve of PDMS with CSA-13
A
Weight % (%)
Temperature (°C)
105
100
90
80
70
60
50
40
30
20
15
25
100
200
300
400
500
600
700
800
850

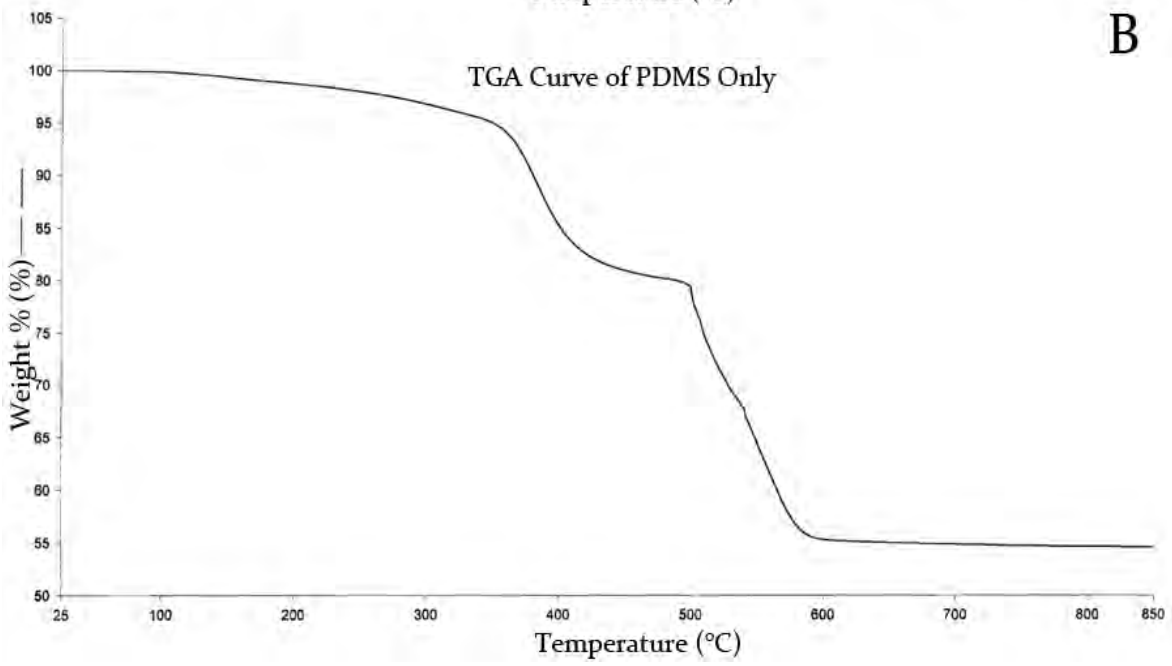
TGA Curve of PDMS Only
B
Weight % (%)
Temperature (°C)
105
100
95
90
85
80
75
70
65
60
55
50
25
100
200
300
400
500
600
700
800
850

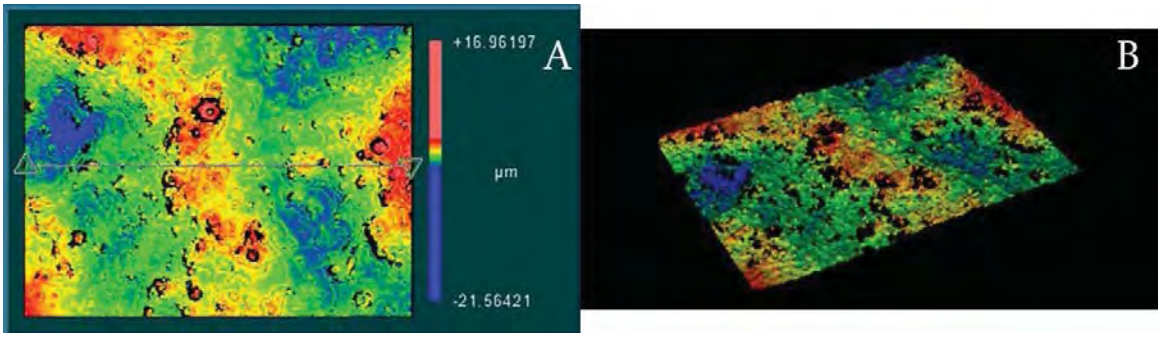

Figure 6.5: Images collected during the optical profilometry analysis of the PDMS with CSA-13 coating. (A) Two-dimensional image of the surface of a PDMS coating that had CSA-13 added to it. The blue regions indicated lower areas whereas the pink areas indicated high points of the surface. These surface characteristics were present in all samples analyzed. The black areas that are present are those areas that had vertical surfaces in the polymer, which cannot be analyzed by optical profilometry because interference patterns do not develop. (B) Three-dimensional rendition of the same area of a surface as in (A). The black areas were more prominent, yet the model outlined the undulating, porous nature of the coating.

CHAPTER 7

ESTABLISHING AN *IN VIVO* ANIMAL MODEL OF BIOFILM IMPLANT-RELATED OSTEOMYELITIS TO TEST COMBINATION BIOMATERIALS USING BIOFILMS AS INITIAL INOCULA

7.1 Introduction

The animal work presented in this chapter has been accepted for publication and a copy of the submitted manuscript is provided as Appendix E at the end of this dissertation. According to a careful literature review, this work represents the first animal model in the literature that used well-established biofilms as initial inocula to produce a positive signal of infection. The rationale for developing this model was provided in Chapter 3 and relates to Specific Aim 3 from Chapter 2, section 2.4. In addition, the development of this model made it possible to test the CSA-13 active release coating in the definitive animal model study that will be presented in Chapter 8.

Based on the observations and information discussed in Chapter 3, it was hypothesized that a sizeable portion of biofilm-related infections, including those that accompany the use of medical devices, may be the result of contamination with bacteria residing in biofilms from natural ecosystems as opposed to planktonic bacteria contaminating a site. If supported, this hypothesis would suggest that using biofilms as

initial inocula, as opposed to planktonic bacteria, to model clinically relevant infection scenarios may provide deeper insight into how biofilm-related infections may be treated and eradicated using current or novel therapies, such as antimicrobial eluting coatings.

In an attempt to address the sporadic nature of biofilm infection development in animal models, wherein planktonic cells are used as initial inocula, the goal of this work was to test the above hypothesis and establish a reproducible experimental model of biofilm implant-related osteomyelitis in sheep. More specifically, in this study, biofilms of MRSA were grown on the surface of PEEK membranes using the membrane biofilm reactor discussed in Chapter 4.[40] These biofilms were placed in apposition to the proximal medial aspect of a sheep tibia, on the bare cortical surface stripped of periosteum, and subsequently covered by a simulated fracture fixation plate (Figure 7.1). As such, this study modeled a massively contaminated Type IIIB Gustilo open fracture,[66] wherein, in a worst case clinical scenario, biofilms from natural ecosystems may contaminate a wound site and be compressed between bone and a fracture fixation plate.[257,258]

7.2 Materials and Methods

7.2.1 Biofilm Growth

The growth of biofilms in this project was the same as the growth of biofilms in all previous studies of this dissertation. These methods can be found in Chapter 4. To transport these membranes, they were kept in 5 mL of BHI broth (modified) and removed aseptically when they were ready to be placed in apposition to the bone of a sheep.

7.2.2 Stainless Steel Plates

The SS plates used in this study were machined from the same medical grade 316L SS and with the same dimensions as those plates presented in Chapter 5 (see Figure 5.1). Prior to implantation, these plates were cleaned and passivated following ASTM standard F86-04, then sterilized by autoclave. Note: no plates were coated with PDMS or CSA-13 for this pilot work.

7.2.3 Surgical Procedure and Postsurgical Monitoring

All animal work was performed with approval from the Institutional Animal Care and Use Committee (IACUC) and the Environmental Health and Safety (EHS) department at the University of Utah. For this study, 2-3-year-old female Columbia Cross sheep, weighing 90 ± 20 kg, were selected. This species of sheep has a flat area of bone on the proximal medial aspect of the tibia with a surface area that was suitable for securing of the plates with transcortical screws. A total of n=10 sheep were used in this study with n=5 being treated with biofilm to serve as positive controls of infection (Group 1), and n=5 serving as negative controls of infection (Group 2). The 5 negative control sheep were treated with PEEK membranes that had been run through the modified CDC biofilm reactor without bacterial inoculation.

Prior to surgery, the sheep were fasted for >12 hours. Since the goal of this work was to develop a positive signal of infection, no antibiotics were administered. Sheep were initially anesthetized using an intravenous (IV) injection of either ketamine (5 mg/kilogram (kg)) and diazepam (0.5 mg/kg) or propofol (3-7 mg/kg) to allow for endotracheal tube intubation. Following intubation, the sheep were placed in the supine

position and maintained under anesthesia with isoflurane to effect (ranged from ~2-3%). An IV catheter was placed in the left forelimb and 0.9% saline was administered at a rate of 10 mL/kg/hour (hr). Veterinary surgical and equipment technicians monitored the sheep's heart rate, temperature, carbon dioxide and oxygen levels, and respiration throughout the procedure.

The right hind limb of each sheep was circumferentially clipped free of hair/wool, from immediately above the hoof to the groin, and then scrubbed and prepped with betadine and alcohol treatment. The hoof was isolated in a sterile rubber glove and wrapped with sterile VetWrap (Fisher Scientific). After sterile draping, the proximal medial aspect of the leg and the region of the incision was treated with Chloraprep (Fisher Scientific) solution to further sterilize the skin.

An anterior midline sagittal incision was made from the region of the tibial tuberosity and extending distally, parallel to the anterior margin of the tibia. This incision was placed away from the plate and biofilm implantation site to avoid contamination of the site during wound healing. Dissection was carried medially and posteriorly, close to the bone, lifting the skin with the attached subcutaneous tissues from the surface of the medial tibial flare.

Since this study modeled a Type IIIB Gustilo open fracture—which may consist of periosteal stripping, bone exposure and massive contamination[66]—a 2 cm x 5 cm area of periosteum was removed from the proximal medial aspect of each sheep tibia (Figure 7.1A). On the bare cortical surface, the positions of a proximal and distal plate were templated by sequentially drilling and placing transcortical screws through a SS plate. The screws were not tightened at this stage. This technique allowed compensating for

any irregularity in the “flat surface” of the tibia, tapped each hole and prevented thread stripping in the thin bone. This prepositioning avoided spurious contamination of the site when placing the infectious biofilm.

A PEEK membrane (with or without biofilm, depending upon the animal group) was aseptically removed from the 5 mL of BHI broth (modified) using sterile forceps. The corner of the membrane was touched against a sterile towel, removing excess broth but not biofilm, and preventing broth from contaminating the surgical field. The membrane was placed into the well of a SS plate and the fluid that remained on the membrane allowed it to adhere to the metal plate due to fluid cohesive forces.

Using careful, aseptic technique, the SS plate/PEEK membrane construct was placed in apposition to the tibia with the PEEK membrane residing between the bone and plate. Each plate was secured to the bone using 2.7 mm diameter x 10 mm length cortical bone screws (self tapping; catalog #ST270.10, Veterinary Orthopaedic Implants). This process was performed twice in each sheep such that each sheep was treated with two PEEK membranes and two plates (Figure 7.1B). The rationale for using two plates was to have one available for microbiological analysis and one for histological analysis at the end of the study. To the best of the surgeons’ ability, the two plates had a space of ~1cm between them. However, anatomical variation existed amongst the sheep and not all were able to maintain exactly 1 cm of space between them.

After plate placement, a swab of the cortical bone surface was collected to determine if bacteria had already begun to dislodge away from the biofilm on the PEEK membrane. The surgical site was closed with interrupted 2-0 Vicryl (catalog #J339H, Ethicon) subcutaneous sutures and a running subcuticular 2-0 Proline (catalog #8533H,

Ethicon) suture. A swab of the incision site was taken to determine if bacteria were present on the skin. Prior to wrapping the surgical site, the leg was cleaned with saline and isopropyl alcohol to kill bacteria that may have been present on the skin. This helped to reduce the risk of cross contamination throughout the animal facility and between animals.

For postoperative analgesia, each sheep was given an epidural dose of morphine (0.1 mg/kg) and two fentanyl patches (100 μg/hr) were placed in a shaved area on the left forelimb. An injection of flunixin (1.1 mg/kg) was administered to diminish inflammation. Postanesthesia monitoring extended until the animals could stand on their own, as well as eat and drink.

7.2.4 Surgical Follow Up

Throughout the course of the study, each sheep was monitored by the author and his team and a veterinarian in the animal quarters to assess any symptoms of pain and distress. Under veterinary supervision, animals that showed signs of pain or distress were treated with Buprenex (0.01 mg/kg) or additional fentanyl patches. If excessive inflammation was present, they were further treated with rimadyl (4.4 mg/kg).

Using a clinical grading system, based on the hallmarks of infection: calor (heat), rubor (redness), dolor (pain), and tumor (swelling), the sheep were monitored daily for a 12-week period for these signs of infection. A daily rectal temperature of each sheep was taken. The animals were also monitored for limping, lethargy, irritability, and going “off feed” and/or water. Based on these criteria, a four-tiered clinical grading system was established.

Grade I, or no infection, consisted of the signs of healing normally seen with surgical trauma and that resolved within 1 to 2 weeks of surgery. These signs included slight redness at the surgical site, mild warmth (to the touch), mild inflammation, a closed suture line, healed within 2 weeks, the sheep eating and drinking, a normal rectal temperature (for these sheep normal temperature was between 101.5° Fahrenheit (F) and 102.8° F), and no signs of distress or limping. A Grade II infection included increased redness, a warmer surgical site with moderate inflammation, evidence of suture line dehiscence, irritable behavior, normal temperature and not limping. Sheep were euthanized if they displayed signs of a Grade III infection. This grade was characterized by significant redness and palpable heat at the surgical site, an open suture line with drainage, significant inflammation, tenderness, lethargy, fever, off feed and/or water, and positive bacterial growth on wound culture. A Grade IV infection was defined, but never allowed to develop in any of the animals. This included excessive heat, excessive inflammation, purulent drainage, implant exposure, excessive limping, local tenderness, off feed and/or water, lethargy, and fever.

7.2.5 Bone Labeling

As stated by Bloebaum *et al.*,[259] "Fluorochrome labeling is a well established method of measuring the mineral apposition rate (MAR), at which osteoid matrix, produced by osteoblast cells, is deposited and mineralized to form new bone."

In this study, calcein fluorochrome (catalog #C-0875, Sigma-Aldrich) was used as a nonantibacterial agent to label bone and to calculate the MAR, i.e., the growth rate of the sheep bone and also provided an indication of bone viability. The method by which

this works is after the calcein is injected, it is taken up by osteoblast cells and released into the matrix of newly forming bone. After processing, calcein fluorochrome can be observed in tissue samples as they are imaged using an excitation wavelength of 495 nm and emission of 515 nm. The imaging that was performed in this study is described in section 7.2.10.

Calcein was prepared in reverse osmosis water to a final concentration of 30 mg/mL. The pH was adjusted to 7.2-7.4, filtered using a 0.22 μm filter for sterility and the solution administered IV at 0.33 mL/kg of body weight. Two separate injections were given: one 16 days and one 5 days prior to the established 12-week end point of each sheep to create a double label in the bone as well as label viable bone. The infected sheep that were euthanized prior to the 12-week end point did not receive calcein injection.

7.2.6 Euthanasia and Microbiological Sample Collection

Sheep were euthanized at the end of 12 weeks, or once a Grade III infection was determined to exist. To euthanize, animals were initially sedated with an IV injection of ketamine (5 mg/kg) and diazepam (0.5 mg/kg) in order to collect a 5 mL blood sample for microbiological analysis. Euthanasia was then performed by IV injection of beuthanasia (1 mL/4.5 kg) solution.

A swab of the incision site (~1 cm^2 area) was taken and streaked onto Columbia blood agar for semiquantitative analysis. More specifically, 1+ growth was defined as having growth in the first zone of streaking, 2+ having growth in the second zone and 3+ having growth in the third zone. The agar plate was incubated overnight at 37° C. Next,

the skin at and surrounding the incision site was prepped using chlorhexidine/isopropyl alcohol antiseptic. A scalpel was used to aseptically reopen the incision site and a swab of the subdermal tissue was collected to determine if bacteria had penetrated into the soft tissues superficial to the plates and PEEK membranes. This swab was also cultured on Columbia blood agar.

One of the SS plates was randomly selected and the underlying PEEK membrane was removed and placed into 5 mL of 10% BHI broth (modified). The sample was vortexed for 1 minute, sonicated for 10 minutes and allowed to recover in the broth at room temperature for 20 minutes (to allow the bacteria to convert from the biofilm to planktonic phenotype) before performing a 10-fold dilution series (plated in duplicate) to quantify the number of CFU/PEEK membrane.

The SS plate that had been removed was then secured to the bone once again so that radiographs could be taken. The tibia was then disarticulated and used for gross photographic and radiographic analysis.

7.2.7 Gross Photography/Radiography

Gross photography of the soft tissues and bone were collected throughout the sampling/dissection process. Radiographs were obtained using a cabinet x-ray system (43855A Model, Faxitron X-Ray Corporation) set at 70 kilovolts (kV) for 2 ½ minutes.

7.2.8 Tissue Embedment/Sectioning

After radiographic imaging, all of the soft tissue was dissected from the bone with the exception of the tissue that was directly over the undisturbed SS plate. The sample

was then fixed in modified Karnovsky's fixative[260] using 3 x 24-hour changes. Following fixation, the bone was rinsed in reverse osmosis water for 10 minutes and cut into two sections separating the two SS plates from one another. The plate that had been removed in order to access the PEEK membrane for microbiology was again removed and the biofilm on the underlying bone imaged with SEM. The remaining bone section, with plate and PEEK membrane intact, was used for histological analysis.

After cutting, both bone samples were placed in 70% ethanol for 24 hours to initially dehydrate them. The bone for SEM imaging was further dehydrated by hand using ascending concentrations (from 70%, to 95% to 100%) of ethanol, then coated with gold using a Hummer 6.2 sputter coater and imaged using SEM.

The bone sample for histology was also dehydrated using increasing concentrations of ethanol. However, this was performed in a Tissue-Tek VIP (Miles Scientific) instrument. It was then placed into a solution of 80% methylmethacrylate and 20% N-butyl (the combination of these two solutions is referred to as Solution A), and mixed for 5 days to infuse the tissues. The Solution A was poured out and a fresh aliquot of Solution A, mixed with 2.5 g/Liter (L) of perkadox (the catalyst for polymerization), was added to the sample. The sample was kept in a dessicator at 4° C for 7 days. Finally, 5 g/L of perkadox was added to another batch of fresh Solution A and exchanged for the used mixture in the container and the sample was kept in a desiccator at 4° C for an additional 9 days. Samples were then placed in a new container and Solution A with 5 g/L of perkadox was added and polymerized in 2 cm layers using ultraviolet light. Each layer required 48 hours to fully polymerize. The final product resulted in a PMMA embedded sample containing the bone, PEEK membrane, stainless steel plate and soft

tissue regions. This embedment procedure has been published by Dr. Bloebaum's group previously.[261-265]

Once embedded, tissue samples were cut using a band saw to remove excess PMMA and isolate the area of interest. Samples were further sectioned into ~2 mm sections using a diamond blade water saw. Radiographs of the sections were obtained following the same procedure outlined above. One face of a section was then polished, and gold coated for SEM analysis.

7.2.9 SEM Analysis

SEM analysis was performed using a JEOL 6100 LaB_6 filament SEM to qualitatively examine bone and/or biofilm morphology in the region where a SS plate/PEEK membrane construct was implanted. For those bone samples that had the SS plate removed, secondary electron images were collected of the cortical bone surface to examine the morphology of the bone and/or biofilm where the PEEK membrane had been present. For those samples that were sectioned in PMMA, BSE images were collected to examine the varying levels of mineralization, how the infection influenced the periosteal response in bone, and cortical bone activity.

7.2.10 MAR Analysis

The procedure for collecting MAR data was based on the published work of Bloebaum *et al.*[257] In short, after sample sections had been imaged using SEM, the polished surfaces were glued to a slide and further ground to ~50-60 μm thickness for MAR analysis. Images were first collected using a mercury lamp Nikon Labophot

microscope to detect the presence of calcein double-labeled osteons of the host bone. Three slides from each sheep were analyzed. From each slide, five osteons were randomly selected in the cortical/periosteal bone region beneath a SS plate and a total of eight measurements were made along the span of each double label using ImagePro Plus software. The MAR of bone was calculated using the following formula:

$$\text{MAR } (\mu\text{m/day}) = \Sigma_x(e)(\pi/4)/nt$$

where Σ_x is the sum of all the measurements between double labels, e is the micrometer calibration factor (μm), (π/4) is the obliquity correction factor, n is the total number of measurements, and t is the time interval between calcein injections expressed in days.

7.2.11 Histology

For histological analysis, sample slides were further ground to a thickness of 40-50 μm and stained with hematoxylin and eosin (H&E) stain. For H&E staining, Mayer's solution was preheated to 50° - 55° C. Slides were placed in the Mayer's solution for 5 minutes, rinsed and dried. Slides were then placed in Clarifier for 4 minutes, rinsed, placed in Bluing Reagent for 4 minutes, rinsed again and dried with a Kimwipe. Finally, slides were counterstained by dripping Acid Fuschin/5% Acetic Acid solution for 35-45 seconds and dipped in 100% ethanol for 30 seconds.

Macroscopic images of slides were collected using a Nikon SMZ800 macroscope. Higher magnification images were collected using a Nikon Eclipse E600 microscope. Using a modified histopathologic grading scale of Smeltzer *et al.*,[234] an outside observer,

who was blinded to the samples in the study, examined the slides to determine what level of osteomyelitis was present in the bone and or surrounding tissue regions. Osteomyelitis was indicated by the presence of bacteria, as determined by the microbiological analysis, in conjunction with chronic inflammation and bone necrosis. Cortical bone growth/response was not an indicator of infection as it was present in all five sheep from Group 1 and three from Group 2. Thus, it appeared to be a normal bone response to the surgical trauma and implantation. The modified Smeltzer *et al*. grading scale is provided in Table 7.1.

7.2.12 Statistical Analyses

From a Kaplan-Meier survival curve, a Log-Rank test was used to examine the statistical significance in survival times between those sheep treated with biofilm and those that were not. A separate Log-Rank test was used to compare the time it took for animals in both groups to become infected. Time to infection differed from survival time since some sheep in Group 1 survived the full 12 weeks of the study, but displayed signs of infection very early on.

Because the number of bacteria collected from PEEK membranes of those sheep in Group 1were not normally distributed, the nonparametric Mann-Whitney U test was used, as opposed to a student's *t* test, to compare the number of bacteria that were collected on the PEEK membranes of Group 1 and Group 2 animals. In all instances, an alpha level of 0.05 was established to define statistical significance. All statistical data were analyzed using SPSS 17.0 software.

7.3 Results

7.3.1 Surgical Follow Up

A survival curve including each of the 10 sheep in this study was plotted using a Kaplan-Meier survival curve (Figure 7.2A). Two of the five sheep in the biofilm treated sheep (Group 1) were euthanized at 3 weeks due to a Grade III infection. The other three survived to the 12-week end point, but each of those three sheep displayed Grade II signs of infection during the 12-week monitoring period. Furthermore, each of the five sheep in Group 1 displayed signs of inflammation and abscess formation between day 4 and 11 after surgery. In contrast, all five of those sheep in Group 2 survived to the 12-week end point with minimal acute inflammation and no signs of infection at any point in the study. The Log-Rank test indicated that the difference in survival among the two groups was not significant ($p=0.184$). However, when time to infection was analyzed, there was a significant difference ($p=0.002$) between the groups (Figure 7.2B). This difference corroborated with the microbiological data.

7.3.2 Microbiology

Microbiological data showed that PEEK membranes collected from Group 1 sheep contained an overall log density of 5.32 ± 5.41 $\log_{10}$ CFU/PEEK membrane. No bacteria were detected on the PEEK membranes of Group 2 sheep. When compared using the Mann-Whitney U test, this difference was statistically significant ($p=0.008$).

All of the swabs taken from all animals showed between 1+ and 2+ growth of normal flora bacteria at the incision site. In three out of five of the Group 1 sheep, subdermal swabs detected 2+ growth of bacteria in the tissues surrounding the SS plates,

whereas swabs taken of the remaining two sheep detected no growth of bacteria. All of the culture swabs collected from Group 2 sheep were negative for growth.

These data indicated that the microbiological findings correlated with the clinical observations of the sheep, wherein those treated with biofilm (Group 1) suffered a Grade II or higher infection, and those not treated with biofilm (Group 2) did not suffer from infection.

Notably, when removing the SS plates for microbiological analysis, it was observed that in each of the five Group 1 sheep, the bone screws had become completely loose and in one animal the plates had even shifted position. This was due to bone resorption around the screws, which was a result of infection as indicated by SEM analysis and histological results (see sections 7.3.4 and 7.3.6). No screw or plate loosening was observed in Group 2 sheep and it was also interesting to observe that in Group 2 sheep, the cortical bone began to grow on/attach to the PEEK membranes, which made it difficult to remove them for quantification. In contrast, the PEEK membranes in the infected sheep had no attachment of bone to them and were easily removed.

7.3.3 Gross Photography/Radiography

Gross photographs provided evidence that an abscess formed in the surgical area of Group 1 sheep, whereas no abscess formation was seen in sheep from Group 2 (Figure 7.3). Furthermore, signs of infected tissue, including pus and significant inflammatory and cortical bone response, could be seen in Group 1 sheep once the skin was resected (Figure 7.3B). In contrast, only a thin membrane of tissue grew over the plates in Group 2 sheep with minimal periosteal/cortical bone response (Figure 7.3D).

Radiographic evidence also suggested that in Group 1 sheep, "moth eaten," osteomyelitic bone was visible (Figure 7.4A). This result was particularly apparent in the microradiographs that were taken of bone sections after they had been embedded and cut (Figure 7.4B). From these sections a significant cortical bone response and an endosteal response indicative of responsive new bone formation could be seen in Group 1 sheep. No such response was seen in Group 2 (Figure 7.4C, D).

7.3.4 SEM Analysis

Due to the natural complexity of the cortical bone surface of sheep and components that resembled bacteria, it was difficult to confirm that there were biofilm dwelling bacteria on the cortical bone surface of Group 1 sheep using SE electron SEM imaging. Although it did appear that the bone surfaces of Group 1 sheep had more degradation and trauma when compared to the bone surfaces of Group 2 sheep, the differences were not deemed substantial enough to support any conclusions. On the other hand, BSE images of the bone sections were much more indicative of bone trauma and infection.

More specifically, in Group 1 sheep, BSE images indicated that there was a considerable amount of bone resorption directly underneath the stainless steel plate (Figure 7.5A) and near the bone screws (Figure 7.5B), which supported the observation mentioned above that these screws were loose, whereas no signs of bone resorption were apparent in any sheep from Group 2 (Figure 7.5C, D). Furthermore, a much larger gap was seen between the cortical bone surface and plate of Group 1 sheep when compared to Group 2. More specifically, the distance from the bone to the plate surface in Group 2

was ~20-50 microns, whereas in Group 1 the gap was much larger and ranged from 200-800 microns. As will be seen in the histopathological results, this larger gap in Group 1 sheep was due to fibrous tissue formation and chronic inflammation, which the microbiology data confirmed to be the result of infection.

7.3.5 MAR/Bone Viability Analysis

MAR results indicated that in Group 1 sheep, the average bone remodeling rate was ~1.5 μm/day. In Group 2 sheep the average rate was ~1.2 μm/day. Images of double labels in the periosteal regions of Group 1 sheep showed that an intense remodeling response was present (Figure 7.6A). However, typical double labels of osteons were seen in the cortical bone regions (Figure 7.6B). No significant response was seen in the periosteal regions of sheep in Group 2 and osteon structures were present in the cortical bone region indicative of remodeling (Figure 7.6C, D). Notably, calcein double labels further indicated bone viability.

7.3.6 Histology

Sections stained with H&E showed that there was an observable difference between the bone and soft tissues of Group 1 and Group 2 sheep. More specifically, when compared to the modified Smeltzer *et al*. histopathological grading scale (Table 7.1), the three sheep in Group 1 that survived to the 12-week endpoint displayed signs of a Grade 4 osteomyelitis as indicated by moderate to severe chronic inflammation with significant intramedullary fibrosis and multiple foci of sequestra (Figure 7.7). These sheep also displayed Grade 3 cortical bone growth. The other two sheep in Group 1,

which survived to 3 weeks, displayed Grade 3-4 osteomyelitis with Grade 2 cortical bone growth. None of the five sheep in Group 2 showed signs of osteomyelitis and were scored with a Grade 0 osteomyelitis. However, three of the five sheep in Group 2 did display Grade 2 cortical bone growth, whereas the other two were scored with Grade 0 cortical bone growth. Taken together, these results suggested that cortical bone growth/response could have been due to surgical trauma or the presence of infection, yet a notable difference in bone morphology was present in those that were infected versus those that had a response due to surgical trauma. More specifically, those that had infection showed signs of "moth eaten" bone that had jagged edges due to resorption/bacterial presence, whereas those with a cortical bone response due to surgical trauma had woven bone formation with little indication that resorption was occurring.

7.4 Discussion

Using biofilms as initial inocula in this study addressed three major limitations, which were outlined in Chapter 3, that may accompany the use of planktonic bacteria in animal models of infection. These animal models include those that are designed to develop combination products of biomaterial coatings and other antimicrobials. To reiterate, these three limitations are 1) Planktonic cells may be cleared by the immune system more readily than cells residing in a biofilm. Thus, when planktonic cells are used in *in vivo* models, it may be that they are eradicated before they can form biofilms. As mentioned, this may contribute to the low reproducibility for the induction of osteomyelitis. 2) It is becoming ever more evident that planktonic bacterial cells are more susceptible to antibiotics than those residing in a biofilm. If antibiotics are

administered prophylactically immediately following inoculation, they may affect planktonic bacteria more effectively and rapidly than they would biofilm bacteria. 3) When planktonic bacteria are added to the body, the possibility exists for them to be dispersed rapidly away from the site of initial inoculation due to the presence of flowing fluids in the body. This could dilute the concentration of bacteria per given area—potentially making it easier for the body to handle the bacterial load and prevent biofilm formation in the tissue or on a medical device.

Notably, osteomyelitis developed in all five sheep from Group 1 of this study treated with biofilm, which strongly supported the hypothesis that using biofilms as initial inocula would cause infection. The hypothesis was further supported, and the data made significantly stronger, by the fact that none of the sheep from Group 2 became infected. This 100% vs. 0% rate of infection provided a promising outcome for future tests of combination biomaterials for device development to be performed in a repeatable fashion using this model.

Despite these promising results, there is one crucial factor to take into consideration. In the above study, biofilms were grown for a 48-hour period, rinsed to remove loosely adherent or nonadherent cells, and transferred in a broth solution prior to using them as initial inocula. These steps were undertaken in an attempt to reduce the possibility of having planktonic cells present. However, the potential still existed that a portion of cells present could have been in the planktonic phenotype. As such, the question may arise: was it the biofilm bacteria or the planktonic bacteria that caused infection? Two responses can be given.

First, it is likely impossible with current technologies to separate all planktonic bacteria from those that reside in the biofilm phenotype such that an inoculum with biofilm bacteria alone is absolutely definitive. Yet, it is also unlikely that such a distinct separation exists between planktonic and biofilm bacteria in natural ecosystems. This may suggest that using an inoculum that has a mixture of the two, with those in the biofilm phenotype being more heavily selected, is clinically relevant.

Second, an additional animal model of infection has recently been developed in Dr. Bloebaum's lab to test the ability of the same MRSA strain as was used in this study to cause infection when inoculated in the planktonic phenotype. When the onset of infection was compared between these two animal models, there was a drastic difference in the rapidity and severity of infection that set in with the planktonic bacteria. In that instance, none of the animals survived past 11 days. In contrast, those that were treated with biofilms as initial inocula displayed signs of infection that were much less severe and which progressed at a much slower pace. More specifically, those animals displayed limited signs of pain or distress even out to 12 weeks, but each of them developed significant osteomyelitis.

This contrast in the speed and severity of infection may provide clinical evidence that using biofilms as initial inocula is more correlative to biofilm-related infections that are present in patients. In patients, biofilm-related infections appear to be latent infections that develop slowly over time and which may persist for extensive periods. This may be due to the quiescent nature of biofilms and the fact that they have already established a community. Planktonic bacteria have yet to develop a community and it

appears that their "goal" in nearly every ecosystem is to find a location to colonize and then begin to develop a biofilm community.

So although this animal model provides a promising step in the direction of using biofilms as initial inocula, there are many factors to take into account: a host's health, the pathogenicity of an organism, the ability for an organism to develop into a biofilm, the degree of contamination, and the ratio of cells in the planktonic phenotype to those in the biofilm phenotype. Thus, this issue of planktonic vs. biofilm infection is still a limitation and will require additional future testing to overcome the challenges of separating the bacterial phenotypes before more definitive statements can be made.

Nevertheless, the biofilms in this study appeared to have a gradual adverse, localized clinical effect on the sheep. More specifically, osteomyelitis developed slowly, and persisted without significant signs of distress in 3 of 5 of the animals in Group 1.

Importantly, there were no sclerosing agents used in this study to promote the development of osteomyelitis, whereas in previous studies these noxious agents have been commonly used to initially kill bone and/or tissue with the intent to make it more susceptible to infection. In addition, the model in this study also appeared to circumvent the problem of low reproducibility for the induction of osteomyelitis, which was cited by Gaudin *et al*. as an important limitation of animal models of osteomyelitis.

In two of the sheep from Group 1, bacteria were not detected in the surrounding tissue regions of the stainless steel plate. This was likely due to the limited area of sampling with the swab culture technique. Bacteria may not have been in those tissue regions, and thus were not detected. However, bacteria were collected from the PEEK membranes of both of these sheep, which corroborated with the SEM, MAR and

histopathological data—all of which supported the conclusion that biofilm-related infection had developed.

At least three limitations accompanied this study and will need to be addressed with future work. First, these results are based on the use of a single species of microorganism and although the outcomes are hypothesized to be similar to other biofilm forming organisms, different organisms may lead to different results. More specifically, although *S. aureus* is a common cause of metal, device-related infections,[59] a wide variety of other organisms can cause biofilm-related infections including *P. aeruginosa, E. faecalis,* coagulase negative staphylococci, *E. coli, Acinetobacter baumanii, Klebsiella pneumoniae* and others. Second, these results will need to be confirmed with other material types. For example, at least one study has shown that titanium implants have reduced infection outcomes when compared to stainless steel.[266] Third, as this was a developmental model to test the ability of biofilms to cause infection, antibiotics were not used. However, if this were a clinical scenario, prophylactic antibiotics would have accompanied the implantation of the devices. Thus, future work will be needed to address these limitations.

In conclusion, after a careful literature review and consultation with various researchers in the biofilm research community, this appears to be the first animal model utilizing well-established, characterized biofilms of MRSA that were grown under fluid sheer conditions as initial inocula to produce a positive signal of reproducible biofilm-related infection.[57] As such, the model provides a promising outcome in that it may be used by future researchers and clinicians to utilize a reproducible model to examine the therapeutic potential of novel systemic antimicrobials and/or antimicrobial coatings on

biomedical devices to treat and prevent biofilm-related osteomyelitis, as well as other biofilm-related infections. It may be that the use of this and similar animal models using biofilms as initial inocula will result in an important shift in the field of biofilm research that adds onto the work that has been done with planktonic bacteria. This shift may lead to the development of novel antimicrobial therapies, such as coatings on devices, that could help prevent biofilm-related infections in a more effective manner. In short, the development of this experimental model may have tremendous implications in the future of biofilm implant-related infection treatment strategies as well as other biofilm-related infections.

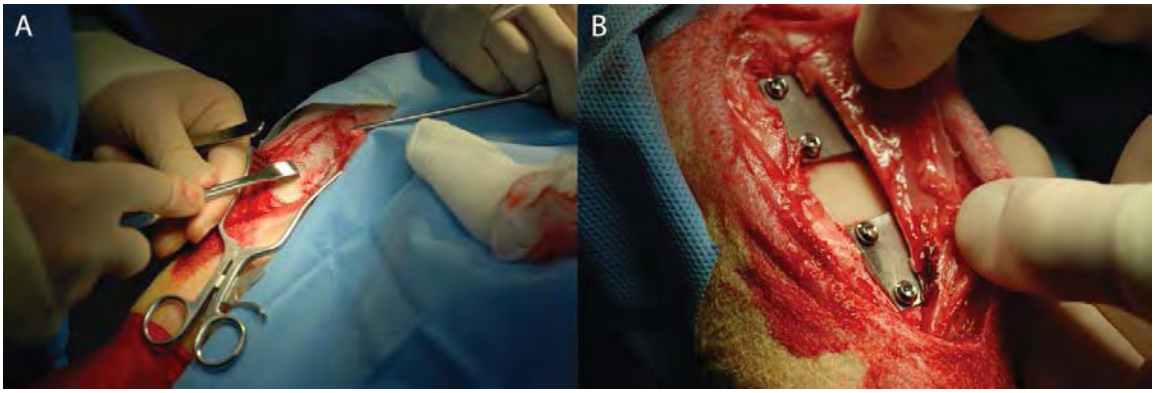

Figure 7.1: Photographs taken during the surgical procedure that was used to secure SS plates to the proximal medial aspect of one of the pilot animals. (A) Photograph of the proximal medial aspect of the right tibia demonstrating removal of a 2cm x 5cm area of periosteum using a periosteal elevator. A template was used in each sheep to standardize the 2cm x 5cm area that was removed. (B) Photograph of the final construct with two stainless steel plates secured to the proximal medial aspect of the tibia. There was a ~1cm gap existed between the two plates and each of the plates had a PEEK membrane in the underside well in direct apposition to the bare cortical bone surface.

Table 7.1: Histological parameters and scoring system.

Intra- and peri-osseous chronic inflammation
0 Not present
1 Minimal to mild chronic inflammation with no significant fibrosis
2 Moderate to severe chronic inflammation with no significant fibrosis
3 Minimal to mild chronic inflammation with significant fibrosis
4 Moderate to severe chronic inflammation with significant fibrosis
Bone necrosis
0 No evidence of necrosis
1 Single focus of necrosis without sequestrum formation
2 Multiple foci of necrosis without sequestrum formation
3 Single focus of sequestrum
4 Multiple foci of sequestra
Cortical bone response
0 No cortical bone response
1 Cortical bone growth that does not extend beyond plate border
2 Cortical bone growth that begins to extend beyond plate border
3 Cortical bone growth that covers a plate part way
4 Cortical bone growth that covers a plate entirely

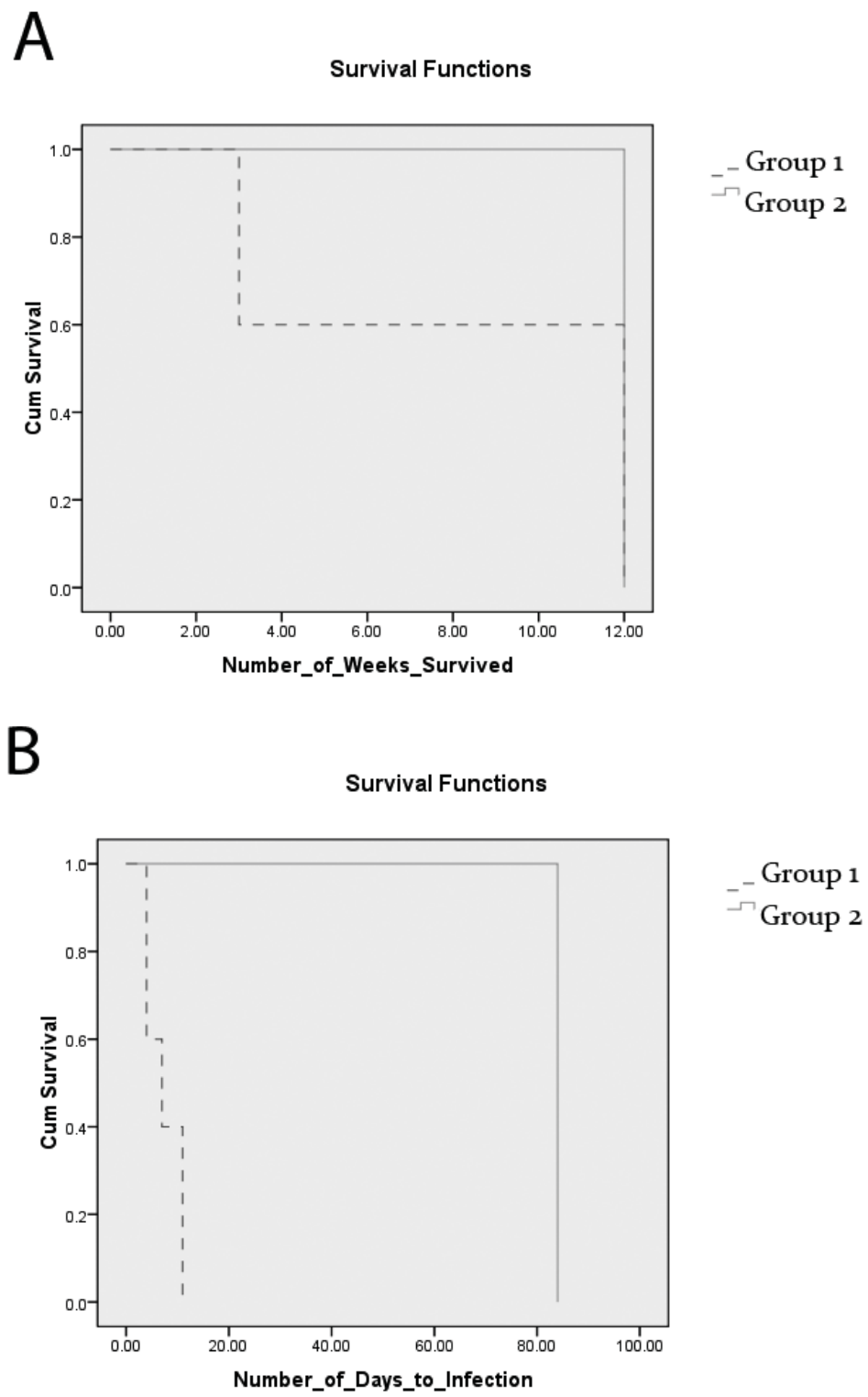

Figure 7.2: Kaplan-Meier curves indicating the survival and time to infection of each pilot animal. (A) Kaplan-Meier survival curve for each sheep in Group 1 and Group2. (B) Kaplan-Meier curve of the time it took for each sheep to display signs of infection.

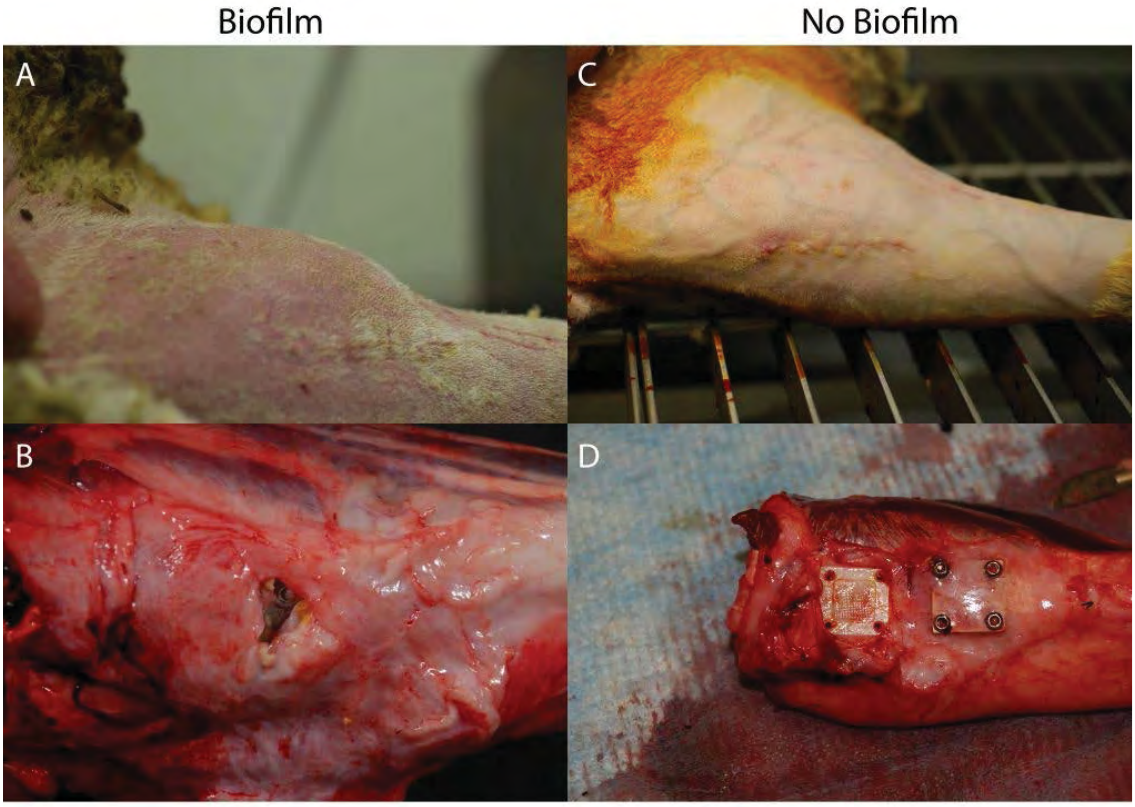

Figure 7.3: Photographs of sheep tibiae that were taken during necropsies. Left column: photographs of a sheep treated with biofilm. Right column: photographs of a sheep not treated with biofilm. (A) Representative photograph of the proximal medial aspect of a sheep tibia from Group 1 that suffered from infection. In this particular sheep, this abscess developed on day 11 postsurgery. (B) Once the skin was resected from the infected sheep shown in Figure 24A, pus could be seen as well as a significant cortical bone/periosteal response in the infected region. This sheep had positive growth for MRSA. (C) Additional photograph of a sheep tibia from Group 2. No abscess formation was seen in any of the sheep from Group 2. (D) Once the skin was resected away from the sheep tibia shown in Figure 24C, a thin, fibrous membrane was observed to have grown over the stainless steel plates. In addition, the bone had grown up to the edges of the plates and no further (Grade 0 cortical bone growth). The plate that was removed was used for microbiological analysis. No bacteria were detected in/on the tissues or on the PEEK membrane.

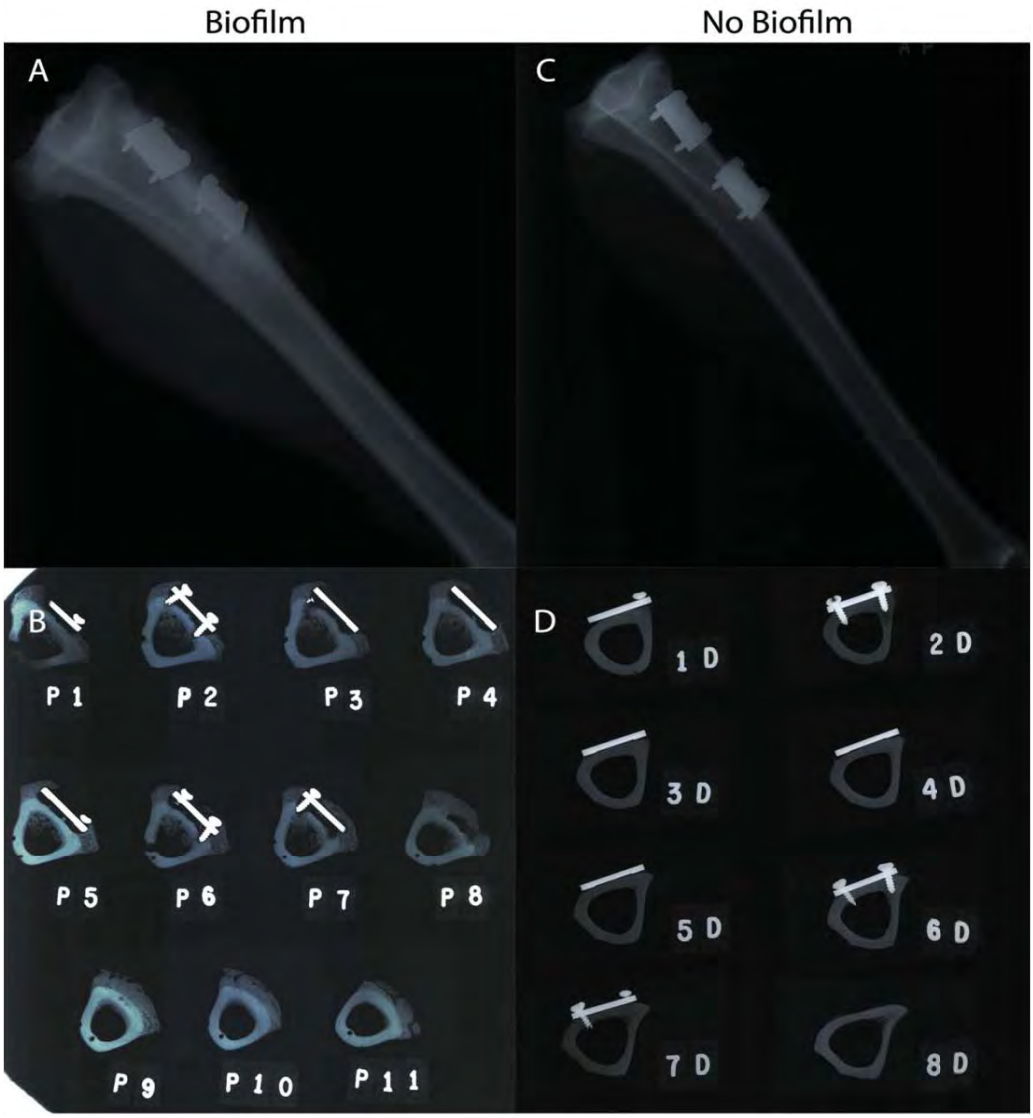

Figure 7.4: Radiographs that were collected from pilot sheep at the time of necropsy. Left column: radiographs of a sheep treated with biofilm. Right column: radiographs of a sheep not treated with biofilm. (A) Macroradiograph of the tibia of the sheep photographed in Figure 24A. From this radiograph, the authors were able to detect signs of "moth eaten," osteomyelitic bone. Similar radiographs were collected from all sheep in Group 1. (B) Once the bone was embedded and sectioned, microradiographs of the same sheep from (A) indicated that in addition to mothy cortical bone, a significant endosteal response was also present suggesting that infection was present in the medullary canal. (C) No "moth eaten" bone was detected in the radiograph of the sheep tibia from Figure 24C. This same result was seen in all of the sheep from Group 2. (D) Microradiographs of the embedded, sectioned samples from the sheep presented in (C) suggested that there was no endosteal or cortical bone response.

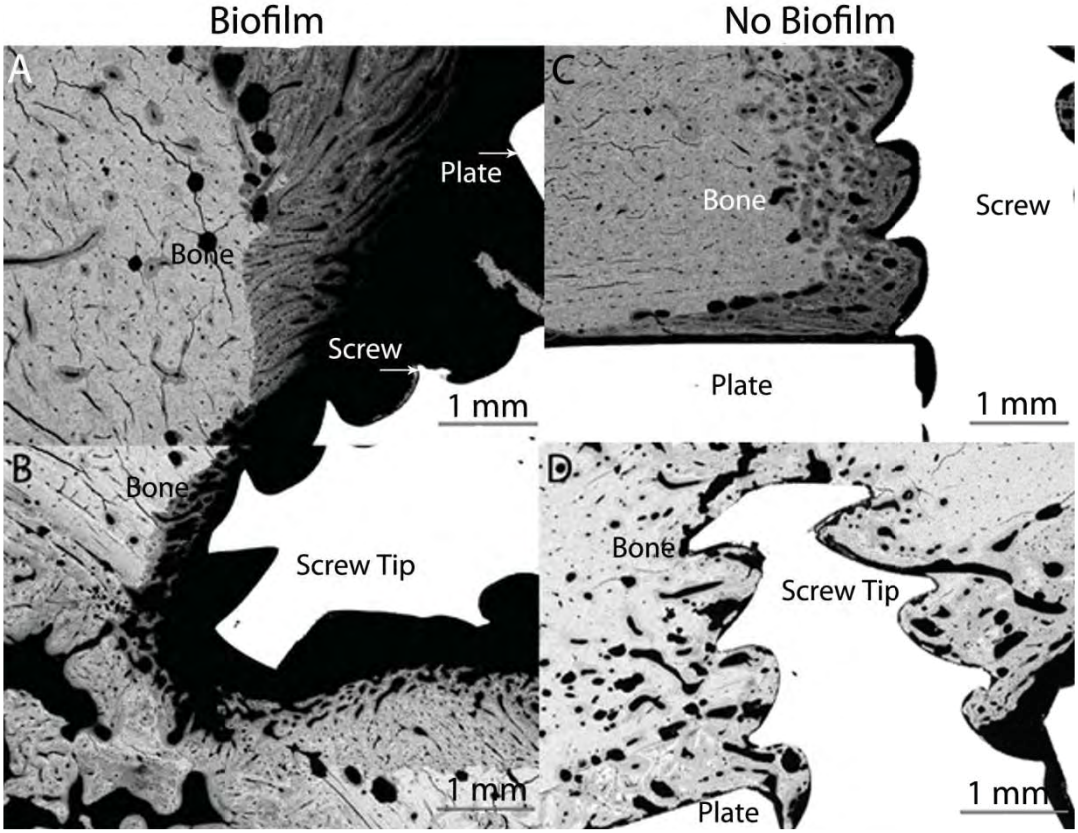

Figure 7.5: SEM images of bone screws and resorption patterns in representative pilot sheep. Left column: BSE images of a sheep treated with biofilm. Right column: BSE images of a sheep not treated with biofilm. Original magnification for all images was 20x. (A) Representative BSE image of a cortical bone surface underneath a stainless steel plate of an infected sheep. Note the resorption away from the bone screw and plate itself as well as the abnormal morphology (wispy, moth eaten appearance) of the bone, which was believed to be a result of infection. Darker bone was indicative of bone that was not yet mineralized, but rather, undergoing remodeling. (B) Additional BSE image from the same sheep as (A) with bone resorption occurring in the distal area of the bone screw. (C) Additional representative BSE image of cortical bone beneath a stainless steel plate in a sheep that was not infected. Note the smooth, morphologic difference in this bone compared to that of bone shown in (A). This bone grew up to the surfaces of the bone screw and plate with normal bone morphology. (D) BSE image of the distal region of a bone screw in a sheep from Group 2. No signs of resorption were present.

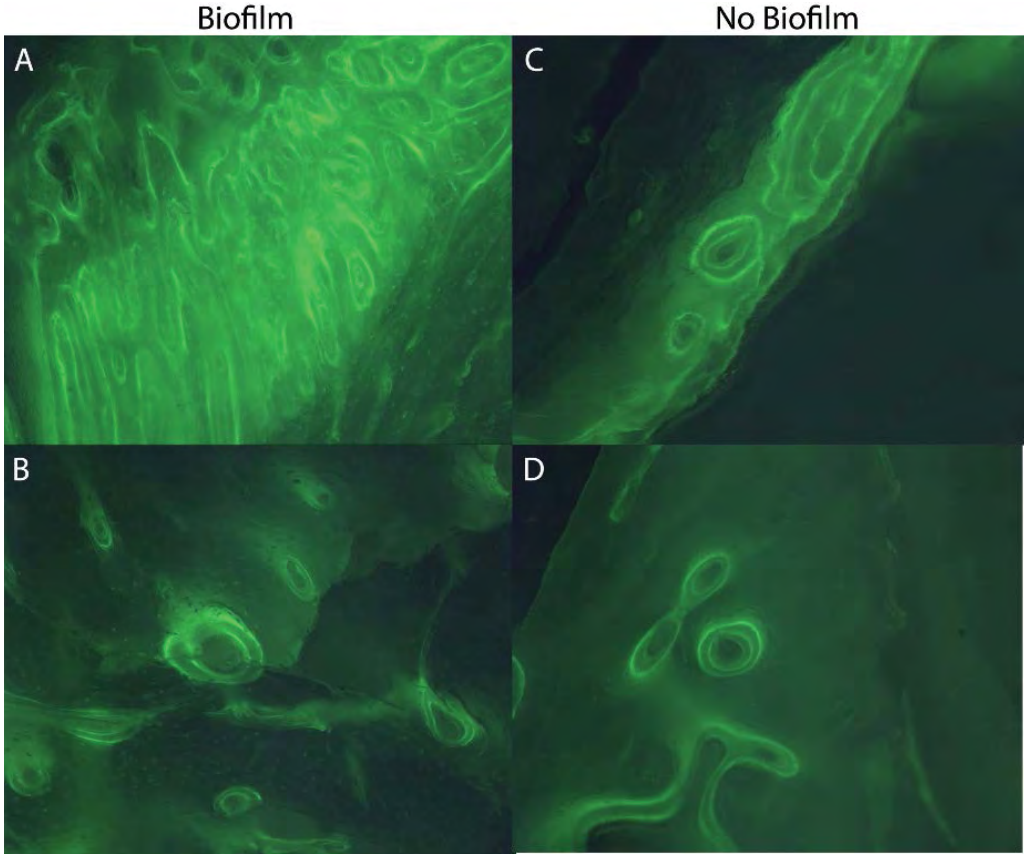

Figure 7.6: MAR images of periosteal regions and cortical bone regions of pilot sheep. Left column: double label images of sheep bone treated with biofilm. Right column: double label images of sheep bone not treated with biofilm. Original magnification of all images was 20x. (A) Image of calcein double labels in a region directly underneath a stainless steel plate of an infected sheep. This type of remodeling was indicative of bone that was attempting to remodel in the presence of infection. (B) Cortical bone region more distal to the stainless steel plate than the image collected in (A). This image indicated that in addition to areas of intense remodeling, there were areas of typical bone remodeling within the cortical bone of sheep that were infected. (C) For comparison, this image of calcein double labels was taken in the same region as the image from (A), but in a sheep that was not infected. (D) Also for comparison, this image of calcein double labels was taken in the same region as (B), but in a sheep that was not infected.

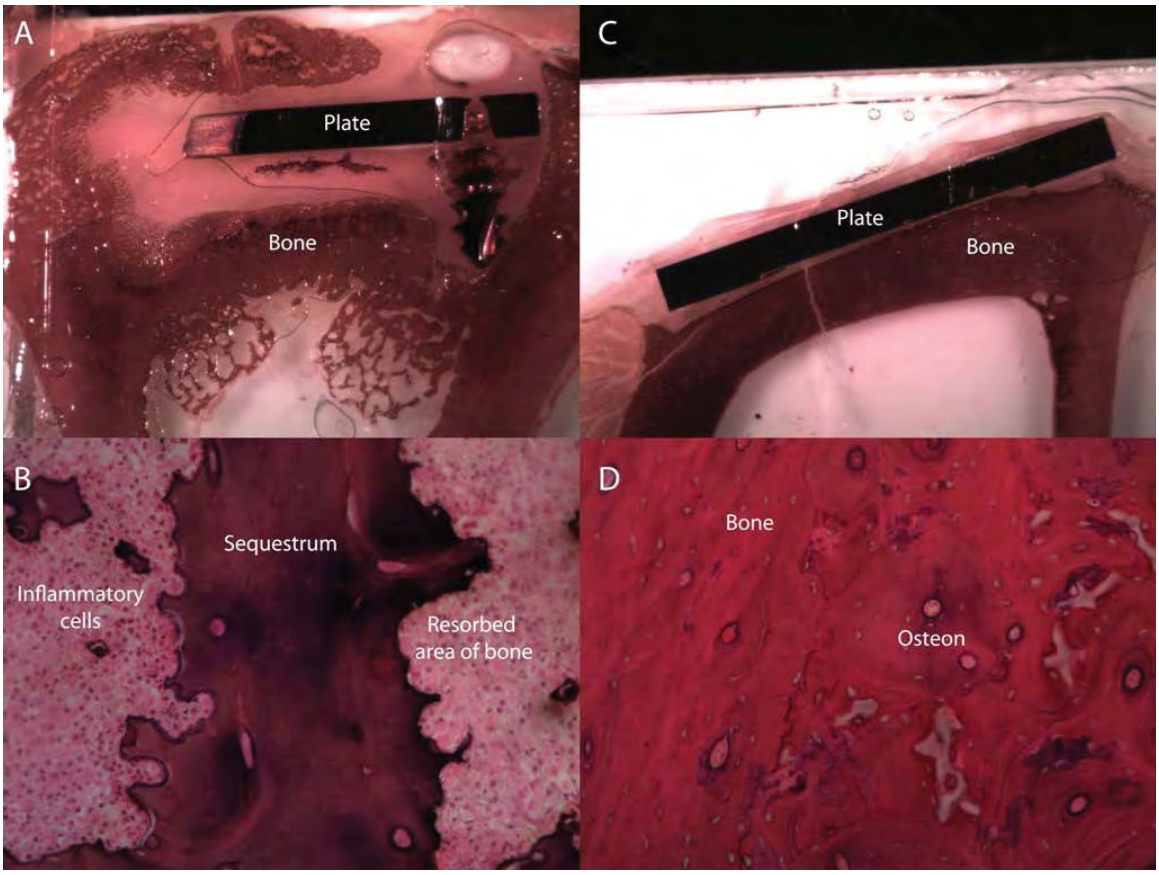

Figure 7.7: Images of histological sections indicating the bone response, sequestrum formation and inflammation in representative pilot sheep. Left column: images of H&E stained bone sections from a sheep treated with biofilm. Right column: images of H&E stained bone sections from a sheep not treated with biofilm. (A) Macroscopic image of bone from an infected sheep. Note the significant cortical bone response, the gap between the plate and bone surface, the endosteal bone response and the focus of sequestrum in the periosteal region. Taken together, these tissue responses were indicators that infection was present. Original magnification was 10x. (B) Microscopic image of the sequestrum seen in (A). The sequestrum had a jagged surface (sign of resorption) and large amounts of inflammatory cells in its surroundings; indicators that bacteria were present and that chronic inflammation had persisted. Original magnification was 20x. (C) Macroscopic image of bone from a sheep that was not infected. Note the apparent differences in tissue morphology between this sample and that from the infected sheep. Original magnification was 10x. (D) Image of a similar region of as that analyzed in (B). Note the lack of sequestrum, resorption or chronic inflammation. In contrast, this bone had normal lamellar structure. Original magnification was 20x.

CHAPTER 8

IN VIVO EFFICACY OF THE NOVEL CSA-13 ACTIVE RELEASE COATING TO PREVENT BIOFILM IMPLANT-RELATED OSTEOMYELITIS

8.1 Introduction

In this chapter, data will be provided regarding the definitive animal study that was used to test the ability of the novel CSA-13 active release coating to prevent biofilm implant-related osteomyelitis. The work that will be presented in this Chapter specifically addressed Aim 3 of the overall study that was outlined in Chapter 2, section 2.4. The specific hypothesis of this work was that when used as an active release agent in a device coating, CSA-13 would prevent biofilm implant-related osteomyelitis from developing *in vivo*.

8.2 Materials and Methods

8.2.1 Biofilm Growth

The method of growing biofilms for this study was the same as in all of the previous studies outlined in this dissertation.[40] Specifically, biofilms were grown on PEEK membranes as outlined in Chapter 4, placed in 5 mL of 10% BHI broth (modified) and inoculated in sheep using the same protocol as the pilot animal study from Chapter 7.

8.2.2 Stainless Steel Plate

The SS plates that were used for this study were manufactured to the same dimensions, made of the same medical grade SS, processed, dip coated with PDMS or PDMS/CSA-13 and cured following the same protocol as outlined in Chapters 4 and 5.

8.2.3 Surgical Procedure and Postsurgical Monitoring

As was the case with the pilot study from Chapter 7, this animal work was performed with the approval of the IACUC and EHS department at the University of Utah. The surgical procedure was the same as that outlined in Chapter 7. The difference between the pilot study and this definitive study was that the SS plates were coated in this portion of the study and the number of animals in each group were expanded. More specifically, a total of n=27 animals were separated into three groups of n=9. Group 1 sheep were those that were treated with PDMS only coated plates and biofilm (positive control). Group 2 sheep received SS plates that were coated with PDMS/CSA-13 and biofilm (treatment group) and Group 3 sheep received PDMS only coated plates and no biofilm (negative control). Table 8.1 provides a detailed description of the animals that were used and their specific treatments. Sheep were monitored on a daily basis using the same clinical grading system as outlined in Chapter 7.

8.2.4 Bone Labeling

Calcein was used in this study to double label the bone and determine the MAR in these sheep as was done in the pilot study.

8.2.5 Euthanasia and Sample Collection

Sheep were euthanized once they reached a 12-week end point or a Grade III infection. Microbiological samples, gross photographs, radiographs, MAR analysis, SEM analysis and histological analysis were collected and performed following the same protocols outlined in Chapter 7. However, in addition to swabbing the incision site and subdermal tissues, a swab of the cortical bone surface of each sheep was aseptically taken at the time of necropsy to determine if bacteria were still present on the surface of the bone. This swab covered approximately 1/2 $inch^2$ of surface area next to the SS plate that was selected for microbiologic analysis.

With respect to histological analysis, in addition to H&E staining, Sanderson's rapid bone stain was also used to stain PMMA sections in order to more accurately assess tissue response, bone quality, and regions of remodeling.

8.2.6 Statistical Analysis

From a Kaplan-Meier survival curve, a Log-Rank test was used to examine the statistical significance in survival times between those sheep treated with biofilm and those that were not. A separate Log-Rank test was used to compare the time it took for animals in each Group to become infected. Time to infection differed from survival time since many sheep in Group 1 survived the full 12 weeks of the study, but displayed signs of infection very early on.

Because the number of bacteria collected from PEEK membranes were not normally distributed, the nonparametric Kruskal Wallis test was used for analysis, as opposed to an ANOVA, to compare the number of bacteria that were collected on the

PEEK membranes of Group 1, Group 2 and Group 3 animals. In all instances, an alpha level of 0.05 was established to define statistical significance. All statistical data were analyzed using SPSS 17.0 software.

8.3 Results

8.3.1 Surgical Follow Up

A survival curve including each of the 27 sheep in this study was plotted using a Kaplan-Meier survival curve (Figure 8.1A). The reason that one sheep in Group 1, two sheep in Group 2 and three sheep in Group 3 went slightly longer than the 12-week end point was due to logistical reasons for euthanasia.

Three of the nine sheep in the PDMS only/biofilm treated group (Group 1) were euthanized early due to a Grade III infection. Two other sheep in Group 1 were euthanized just days prior to the 12-week endpoint, due to the fact that each of them had the operative leg break during routine observation. Both of these breaks occurred in the tibia near the inferior SS plate that had been implanted and it was believed that these breaks occurred as a result of osteomyelitis (Grade II infection) that had weakened the bone. These five sheep in Group 1 that were euthanized early did not receive a double label of calcein. The remaining four sheep in Group 1 survived to the 12-week end point. Each of those four sheep displayed Grade II signs of infection during the 12-week monitoring period. Furthermore, each of the nine sheep in Group 1 displayed signs of inflammation and abscess formation between day 3 and 18 after surgery.

Eight of nine sheep in Group 2 survived to the 12-week end point with minimal acute inflammation that resolved within the first week or two and no signs of infection at

any point in the study. One sheep from Group 2 was euthanized at 5 weeks due to a chronic limp that was not related to infection, but rather it appeared to have a small, incomplete fracture that may have developed due to surgery. This sheep did not receive a calcein double label.

One sheep from Group 3 had a large abscess develop 11 days following surgery and was euthanized as it displayed signs of a Grade III infection. This sheep likewise did not receive a calcein double label. The remaining eight sheep in Group 3 showed no signs of infection and their acute inflammation resolved within one or two weeks following surgery.

The Log-Rank test indicated that there was no statistically significant difference in survival times between any of the groups ($p=0.122$). There was no statistically significant difference in the time to infection between Group 2 and Group 3 sheep ($p=0.839$; Figure 8.1B). Yet there was a difference in the time to infection between Group 1 and both Group 2 ($p=0.000$) and Group 3 ($p=0.000$) sheep (Figure 8.1B). These differences corroborated with the microbiological data.

8.3.3 Microbiology

From the swabs that were taken of the subdermal tissues immediately after the SS plates had been secured to the bone during surgery, it was found that MRSA bacteria were released from the biofilm onto the bone surface and into the surrounding tissues within minutes after inoculation for Groups 1 and 2. No bacteria were cultured from those sheep in Group 3 at the time of surgery.

At necropsy, microbiological data showed that all sheep had between 1+ and 2+ growth of bacteria on their skin near the incision site. These were found to be normal

flora bacteria. All sheep in Group 1 had between 2+ and 3+ growth in the subdermal tissues and from the bone swabs. No sheep in Group 2 had growth in the subdermal tissue. The one sheep in Group 2 that was euthanized at 5 weeks did have one colony of MRSA growth from the bone swab that was taken, whereas none of the remaining eight that survived to 12 weeks had growth on the bone surface. Interestingly, the one sheep from Group 3 that had a large abscess and soft tissue infection had no growth in the subdermal tissues by culture. It was concluded that the infecting organism was not culturable by the methods used in this study. However, the clinical indications suggested that the tissue was highly infected. One additional sheep from Group 3 had growth of *Corynebacterium* from the bone swab, but never had indications of infection during the monitoring period. No other sheep from Group 3 had growth from the bone swab.

PEEK membranes collected from Group 1 sheep contained an overall $\log_{10}$ density of 6.11 ± 0.89 CFU/PEEK membrane. No bacteria were detected on the PEEK membranes of Group 2 sheep. There was no detectable growth on the PEEK membrane of the sheep in Group 3 that had a soft tissue infection. However, the same sheep from Group 3 that had growth from the bone swab also had 2.39 $\log_{10}$ CFU of *Alloiococcus otitis* and *Corynebacterium* on a PEEK membrane at the time of necropsy, but again that sheep did not show signs of infection during the 12-week monitoring period. When compared using a Kruskal Wallis test with the Mann Whitney U test used for post hoc analysis, it was found that there was no difference in bacterial numbers from PEEK membranes between Group 2 and Group 3 ($p=0.730$), whereas there was a difference between Group 1 and both Group 2 ($p=0.000$) and Group 3 ($p=0.000$).

These data indicated that the microbiological findings correlated with the clinical observations of the sheep, wherein those treated with biofilm and no CSA-13 (Group 1) suffered a Grade II or higher infection, and those treated with biofilm and CSA-13 (Group 2) did not suffer from infection. One sheep from Group 3 suffered a soft tissue infection and another had positive growth on the PEEK membrane and bone swab, but no signs of infection.

Notably, when removing the SS plates for microbiological analysis, it was observed that in each of the Group 1 sheep, the bone screws had become completely loose and in three animals the plates had lifted off the surface of the bone. This was due to bone resorption around the screws, which was a result of infection as indicated by SEM analysis and histological results (see SEM and Histology results). No screw or plate loosening was observed in Group 2 or Group 3 sheep and it was also interesting to observe that in Group 2 and Group 3 sheep, the cortical bone began to grow on/attach to the PEEK membranes, which made it difficult to remove them for quantification. In contrast, the PEEK membranes in the infected sheep had no attachment of bone to them and were easily removed.

8.3.4 Gross Photography/Radiographic Analysis

Gross photographs of the sheep limbs provided evidence that an abscess formed in the surgical area of Group 1 sheep (Figure 8.2A). No abscess formation was seen in sheep from Group 2 (Figure 8.2C) and only one had abscess formation in Group 3 (Figure 8.2E). Furthermore, signs of infected tissue, including pus and necrotic tissue, could be seen in Group 1 sheep once the skin was resected (Figure 8.2B). In contrast,

only a thin membrane of tissue grew over the plates in Group 2 (Figure 8.2D) and Group 3 (Figure 8.2F) sheep.

Radiographic evidence suggested that in Group 1 sheep, "moth eaten," osteomyelitic bone was visible (Figure 8.3A). This result was particularly apparent in the microradiographs that were taken of bone sections after they had been embedded and cut (Figure 8.3B). From these sections a significant cortical bone response and an endosteal response indicative of responsive new bone formation could be seen in Group 1 sheep. No such response was seen in Group 2 (Figure 8.3C, D) or Group 3 (Figure 8.3E, F) sheep.

8.3.5 SEM Analysis

In those sheep treated with biofilm and PDMS only coated plates (Group 1), BSE images indicated that there was a considerable amount of bone resorption directly underneath the SS plates with sequestrum formation caused by the presence of biofilm (Figure 8.4A). Similar patterns of resorption were seen near the bone screws (Figure 8.4B), which supported the observation mentioned previously that these screws were loose due to bone resorption caused by osteomyelitis. There were no screws loose in those sheep treated with CSA-13 (Group 2). In addition, the cortical bone surface that had been in direct contact with biofilms on PEEK membranes appeared to be viable in all nine sheep from Group 2 (Figure 8.4C). In the screw regions of Group 2 sheep, bone remodeling had occurred consistent with surgical trauma (Figure 8.4D). In those sheep that were treated with PDMS only coated plates and no biofilm (Group 3), bone remodeling was seen directly underneath the SS plates and near the screws similar to the CSA-13 treated sheep (Figure 8.4E & F).

A larger gap of fibrous and inflammatory tissue was seen between the cortical bone surface and SS plate of Group 1 sheep when compared to Group 2 or Group 3. More specifically, the distance from the bone to the plate surface in Group 1 was ~1,179 ± 1,257 microns. In Group 2 and Group 3, the gap was 316 ± 382 and 456 ± 313, respectively. As will be seen in the histopathological results, the larger gap in Group 1 sheep was due to fibrous tissue formation and chronic inflammation related to the presence of infection that was confirmed by microbiological sampling.

8.3.6 MAR Analysis

MAR results indicated that in Group 1 sheep, the average bone remodeling rate directly underneath the SS plate was 1.71 ± 0.12 μm/day. In Group 2 sheep the average rate was 1.53 ± 0.32 μm/day and in Group 3 sheep, the average was 1.31 ± 0.15 μm/day. The MAR of host bone in the cortical region opposite of the SS plates were 1.19 ± 0.09 for Group 1, 1.06 ± 0.16 for Group 2, and 1.00 ± 0.15 for Group 3. Images of double labels in the periosteal regions of Group 1 sheep showed that an intense remodeling response was present (Figure 8.5A). Importantly, no double labels were seen in those areas where bone chips/and or sequestra were located (Figure 8.5B, C & D) suggesting that the bone chips and sequestra were not viable. This was likely due to the presence of biofilm bacteria on PEEK membranes that caused sequestra to form and killed the bone. Typical double labels of osteons were seen in the cortical bone regions of the host bone (Figure 8.5E).

In Group 2 sheep, double labeled osteon structures were present in the cortical bone region where bacteria had been placed indicative of bone remodeling (Figure 8.5E).

A similar response was seen in Group 3 sheep and bone was observed growing into the interstices of the PEEK membrane (Figure 8.5F). Notably, calcein double labels indicated local/regional bone viability in all Groups.

8.3.7 Histological Analysis

Histological sections from Group 1 sheep corroborated with the radiographs and SEM images. There were signs of "moth eaten" bone, a significant inflammatory response, and fibrous tissue formation (Figure 8.6A). In addition, multiple foci of sequestra were detected and necrotic bone that preceded sequestrum formation was seen (Figure 8.6A). Sheep in Group 1 that were euthanized within one or two weeks of surgery had early signs of bone resorption and necrosis, but it had not yet progressed to the point of sequestrum formation (Figure 8.6B). Nevertheless, inflammatory cells were present in the area where the biofilm-ridden PEEK membrane had been placed, fibrosis had occurred and there were signs of responsive new bone formation in the periosteal and endosteal regions (Figure 8.6B).

Group 2 sheep did not show signs of necrotic tissue in those regions that were in direct contact with PEEK membranes that had biofilms on them (Figure 8.6C). Rather the bone was viable, remodeling and there were few inflammatory cells and a reduced fibrous capsule compared to Group 1 sheep (Figure 8.6D). The results of Group 2 were similar in Group 3 sheep (Figure 8.6E & F).

Table 7.1, which was used to grade histological sections in the pilot study from Chapter 7, was used once again to grade the histological sections from these sheep. The results for this portion of the study are provided in Table 8.2. This table shows the

number of sheep from each group and the degree to which inflammation, necrosis and cortical bone response were present. Significant inflammation was present in Group 1 sheep, with mild to moderate inflammation mostly present in Group 2 and Group 3 sheep. Seven out of nine sheep from Group 1 had necrotic bone and/or multiple foci of sequestra underneath SS plates. No sheep from Group 2 showed signs of necrosis or sequestra in bone underneath the SS plate. Likewise, no signs of necrotic bone or sequestra were present in Group 3 sheep. A cortical bone response was present in all sheep near the edges of SS plates and was a natural result of surgical trauma.

8.4 Discussion

In order to address previous limitations that have accompanied the development of active release coatings (see Chapter 2, section 2.5.3), this study was designed to test a novel active release coating by exposing it to well-established biofilms of MRSA as opposed to planktonic bacteria. The fact that CSA-13 was able to prevent infection in 100% of sheep in Group 2 indicated that the *in vitro* work (see Chapter 5) was performed in a translational manner. Taken together, these *in vitro* and *in vivo* studies have the potential to influence the development of antimicrobial coated devices in the future.

Perhaps the most telling difference between the sheep in Group 1 that were treated with PDMS only coated plates and biofilms, and the other two groups of sheep was the microbiologic data. More specifically, the fact that only one colony of bacteria was detected in a single sheep in Group 2 and 0% were infected strongly indicated that CSA-13 acted as a potent active release agent within the PDMS-based coating system to prevent biofilm implant-related osteomyelitis. Furthermore, the fact that one sheep out of

nine (11%) became infected in the negative control group, i.e., those that had PDMS only coated implants and no biofilm (Group 3), provided further evidence that CSA-13 had the ability to prevent infection that may have been related to the surgical procedure itself.

Sheep in Group 1 displayed multiple signs that were indicative of chronic osteomyelitis. For example, multiple foci of sequestra could be seen from SEM and histologic analysis, the bone surface was "moth eaten" in the majority of sheep in that Group, very high inocula of bacteria were confirmed to be present in the subdermal tissues, on the bone surface and on the PEEK membranes of all nine sheep, and the infection seemed to progress slowly over time similar to what has been observed with chronic osteomyelitis clinically when biofilm was present.[16]

No signs of osteomyelitis were present in Group 2 sheep. In contrast, despite the fact that the cortical bone surface in this Group of sheep had been directly exposed to PEEK membranes that had biofilms grown on them, the bone surface of each sheep appeared healthy with signs that bone was remodeling. This further indicated that CSA-13 did not have a toxic effect to the bone. Furthermore, although there was minimal foreign body response, the surrounding tissue regions showed no signs that CSA-13 had an adverse effect on tissue healing and the ability of bone to remodel.

Despite one soft tissue infection in a sheep from Group 3, no sheep in that Group suffered from osteomyelitis and the bone was able to grow throughout the interstices of the PEEK membrane, suggesting that the PEEK may have had an osteoconductive effect.

Similar to the results that were seen in the pilot work to establish this animal model, all sheep that were treated with biofilm in Group 1 became infected. This result further established the consistency with which this animal model may be used for future

testing of biomaterial device development and chronic osteomyelitis for other types of applications.

From the histological grading scale, it was apparent that those sheep with PDMS only coated plates and no biofilm had the least amount of inflammation, necrosis and cortical bone response. This was likely due to the fact that Group 1 and Group 2 sheep had bacteria present. Although CSA-13 was able to prevent infection, results from the histological grading scale indicated that bacteria still had time to cause a moderate to significant inflammatory response to develop in four sheep. Nevertheless, it may be that if these animals were monitored for longer than 12 weeks, the inflammation may have reduced over time.

In conclusion, the results of this definitive animal study indicated that CSA-13 may have significant promise to be used as an active release agent to prevent biofilm implant-related infections. Furthermore, in addition to work that is currently being performed by Dr. Paul Savage's group, which has demonstrated that CSA-13 has a low risk of toxicity, this work demonstrated that CSA-13 may be used safely as an active release agent. As this active release coating is developed further, it may have the ability to help reduce rates of infection that adversely affect the use of fracture fixation devices as well as other biomedical materials.

Table 8.1: Outline of the different groups of sheep, the number of animals in each group, the coating type that was present in each and whether or not they were treated with biofilm.

Group (Number of Animals)	**Coating Type**	**Biofilm Treatment**
Group 1 - Positive Control (n=9)	PDMS Only	Biofilm
Group 2 - Treatment Group (n=9)	PDMS/CSA-13	Biofilm
Group 3 - Negative Control (n=9)	PDMS Only	No Biofilm

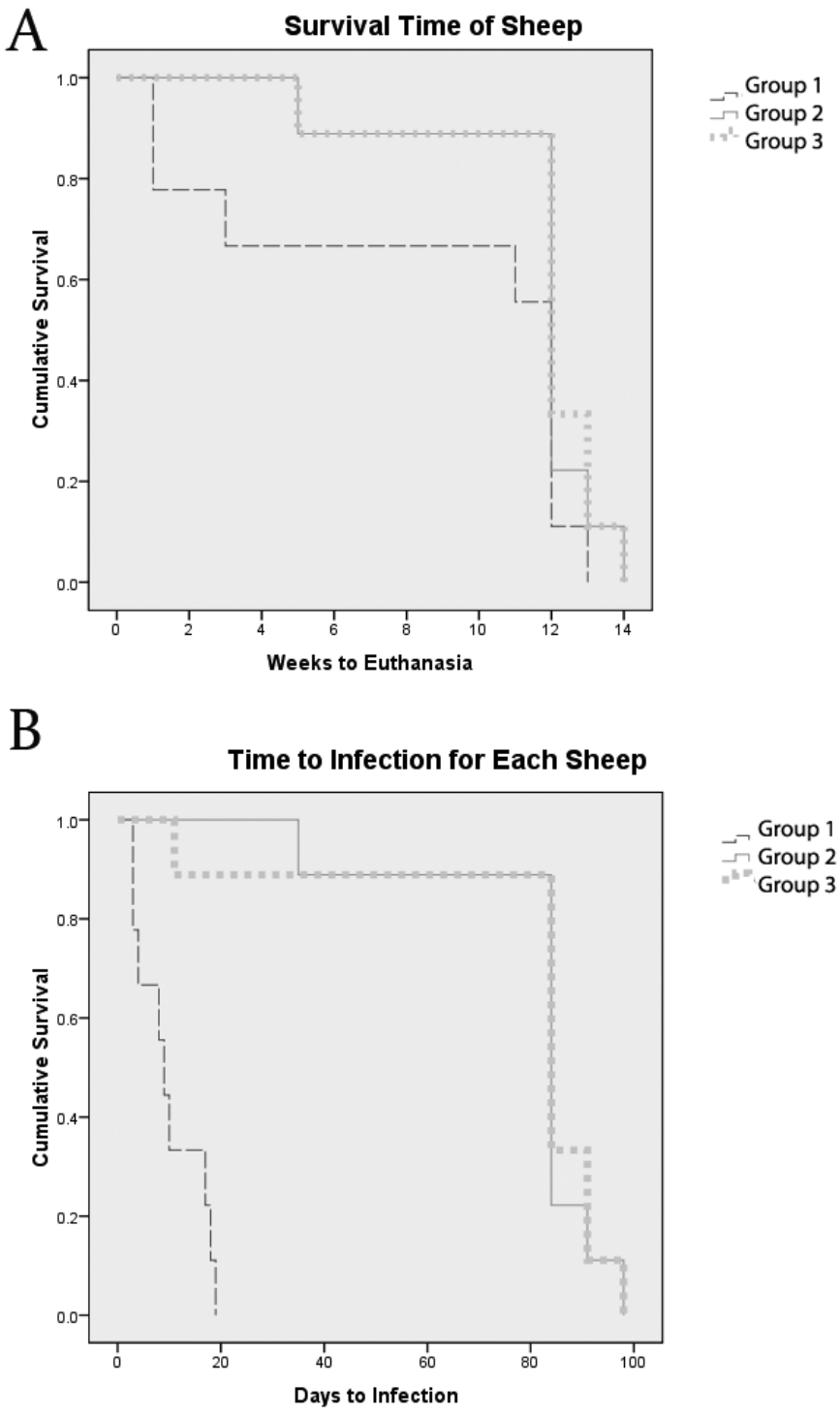

Figure 8.1: Kaplan-Meier curves indicating the survival and time to infection of each animal in the definitive study group. (A) Kaplan-Meier survival curve outlining the number of weeks that each sheep survived during the course of the study. (B) Kaplan-Meier curve indicating the time it took for each sheep to show signs of infection.

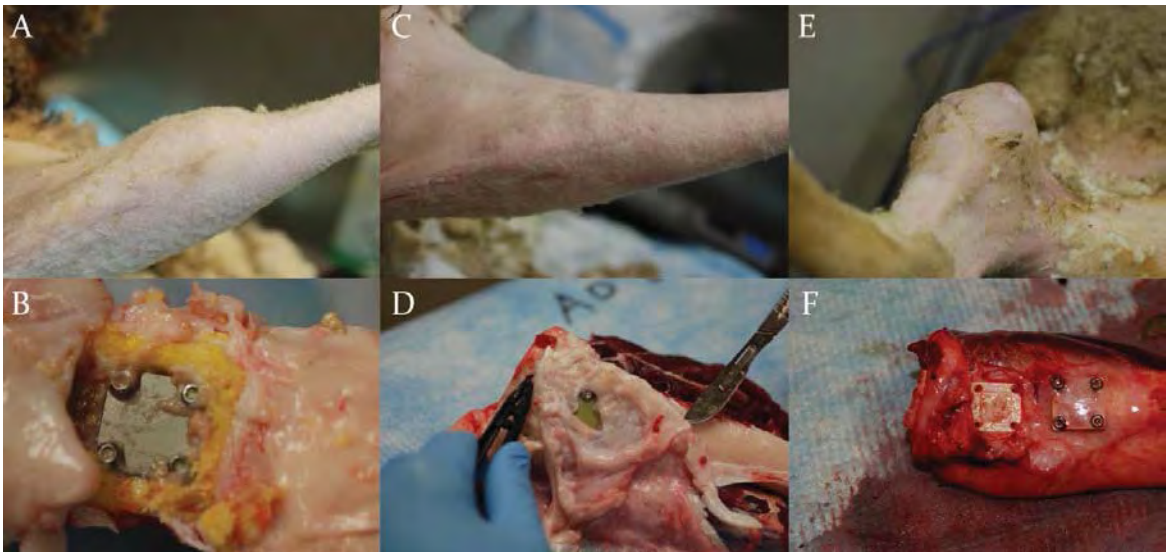

Figure 8.2: Photographs of the tibiae of sheep indicating infection and lack thereof amongst the different animal Groups. (A) Photograph of an abscess that was present in the proximal medial aspect of a sheep tibia from Group 1. (B) Photograph of the subdermal tissue of a sheep from Group 1. Note the presence of necrotic (brown next to plate) and inflammatory tissue (yellow). (C) Photograph of the proximal medial aspect of a sheep tibia from Group 2. (D) Photograph of the subdermal tissue in a sheep that was treated with CSA-13. The yellowing of the plate was likely due to the calcein green that was injected. A thin membrane of tissue had grown over the plates. (E) Photograph of the abscess that was present in the one sheep from Group 3 that had a soft tissue infection. (F) Photograph of the subdermal tissue in a sheep from Group 3. One plate had been removed prior to this picture being taken, but note the thin fibrous membrane that was still intact over the other SS plate.

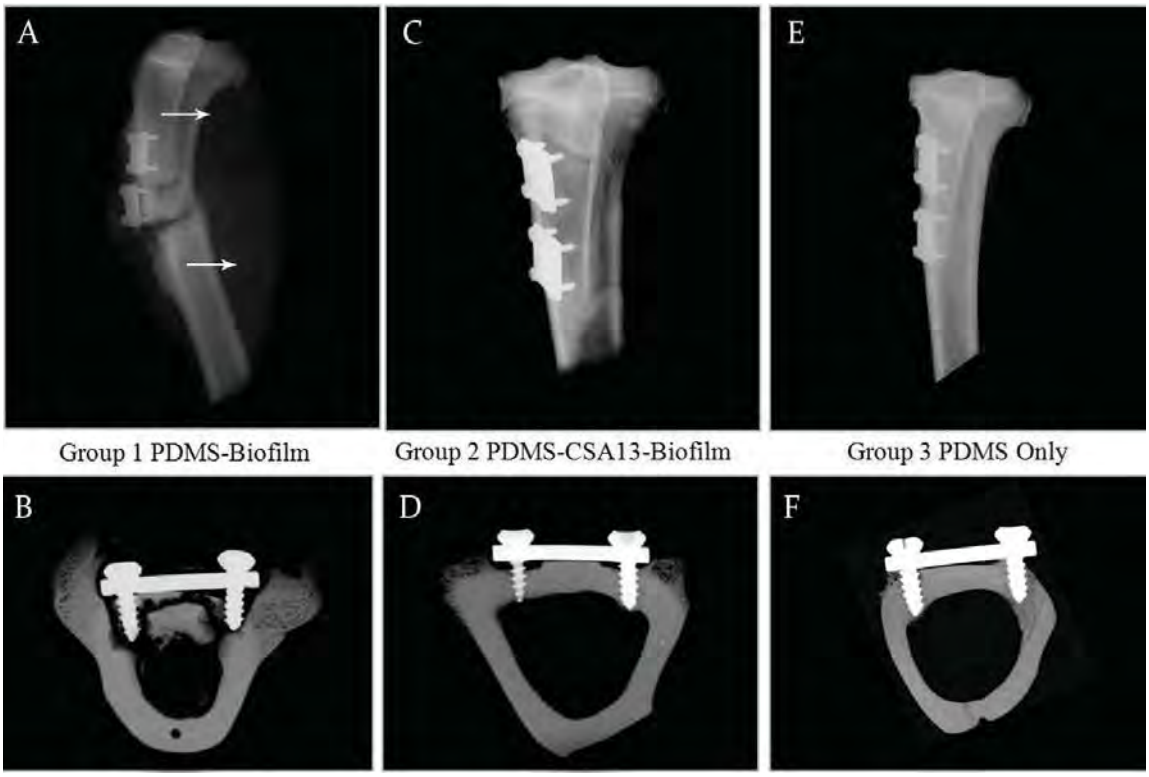

Figure 8.3: Representative radiographs indicating osteomyelitis and lack thereof in sheep from each Group. (A) Radiograph of the tibia of a sheep from Group 1 that suffered from osteomyelitis. This radiograph is from one of the sheep that broke its leg during a routine checkup. Note the "moth eaten" bone in the inferior and superior regions of the SS plates (arrows). (B) Microradiograph of a bone section (Group 1 sheep) that was cut after it had been embedded in PMMA. This radiograph provides evidence for why the bone screws were loose in Group 1 sheep; the screws had lost contact with the host bone. The infection had caused the screws to come loose, contributed to resorption of bone throughout the cortical bone regions, which led to the "moth eaten" appearance. (C) Radiograph of a tibia from a sheep that was treated with CSA-13-coated plates (Group 2). (D) Microradiograph of a bone section from a sheep treated with CSA-13-coated plates. The edging effect that is seen near the bone screws was consistent in all nine sheep from Group 2. (E) Radiograph of a tibia from a sheep in Group 3. (F) Microradiograph of a bone section from a sheep in Group 3.

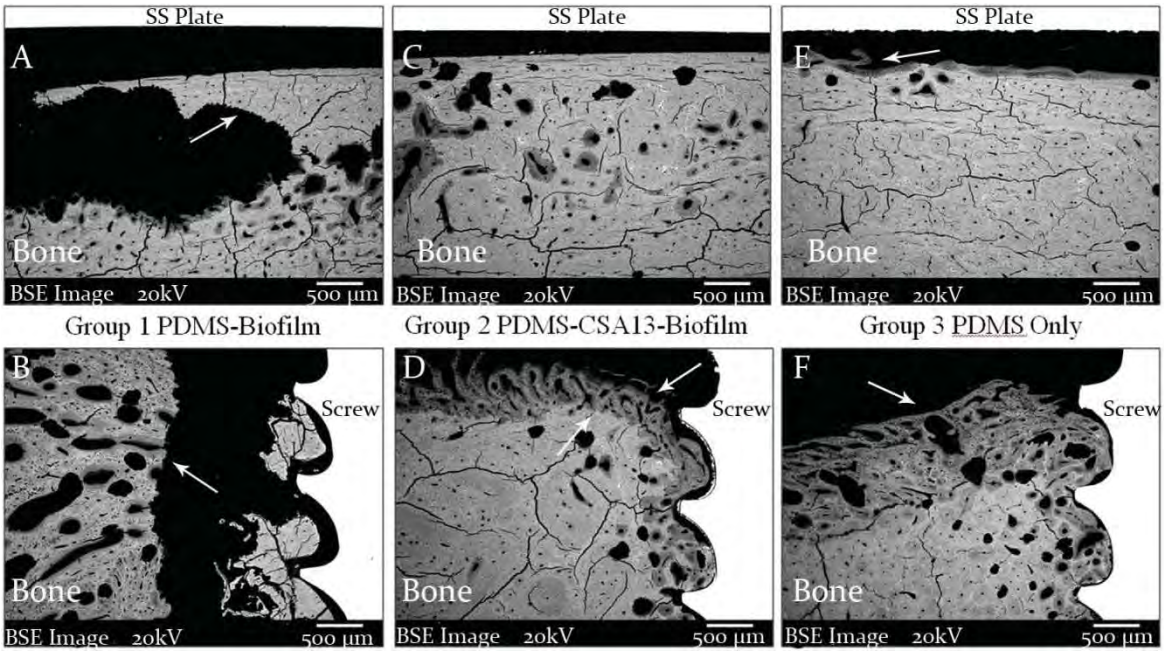

Figure 8.4: SEM images of bone directly underneath SS plates and near cortical bone screws in sheep from each Group (all 30x original magnification). (A) SEM micrograph of the cortical bone surface directly underneath a SS plate that was from a sheep in Group 1. The arrow indicates an area of significant resorption that likely prefaced the formation of a sequestrum in the periosteal region. Resorption was indicated by the presence of jagged bone edges as a result of osteoclast activity and infection (as will be seen in the Histology section). Cracks that can be seen in the bone were an artifact of processing. (B) SEM micrograph of an area near a bone screw in a sheep from Group 1. The arrow again indicates an area of resorption. Note the presence of bone chips next to the screw and the gap between the bone chips and the resorbed bone surface. This gap provided an indication as to why the screws were loose in Group 1 sheep. (C) SEM micrograph of a cortical bone surface underneath a SS plate from a sheep in Group 2 (CSA-13 treated). The bone surface itself looked healthy and had no signs of resorption in the area where bacteria had been placed. (D) The arrow that is facing up in this SEM micrograph indicates the jagged border where bone resorption had occurred whereas the arrow that is facing down points to the new bone that formed. The screw was in close contact with the bone surface. (E) SEM micrograph of the cortical bone surface underneath a SS plate that had been coated with PDMS only. Minor areas of remodeling were seen in this region of sheep from Group 3. (F) SEM micrograph of a bone region from a sheep in Group 3. Bone remodeling was seen (arrow), but there were no indications that resorption had occurred as it had in Group 2 sheep. The remodeling in this bone was likely a result of surgical trauma, and the bone grew close to the screw surface.

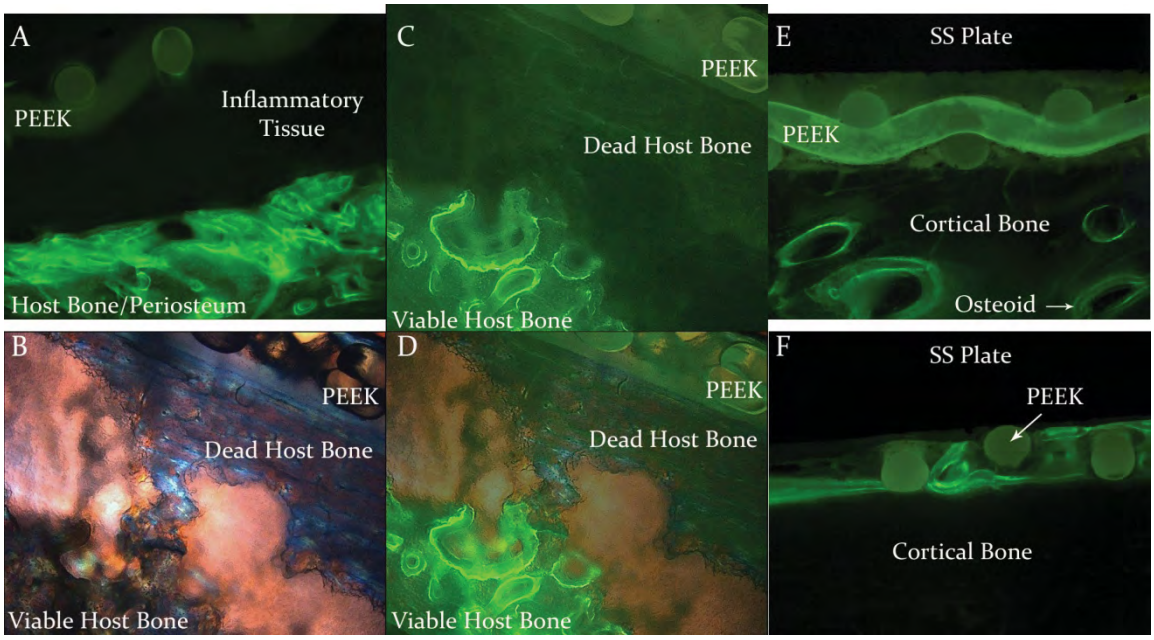

Figure 8.5: MAR images of infected bone, remodeling bone and cortical bone in representative sheep from each Group. (A) Fluorescent microscope image of calcein double labels that were present in the periosteal region directly underneath a SS plate of a sheep from Group 1. Initially, the PEEK membrane that had biofilm grown on it was placed in apposition to the host bone. Inflammation and fibrous capsule formation caused the PEEK membrane and the SS plate to lift off the surface of the bone. Periosteal growth in Group 1 sheep was highly responsive as a result of infection. (B) Polarized light image of a sequestrum in a sheep from Group 1. (C) Same image as in (B), but with fluorescent double labels. (D) Combined image of (B) and (C). Areas of viable bone and dead bone are labeled. Viable areas are indicated by the presence of calcein labels whereas dead bone is void of double labels. The PEEK membrane can be seen in apposition to the dead host bone. (E) Fluorescent microscope image of calcein double labels in the periosteal/cortical bone region of a sheep from Group 2. Note the lack of periosteal response and typical osteoid growth despite the fact that bacteria had been present on the PEEK membrane. (F) Fluorescent microscope image of the periosteal/cortical bone region of a sheep from Group 3. This image demonstrates how the bone grew throughout the interstices of the PEEK membrane without any significant periosteal response.

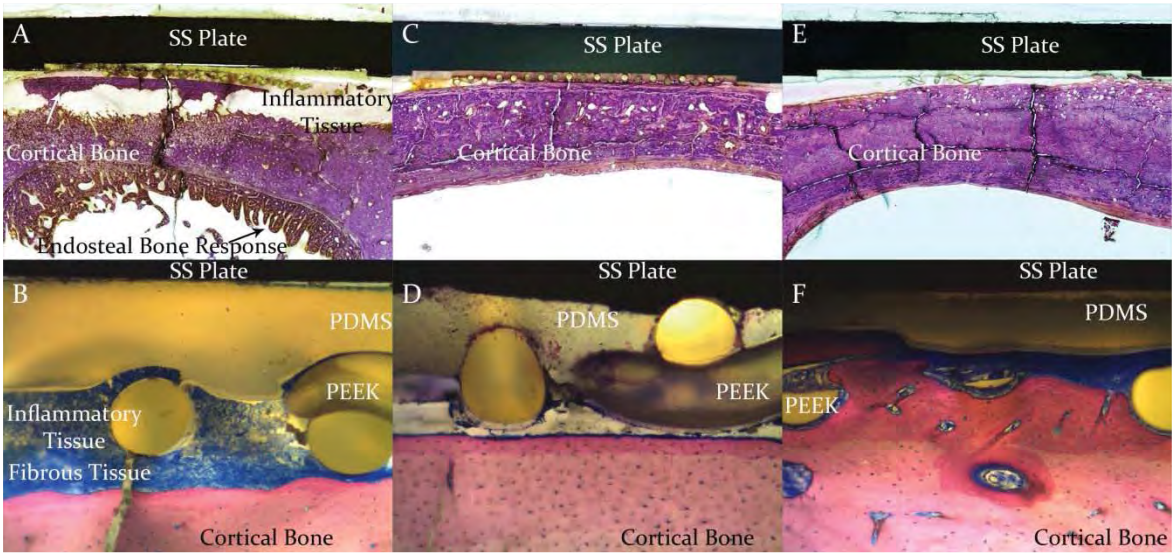

Figure 8.6: Images of histological sections from representative sheep in each Group. (A) H&E stained section of bone embedded in PMMA. The SS plate can be seen at the top of the picture; the white arrow points to an area of necrotic bone that likely prefaced the formation of a sequestrum. The black arrow points to the significant endosteal bone response and a similar response could be seen in the periosteal region underneath the plate. (B) Bone section stained with Sanderson's rapid bon stain. Inflammatory cells and a fibrous capsule can be seen in the area where a PEEK membrane with biofilm had been placed. Early signs of bone necrosis were seen in this section as indicated by the wavy morphology of the bone that likely preceded resorption. (C) H&E section of bone from a sheep in Group 2. In contrast to the sheep from Group 1, the bone was healthy even after being exposed to a PEEK membrane that had biofilm on it. (D) Sanderson's bone stain of a sheep from Group 2. Despite the fact that bacteria had been present on the PEEK membrane, there was minimal foreign body reaction and the bone surface was healthy. New bone formation was indicated by the darker pink area of bone that was not yet mineralized. Mineralized bone is lighter pink after Sanderson's bone staining. (E) H&E section of bone from a sheep in Group 3. This bone was also healthy in an area where the PEEK had been present. (F) Sanderson's bone stained section from a sheep in Group 3. The newly forming bone could be seen integrating throughout the interstices of the PEEK membrane. Inflammatory cells could be seen in this section as a natural response to a foreign body (PEEK and SS plate) being present.

Table 8.2: Results of comparing the histological sections of each sheep to Table 7.1 provided in Chapter 7. These results indicated that inflammation was present in sheep from all groups, with the highest level of inflammation being present in Group 1 sheep. Furthermore, bone necrosis was primarily seen in sheep from Group 1. A cortical bone response was also seen in sheep from each group, but this was a normal response to surgical trauma.

Inflammation	**# of Sheep From Group 1**	**# Sheep From Group 2**	**# Sheep From Group 3**
0	0	1	5
1	2	4	3
2	3	3	1
3	0	1	0
4	4	0	0
Bone Necrosis			
0	2	9	9
1	0	0	0
2	2	0	0
3	0	0	0
4	5	0	0
Cortical Bone Response			
0	2	2	3
1	3	1	5
2	2	4	0
3	1	1	0
4	1	1	1

CHAPTER 9

CONCLUDING REMARKS

9.1 Dissertation Highlights

Considered together, the work that was performed in this dissertation has led to or may lead to five areas of development that have the potential to contribute to the fields of bioengineering and biofilm research. The first was the development of an animal model that has the potential to contribute to the future development of combination biomedical materials with active release antimicrobial coatings, biofilm implant-related infection studies, other biofilm-related infection studies and clinical infection prevention strategies.

After a careful literature search, the animal model developed in this project appears to be the first model to incorporate well-established biofilms of MRSA that were grown under fluid sheer forces in a biofilm reactor as initial inocula in order to model the predominant phenotype of bacteria from natural ecosystems that have the potential to contaminate open wound sites. One of the most exciting aspects of this model is that it may provide additional insight into how biofilm infections develop over time in a slow, chronic and somewhat mild fashion similar to what is seen in clinical settings.

The second contribution was the development of an active release coating that incorporated a novel antimicrobial compound as its active release agent and which was effective in preventing infection in 100% of animals that were treated with viable

biofilms of MRSA. Currently, there are a limited number of biomedical devices or products that utilize active release coatings. As outlined in Chapter 2, it is believed that there is a paucity of active release coatings in clinical use due to three important limitations. To reiterate, these are a dependence on MIC values to treat biofilm-related infections, inaccurate *in vitro* tests that do not model physiologically relevant environments and the use of planktonic bacterial cells as initial inocula as opposed to bacteria that reside in the biofilm phenotype as they do in natural ecosystems. The work that was performed in this dissertation addressed each of these limitations and the data indicated that in doing so, an active release coating was developed with *in vitro* and *in vivo* success. Importantly, the *in vivo* work in this study, and other work that has been performed by Dr. Paul Savage's group (unpublished data), have shown that CSA-13 has limited to no toxic effects on host cells and tissues. These data may have significant future implications to translate this coating for FDA approval in human clinical trials.

The third contribution was the development and use of a flow cell system to optimize and test the efficacy of an active release coating on SS plates under *in vitro* conditions. The *in vitro* conditions were specifically designed to model the *in vivo* environment in which the coated SS plates would be tested. These tests suggested that an 18% w/w concentration of CSA-13 would be needed to effectively eradicate biofilms of MRSA to less than 10^2 cells in a 24-hour period. These findings were particularly important compared to the preliminary work that was done with the CSA-13 active release coating in stagnant broth solutions. In stagnant broth solution, only 10% w/w CSA-13 was needed to reduce MRSA biofilms to similar levels. Thus, the fact that higher amounts of CSA-13 were needed to eradicate biofilms under flow conditions

supported the proposal that when stagnant broth solutions are used by investigators, they may not adequately reflect the amount of antimicrobial that may be necessary to eradicate biofilms.

The *in vitro* work further highlighted the fact that MIC values are limited when it comes to fighting biofilm implant-related infection. In this study, the *in vitro* work suggested that the concentration of CSA-13 that was needed to eradicate biofilms ranged from approximately 60 μg/mL in the first 4 hours to approximately 20 μg/mL by 24 hours. By comparison, the MIC of CSA-13 against planktonic cells of the MRSA isolate that was used in this study was found to be 0.25 μg/mL. In order to kill biofilms of MRSA, CSA-13 had to be present in concentrations that were 85x - 240x greater than the MIC. This same trend is very commonly seen with antibiotics as was shown by Nickel *et al*. (refer to Chapter 1) and others. Their work has shown that it is very common for concentrations of antibiotics to be required at several hundred to more than a thousand times their MIC values to be even marginally effective against biofilms.

Perhaps the most poignant aspect of the *in vitro* work that was performed in this dissertation was the fact that it translated well to the *in vivo* animal model. This was shown by the fact that when CSA-13 was used as an active release agent, it was able to prevent osteomyelitis in 100% of the animals in which it was tested. These *in vivo* results supported the hypothesis that an 18% w/w concentration of CSA-13 would be sufficient to reduce the number of bacteria in a biofilm to clinically acceptable levels. Thus, the *in vitro* system that was developed may be used by other investigators to more effectively perform initial *in vitro* work that is intended to develop biomedical devices with active release coatings in a translational manner, though further *in vitro* and *in vivo*

investigations using different coatings and antimicrobials will be required to confirm this hypothesis.

The fourth contribution that has the potential to extend from this project was the development of a membrane biofilm reactor. After a careful literature search, this reactor appears to be the first biofilm reactor to have been developed with the specific intent of growing biofilms that can be used as initial inocula in an animal model of biofilm-related infection. Importantly, the reproducibility of this reactor directly corresponded to the protocol that was rigidly followed to grow biofilms on the surface of PEEK membranes. There are two major benefits that may accompany the development of this reactor and they are 1) the size of PEEK membrane can be modified in this reactor to grow essentially any number of bacteria that an investigator desires. 2) An investigator can change the type of material such that instead of using PEEK, biofilms could be grown on a different type of polymeric material, metallic material or even on a biological sample(s). Thus, this reactor is diverse and has the potential to lead to a variety of applications in biofilm research, antimicrobial and combination biomaterials development.

The fifth important aspect of this work that may have the potential to expand the literature was the use of a novel antimicrobial compound, CSA-13, that demonstrated significant potential to address the limitations of current antibiotic therapies. Pharmaceutical companies are currently at a standstill with regard to developing additional antibiotics and/or antimicrobials for clinical use. There are three main reasons for this standstill. 1) Regulatory costs are prohibitively expensive for companies to produce new drugs. 2) Companies are concerned that bacteria will quickly develop

resistance to any new antibiotic that is introduced, which would ultimately result in reduced sales of a product. 3) Despite the fact that an antimicrobial compound may be highly effective against bacteria, manufacturing costs may cripple the ability of a compound to be produced on a commercial scale. With the exception of the regulatory costs that are associated with drug or device development, CSA-13 may have the ability to address the latter two limitations.

Due to its rapid attack and nonspecific method of action against bacteria, CSA-13 carries a significantly reduced risk of engendering bacterial resistance compared to traditional antibiotic compounds. It can also be manufactured on a commercial scale for a fraction of the cost that other compounds require to be manufactured. In addition, based on the results of the animal work in this study, in conjunction with much of the testing that has been done by Dr. Savage and his colleagues, CSA-13 appears to have limited toxic effects to eukaryotic cells at bactericidal concentrations. All of these properties of CSA-13 are promising and suggest that it may be effective when used as an active release agent of biomedical device coatings.

9.2 Future Work

There are several important projects that need to be performed in order to validate and add upon the work that was completed in this dissertation. To date, the work that has been done with CSA-13 has shown that it is a very promising antimicrobial as far its efficacy is considered. The next step, then, will be to demonstrate that CSA-13 is a safe product to use. Studies to test the safety of CSA-13 are in fact already under way. This dissertation encompassed the first half of a NIH-funded project. The second half of the

funded project has been designed to test the safety of CSA-13. To do so, three tests will be performed. First, the effect of CSA-13 on fracture healing will be determined. This will be done by creating an osteotomized fracture in a group of sheep that will be reduced with a fracture fixation plate that is coated with the CSA-13 active release coating. Another group of animals will have a fracture reduced with a plate that is uncoated. At the endpoint of this study, the sheep bones will be tested mechanically using a four-point bend test to determine the strength of fractures. As such, it will be determined if CSA-13 has any adverse effect on fracture healing. Second, in conjunction with fracture healing analysis, end organ analysis will be performed. This will be done with tritiated CSA-13. As samples of end organs and tissues are collected, the amount of CSA-13 will be determined by scintillation counting. The third method by which the safety of CSA-13 will be determined has already taken place. This was done by performing surgeries on a group of sheep that were treated with SS plates coated with the CSA-13 active release coating in the absence of bacteria. This was done to determine the effect of CSA-13 alone on host tissue(s) in the absence of a fracture and in the absence of bacteria.

In addition to these studies, plans are also underway to test the active release coating that was developed in this project on a variety of other biomedical devices including total joint replacement devices, intramedullary nails, external fixators, catheters, endotracheal tubes, etc. The efficacy of CSA-13 as a wound care product, lavage solution, injectable solution and systemic antimicrobial is also being investigated.

All in all, Dr. Bloebaum's group has met with multiple biomedical device companies that have shown tremendous interest in the CSA-13 technology that has been developed as part of this dissertation. At this time, negotiations are currently in progress

between venture groups, investors, companies and the University of Utah to develop a collaborative effort that can translate CSA-13 to clinical applications. Thus, the future outlook is bright for CSA-13 to potentially help millions of patients who suffer from biofilm implant-related infections.

9.3 Conclusion

It is likely safe to say that when Antony van Leeuwenhoek observed animalcules for the first time, he did not foresee this day, wherein those animalcules would be defined as biofilms that are now known to have dramatic influence on the daily life of each human being. Similarly, if Aristotle were able to now see the functions of the world, he would perhaps be dumbfounded that spontaneous generation, or Aristotelian abiogenesis, continues to be disproven in dramatic fashion by the copious amounts of data that suggest that life does not arise *ex nihilo*. In stark contrast, Dr. Bill Costerton has had the opportunity to directly observe the impact that his research has had on the world. As such, he, along with the rest of the scientific community, has had the ability to see that biofilms may adversely or beneficially influence many facets of life.

As far as their beneficial influence is concerned, biofilms aid in sewage treatment, plant growth, plant and human waste decomposition, oxygen production, and gastrointestinal functions of all known animal species. Unfortunately, if biofilms come in contact with tissues that have not evolved to coexist in a beneficial manner, these tissues are at significant risk to become infected due to the fact that biofilms "see" these tissues as carbon and energy sources. Infection becomes even more problematic if a biomedical device has been implanted in a human patient. In this instance, in addition to having a

carbon and energy source, an abiotic, colonizable surface is presented to biofilms, to which they preferentially adhere. This paradigm leads to biofilm implant-related infection that constitutes one of the most difficult-to-treat pathologies in current healthcare systems.

Antibiotics are becoming ever more limited in their ability to address this problem due to their lack of efficacy against bacteria that reside in the biofilm phenotype. The future outlook is bright, however, as investigators discover and develop novel antimicrobial compounds that specifically address the limitations of antibiotics. One of the most promising of these novel antimicrobial compounds is CSA-13. Currently, there are multiple NIH-funded studies that are taking place to further test the efficacy of CSA-13, manufacture it on a commercial scale, and at least one study is taking place to test the safety of CSA-13 in human trials. To date, the results of these projects have strongly suggested that CSA-13 will be able to be manufactured on a commercial scale at relatively low cost, that it is highly efficacious against planktonic and biofilm bacteria both *in vitro* and *in vivo* and that it may have limited toxicity *in vivo*.

Although the author is candidly aware that future testing must be performed to validate these findings, there is reason to be optimistic that CSA-13 may be an effective alternative to current combination antibiotic therapies; in particular for it to be used in a novel active release coating to prevent biofilm implant-related infections in patients who are implanted with a biomedical device(s).

APPENDIX A

USING BIOFILMS AS INITIAL INOCULA IN ANIMAL MODELS OF BIOFILM-RELATED INFECTION

212
Society For Biomaterials

Review

Using biofilms as initial inocula in animal models of biofilm-related infections

Dustin L. Williams,[1,2,3] J. William Costerton[4]

[1]George E. Wahlen Department of Veterans Affairs Medical Center, Salt Lake City, Utah
[2]Department of Bioengineering, University of Utah, Salt Lake City, Utah
[3]Department of Orthopaedics, University of Utah, Salt Lake City, Utah
[4]Center for Genomic Sciences, Allegheny-Singer Research Institute, Pittsburgh, Pennsylvania

Received 27 July 2011; revised 13 September 2011; accepted 24 September 2011
Published online in Wiley Online Library (wileyonlinelibrary.com). DOI: 10.1002/jbm.b.31979

Abstract: One of the most practical strategies that has been undertaken to fight biofilm implant-related infections has been the development of coatings on biomaterial devices that can elute antimicrobials into regions of patients' tissues. To date, the majority of animal studies that have been developed to model infections that accompany the use of these materials have primarily involved an initial inoculum of planktonic bacterial cells from batch cultures. Although valuable, data that have been derived from these experiments may not provide important clinical insight into how bacteria in well-established, mature biofilms impact device-related and other clinical infections when they contaminate a patient site or implanted device. In this review, a discussion is presented on the impact that a shift in biofilm research may have if initial inocula of well-established, mature biofilms are used to model biomaterial device-related infections in animal models. © 2011 Wiley Periodicals, Inc. J Biomed Mater Res Part B: Appl Biomater 00B: 000–000, 2011.

Key Words: initial inocula, planktonic, biofilm, future research, animal model

How to cite this article: Williams DL, Costerton JW. 2011. Using biofilms as initial inocula in animal models of biofilm-related infections. J Biomed Mater Res Part B 2011: 00B: 000–000.

THE USE OF PLANKTONIC CELLS IN ANIMAL MODELS

Currently, combination biomaterials and coatings are being developed for the treatment and prevention of biofilm-related infections. The majority of animal studies that are used to model infections related to these materials primarily involve the use of an initial inoculum of planktonic bacterial cells from batch cultures.[1–24] The expectation has been that these planktonic cells would attach to the surface of a biomaterial, medical device, or surrounding tissue and subsequently form a biofilm. Although valuable, data that have been derived from these experiments may not provide clinicians and biomaterials scientists additional clinical insight into how bacteria that reside in well-established, mature biofilms impact device-related and other human infections when they initially contaminate an implant site.

Following several decades of important observations from investigators that bacteria preferentially adhere to solid surfaces and to one another,[25,26] in 1978 Costerton et al. formally hypothesized that bacteria in nature reside primarily in the biofilm phenotype.[27] Strong support for this hypothesis continues to be shown in the literature that involves collecting, analyzing, imaging, and characterizing bacterial biofilms found in nature, human tissues, and clinically retrieved devices.[28–34] Additionally, since the initial hypothesis of Costerton et al., estimates have suggested that 99.9% of bacteria in natural ecosystems reside in the biofilm phenotype.[35] Intriguingly, The Centers for Disease Control has estimated that 65% of all infections in humans are biofilm related.[36] A public announcement from The National Institutes of Health placed that estimate at 80% (see announcement PA-07-288).

On the basis of these observations and information, it is important to consider that when bacteria come in contact with wound sites, biomaterials, or portals of entry in humans, that is, inoculate patients, there is strong evidence to suggest that the majority of these bacteria are inherently residing in well-established, mature biofilms. A specific example of this scenario is that of a patient who suffers

Correspondence to: D. L. Williams; e-mail: dustin.williams@utah.edu
Contract grant sponsor: National Institute of Arthritis and Musculoskeletal and Skin Diseases; contract grant number: R01AR057185.
Contract grant sponsor: Office of Research and Development, Rehabilitation R&D Service.
Contract grant sponsor: George E. Wahlen Department of Veterans Affairs, Salt Lake City, UT

from a Type IIIB open fracture, which is reduced with a fracture fixation device.

A Type IIIB severe fracture has been defined by Gustilo et al.[37] as having "extensive soft-tissue injury loss with periosteal stripping and bone exposure" that "is usually associated with massive contamination." Rates of infection that accompany these open fractures reach 50%[38–40] and 60% in at least one reported instance.[41] The potential for these fractures to be massively contaminated is highlighted by the work of Bakken[42] and Torsvik et al.[43] who have shown that even 1 g of soil may contain between 10^7 or 10^{10} bacteria, the majority of which are estimated to reside in the biofilm phenotype.[35] The presence of these bacteria in soil expose fracture fixation devices to biofilm formation on the surface.

However, in all animal models of open fracture infections to date, planktonic bacteria have been used as initial inocula. The same is true for other animal models of biofilm device-related infections.

LIMITATIONS OF USING PLANKTONIC CELLS AS INITIAL INOCULA

At least three proposed rationales can be given for why the use of planktonic cells has potentially limited investigators' abilities to detect clinically relevant outcomes of device biofilm-related infections. (1) Planktonic cells are more readily cleared by the immune system than cells residing in a biofilm.[44–46] Furthermore, animals typically have immune systems that are innately advantaged compared with those of humans. Thus, when planktonic cells are used in *in vivo* models, it may be that the majority are eradicated before they can form biofilms. This may contribute to the low reproducibility for the induction of osteomyelitis, which has been suggested by Gaudin et al.[47] as a common problem with animal models of osteomyelitis. (2) It is well documented that planktonic bacterial cells are more susceptible to antibiotics than those residing in a biofilm.[48,49] Therefore, if antibiotics are administered immediately following inoculation, they may affect planktonic cells more effectively than they would biofilm cells. (3) When planktonic cells are added to an *in vivo* system, the possibility exists that they may be dispersed rapidly away from the site of initial inoculation, which would dilute the concentration of bacteria per given area—potentially making it easier for the body to handle the bacterial load and prevent attachment to a medical device.

In addition to these limitations that may accompany the use of planktonic cells as initial inocula, investigators have depended heavily on minimum inhibitory concentrations (MIC) to determine the dose of antimicrobial that should be delivered, either from a device coating or intravenously, to prevent and/or treat biofilm-related infections. The limitation of the MIC value in this specific instance is that it is based on data derived from planktonic cells from batch culture. Specifically, a MIC is defined by the Clinical and Laboratory Standards Institute (CLSI) as the dose of antimicrobial that is needed to result in a three log reduction ($10^5 \rightarrow 10^2$) of planktonic bacteria over a 24-h period (see CLSI standard M26-A). Antimicrobial efficacy tests as standardized by the Environmental Protection Agency (e.g., SOP Number: MB-09-04 and SOP Number: MB-06-05) are also based on planktonic bacterial responses. At least one standard of the American Society for Testing and Materials (ASTM E645-07) was found to recommend that microbicides be tested against biofilms. Citing these planktonic cell-based standards, Ceri et al. suggested that additional standards must be developed to treat and/or prevent recurring and untreatable infections that are the result of biofilm contamination and/or subsequent biofilm formation on medical devices.[50]

NUMBER OF BACTERIA IN A BIOFILM THAT MAY BE USED AS INITIAL INOCULA

It does not appear that all biofilms carry the same infectious potential and we propose that most have minimal pathogenicity. If the opposite were true, it is likely that many more people would suffer from infections including gingivitis, periodontitis, sinusitis, conjunctivitis, cellulitis, gastroenteritis, vaginitis, and/or colitis. Each human being is colonized with billions of bacteria, the majority of which appear to reside in well-established biofilms.[51] As such, infection may be considered an anomaly that extends beyond the normal host/bacterial relationship. Infection may also occur as humans are exposed to well-known pathogens that reside in biofilms from soil samples, on grocery carts, in food, within the human microbiome, on office desks, in shower heads, women's purses, grocery bags, and a plethora of other locations all over the world.

The number of bacteria that should be used as initial inocula in animal models is application dependent. Conditions may be considerably different in an animal that is intended to model a patient of total joint replacement, or some other elective surgery. Elective surgeries are performed under scrupulously aseptic conditions, yet despite these efforts, rates of infection still range from 1 to 4% and at times higher.[52–59] If an animal model were used to replicate an elective surgery scenario for biomaterial development, it may be more appropriate to use a low number biofilm as the initial inoculum than what might be used for a massively contaminated open fracture model. Additional consideration would also need to be taken for the inclusion of organisms associated with human skin. Similarly, the use of planktonic or biofilm bacteria is application dependent.

When biofilms are grown in the laboratory, it is common to see them reach incredibly high numbers—on the order of 10^7 or 10^{10} cells/given area. Biofilms that contain high numbers of cells can also be found in nature.[25,27,29,42,43] Similarly, bacterial cells that have been directly observed on and in the human body have been shown to reside in the biofilm phenotype.[51,60] Biopsy punches of human skin have been estimated to contain $\sim 10^6$ cells/cm^2 and it is well documented that the hardy biofilm former, *Staphylococcus epidermidis*, comprises a large portion of these resident commensal bacteria.[51,61,62] In the large intestine, several hundred grams of bacteria can be found with numbers reaching an astounding 10^{11} or 10^{12} cells/g of tissue

comprised of hundreds of species.[51,63,64] Notably, 60% of fecal solids have been shown to be comprised of bacteria.[65]

Although biofilms are ubiquitous and they tend to dwell in communities that can have very high numbers of cells, it may nevertheless be incorrect to assume that wound sites or surgical sites only become infected when they are contaminated with high number biofilms. To the contrary, a biofilm, or a portion of biofilm that has broken off, that contaminates a wound site may consist of as few as 10^2 or 10^4 cells, if not fewer.

Consider the paradigm of a patient who undergoes elective surgery, such as total joint replacement. After the patient's skin is prepped, 10^6 cells/cm^2 of normal flora may be reduced in number to less than 10^3 cells/cm^2 (a 99.9% reduction, which is the most common claim of antiseptics). Note that the majority of these have been shown to reside in the biofilm phenotype. Importantly, groups have shown that even following antiseptic treatment, viable cells continue to reside several layers deep in skin,[66,67] and one of us (J.W.C.) has observed matrix-enclosed bacterial biofilms between stratified squamous cells in the distal five to seven layers of human prepped skin (unpublished observations). During surgery, these cells would have direct access to tissue throughout a patient's integument, while an incision is made, and they would also have direct access to the surfaces of transcutaneous or other implanted biomaterials. As there is no data in the literature that involves small number biofilms contaminating wound and/or surgical sites, surgeons, and investigators are left to wonder what effect these might have on the development of infection in these scenarios.

There are myriad other paradigms that could be considered with similar scenarios of low numbers of cells within a biofilm contaminating wound and/or surgical sites. What remains is the fact that hypothesis driven research needs to be undertaken to determine the impact that low number biofilms have on human health as they attach to and form on the surface of biomaterial devices. Furthermore, to our knowledge, there is no comparative study in the literature to determine the effect that fewer versus higher numbers of cells in a biofilm, which derive from the same bacterial strain(s), have on the formation of biofilms on biomaterials. For now, the understanding of critical doses required to cause infection are based solely on concentrations of planktonic bacteria.

THE 10^5 RULE MAY NOT APPLY TO BIOFILM

Studies have shown that to prevent infection, bacterial loads must be kept below 10^5 cells per gram of tissue[66,68–71] and this is the rule of thumb used by various clinicians as an indicator of infection. However, this number is strain dependent and is based on planktonic bacterial cell counts. Citing Bowler,[72] Edwards and Harding have stated that, "The clinical relevance of the theory that bacterial counts of over 10^5 represent clinical infection has been questioned."[68] In addition, it may be that smaller numbers of cells are required to cause infection if they reside in the biofilm phenotype. Indeed, the ability of low number, mature biofilms to resist antimicrobial treatment may enhance our understanding of how bacteria cause infection when initial inocula are on the order of thousands or tens of thousands of cells as opposed to the hundreds of thousands or hundreds of millions in planktonic form that are commonly used for *in vivo* studies.

Wolcott et al.[73] have recently undertaken a study wherein they showed that in the early stages of development, biofilms were more sensitive to antimicrobials when compared with biofilms that had matured for more than 24 or 48 h. Their data further suggested that even if similar numbers of cells were present, the maturity, and not so much the number of cells within the biofilm, had a significant influence on its ability to resist antimicrobial perturbations. Their work was designed to model a specific clinical application and effectively addressed those scenarios. Importantly, however, this work also followed the predominant pattern of biofilm research wherein enormous numbers of cells accumulated over time within the biofilm growth system.

Yet, as mentioned above, it may not always be accurate to analyze biofilms as they undergo an increase in their number of cells. Although dynamic, biofilms in real life systems typically do not display the same growth rates as those generated under optimal conditions in the laboratory. Rather, in natural systems biofilms increase in cellular number over a longer period of time, mature to a level of equilibrium and when challenged by modifications in their environment, they respond appropriately. The hypothesis is that these equilibrated, matured, slow growing biofilms are what primarily contaminate wound sites, parenteral routes and medical devices within humans. Thus, to model contamination of a wound site with matured, equilibrated biofilms, similar to how they are found in nature, studies may benefit from growing biofilms to threshold levels, allowing them to mature, and then exposing them to wound sites, antibiotics or other antimicrobial agents in *in vitro* and/or *in vivo* systems.

FUTURE METHODS OF GROWING BIOFILM FOR USE AS INITIAL INOCULA

Connell et al.[74] have recently developed a remarkable method of growing biofilms in small numbers using micron sized "lobster traps." Although countless possibilities exist for *in vitro* experimentation with these traps, they are currently limited in that they are adhered to a solid surface. However, modifications to the substrate could make it possible for them to be used as initial inocula in an *in vivo* model.

Recently, a modified CDC biofilm reactor system has been developed to grow biofilms on the surface of polyetheretherketone (PEEK) membranes. Biofilms of methicillin-resistant *Staphylococcus aureus* (MRSA) were shown to develop into three-dimensional pillar like structures on the surface of these membranes.[75,76] *In vitro* and *in vivo* work is currently being performed to test the efficacy of a novel antimicrobial coating on simulated fracture fixation plates against these MRSA biofilms. To date, in 14 out of 14 animals, work has indicated that when these biofilms are used

as initial inocula in the absence of antimicrobial treatment, they caused osteomyelitis to develop and persist up to a 12 week end point.

Despite these promising results, there is one crucial factor to take into consideration. In the above study, biofilms were grown for a 48-h period, rinsed to remove loosely adherent or nonadherent cells, and transferred in a broth solution prior to using them as initial inocula. These steps were undertaken in an attempt to reduce the possibility of having planktonic cells present. However, the potential still existed that a portion of cells present could have been in the planktonic phenotype. As such, the question may arise; was it the biofilm bacteria or the planktonic bacteria that caused infection? Two responses can be given.

First, it is likely impossible with current technologies to separate all planktonic bacteria from those that reside in the biofilm phenotype such that an inoculum with biofilm bacteria alone is absolutely definitive. Yet, it is also unlikely that such a distinct separation exists between planktonic and biofilm bacteria in natural ecosystems. This may suggest that using an inoculum that has a mixture of the two, with those in the biofilm phenotype being more heavily selected, is clinically relevant.

Second, an additional animal model is currently being used to test the ability of the MRSA strain discussed above to cause infection when inoculated in the planktonic phenotype from batch culture. When the onset of infection was compared between these two animal models, there was a drastic difference in the rapidity and severity of infection that set in with the planktonic bacteria. In that instance, none of the animals survived past 11 days. In contrast, those that were treated with biofilms as initial inocula displayed signs of infection that were much less severe and which progressed at a much slower pace. More specifically, those animals displayed limited signs of pain or distress even out to 12 weeks, but each of them developed a significant osteomyelitic infection.

This contrast in the speed and severity of infection may provide clinical evidence that using biofilms as initial inocula is more correlative to biofilm-related infections that are present in patients. In patients, biofilm-related infections appear to be latent infections that develop slowly over time and which may persist for extensive periods.[33] So although these current animal models provide a promising step in the direction of using biofilms as initial inocula, there are many factors to take into account: a host's health, the pathogenicity of an organism, the ability for an organism to develop into a biofilm, the degree of contamination, the ratio of cells in the planktonic phenotype to those in the biofilm phenotype, and so forth. Thus, this issue of planktonic versus biofilm infection is still a limitation and will require additional future testing to overcome the challenges of separating the bacterial phenotypes before more definitive statements can be made.

At this time, with the variety of biofilm reactor devices that are currently available, such as the CDC biofilm reactor, the modified CDC biofilm reactor, the Drip Flow Biofilm Reactor, and "lobster traps," the outlook is promising for a transition in biofilm investigation to occur from the *in vitro* paradigm to the *in vivo* setting.

CONCLUDING DISCUSSION

During the design process of an animal study, in particular an infection model, investigators often take careful consideration to select animals that have not been influenced by antibiotic feed, those that have not been specially treated in some manner at a housing facility, and, depending on the study design, those that have not been genetically modified or otherwise altered to influence the outcomes of a study. In contrast, investigators tend to select animals that come from natural environments so as to select a group that will model an uninfluenced, random sample. A similar process should be used when selecting bacterial isolates. These should be derived, as closely as possible, from natural systems and grown under conditions that are conducive to their environment and phenotype. This may be the biofilm phenotype and in other cases, the planktonic.

In summary, as an isolate(s) is selected for application in an animal model of infection, or as one is selected for specific *in vitro* testing, such as an antimicrobial eluting biomaterial, we recommend that, depending on the specific application, (1) the isolate be derived from a primary culture, either from a patient or natural environment, that has not been passaged numerous times, (2) that it be grown under conditions that will promote biofilm formation to the nearest possible extent as they are found in their natural environment and, (3) that biofilms be applied in numbers that, as closely as possible, model clinical and/or environmental scenarios to which biomaterials may be exposed.

The impact of biofilm-dwelling bacteria on human health is becoming ever more apparent. Chronic wounds are now considered to be the result of acute infection that begins with biofilm contamination as opposed to a nonhealing wound that is later contaminated and suffers from biofilm formation/infection.[77–80] Heart disease is now indicated to be compounded by biofilm dwelling bacteria from oral plaque that enter the vasculature.[81,82] Overall human health is believed to be significantly influenced by an intricate balance of biofilm dwelling bacteria in gut flora.[63] In short, the impact of biofilms on human well-being and disease cannot be overestimated.

Looking to the future of biofilm and biomaterials research, additional approaches for *in vitro* analyses and design modifications to *in vivo* models that encompass the use of preformed, well-established, sessile communities of mature biofilms that model those found in nature, in patients and within the environment, can be envisioned. As studies are undertaken to analyze the impact of low number biofilms on infection outcomes, results may indicate that less than 10^5 cells/gram of tissue, or per area, will be required to cause infection.

If the efficacy of antimicrobials are tested against high and low number biofilms, those on the order of 10^7–10^9 cells and 10^2–10^4, respectively, we may uncover deeper insights into the concentrations of antimicrobial in, for example, antimicrobial eluting biomaterials, that are needed

to prevent and eradicate biofilm-related infections from developing. We can only wonder at this time how many antimicrobials and antimicrobial eluting biomaterials have been prevented from progressing to clinical, home, industrial, and/or environmental use based on the fact that MIC values, which are primarily the result of planktonic cellular response, have been used to determine the amount that was needed to eradicate bacteria residing in well-established biofilms.

The opposite may be true as well. There is no indication that antibiotics that have been put into clinical use have shown efficacy against low and/or high number biofilms on implants. Although this trend may change as an understanding of the role of biofilm increases, this paradigm has potentially been a contributing factor to the development of antibiotic resistance. More specifically, in various systems, bacteria residing in biofilms may have been exposed to lower concentrations than are needed to prevent their growth and eradicate them within *in vitro* and *in vivo* systems. However, a cavalier approach of simply increasing dosages of antimicrobials alone or used in eluting biomaterials could potentially lead to toxic effects *in vivo* and cause additional problems. Thus, future work will be needed to elucidate the efficacy and toxicity of antimicrobials used alone or in eluting biomaterials against biofilms in clinical studies.

In conclusion, the impact that low number biofilms have on human infection as well as using well-established, mature biofilms as initial inocula for *in vitro* and *in vivo* models may help further the optimization of antimicrobial treatments, such as those used in coatings on biomaterials. In addition, the understanding of the impact that biofilms from natural systems have as initial contaminants of wounds may also be increased. Most importantly, a shift in the use of biofilms for inoculation methods and analytical techniques may help biomaterial researchers take a step forward, and thus obtain the advantage in the battle against biofilm implant-related infections.

ACKNOWLEDGMENTS

The content is solely the responsibility of the authors and does not necessarily represent the official views of the National Institute Of Arthritis And Musculoskeletal And Skin Diseases or the National Institutes of Health. The authors also wish to thank Dr. Roy Bloebaum for his insightful comments and review of the manuscript throughout the writing process.

REFERENCES

1. Buret A, Ward KH, Olson ME, Costerton JW. An *in vivo* model to study the pathobiology of infectious biofilms on biomaterial surfaces. J Biomed Mater Res 1991;25:865–874.
2. Cirioni O, Mocchegiani F, Ghiselli R, Silvestri C, Gabrielli E, Marchionni E, Orlando F, Nicolini D, Risaliti A, Giacometti A. Daptomycin and rifampin alone and in combination prevent vascular graft biofilm formation and emergence of antibiotic resistance in a subcutaneous rat pouch model of staphylococcal infection. Eur J Vasc Endovasc Surg 2010;40:817–822.
3. Lambe DWJ, Ferguson KP, Mayberry-Carson KJ, Tober-Meyer B, Costerton JW. Foreign-body-associated experimental osteomyelitis induced with *Bacteroides fragilis* and *Staphylococcus epidermidis* in rabbits. Clin Orthopaedics Related Res 1991;266:285–294.
4. Darouiche RO, Farmer J, Chaput C, Mansouri M, Saleh G, Landon GC. Anti-infective efficacy of antiseptic-coated intramedullary nails. J Bone Joint Surg 1998;80:1336–1340.
5. Darouiche RO, Mansouri MD. Dalbavancin compared with vancomycin for prevention of *Staphylococcus aureus* colonization of devices in vivo. J Infect 2005;50:206–209.
6. Darouiche RO, Mansouri MD, Gawande PV, Madhyastha S. Antimicrobial and antibiofilm efficacy of triclosan and dispersin B combination. J Antimicrobial Chemotherapy 2009;64:88–93.
7. Darouiche RO, Mansouri MD, Zakarevicz D, AlSharif A, Landon GC. In vivo efficacy of antimicrobial-coated devices. J Bone Joint Surg 2007;89:792–797.
8. Davis SC, Ricotti C, Cazzaniga A, Welsh E, Eaglstein WH, Mertz PM. Microscopic and physiologic evidence for biofilm-associated wound colonization in vivo. Wound Repar Regenerat 2008;16: 23–29.
9. Dohar JE, Hebda PA, Veeh R, Awad M, Costerton JW, Hayes J, Ehrlich GD. Mucosal biofilm formation on middle-ear mucosa in a nonhuman primate model of chronic suppurative otitis media. Laryngoscope 2005;115:1469–1472.
10. Elasri MO, Thomas JR, Skinner RA, Blevins JS, Beenken KE, Nelson CL, Smeltzer MS. *Staphylococcus aureus* collagen adhesin contributes to the pathogenesis of osteomyelitis. Bone 2002;30: 275–280.
11. Fernandez-Hidalgo N, Gavalda J, Almirante B, Martin M-T, Onrubia PL, Gomis X, Pahissa A. Evaluation of linezolid, vancomycin, gentamicin and ciprofloxacin in a rabbit model of antibitoic-Locl technique for *Staphylococcus aureus* catheter-related infection. J Antimicrobial Chemotherapy 2010;65: 525–530.
12. Hansen LK, Berg K, Johnson D, Sanders M, Citron M. Efficacy of local rifampin/minocycline delivery (AIGISRX®) to eliminate biofilm formation on implanted pacing devices in a rabbit model. Int J Artificial Organs 2010;33:627–635.
13. Hart E, Azzopardi K, Taing H, Graichen F, Jeffery J, Mayadunne R, Wickramaratna M, O'Shea M, Nijagal B, Watkinson R, O'Leary S, Finnin B, Tait R, Robins-Browne R. Efficacy of antimicrobial polymer coatings in an animal model of bacterial infection associated with foreign body implants. J Antimicrobial Chemotherapy 2010; 65:974–980.
14. Keeling WB, Myers AR, Stone PA, Heller L, Widen R, Back MR, Johnson BL, Bandyk DF, Shames ML. Regional antibiotic delivery for the treatment of experimental prosthetic graft infections. J Surg Res 2009;157:223–226.
15. Li B, Brown KV, Wenke JC, Guelcher SA. Sustained release of vancomycin from polyurethane scaffolds inhibits infection of bone wounds in a rat femoral segmental defect model. J Control Release 2010;145:221–230.
16. Lucke M, Schmidmaier G, Sadoni S, Wildemann B, Schiller R, Haas NP, Raschke M. Gentamicin coating of metallic implants reduces implant-related osteomyelitis in rats. Bone 2003;32:521–531.
17. Mayberry-Carson KJ, Tober-Meyer B, Smith JK, D.W. Lambe J, Costerton JW. Bacterial adherence and glycocalyx formation in osteomyelitis experimentally induced with *Staphylococus aureus*. Infect Immunity 1984;43:825–833.
18. Reid SD, Hong W, Dew KE, Winn DR, Pang B, Watt J, Glover DT, Hollingshead SK, Swords WE. *Streptococcus pneumoniae* forms surface-attached communities in the middle ear of experimentally infected chinchillas. J Infect Dis 2009;199:786–794.
19. Zou G-Y, Shen H, Jiang Y, Zhang X-L. Synergistic effect of a novel focal hyperthermia on the efficacy of rifampin in staphylococcal experimental foreign-body infection. J Int Med Res 2009; 37:1115–1126.
20. Brin YS, Golenser J, Mizrahi B, Maoz G, Domb AJ, Peddada S, Tuvia S, Nyska A, Nyska M. Treatment of osteomyelitis in rats by injection of degradable polymer releasing gentamicin. J Control Release 2008;131:121–127.
21. Xie Z, Liu X, Jia W, Zhang C, Huang W, Wang J. Treatment of osteomyelitis and repair of bone defect by degradable bioactive borate glass releasing vancomycin. J Control Release 2009;139: 118–126.
22. Krasko MY, Golenser J, Nyska A, Nyska M, Brin YS, Domb AJ. Gentamicin extended release from an injectable polymeric implant. J Control Release 2007;117:90–96.

23. Williams D, Bloebaum R, Petti CA. Characterization of *Staphylococcus aureus* strains in a rabbit model of osseointegrated pin infections. J Biomed Mater Res A 2008;85:366–70.
24. Chou TGR, Petti CA, Szakacs J, Bloebaum RD. Evaluating antimicrobials and implant materials for infection prevention around transcutaneous osseointegrated implants in a rabbit model. J Biomed Mater Res A 2010;92:942–952.
25. ZoBell CE. The effect of solid surfaces upon bacterial activity. J Bacteriol 1943;46:39–56.
26. Costerton JW. The Predominance of biofilms in natural and engineered ecosystems. In: Costerton JW, editor. The biofilm primer. Heidelberg: Springer; 2007. pp 5–13.
27. Costerton JW, Geesey GG, Cheng KJ. How bacteria stick. Sci Am 1978;238:86–95.
28. Lawrence JR, Korber DR, Hoyle BD, Costerton JW, Caldwell DE. Optical sectioning of microbial biofilms. J Bacteriol 1991;173: 6558–6567.
29. Geesey GG, Richardson WT, Yeomans HG, Irvin RT, Costerton JW. Microscopic examination of natural sessile bacterial populations from an alpine stream. Can J Microbiol 1977;23: 1733–1736.
30. James GA, Swogger E, Wolcott R, Pulcini Ed, Secor P, Sestrich J, Costerton JW, Stewart PS. Biofilms in chronic wounds. Wound Repair Regen 2008;16:37–44.
31. Feazel LM, Baumgartner LK, Peterson KL, Frank DN, Harris JK, Pace NR. Opportunistic pathogens enriched in showerhead biofilms. Proc Natl Acad Sci USA 2009;106: 16393–16399.
32. Dowd SE, Sun Y, Secor PR, Rhoads DD, Wolcott BM, James GA, Wolcott RD. Survey of bacterial diversity in chronic wounds using pyrosequencing, DGGE, and full ribosome shotgun sequencing. BMC Microbiol 2008;6:43.
33. Gristina AG, Costerton JW. Bacteria-laden biofilms: A hazard to orthopedic prostheses. Infect Surg 1984;3:655–662.
34. Marrie T, Nelligan J, Costerton J. A scanning and transmission electron microscopic study of an infected endocardial pacemaker lead. Circulation 1982;66:1339–1341.
35. Wimpenny J, Manz W, Szewzyk U. Heterogeneity in biofilms. FEMS Microbiol Rev 2000;24:661–671.
36. Costerton JW. Cystic fibrosis pathogenesis and the role of biofilms in persistent infection. Trends Microbiol 2001;9:50–52.
37. Gustilo RB, Mendoza RM, Williams DN. Problems in the management of type III (severe) open fractures: A new classification of type III open fractures. J Trauma 1984;24:742–746.
38. Gustilo RB, Merkow RL, Templeman D. The management of open fractures. J Bone Joint Surg 1990;72:299–304.
39. Zalazras CG, Marcus RE, Levin S, Patzakis MJ. Management of open fractures and subsequent complications. J Bone Joint Surg 2007;89:884–895.
40. Johnson EN, Burns TC, Hayada RA, Hospenthal DR, Murray CK. Infectious complications of open type III tibial fracture amon combat casualties. Clinical Infect Dis 2007;45:409–415.
41. Lambert EW, Simpson RB, Marzouk A, Unger DV. Orthopaedic injuries among survivors of USS cole attack. J Orthopaedic Trauma 2003;17:436–441.
42. Bakken LR. Separation and purification of bacteria from soil. Appl Environ Microbiol 1985;49:1482–1487.
43. Torsvik V, Goksoyr J, Daae FL. High diversity in DNA of soil bacteria. Appl Environment Microbiol 1990;56:782–787.
44. Cerca N, Jefferson KK, Oliviera R, Pier GB, Azeredo J. Comparative antibody-mediated phagocytosis of *Staphylococcus epidermidis* cells grown in a biofilm or in the planktonic state. Infect Immunity 2006;74:4849–4855.
45. Leid JG, Willson CJ, Shirtliff ME, Hassett DJ, Parsek MR, Jeffers AK. The Exopolysacharide alginate protects *Pseudomonas aeruginosa* biofilm bacteria from IFN-γ-mediated macrophage killing. J Immunol 2005;175:7512–7518.
46. Donlan RM. Biofilms Associated with medical devices and implants. In: Jass J, Surman S, Walker J, editors. Medical Biofilms: Detection, Prevention, and Control; Chichester West Sussex, England: John Wiley and Sons Ltd; 2003. pp 29–96.
47. Gaudin A, Valle GAD, Hamel A, Mabecque VL, Miegeville A-F, Potel G, Caillon J, Jacqueline C. A new experimental model of acute osteomyelitis due to methicillin-resistant *Staphylococcus aureus* in rabbit. Lett Appl Microbiol 2011;52:253–257.
48. Nickel JC, Ruseska I, Wright JB, Costerton JW. Tobramycin resistance of *Pseudomonas aeruginosa* cells growing as a biofilm on urinary catheter material. Antimicrobial Agents Chemotherapy 1985;27:619–624.
49. Melchior MB, Fink-Gremmels J, Gaastra W. Comparative assessment of the antimicrobial susceptibility of *Staphylococcus aureus* isolates from bovine mastitis in biofilm versus planktonic culture. J Veterinary Med Part B 2006;53:326–332.
50. Ceri H, Olson ME, Morck DW, Storey DG. Minimal biofilm eradication concentration (MBEC) assay: Susceptibility testing for biofilms. In: Pace JL, Rupp ME, Finch RG, editors. Biofilms, Infection, and Antimicrobial Therapy. Boca Raton: CRC Press; 2006. pp 257–269.
51. Costerton JW. The microbiology of the healthy human body. In: Costerton JW, editor. The Biofilm Primer. Heidelberg: Springer; 2007. pp 107–128.
52. Brandt C, Hott U, Sohr D, Daschner F, Gastmeier P, Ruden H. Operating room ventilation with laminar airflow shows no protective effect on the surgical site infection rate in orthopedic and abdominal surgery. Annals Surg 2008;248:695–700.
53. Sponseller PO, Shah SA, Abel MF, Newton PO, Letko L, Marks M. Infection rate after spine surgery in cerebral palsy is high and impairs results. Clin Orthopaedics Related Res 2010;468: 711–716.
54. Kaltsas DS. Infection after total hip arthroplasty. Annals Royal College Surgeons England 2004;86:267–271.
55. Tate A, Yazdany T, Bhatia N. The use of infection prevention practices in female pelvic medicine and reconstructive surgery. Current Opin Obstetrics Gynecol 2010;22:408–413.
56. Pozo JLD, Patel R. Infection associated with prosthetic joints. New England J Med 2009;361:787–794.
57. Murray CK. Epidemiology of infections associated with combat-related injuries in Iraq and Afghanistan. J Trauma 2008;64: S232–S238.
58. Owens BD, John F. Kragh J, Macaitis J, Svoboda SJ, Wenke JC. Characterization of extremity wounds in operation iraqi freedom and operation enduring freedom. J Orthopaedic Trauma 2007;21: 254–257.
59. Zimmerli W. Prosthetic-joint-associated infections. Best Practice Res Clin Rheumatol 2006;20:1045–1063.
60. Thomas JG, Nakaishi LA. Managing the complexity of a dynamic biofilm. J Am Dental Assoc 2006;137:10S–15S.
61. Grice EA, Kong HH, Renaud G, Young AC, Bouffard GG, Blakesley RW, Wolfsberg TG, Turner ML, Segre JA. A diversity profile of the human skin microbiota. Genome Res 2008;18:1043–1050.
62. Kloos WE, Musselwhite MS. Distribution and persistence of *Staphylococcus* and *Micrococcus* species and other aerobic bacteria on human skin. Appl Microbiol 1975;30:381–395.
63. Guarner F, Malagelada J-R. Gut flora in health and disease. Lancet 2003;361:512–519.
64. Simon GL, Gorbach SL. Intestinal flora in health and disease. Gastroenterology 1984;86:174–193.
65. Stephen AM, Cummings JH. The microbial contribution to human faecal mass. J Med Microbiol 1980;13:45–56.
66. Fry DE, Fry RV. Surgical site infection: The host factor. AORN J 2007;86:801–814.
67. Hendley JO, Ashe KM. Effect of topical antimicrobial treatment on aerobic bacteria in the stratum corneium of human skin. Antimicrobial Agents Chemotherapy 1991;35:627–631.
68. Edwards R, Harding KG. Bacteria and wound healing. Curr Opin Infect Dis 2004;17:91–96.
69. Robson MC, Heggers JP. Bacterial quantification of open wounds. Military Med 1969;134:19–24.
70. Krizek TJ, Robson MC, Kho E. Bacterial growth and skin graft survival. Surg Forum 1967;18:518.
71. Murphy RC, Robson MC, Heggers JP, Kadowaki M. The effect of microbial contamination on musculocutaneous and random flaps. J Surg Res 1986;41:75–80.
72. Bowler PG. The 10^5 bacterial growth guideline: Reassessing its clinical relevance in wound healing. Ostomy Wound Manage 2003;49:44–53.

73. Wolcott RD, Rumbaugh KP, James G, Schultz G, Phillips P, Yang Q, Watters C, Stewart PS, Dowd SE. Biofilm maturity studies indicate sharp debridement opens a time-dependent therapeutic window. J Wound Care 2010;19:320–328.
74. Connell JL, Wessel AK, Parsek MR, Ellington AD, Whiteley M, Shear JB. Probing prokaryotic social behaviors with bacterial "lobster traps". mBio 2010;1:e00202–00210.
75. Williams DL, Haymond BS, Bloebaum RD. Use of delrin plastic in a modified CDC biofilm reactor. Res J Microbiol 2011;6: 425–429.
76. Williams DL, Woodbury KL, Haymond BS, Parker AE, Bloebaum RD. A modified CDC biofilm reactor to produce mature biofilms on the surface of PEEK membranes for an in vivo animal model application. Curr Microbiol 2011;62: 1657–1663.
77. Serralta VW, Harrison-Balestra C, Cazzaniga AL, Davis SC, Mertz PM. Lifestyles of bacteria in wounds: Presence of biofilms? Wounds 2001;13:29–34.
78. Mertz PM. Cutaneous biofilms: Friend or foe? Wounds 2003;15: 129–132.
79. Percival SL, Bowler PG. Biofilms and their potential role in wound healing. Wounds 2004;16:234–240.
80. James G, Swogger E, deLancey-Pulcini E. Biofilms in chronic wounds. In: Costerton JW, editor. The Role of Biofilms in Device-Related Infections. Heidelberg: Springer; 2009. pp 11–14.
81. Okuda K, Ishihara K, Nakagawa T, Hirayama A, Inayama Y, Okuda K. Detection of *Treponema denticola* in atherosclerotic lesions. J Clin Microbiol 2001;39:1114–1117.
82. Chiu B. Multiple infections in carotid atherosclerotic plaques. Am Heart J 1999;138(Part 2):S534–S536.

APPENDIX B

A MODIFIED CDC BIOFILM REACTOR TO PRODUCE MATURE BIOFILMS ON THE SURFACE OF PEEK MEMBRANES FOR AN *IN VIVO* ANIMAL MODEL APPLICATION

Curr Microbiol (2011) 62:1657–1663
DOI 10.1007/s00284-011-9908-2

A Modified CDC Biofilm Reactor to Produce Mature Biofilms on the Surface of PEEK Membranes for an In Vivo Animal Model Application

Dustin L. Williams · Kassie L. Woodbury · Bryan S. Haymond · Albert E. Parker · Roy D. Bloebaum

Received: 29 November 2010 / Accepted: 17 February 2011 / Published online: 25 March 2011

Abstract Biofilm-related infections have become a major clinical concern. Typically, animal models that involve inoculation with planktonic bacteria have been used to create positive infection signals and examine antimicrobial strategies for eradicating or preventing biofilm-related infection. However, it is estimated that 99.9% of bacteria in nature dwell in established biofilms. As such, open wounds have significant potential to become contaminated with bacteria that reside in a well-established biofilm. In this study, a modified CDC biofilm reactor was developed to repeatably grow mature biofilms of *Staphylococcus aureus* on the surface of polyetheretherketone (PEEK) membranes for inoculation in a future animal model of orthopaedic implant biofilm-related infection. Results indicated that uniform, mature biofilms repeatably grew on the surface of the PEEK membranes.

Keywords Biofilm · Modified · Reactor · CDC · Membrane · Repeatability

D. L. Williams · R. D. Bloebaum (✉)
Department of Bioengineering, University of Utah, Salt Lake City, UT, USA
e-mail: roy.bloebaum@hsc.utah.edu

D. L. Williams
e-mail: dustin.williams@utah.edu

K. L. Woodbury · B. S. Haymond · R. D. Bloebaum
Department of Veterans Affairs, Bone and Joint Research Laboratory (151F), Salt Lake City, UT, USA

A. E. Parker
Center For Biofilm Engineering, Montana State University, Bozeman, MT, USA

R. D. Bloebaum
Department of Orthopaedics, University of Utah School of Medicine, Salt Lake City, UT, USA

Introduction

Biofilms have become a major research interest in recent years. For example, the role of biofilms in chronic orthopaedic device-related infections has been particularly concerning as highlighted by the failed attempts of orthopaedic surgeons to treat patients who are adversely affected by biofilm formation on and near orthopaedic devices [3, 5, 16]. These patients often require expensive and compromising revision surgery, implant removal or, in a worst case scenario, amputation. Death can also be a devastating outcome. Biofilm-related infections similarly affect injured military personnel, in particular, those suffering from severely contaminated blast injuries in the current Afghanistan and Iraq conflicts [13, 14].

In an attempt to prevent these biofilm-related infections from developing near or on orthopaedic devices, animal models have been used to create positive infection signals and to examine antimicrobial strategies for treatment [4, 7, 8, 17]. Typically, these animal models have consisted of implanting a device in conjunction with inoculation of planktonic (free-floating) bacteria near the device. The expectation has either been that planktonic cells will form a biofilm on or near the implant and result in biofilm-related infection, or that planktonic cells alone will develop infection.

However, since the 1978 hypothesis of Costerton et al. [6] that bacteria in nature preferentially aggregate in biofilms, it has been estimated that approximately 99.9% of bacteria in nature dwell in biofilms [11, 12]. Moreover, Bakken [1] has shown that 1 g of fertile soil can contain up to 5 billion bacterial cells. If contaminated with even 1 or 2 g of soil, it is plausible that open fractures or other types of open wounds may have significant contamination with very high inocula of bacteria residing in well-established biofilms. Therefore, in vivo models of infection that

involve the use of well-established biofilms may contribute to our understanding of biofilm-related infection as well as methods of safely eradicating the biofilm and related infection without surgery and implant removal.

In this study, a modified CDC biofilm reactor was developed to grow well-established *Staphylococcus aureus* biofilms on the surface of polyetheretherketone (PEEK) membranes. It is intended for these biofilm-ridden membranes to be used to inoculate future animal models of biofilm-related infection, pending confirmation that mature, uniform and viable biofilms can be repeatably formed on the PEEK membranes.

Materials and Methods

Isolate Selection

A freshly cultured, clinical isolate of methicillin-resistant *S. aureus* (MRSA) was collected from a patient and used for this study. More specifically, a patient who underwent knee surgery developed infection and an aspirate was sent to ARUP Laboratories, Salt Lake City, UT for characterization and susceptibility testing. The isolate was characterized as MRSA based on resistance to penicillin and oxacillin using the Kirby Bauer disc diffusion technique. Preliminary work indicated that the isolate was a biofilm former following black colony formation on Congo Red agar and detection of the *icaADBC* gene cluster. When grown as a biofilm and used as initial inocula, biofilms of this strain caused osteomyelitis in a pilot animal model of biofilm implant-related infection (unpublished data).

Modified Design of the CDC Biofilm Reactor

The CDC biofilm reactor was purchased from Biosurface Technologies (Bozeman, MT). The original design of the reactor is provided in Fig. 1a. A modified lid was designed and machined using a local machine shop. The modified lid contained four slots into which guillotine-like holders (20 cm in length with a 3 mm groove down the middle of the interior portion) made of ultra-high-molecular-weight-polyethylene (UHMWPE) were inserted (Fig. 1b). Into the guillotine holders were placed PEEK membranes that were held in place between two 316L stainless steel plates with a 0.64 cm^2 opening (Fig. 1b). A photograph of the modified reactor is provided in Fig. 1c. All other aspects of the reactor were the same as the original CDC biofilm reactor.

Biofilm Growth in Reactor

The modified reactor held eight PEEK membranes with two membranes in each of the four guillotine holders (see Fig. 1). PEEK membranes were first sonicated for 10 min in detergent, rinsed under running reverse osmosis water for 10 min, sonicated in reverse osmosis water for 10 min and rinsed once again using 70% ethanol. The reactor was then assembled and all components autoclaved before use.

Following American Society for Testing and Materials (ASTM) standard E2562-07, the modified reactor was run under the following conditions: approximately 1.5×10^8 bacterial cells were inoculated into 500 ml of brain heart infusion (BHI) broth (modified) in the biofilm reactor. The rotator was stirred at 130 rpm, and the unit was placed in an incubator set at 28.5°C for 24 h. A 10% BHI broth (modified) solution was then flowed through the reactor at 6.94 ml/min for 24 h.

Sample Fixation, Dehydration and Imaging

To qualitatively observe the biofilms that had developed, eight membranes were imaged using SEM. For imaging preparation, membranes were removed from the reactor, placed in 2.5% glutaraldehyde for 24 h and then dehydrated using ascending grades of ethanol with 3 × 20 min exchanges of each up to 100%. Samples were dried in a desiccator overnight, sputter coated with ~3 nm of gold, and imaged using a FEI NOVANano SEM 600.

On two membranes, the Filmtracer™ LIVE/DEAD® stain (Invitrogen, Carlsbad, CA) was used in conjunction with confocal laser scanning microscopy (CLSM) to qualitatively observe the degree of live versus dead bacteria on the membrane. The biofilms were observed using a FV-1000 XY inverted CLSM microscope with a 60× water objective.

Bacterial Quantification

In order to determine uniformity, following eight separate runs of the modified biofilm reactor, a total of 64 PEEK membranes were used to quantify the number of bacteria that grew on the surface of each membrane. The membranes from each run were randomly assigned to one of two treatment groups (i.e., with four membranes per group).

Following growth in the reactor, the four membranes in Group 1 were removed from the guillotine holders, rinsed 3× in 6 ml of saline, placed on a shaker at 100 rpm for 20 min and allowed to remain stationary for 1.5 h. The membranes were then vortexed for 1 min, sonicated at 47 kHz and 1.8 W/cm^2 for 10 min, allowed to recover from sonication for 20 min and then enumerated using a 10-fold dilution series. 100 µl of each dilution (1:10–1:10,000,000) was plated onto Columbia blood agar and incubated overnight at 37°C. The following day, the colony forming units (cfu) were counted to determine the number of bacteria per membrane (cfu/membrane). Fifteen randomly selected membranes were imaged by

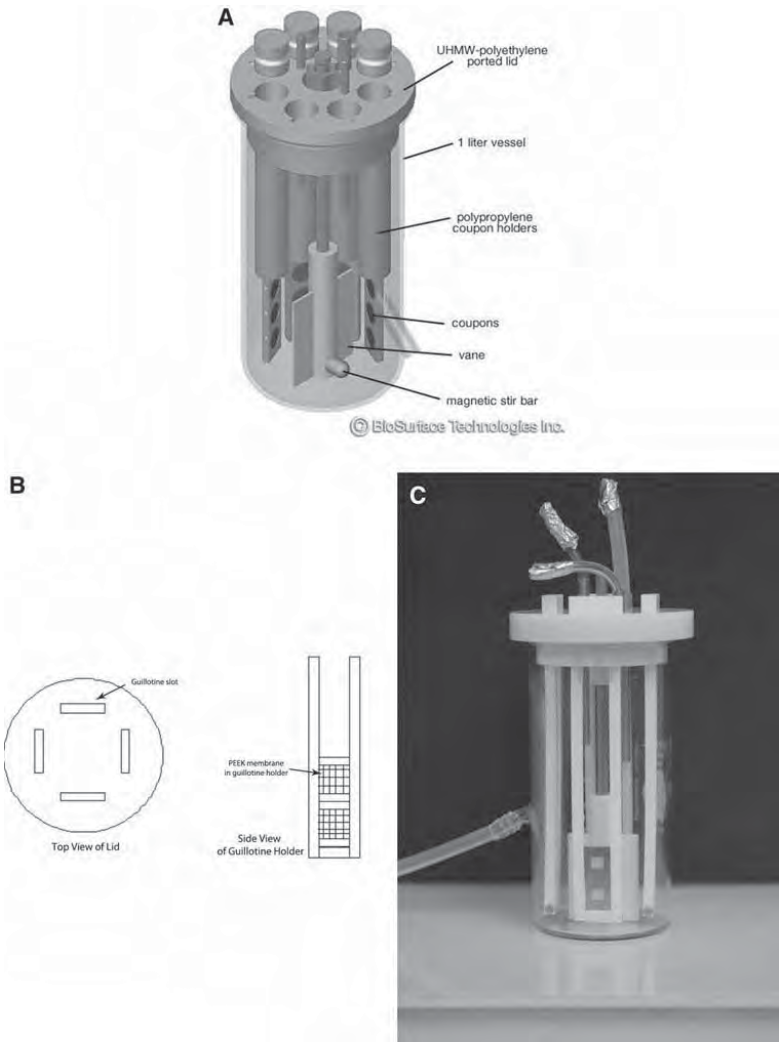

Fig. 1 **a** Schematic diagram of the CDC biofilm reactor. **b** Schematic diagram of the modified CDC biofilm reactor lid and guillotine-like holder. **c** Photograph of the completed modified CDC biofilm reactor

SEM to confirm that bacteria had been removed from the surface.

The rationale for shaking the membranes at 100 rpm for 20 min was to model the car ride that they will be exposed to when they are transported from the lab to the site of animal surgery. Furthermore, the four membranes in Group 1 were allowed to remain stationary for 1.5 h to model the time that they will be stationary whilst the surgical facility and animals are prepped for surgery before inoculation. Group 2 membranes were treated in the same manner as those in Group 1 with the exception that they were allowed to remain stationary for 3 h as opposed to 1.5 h so as to model the time that they will remain stationary during the first surgery of the future animal model.

The density of bacteria in cfu/membrane was recorded for each PEEK membrane and then $\log_{10}$ transformed. For each of the two treatment groups separately, an ANOVA was fit, with run as a random effect, to calculate the mean and repeatability standard deviation (SD) of the log densities on the PEEK membranes over the eight reactor runs.

Another ANOVA, with group as a fixed effect and run as a random effect, was used to compare the group means and to calculate the repeatability SD for both groups pooled together. These statistics were used to determine if any difference in bacterial response could be seen between membranes that were allowed to remain in a dilute broth solution for varying periods of time. The analyses also showed the percentage of the repeatability variance attributable to within- and between-run sources.

Results

Growth on PEEK Membranes Within the Biofilm Reactor

Images collected of the PEEK membranes following growth, sample fixation and dehydration indicated that copious amounts of biofilm formed on the membrane surfaces (Fig. 2a). Furthermore, each of the three indicators

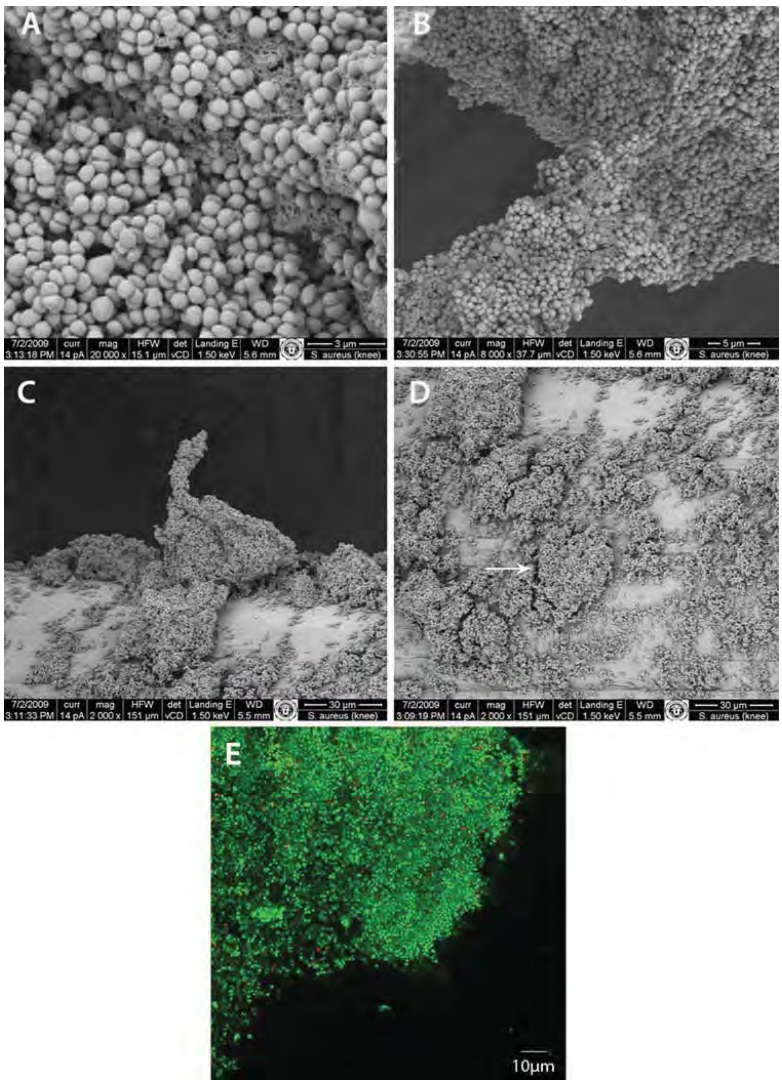

Fig. 2 **a** Representative SEM image of the *S. aureus* biofilm. **b** Additional image of the EPS providing a scaffold for bacterial cells within the biofilm to create a bridge from one surface of the PEEK membrane to another. **c** Representative image showing a three-dimensional structure of the biofilm extending vertically from the surface of the PEEK membrane. **d** Representative image showing possible water channels within the biofilm structure (*arrow*). **e** The LIVE/DEAD® stain showed living cells as *green* and dead cells as *red*. This image shows a representative Z projection slice of the *S. aureus* biofilm collected using CLSM and indicates that the cells within the biofilm were predominantly living with an estimated ratio of live to dead cells being 1000:1. Original magnification was ×60 (color images can be seen in the online version or upon request to the authors)

that a mature biofilm had developed were detected [10], i.e., significant EPS production (Fig. 2a and b), three-dimensional structures of mushroom- or pillar-like formations (Fig. 2c) and possible water channel development (Fig. 2d) were observed upon SEM analysis. In addition, the EPS matrix appeared to act as a scaffold to which the bacteria attached to create a "bridge" that connected cells of the biofilm from one strand of the PEEK membrane to another (Fig. 2b). These results indicate that mature biofilms did form on the surface of PEEK membranes when grown within the modified membrane reactor.

Notably, although the temperature of the incubator was set at 28.5°C, the recorded temperature of the broth after the first 24 h of each run was 28.1 ± 1.2. After 48 h of growth, the broth temperature from each run was 29.8 ± 0.5.

Bacterial Quantification

The number of bacteria on each PEEK membrane was quantified following eight separate runs of the reactor, with eight membranes per run, and four membranes randomly assigned to each of two treatment groups to confirm uniformity. The data are shown in Fig. 3.

Mean log densities and repeatability SDs for each of the two groups individually and also for all 64 membranes pooled together are given in Table 1. The table corroborates what is evident in Fig. 3: the two groups have similar means and repeatability SDs. A 90% confidence interval for the difference of the Group 1 mean log density subtracted from the Group 2 mean log density was found to be (0.06, 0.19), which indicates statistical equivalence between the two group means at a significance level of 5% as long as mean differences up to 0.19 are considered to be negligible.

Taken together, these results show that copious amounts of *S. aureus* biofilm formed on the surface of each PEEK membrane within the reactor and that the mean log densities for the two treatment groups were statistically equivalent. Furthermore, the biofilm log density exhibited acceptable repeatability from run to run under the conditions described.

SEM images of the PEEK membranes that were collected after the quantification process indicated that only

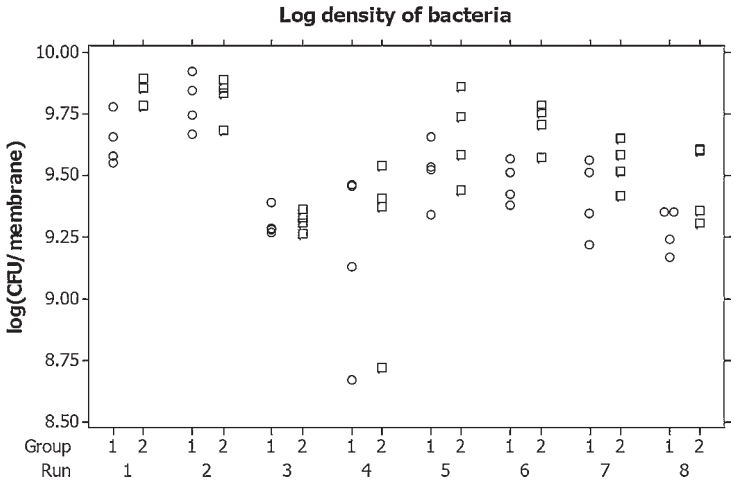

Fig. 3 An individual value plot of the log density of bacteria per PEEK membrane. Group 1 (*open circle*) membranes were those that were allowed to remain stationary for 1.5 h before quantification. Group 2 (*open square*) membranes were those that were allowed to remain stationary for 3 h before quantification. Each point represents one membrane

Table 1 Statistical characteristics for each of the two treatment groups, and both groups pooled together

Group	Mean	SE	Repeatability SD	Percentage contribution	
				Within run (%)	Between run (%)
1	9.45	0.0296	0.2020	17	83
2	9.58	0.0297	0.2162	15	85
Both 1 and 2	9.51	0.0203	0.2130	14	86

The standard error (SE) of the mean and the repeatability SD are based on four membranes per run. These results demonstrate the uniformity of the biofilm formation on the PEEK membranes

sparse microcolonies of bacteria remained on the surface. As such, the number of bacteria in the microcolonies was inconsequential with respect to the billions of cells that were enumerated (SEM images not shown).

Discussion

An increased understanding of the important role of biofilms in device-related and chronic infections suggests that in vitro and in vivo studies may be strengthened with the use of mature biofilms as opposed to the application of planktonic bacteria alone. This study highlighted the ability of the CDC biofilm reactor to be modified in such a way that mature biofilms could be grown on a biocompatible polymer surface that can later be applied towards in vivo experimentation. Taken together, the hypothesis that mature biofilms would develop on the surface of PEEK membranes in a repeatable fashion was supported.

Interestingly, during the optimization of the modified reactor, it was found that when the unit was placed in an incubator set at 37°C, biofilms did not form as well as when they were grown at 28.5°C. More specifically, when grown at 37°C, there was no biofilm growth on the PEEK membranes by visual observation, whereas at 28.5°C, copious amounts of biofilm could be seen. Since our group was interested in having $\sim 10^9$ cells/membrane, no further runs at 37°C were performed. Nevertheless, this finding was similar to that of Rode et al. [15]. They found that several clinical and food-related isolates of *S. aureus* produced biofilms optimally near 30°C.

The overall mean bacterial log density was 9.51 log (cfu/membrane), and the repeatability SD was 0.2130. As a comparison, in the 13 experiments described by Buckingham-Meyer et al. [2], *S. aureus* ATCC 6538 biofilm grown in the CDC reactor on glass coupons exhibited a mean of 8.3 log (cfu/cm^2) and a repeatability SD of 0.224 (based on two coupons). In a different set of 12 experiments, Buckingham-Meyer et al. [2] grew *Pseudomonas aeruginosa* biofilm in the CDC reactor on glass coupons, with a mean of 8.5 log (cfu/cm^2) and a repeatability SD of 0.211. Goeres et al. [9] grew *P. aeruginosa* biofilm in the CDC reactor on polycarbonate coupons over nine experiments and reported a mean of 7.06 log (cfu/cm^2) and a repeatability SD of 0.510 (based on two coupons per experiments). Thus, the biofilm bacteria grown on PEEK membranes in the modified CDC reactor exhibited acceptable run to run repeatability in our study.

Demonstrating that biofilm growth on the PEEK membranes was repeatable from run to run was an important aspect of this project. More specifically, if these biofilms of *S. aureus* on PEEK membranes are to be used in future animal models, it is important that individual animals receive statistically equivalent biofilm challenges. Therefore, the statistical equivalence of the biofilm grown on membranes in each of the treatment groups suggests that these biofilms will be used reliably and repeatably in a future animal model of device-related infection.

Acknowledgments This material is based upon study supported by the Office of Research and Development, Rehabilitation R&D Service, Department of Veterans Affairs, Salt Lake City, UT. The project described was also supported by Award Number R01AR057185 from the National Institute Of Arthritis And Musculoskeletal And Skin Diseases. The content is solely the responsibility of the authors and does not necessarily represent the official views of the National Institute Of Arthritis And Musculoskeletal And Skin Diseases or the National Institutes of Health. This study was also supported by the Albert and Margaret Hofmann Chair and the Department of Orthopaedics, University of Utah School of Medicine, Salt Lake City, UT. The authors also acknowledge the help of Brad Isaacson, PhD for his contributions to the design of the modified CDC biofilm reactor and Dennis Romney for machining the modified reactor parts.

References

1. Bakken LR (1985) Separation and purification of bacteria from soil. Appl Environ Microbiol 49:1482–1487
2. Buckingham-Meyer K, Goeres DM, Hamilton MA (2007) Comparative evaluation of biofilm disinfectant efficacy tests. J Microbiol Methods 70:236–244
3. Campoccia D, Montanaro L, Arciola CR (2006) The significance of infection related to orthopedic devices and issues of antibiotic resistance. Biomaterials 27:2331–2339
4. Chou TG, Petti CA, Szakacs J et al (2010) Evaluating antimicrobials and implant materials for infection prevention around transcutaneous osseointegrated implants in a rabbit model. J Biomed Mater Res A 92:942–952
5. Costerton JW (2005) Biofilm theory can guide the treatment of device-related orthopaedic infections. Clin Orthop Relat Res 437:7–11
6. Costerton JW, Geesey GG, Cheng KJ (1978) How bacteria stick. Sci Am 238:86–95
7. Darouiche RO, Mansouri MD, Zakarevicz D et al (2007) In vivo efficacy of antimicrobial-coated devices. J Bone Joint Surg Am 89:792–797
8. Darouiche RO, Mansouri MD, Gawande PV et al (2009) Antimicrobial and antibiofilm efficacy of triclosan and Dispersin B combination. J Antimicrob Chemother 64:88–93
9. Goeres DM, Loetterle L, Hamilton MA et al (2005) Statistical assessment of a laboratory method for growing biofilms. Microbiology 151:757–762
10. Jiang X, Pace JL (2006) Microbial biofilms. In: Pace JL, Rupp ME, Finch RG (eds) Biofilms infection and antimicrobial therapy. Taylor and Francis Group, Boca Raton, p 4
11. Wimpenny J, Manz W, Szewzyk U (2000) Heterogeneity in biofilms. FEMS Microbiol Rev 24:661–671
12. Murphy TF, Kirkham C (2002) Biofilm formation by nontypeable Haemophilus influenzae: strain variability, outer membrane antigen expression and role of pili. BMC Microbiol 2:7
13. Murray CK (2008) Epidemiology of infections associated with combat-related injuries in Iraq and Afghanistan. J Trauma 64:S232–S238
14. Owens BD, Kragh JF Jr, Macaitis J et al (2007) Characterization of extremity wounds in operation Iraqi freedom and operation enduring freedom. J Orthop Trauma 21:254–257

15. Rode TM, Langsrud S, Holck A et al (2007) Different patterns of biofilm formation in *Staphylococcus aureus* under food-related stress conditions. Int J Food Microbiol 116:372–383
16. Taubes G (2008) The bacteria fight back. Science 321:356–361
17. Williams D, Bloebaum R, Petti CA (2008) Characterization of *Staphylococcus aureus* strains in a rabbit model of osseointegrated pin infections. J Biomed Mater Res A 85:366–370

APPENDIX C

USE OF DELRIN PLASTIC IN A MODIFIED CDC BIOFILM REACTOR

Research Journal of Microbiology, 2011
ISSN 1816-4935 / DOI: 10.3923/jm.2011.

Use of Delrin Plastic in a Modified CDC Biofilm Reactor

[1,2,3]Dustin L. Williams, [1,2]Bryan S. Haymond and [1,2,3]Roy D. Bloebaum
[1]George E. Wahlen Department of Veterans Affairs Health Care Systems, Salt Lake City, UT, USA
[2]Department of Orthopaedics, University of Utah, Salt Lake City, UT, USA
[3]Department of Bioengineering, University of Utah, Salt Lake City, UT, USA

Corresponding Author: Roy D. Bloebaum, George E. Wahlen Department of Veterans Affairs Health Care Systems, Salt Lake City, UT, USA Tel: (801) 582-1565 x4607 Fax: (801)584-2533

ABSTRACT

In this study, a modified CDC biofilm reactor was designed and the components of the reactor were primarily machined using Delrin plastic. Initially, biofilms grew well using the reactor unit. However, after approximately five runs of the reactor, bacterial growth was inhibited and biofilms no longer formed. To troubleshoot the problem, bacteria were grown in the presence of broth alone or in the presence of broth and Delrin plastic. It was determined that the reactor components containing Delrin plastic prevented growth of bacteria and the formation of biofilm. It appeared that the repeated exposure to autoclave temperature and pressure caused the Delrin plastic to decompose and leach formaldehyde into the broth, which inhibited bacterial growth. Based on these results, we propose that Delrin plastic should not be used in bacterial growth devices.

Key words: Delrin, biofilm, reactor, polymer, components, plastic

INTRODUCTION

Biofilm reactors have become essential tools in Biofilm-related research and have helped to advance our knowledge of Biofilm formation, morphology, the role of Biofilm in medicine and more (Buckingham-Meyer *et al.*, 2007; Mohle *et al.*, 2007; Goeres *et al.*, 2009; Gilmore *et al.*, 2010; Lipp *et al.*, 2010; Williams and Bloebaum, 2010). Primarily, these reactors have been composed of polymeric materials and metal components. Various polymeric materials provide significant advantages in that they can be machined easily, are relatively cheap, can be autoclaved numerous times and in many instances are chemically inert.

In addition, biofilm reactors can be customized to meet specific needs of experimentation. More specifically, we modified the design of the CDC biofilm reactor (Goeres *et al.*, 2005) (Biosurface Technologies, Bozeman, MT) to meet the needs of an *in vivo* model wherein the coupons from the CDC biofilm reactor (Fig. 1a) would have been too large and ultimately ineffective. The modified design of the reactor allowed for membranes made of polyetheretherketone (PEEK) to be placed into a 1 L glass vessel as they were secured in guillotine-like holders that were inserted into a slot of the reactor cap (Fig. 1b). As such, the PEEK membranes were held in the base of the reactor and exposed to shear forces of a swirling vane to promote biofilm production (Stoodley *et al.*, 1999, 2001). In a future study, after biofilms have been grown on the surface of the PEEK membranes, they will be surgically placed into an animal to model biofilm-related infection. PEEK polymer membranes were used in this study because of the known biocompatibility of PEEK (Rivard *et al.*, 2002), the membranes were porous and they provided a large surface area for biofilm formation.

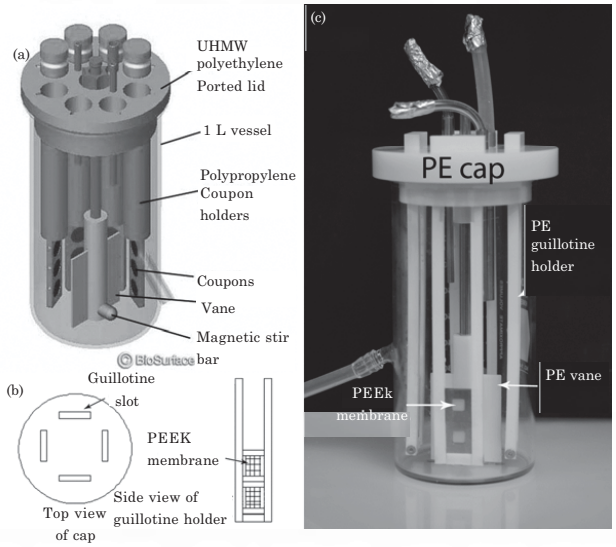

Fig. 1: (a) Schematic drawing of the original CDC biofilm reactor. (b) Schematic drawing of the cap of the modified CDC biofilm reactor and a guillotine-like holder. The holder was designed to hold PEEK membranes in the base of the reactor as they were compressed between two stainless steel plates that had a 0.64 cm^2 opening. The reactor was designed such that biofilms would form on the surface of the PEEK membranes. These membranes will be surgically inserted into an animal to model biofilm-related infection in a future study. (c) Photograph of the modified CDC biofilm reactor showing the final design of the unit. UHMWPE components are labeled with PE to show where the plastic components resided within the reactor unit. The PEEK membranes are shown being held between two stainless steel plates

The goal of this study was to determine if Delrin plastic (also known as polyoxymethylene, acetal or polyformaldehyde) was a suitable material to use for machining of the guillotine-like holders and cap of the modified reactor. As such, bacteria were grown in a broth solution within the reactor, biofilm formation on the PEEK membranes was observed and the number of bacteria on each membrane quantified.

MATERIALS AND METHODS

This study took place between January 2010 and October 2010 and was performed at the George E. Wahlen Department of Veterans Affairs Medical Center in Salt Lake City, UT. A CDC biofilm reactor was purchased from Biosurface Technologies. Delrin plastic was purchased from a local machine shop to make modified reactor components. PEEK membrane was purchased through www.smallparts.com (catalog #B000FMW8EO).

The machinist with whom we consulted had previous experience working only with Delrin plastic. He suggested that we make the guillotine-like holders out of Delrin since it was easy to machine, cheap and could be autoclaved.

The guillotine-like holders were machined to a length of 20 cm with a groove of 3 mm into which stainless steel plates could be inserted (Fig. 1b). Stainless steel screws were used to hold the guillotine-like holders together. A cap was also machined having four slots into which the holders could be inserted (Fig. 1b).

Following machining of the Delrin plastic parts for the modified reactor, the reactor was assembled such that eight PEEK membranes were lowered into the reactor as they were held in the guillotine-like holders (four holders held two membranes each for a total of eight PEEK membranes within the modified reactor unit). As such, the membranes could be exposed to shear forces of a swirling paddle in the base of the reactor (Fig. 1b). After rinsing the reactor thoroughly with distilled water, it was autoclaved prior to use.

To grow the biofilms, the reactor was filled with 500 mL of brain heart infusion broth (modified) and aseptically inoculated with ~1.5×10^8 cells of methicillin-resistant *Staphylococcus aureus*. The paddle was swirled at 130 rpm and the unit was incubated on a hot plate set at 34°C for 24 h. A flow of 10% brain heart infusion broth (modified) was flowed through the reactor for an additional 24 h.

RESULTS

For approximately five runs of the modified reactor, biofilms developed on the surface of the PEEK membranes with an average of ~3×10^9 cells per membrane. However, as we used the modified reactors over approximately five runs, we began to notice that there was more than a 3 log reduction in the number of cells within our biofilms. After another three to five runs of the reactor, bacterial growth within the reactor was inhibited completely, with no growth in the broth or on the membranes of the reactor system.

To troubleshoot the problem, we grew bacteria in 500 mL of broth alone within the biofilm reactor. The ability of bacteria to grow in the broth while in the presence of PEEK, stainless steel or Delrin plastic was also tested. More specifically, bacteria were grown in 10 mL of broth that contained a 1 cm^2 section of PEEK membrane material, in 10 mL of broth that contained 1 cm^2 of PEEK membrane and a stainless steel plate and in 10 mL of broth and a stainless steel plate alone. Finally, we grew bacteria in the modified reactor that had only the Delrin plastic reactor components in place. Notably, each of the broth samples was inoculated with ~1.5×10^5 bacterial cells.

Results indicated that bacterial growth was overtly evident in all of the broth samples with the exception of the broth that had been exposed to the Delrin plastic. These results further indicated that the Delrin plastic contained or eluted some toxic compound that had been inhibiting bacterial growth and thus biofilm formation.

Based on these findings, we made an updated version of the modified biofilm reactor using Ultra High Molecular Weight Polyethylene (UHMWPE) in place of those parts that were made of Delrin plastic (Fig. 1c). Following more than 10 runs of this autoclaved reactor, we have had no problems with bacterial growth or biofilm formation on the surface of the PEEK membranes.

DISCUSSION

Although there is a paucity of data in the literature with respect to the use of Delrin plastic in bacterial growth devices, Laluppa *et al.* (1997) showed that its use in an *ex vivo* cell expansion system had an adverse effect on the proliferation of hematopoietic progenitor cells

(LaIuppa *et al.*, 1997). Use of Delrin plastic in biomaterials should be limited as it may release toxic formaldehyde into human patients (Kusy and Whitley, 2005). Ohlin and Linder suggested the same (Ohlin and Linder, 1993).

However, in contrast to these reports, Penick *et al.* (2005) were unable to confirm the observation of LaIuppa *et al.* (1997), as they found no inhibition of cellular proliferation in an *in vitro* bioreactor system that contained components made of polyoxymethylene that was autoclaved even up to 20 times, yet they recognized that they used a different cell type and material handling may have contributed to the difference (Penick *et al.*, 2005). Further, in direct response to the suggestion of Kusy and Whitley (2005), Zilberman (2005), argued that there have been no reports of complications due to toxicity with the use of Delrin plastic in biomaterials (particularly dental crowns and bridges), suggesting that it is safe to use clinically (Zilberman, 2005). Clinical data have corroborated those suggestions (Brown and Mayor, 1978; MacAfee and Quinn, 1992).

The results of this investigation had a similar outcome as that of LaIuppa *et al.* (1997). More specifically, results strongly suggested that when Delrin plastic that had been autoclaved numerous times was exposed to the broth in which bacteria were inoculated, bacterial growth was inhibited. From the literature cited above and the material safety data sheet for Delrin plastic, wherein it is stated that if Delrin is exposed to high pressure and high temperature systems numerous times, which in our case was autoclaving, it can begin to decompose, there is strong evidence to suggest that the Delrin plastic in our system began to decompose and released formaldehyde into the broth, ultimately preventing bacterial growth in our modified biofilm reactor. Furthermore, there has been no inhibition of bacterial growth within the reactor unit after the Delrin plastic components were replaced with UHMWPE components.

The difference in cellular viability and proliferation that have been seen by investigators in *in vitro* and *ex vivo* systems may be due to (1) differences in surface area of Delrin that comes in contact with liquid, (2) the machining process of various components and/or (3) the manufacturing process that the Delrin plastic underwent prior to purchase. These possibilities remain to be determined, but may help explain the disparity in results.

In conclusion, the goal of this study was achieved. We determined that in this specific application, i.e., for our modified biofilm reactor system, Delrin plastic was not a suitable material to support growth of bacteria in broth and prevented the formation of biofilm on the surface of PEEK membranes. It is our suggestion that since there is the possibility that Delrin plastic may prevent bacterial growth, that this material not be used to manufacture bacterial growth devices, but that alternate materials such as UHMWPE be used.

ACKNOWLEDGMENTS

This material is based upon work supported by the Office of Research and Development, Rehabilitation R and D Service, George E. Wahlen Department of Veterans Affairs, Salt Lake City, UT. The project described was also supported by Award Number R01AR057185 from the National Institute of Arthritis and Musculoskeletal and Skin Diseases. The content is solely the responsibility of the authors and does not necessarily represent the official views of the National Institute of Arthritis and Musculoskeletal and Skin Diseases or the National Institutes of Health. Work was also supported by the Albert and Margaret Hofmann Chair and the Department of Orthopaedics, University of Utah School of Medicine, Salt Lake City, UT. The authors also acknowledge the help of Brad Isaacson for his contributions to the design of the modified CDC biofilm reactor and Kassie

Woodbury and Bryan Haymond for their contributions in running the modified reactor and quantifying bacteria.

REFERENCES

Brown, S.A. and M.B. Mayor, 1978. The biocompatibility of materials for internal fixation of fractures. J. Biomed. Mater. Res., 12: 67-82.

Buckingham-Meyer, K., D.M. Goeres and M.A. Hamilton, 2007. Comparative evaluation of biofilm disinfectant efficacy tests. J. Microbiol. Methods, 70: 236-244.

Gilmore, B., T. Hamill, D. Jones and S. Gorman, 2010. Validation of the CDC biofilm reactor as a dynamic model for assessment of encrustation foratmion on urological device materials. J. Biomed. Mater. Res. Part B, 93: 128-140.

Goeres, D.M., L.R. Loetterle, M.A. Hamilton, R. Murga, D.W. Kirby and R.M. Donlan, 2005. Statistical assessment of a laboratory method for growing biofilms. Microbiology, 151: 757-762.

Goeres, D.M., M.A. Hamilton, N.A. Beck, K. Buckingham-Meyer and J.D. Hilyard *et al.* 2009. A method for growing a biofilm under low shear at the air-liquid interface using the drip flow biofilm reactor. Nat. Protocols, 4: 783-788.

Kusy, R.P. and J.Q. Whitley, 2005. Degradation of plastic polyoxymethylene brackets and the subsequent release of toxic formaldehyde. Am. J. Orthod. Dentofacial Orthop., 127: 420-427.

LaIuppa, J.A., T.A. McAdams, E.T. Papoutsakis and W.M. Miller, 1997. Culture materials affect *ex vivo* expansion of hematopoietic progenitor cells. J. Biomed. Mater. Res., 36: 347-359.

Lipp, C., K. Kirker, A. Agostinho, G. James and P. Stewart, 2010. Testing wound dressings using an *in vitro* wound model. J. Wound Care, 19: 220-226.

MacAfee, K. and P. Quinn, 1992. Total temporomandibular joint reconstruction with a delrin titanium implant. J. Craniofac. Surg., 30: 160-169.

Mohle, R., T. Langemann, M. Haesner, W. Augustin and S. Scholl *et al.* 2007. Structure and shear strength of microbial biofilms as determined with confocal laser scanning microscopy and fluid dynamic gauging using a novel rotating disc biofilm reactor. Biotechnol. Bioeng., 98: 747-755.

Ohlin, A. and L. Linder, 1993. Biocompatibility of polyoxymethylene (delrin) in bone. Biomaterials, 14: 285-289.

Penick, K.J., L.A. Solchaga, J.A. Berilla and J.F. Welter, 2005. Performance of polyoxymethylene (pom) as a component of a tissue engineering bioreactor. J. Biomed. Mater. Res. Part A, 75: 168-174.

Rivard, C.H., S. Rhalmi and C. Coillard, 2002. *In vivo* biocompatibility testing of peek polymer for a spinal implant system: A study in rabbits. J. Biomed. Mater. Res., 62: 488-498.

Stoodley, P., J.D. Boyle and H.M. Lappin-Scott, 1999. Influence of flow on the structure of bacterial biofilms. Proceedings of the 8th International Symposium on Microbial Ecology, (ISME'99), Halifax, Canada, pp: 107-108.

Stoodley, P., A. Jacobsen, B. Dunsmore, B. Purevdorj, S. Wilson, H.M. Lappin-Scott and J.W. Costerton, 2001. The influence of fluid shear and ALCL3 on the material properties of *Pseudomonas aeruginosa* pao1 and *desulfovibrio* sp. Ex265 biofilms. Water Sci. Technol., 43: 113-120.

Williams, D.L. and R.D. Bloebaum, 2010. Observing the biofilm matrix of *Staphylococcus epidermidis* ATCC 35984 grown using the CDC biofilm reactor. Microsc. Microanal., 16: 143-152.

Zilberman, U., 2005. Formaldehyde from pom brackets. Am. J. Orthod. Dentofacial Orthop., 128: 147-148.

APPENDIX D

OBSERVING THE BIOFILM MATRIX OF *Staphylococcus epidermidis* ATCC 35984 GROWN USING THE CDC BIOFILM REACTOR

Microsc. Microanal. 16, 143–152, 2010
doi:10.1017/S143192760999136X

Microscopy AND Microanalysis

Observing the Biofilm Matrix of *Staphylococcus epidermidis* ATCC 35984 Grown Using the CDC Biofilm Reactor

Dustin L. Williams[1,2,3] and Roy D. Bloebaum[1,2,3,*]

[1]*Department of Veterans Affairs, Salt Lake City, UT 84148, USA*
[2]*Department of Bioengineering, University of Utah, Salt Lake City, UT 84112, USA*
[3]*Department of Orthopaedics, University of Utah, Salt Lake City, UT 84108, USA*

Abstract: Bacteria flourish in nearly every environment on earth. Contributing to their ability to grow in many esoteric locations is their development into a biofilm structure. In an effort to more accurately model the growth environment of biofilms in nature, a Center for Disease Control and Prevention (CDC) biofilm reactor has been developed that mimics nature-like shear forces and renewable nutrient sources. To date, there has been no confirmation by scanning electron microscopy (SEM) that mature biofilms develop on a surface when grown using the CDC biofilm reactor. Three different SEM methods were used to collect images of *Staphylococcus epidermidis* ATCC 35984 that was to be grown using the CDC biofilm reactor. In addition, two different fixative techniques were used in each of the imaging methods. Results indicated that after 48 hours of growth in the reactor, *S. epidermidis* ATCC 35984 does produce a significant network of matrix components and 3D mushroom- or pillar-like structures with signs of water channel development. In conclusion, *S. epidermidis* ATCC 35984 grown using the CDC biofilm reactor does appear to display signs of mature biofilm development. These results could be important for studies wherein mature biofilms are needed for *in vitro* and/or *in vivo* applications.

Key words: biofilm, scanning electron microscopy, fixation, CDC biofilm reactor

Introduction

Biofilms are "Structured communit(ies) of bacterial cells enclosed in a self-produced polymeric matrix and adherent to an inert or living surface" (Costerton et al., 1999). Although largely beneficial to human life in performing niche functions such as biodegradation (Martinkova et al., 2008), oxygen production (Pringault & Garcia-Pichel, 2000), and water treatment (Modin et al., 2008), biofilms do have the negative potential of attaching to biomaterials and subsequently causing biomaterial-related infections in humans (Costerton, 2007*a*).

The pathogenicity of biofilm-dwelling organisms is at least in part attributed to the development of an extracellular polymeric substance (EPS) (Ammendolia et al., 1999). The EPS is highly heterogeneous in its production between organisms and even bacterial growth conditions (Uhlinger & White, 1983; De Beer et al., 1994). Containing between 90% and 98% water, the matrix expresses highly hydrodynamic properties (Christensen & Characklis, 1990; Schmitt & Flemming, 1999; Erlandsen et al., 2004). Furthermore, the EPS matrix can have a variety of forms from honeycomb structures (Thar & Kuhl, 2002; Costerton, 2007*d*; Schaudinn et al., 2007) to complex three-dimensional (3D) networks of fibers wrapping around the surface of the bacteria (Erlandsen et al., 2004).

Not only has the National Institutes of Health suggested that 80% of all clinical illnesses are biofilm-related, it is believed that in nature bacteria dwell largely in biofilm structures (Costerton, 2007*c*). Importantly, and perhaps intuitively, bacterial phenotypes and environments that exist in nature are not the same as bacteria grown in the lab. Differences in nutrient source and concentration can affect bacterial growth rate and biofilm formation. In the lab, microbiologists select planktonic bacteria for almost every application from the bulk solution of a broth growth media or the water surface of an agar plate, whereas the more naturally occurring biofilm bacteria grow at interfaces, on ridges, under varying nutrient conditions, and at times under high shear forces. In summary, the lab environment does not always accurately reflect the natural life cycle of pathogenic or other bacteria (Costerton, 2007*c*).

In an attempt to address these limitations, novel technologies have been developed that propose to grow biofilms in the lab under more natural conditions while maintaining repeatable results (Goeres et al., 2005). One such technology

Received September 1, 2009; accepted December 22, 2009
*Corresponding author. E-mail: roy.bloebaum@hsc.utah.edu

is the Centers for Disease Control and Prevention (CDC) biofilm reactor. The CDC biofilm reactor is a reliable experimental tool for growing a standard biofilm with former evaluation of the repeatability of the procedure (Goeres et al., 2005).

In essence, this unit supplies a continuous flow of nutrient broth through a beaker that contains a swirling paddle that exposes bacteria growing on "coupons" to shear forces. The setup mimics at least two nature-like environments—a renewable nutrient source (the concentration of which the user can adjust as desired) and shear forces that are exposed to the growth substrate and biofilm itself. Previous imaging studies have involved bacteria that were grown using the previously described traditional growth methods (Erlandsen et al., 2004; Priester et al., 2007). However, to date there has not been visual observation by scanning electron microscopy (SEM) to confirm that bacteria grown using the CDC biofilm reactor develop into a mature biofilm, i.e., a biofilm that displays significant EPS production, mushroom- or pillar-like structures, and water channel connections (Jiang & Pace, 2006). Thus, in this study three types of SEM and two fixation techniques were used to observe the biofilm matrix of *Staphylococcus epidermidis* ATCC 35984, a known heavy matrix producer, grown using the CDC biofilm reactor. It was hypothesized that this biofilm grown using the CDC biofilm reactor would display characteristics that reflect a mature biofilm structure. It was further hypothesized that when fixed with a glutaraldehyde-based fixative solution, the EPS would be preserved more readily than with formalin fixation.

A promising field of SEM imaging has been developed that provides the ability to image a biological or otherwise "wet" sample without any preparatory techniques—hypothetically resulting in an image of the sample in its more natural, water-containing condition. These imaging methods are termed environmental SEM (ESEM) and variable pressure, or low vacuum SEM. ESEM conditions include chamber pressures in the range of 20 Torr whereas low vacuum conditions function at around 2 Torr. The purpose of these conditions is to circumvent the need for fixing, dehydrating, and/or coating a sample, which, in the case of biofilms, are believed to alter the morphology of the matrix (Little et al., 1991; Fassel & Edminston, 1999; Priester et al., 2007). However, previous reports have also found that with ESEM damage to biofilms from the beam is evident after only a few minutes of imaging (Little et al., 1991; Priester et al., 2007).

Another mode of SEM imaging requires high vacuum (10^{-4}–10^{-10} Torr) conditions to image a sample making fixation, dehydration, and coating techniques essential. Nevertheless, it has recently been shown that cationic dyes and metal stains, in conjunction with cellular fixation and dehydration techniques, may preserve the biofilm matrix to allow for qualitative interpretation of connection points, matrix structures, and distribution of the components (Erlandsen et al., 2004). Moreover, Priester et al. (2007) determined that even ESEM images of biofilm are enhanced after fixation and cationic dye treatment, albeit without dehydration of the sample.

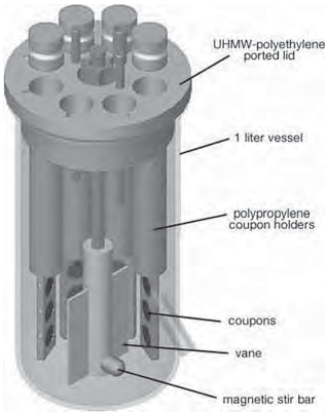

Figure 1. Schematic diagram of the CDC biofilm reactor. Biofilms are grown on the surface of coupons in the base of the reactor. In addition, biofilms are exposed to shear forces as the paddle (vane) swirls broth media across the surface of the coupons.

Therefore, to compare the various SEM imaging techniques, a standard JEOL JSM-6100 lanthanum hexaboride (LaB_6) filament SEM, a FEI high-resolution NOVA NanoSEM, and the FEI Quanta 600 ESEM were used to observe the biofilm matrix of *S. epidermidis* ATCC 35984 grown using the CDC biofilm reactor. Moreover, because many laboratories use 10% buffered formalin or 2.5% glutaraldehyde combined with other chemicals to fix biological specimens, biofilms were treated with one of these two fixative techniques for comparison of matrix preservation.

Materials and Methods

Coupon Passivation

The CDC biofilm reactor (Biosurface Technologies, MT) uses "coupons" that have a $\frac{1}{2}$-in. diameter and $\frac{1}{8}$-in. height on which to grow biofilms (Fig. 1). The biofilms develop on the faces of the coupons as they are exposed to shear forces by a swirling paddle in the base of the reactor. The coupons can be made of nearly any desired material. For this study, commercially pure titanium (cpTi) coupons were used (Biosurface Technologies, Bozeman, MT) to model titanium that is used in implants for joint replacement devices. Prior to growing biofilm on them, the coupons were passivated by first washing them and sonicating them for 10 min in a store-bought detergent. The coupons were then rinsed in running reverse osmosis water, cleaned and sonicated for another 10 min in Alconox detergent, rinsed again in the

same, and placed in ∼35% solution of nitric acid for 30 min. Following nitric acid passivation, coupons were soaked in reverse osmosis water for 10 min then rinsed in running water of the same for an additional 10 min. All equipment, including the coupons, was autoclaved prior to use.

Bacterial Growth

S. epidermidis ATCC 35984 was chosen because of its use in various orthopaedic experiments and its significant production of a slimy layer. The isolate was first grown on Columbia blood agar (Hardy Diagnostics, Santa Maria, CA). From a fresh 24 h culture, a 0.5 McFarland standard of the bacteria was made, which equates to $\sim 1.5 \times 10^8$ bacteria/mL. One mL of the McFarland standard was then inoculated into 500 mL of tryptic soy broth (TSB; Becton Dickinson and Company, Franklin Lakes, NJ) in the CDC biofilm reactor. The reactor was placed on a hot plate set at 38°C, a rotation of 130 rpm, and incubated 24 h. Following this initial 24 h incubation, a continuous flow of 10% TSB was flushed through the reactor at ∼5.8 mL/min for another 24 h. The coupons were then removed and exposed to one of two fixation procedures or imaged immediately in the ESEM.

Glutaraldehyde Fixative

Erlandsen et al. (2004) have shown that low voltage, high-resolution images of biofilm can be observed by SEM with the addition of cationic dyes to fixative solution to enhance the attachment of osmium tetroxide (OsO_4), which aids in fixation and sample conductivity, to the EPS matrix. Thus, in this experiment Ruthenium Red was used as a cationic dye. After running the CDC biofilm reactor, three of the coupons having biofilm grown on them and one untreated, control coupon were initially exposed to a pre-fixative solution containing 2.5% glutaraldehyde (Ted Pella, Redding, CA), 50 mM L-lysine monohydrochloride (Sigma, St. Louis, MO) and 0.75% Ruthenium Red (Ted Pella) in 0.2 M cacodylate buffer, pH 7.4 (Electron Microscopy Sciences, Hatfield, PA). Coupons were soaked in the prefixative for 20 min followed by a 24 h treatment in the same fixative solution excluding the 50 mM L-lysine as per the protocol of Priester et al. (2007).

Coupons were rinsed in cacodylate buffer 3× for 10 min, placed in a 2% solution of osmium tetroxide (OsO_4; Ted Pella) in cacodylate buffer for 2 h and rinsed with cacodylate buffer 3× for 10 min (hereafter, this cationic dye/2.5% glutaraldehyde/OsO_4 treatment routine is simply referred to as 2.5% glutaraldehyde fixative). Following the final rinse, the coupons were placed in increasing concentrations of ethanol, from 70% to 95% to 100%, 3× for 20 min each. Coupons were then dried in a desiccator. Two coupons containing biofilm were coated with gold or carbon prior to imaging. One biofilm-containing coupon was left uncoated for imaging under low vacuum conditions in the NOVA NanoSEM. The control, non-biofilm-containing coupon was imaged under low vacuum conditions in the same instrument to determine if artifacts from the fixation procedure were present.

Formalin Fixative

After running the CDC biofilm reactor, three coupons having biofilm grown on them and one untreated, control coupon were placed in 10% buffered formalin for 24 h and dehydrated in the same manner as the 2.5% glutaraldehyde fixative procedure. Coupons were dried in a desiccator. Two coupons containing biofilm were coated with gold or carbon prior to imaging. One biofilm-treated coupon was left uncoated for imaging under low vacuum conditions in the NOVA NanoSEM. The control, non-biofilm-containing coupon was also imaged under low vacuum conditions to determine if artifacts developed from the fixation procedure.

ESEM Imaging

Following the 48 h growth period in the CDC biofilm reactor, three coupons were removed, placed in 0.9% sterile saline and imaged by ESEM within 30 min of removal. Double-sided carbon sticky tabs were used to attach the coupon to a standard stub (Ted Pella) for mounting onto the stage of the Quanta 600 ESEM. Images were collected with an accelerating potential of 10–20 keV, chamber pressure of 1–20 Torr and 60–100% humidity. Secondary electron images were collected using a gaseous secondary electron detector.

Low Vacuum Imaging

Two uncoated coupons containing biofilms that were treated with either 2.5% glutaraldehyde or 10% buffered formalin were imaged using a NOVA NanoSEM 600 at 7 keV and a chamber pressure of 0.5–2 Torr. Secondary electron images were collected using a secondary electron Helix detector.

High Vacuum Imaging

Following the 2.5% glutaraldehyde and 10% buffered formalin fixation procedures, one coupon each containing biofilm was coated with carbon or gold resulting in a coating layer of approximately 6–8 nm and 4–5 nm, respectively. Biofilms were imaged in a NOVA NanoSEM 600 at 2 keV accelerating potential. Backscatter electron images were collected using a vCD detector.

Results

ESEM Imaging

Initial images were collected at 10 keV and a pressure of 1 Torr. However, the biofilm charged and the images did not

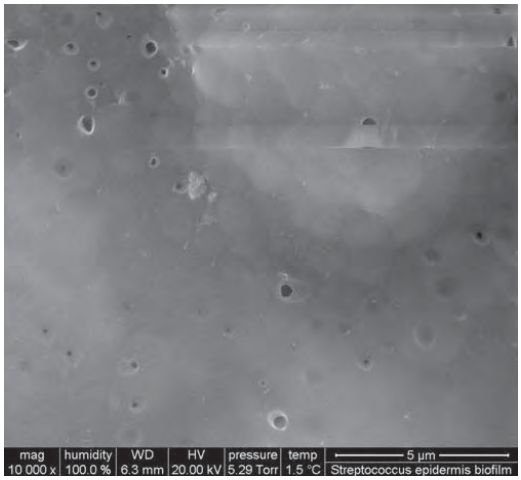

Figure 2. Holes (dark circles) were punctured into the biofilm of *S. epidermidis* ATCC 35984 by the beam after only a few minutes of imaging at 20 keV, 100% humidity, and 5.29 Torr.

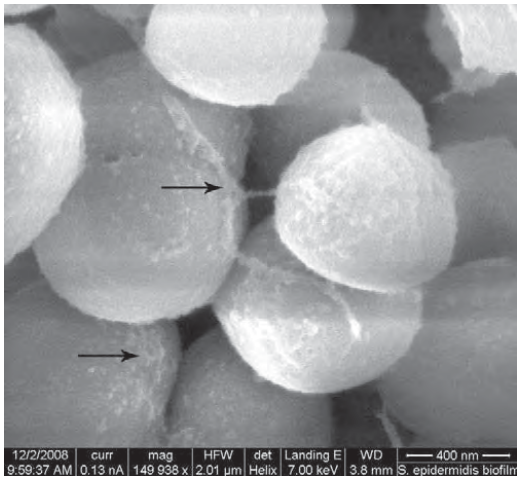

Figure 3. Secondary electron image of an uncoated biofilm of *S. epidermidis* ATCC 35984 under low vacuum conditions. At ~150k× original magnification, nanostructures of the matrix can be seen with components overlaying and attaching to cells (arrows).

resolve well. Therefore, the pressure and accelerating potential were increased to 5.29 Torr and 20 keV, respectively. Notably, no sharp image could be collected with greater than an original magnification of 10,000× (Fig. 2).

Consistent with previous experiments using ESEM imaging (Little et al., 1991; Priester et al., 2007), the biofilm of *S. epidermidis* ATCC 35984 was damaged by the beam after only a few minutes making it difficult to collect useful images (Fig. 2). Nevertheless, the smooth, undulating surface that was seen indicated that a 3D structure of biofilm encapsulated in a slimy substance was present—suggesting that a mature biofilm had developed on the surface of the coupon (Jiang & Pace, 2006).

Low Vacuum Imaging

Images of secondary electrons collected using the Helix detector indicated that without any coating, the structures of the *S. epidermidis* ATCC 35984 biofilm treated with the 2.5% glutaraldehyde fixative could be resolved to a nm scale (Fig. 3). Importantly, under low vacuum conditions the 10% buffered formalin did not appear to preserve the matrix components on the surface of cells (Fig. 4) to the same degree as 2.5% glutaraldehyde (Fig. 5).

The EPS matrix displayed a fibrous network of products similar to what Erlandsen et al. (2004) described as helical duplexes wrapping around cells (Fig. 3) in addition to a mesh of components that appeared to connect cells one to another and create an outer shell of protection to sporadic areas of the biofilm (Fig. 6). The significant production of EPS by the cells indicated that mature biofilms had developed on the surface of the coupons.

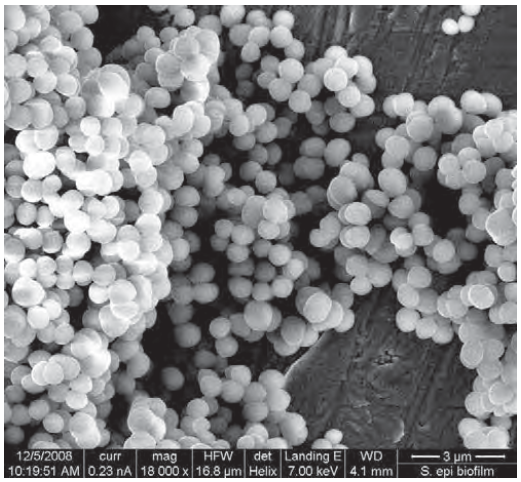

Figure 4. Low vacuum secondary electron image collected of the *S. epidermidis* ATCC 35984 biofilm fixed with formalin. Note the smooth appearance of the cellular surface and the lack of fibers or matrix structures extending off the surface or between cells.

Finally, control coupons that did not contain biofilm, but that were treated with either 2.5% glutaraldehyde or

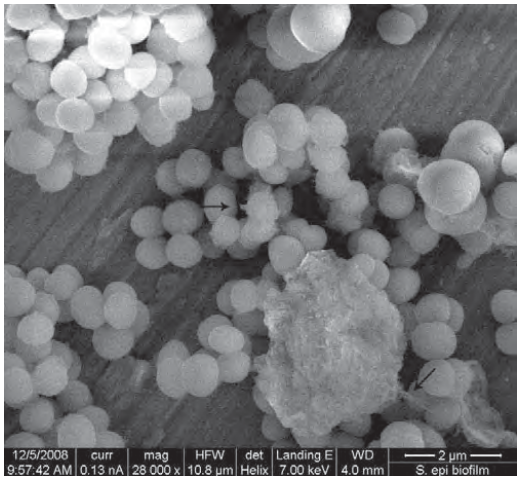

Figure 5. Low vacuum secondary electron image of the *S. epidermidis* ATCC 35984 biofilm fixed with 2.5% glutaraldehyde. Arrows indicate portions of the matrix components connecting cells one to another and extending off the surface.

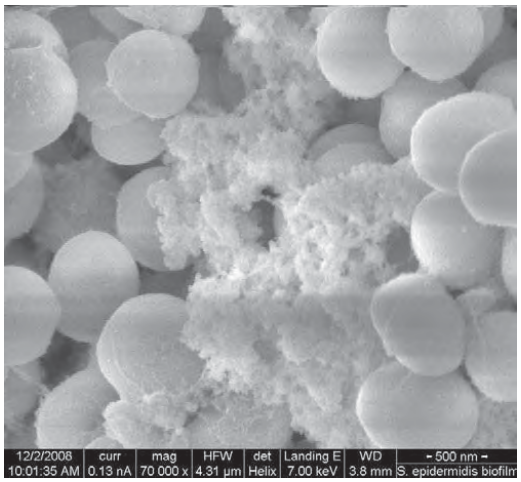

Figure 6. Under low vacuum conditions, a mesh of matrix components is observed. Not only does the mesh connect cells one to another, but it also encapsulates cells, likely protecting them from environmental perturbations.

10% buffered formalin, were imaged under low vacuum. These were to determine if artifacts developed that may result in a misinterpretation of the biofilm matrix or other cellular structures. Results indicated that no residue of any kind was left on the coupons by either treatment.

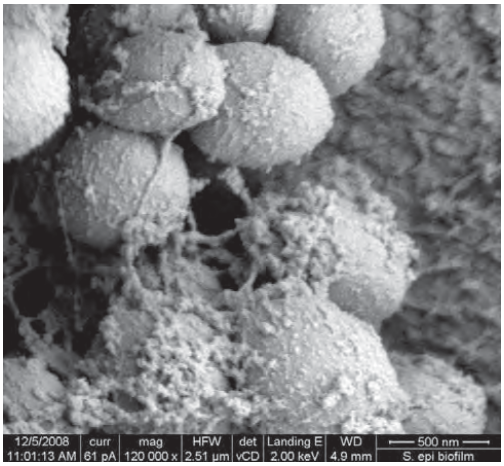

Figure 7. Backscatter electron image of a 2.5% glutaraldehyde-fixed biofilm taken under high vacuum with the vCD detector in the NOVA NanoSEM. Compared to the images collected at low vacuum, the image does appear to be sharper and have greater contrast with reduced charging artifacts.

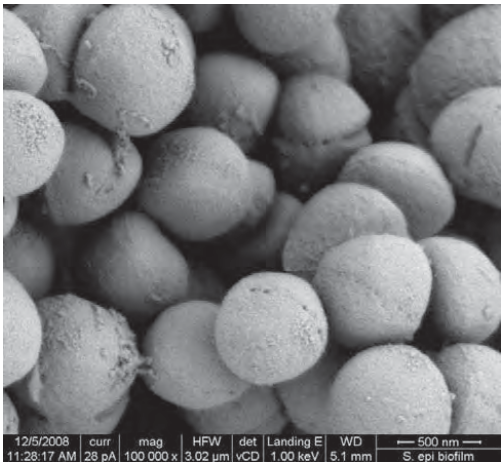

Figure 8. Backscatter electron image of a 10% buffered formalin-fixed biofilm taken at high vacuum with the vCD detector in the NOVA NanoSEM. Fewer matrix components can be seen than the 2.5% glutaraldehyde-fixed biofilm. Compared to the images collected at low vacuum, the image does appear to be sharper and have a greater contrast with reduced charging artifacts.

High Vacuum Imaging

Although the images collected with the NOVA NanoSEM 600 under low vacuum were sharp enough to see nanostruc-

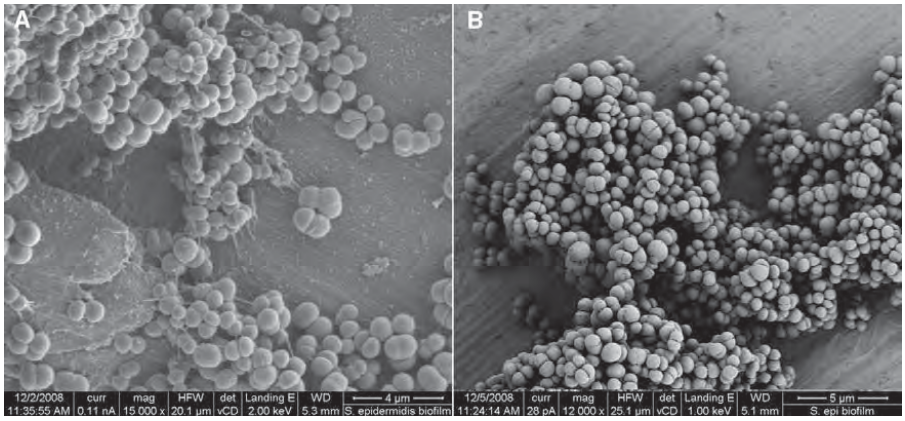

Figure 9. A: Carbon-coated biofilm of *S. epidermidis* ATCC 35984 fixed with 10% buffered formalin. **B:** Gold-coated biofilm of the same organism fixed with 10% buffered formalin. Note the sharper image and more defined contrast in the biofilm coated with gold (**B**).

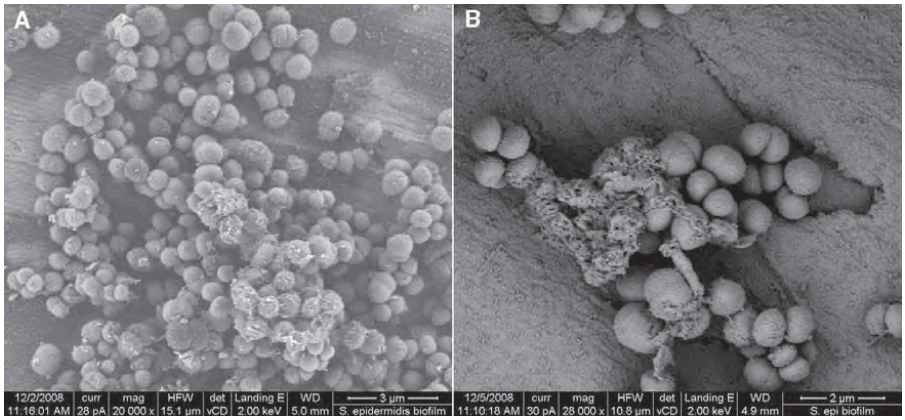

Figure 10. A: Carbon-coated biofilm of *S. epidermidis* ATCC 35984 fixed with 2.5% glutaraldehyde. **B:** Gold-coated biofilm of the same organism fixed with 2.5% glutaraldehyde. Note the sharper image and more defined contrast in the biofilm coated with gold (**B**).

tures of the biofilm matrix, the images collected of 2.5% glutaraldehyde and 10% buffered formalin-fixed biofilms at high vacuum with the vCD detector were not altered by charging and had much higher resolution and sharpness (Figs. 7, 8). In addition, greater detail of the fibers of the EPS matrix could be seen. The fibers had rounded edges, areas that were significantly bundled with a net-like appearance, with other areas having a single fiber spanning the distance of one or several cells (Fig. 7).

Importantly, while imaging biofilms that had been fixed with either 2.5% glutaraldehyde fixative or 10% buffered formalin, those coated with gold did appear to produce sharper, more defined images when compared to carbon-coated biofilms (Figs. 9, 10). Notably, it was thought that the OsO_4 used in the 2.5% glutaraldehyde-treated biofilms was responsible for helping to create a sharper contrast image when compared to 10% buffered formalin-fixed biofilms, but after comparing a gold-coated, 10% buffered formalin-fixed biofilm that was not treated with OsO_4 to a gold-coated, 2.5% glutaraldehyde-fixed biofilm, the contrast and sharpness appeared to be quite similar (Fig. 11).

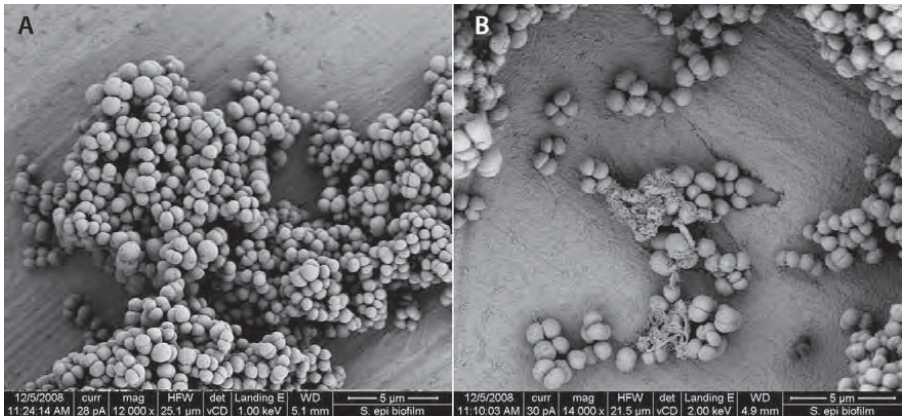

Figure 11. A: Biofilm of *S. epidermidis* ATCC 35984 that has been fixed using 10% buffered formalin and coated with gold. **B:** Biofilm of the same organism that has been fixed 2.5% glutaraldehyde and coated with gold. Notice the similar contrast and sharpness between the images.

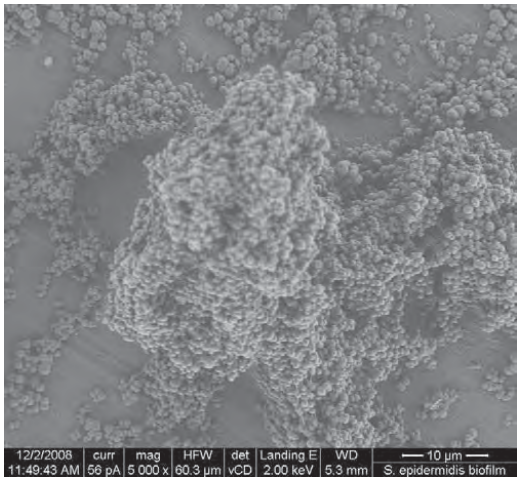

Figure 12. Representative image of a mushroom-like structure that is typical of the biofilm formations that were seen in this study. Note that the top of the mushroom is blurry and in-focus regions are near the coupon surface indicating a vertical rising of the mushroom toward the viewer. Sample was fixed with 10% buffered formalin and coated with carbon.

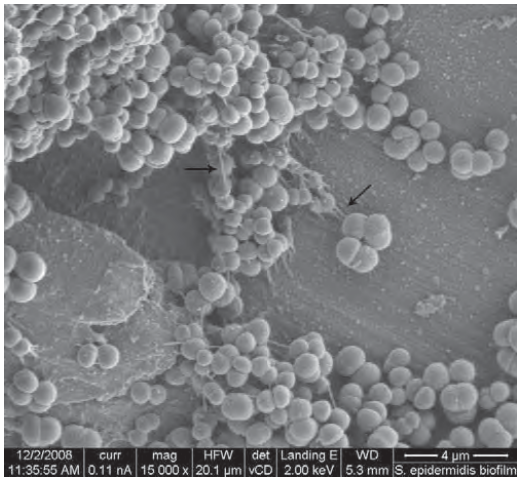

Figure 13. Arrows indicate nanofibers that could be seen within the biofilm structure. These wires appear to connect the cells to one another as well as to the surface of the coupon.

Consistent throughout each of the imaging techniques was the identification of mushroom- or pillar-like structures and signs of water channels that are indicators of mature biofilm development (Fig. 12) (Jiang & Pace, 2006). Interestingly, the 10% buffered formalin-fixed biofilms appeared to display what may have been nanofibers extending between cells, but this may have been shrinkage artifact (Fig. 13).

After comparing several of the biofilms that had been fixed with 2.5% glutaraldehyde or 10% buffered formalin, it was determined that the 2.5% glutaraldehyde-fixed biofilms may contain and preserve more matrix components, but at least some matrix components were maintained by both fixation procedures (Fig. 14). From the various images, it

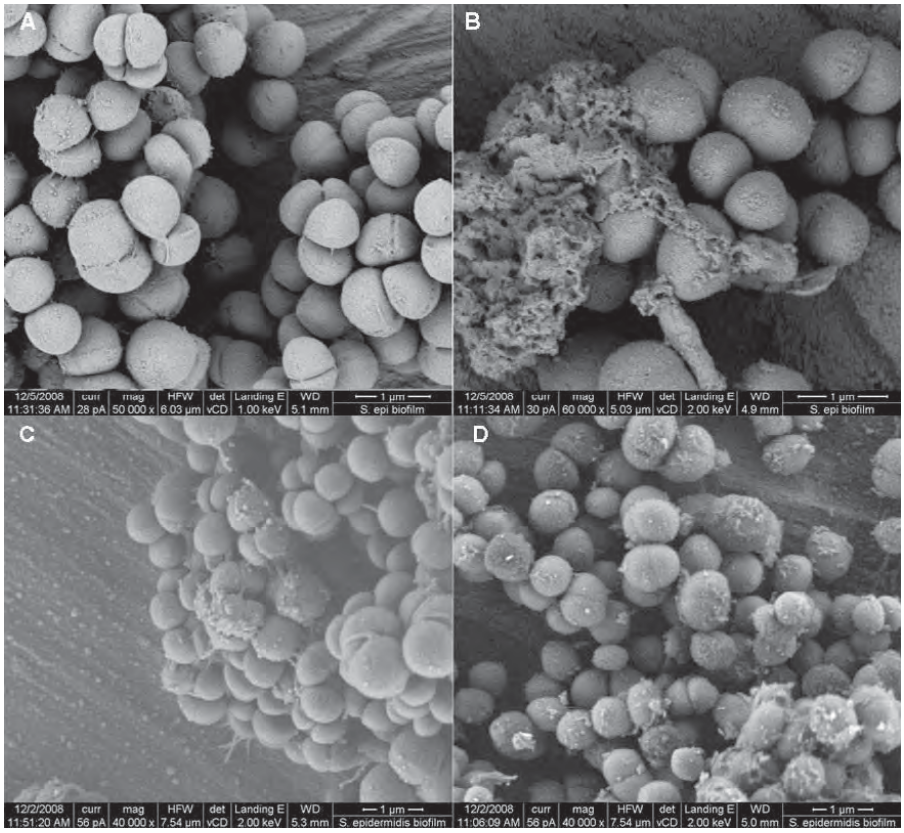

Figure 14. A: Gold-coated biofilm fixed with 10% buffered formalin. Signs of bacterial growth are indicated by the bacterial cells that are dividing. This is a representative image of the thousands of cells that were seen dividing. **B:** Gold-coated biofilm fixed with 2.5% glutaraldehyde. **C:** Carbon-coated biofilm fixed with 10% buffered formalin. **D:** Carbon-coated biofilm fixed with 2.5% glutaraldehyde. Notice that slightly more matrix components seem to be preserved in the 2.5% glutaraldehyde-treated biofilms.

appeared that the EPS components provided significant to moderate coverage of the bacterial cells within the biofilm, supporting previous data that suggests the EPS matrix plays an important role in protecting the cells from environmental perturbations and antimicrobial therapies (De Beer et al., 1994). Interestingly, within the biofilm structures, there were signs of a significant amount of bacterial growth. Indeed, thousands of cells were observed in a dividing state with areas of cellular attachment still being present (Fig. 14A).

Discussion

Images of a *S. epidermidis* ATCC 35984 biofilm grown using the CDC biofilm reactor system were collected using three separate SEM methods: ESEM, low vacuum imaging and high vacuum imaging. In addition, biofilms that had been fixed using either 2.5% glutaraldehyde or 10% buffered formalin were compared with the hypothesis that glutaraldehyde would preserve the biofilm matrix more so than 10% formalin. This hypothesis was developed due to the lack of data regarding this direct comparison of biofilm fixation in the literature. Finally, gold-coated, carbon-coated, and uncoated biofilms were analyzed in conjunction with these fixation techniques under the hypothesis that biofilms grown on the surface of titanium coupons within the CDC biofilm reactor would develop into maturity.

The images collected using ESEM indicated that the biofilm was damaged by the beam after only a few minutes—similar to previous findings (Little et al., 1991; Priester et al., 2007). In addition, sample charging was a problem, and no

high magnification images with high resolution could be collected. However, it must be noted that the quality of images collected using ESEM or SEM can be largely user-dependent. Therefore, it is important to mention that four different users attempted to work with this biofilm under ESEM conditions and the images provided are the sharpest that were able to be taken. In summary, consistent with previous findings (Priester et al., 2007), in its current state of technology, without cationic dyes or some fixation, ESEM does not appear to have the capacity to image biofilms such that the micro or nanostructures of the matrix can be viewed. Indeed, with ESEM alone it was difficult to elucidate the structure of this biofilm matrix beyond its global appearance and shape. However, these data could be very informative in a different application. Nevertheless, the ESEM images did not resolve the biofilm matrix to a level that allowed us to determine if the fixation and dehydration of the biofilms had changed its morphology as has been reported previously (Little et al., 1991; Fassel & Edminston, 1999; Priester et al., 2007).

The images collected in this study suggest that 2.5% glutaraldehyde-fixed biofilm matrix is preserved sufficiently to obtain information concerning its topographical characteristics, connection points with both the cells and substrate as well as nanostructures of the matrix itself. In contrast, biofilms fixed with 10% buffered formalin displayed a lack of matrix components suggesting that formalin, with only one reactive group per molecule, does not preserve the biological components to the same level as 2.5% glutaraldehyde. In both cases, however, cellular division could be seen at the surface of the biofilm suggesting that even after 48 h of growth, the biofilms were rapidly dividing.

Importantly, the EPS matrix and 3D structure of biofilms can vary significantly from one growth environment to another. Other studies have observed the wide variety of biofilm morphologies that can exist in clinical and environmental applications (Costerton et al., 1978; Litzler et al., 2007; Schaudinn et al., 2007). At times, 3D mushroom- or pillar-like formations of biofilms are not seen (Erlandsen et al., 2004; Priester et al., 2007), whereas in this study they were seen. The observation that biofilms grown in the CDC biofilm reactor developed significant EPS and mushroom-like structures was promising. More specifically, as reports highlight the ever-increasing rate of bacterial resistance to antibiotics with biofilms providing even greater resistance (Nickel et al., 1985) and high rates of genetic material exchange (Cvitkovitch, 2001; Costerton, 2007*b*), the use of well-established, mature biofilms in *in vivo* models of clinically relevant infections is important. Thus, the production of mature biofilms in a standardized biofilm reactor system (Goeres et al., 2005) provides strong potential to produce mature biofilms that can be used in *in vivo* applications of implant-related and other chronic infections.

One limitation to this study, however, was that preparatory techniques for SEM imaging did cause water loss and shrinkage of the biological samples. Because of the well-known fact that dehydration can alter biological morphology, the ability to observe water channels throughout the mushroom- or pillar-like structures biofilms was limited. Thus, although ravines, ridges, and crevices were replete throughout mushroom- or pillar-like structures, it could not be concluded that these were water channels, but could be artifacts from shrinkage and water loss. However, the ravines do suggest that water channels may have been present and in combination with significant EPS products and mushroom- or pillar-like structures, there is strong evidence to suggest that mature biofilms did form.

It is becoming apparent that biofilm matrices come in a variety of structures such as the production of honeycomb-like structures or fibrous networks of the *S. epidermidis* isolate observed in this study. Thus, phenotypic characteristics are species dependent, but may also change with maturation of the biofilm. Herein the biofilm was grown for only 48 h, and in future it will be interesting to see what the matrix looks like after 5 or more days of growth in the CDC biofilm reactor.

In conclusion, biofilms grown using the CDC biofilm reactor were found to produce EPS matrix components displaying cell-cell and cell-surface connections as well as mushroom- or pillar-like structures with signs of water channel development. Thus, the hypothesis that bacteria grown in the reactor would produce EPS and show signs of mature development was supported. These data suggest that biofilms grown in this reactor may be useful for future animal models that are used for translational research applications.

Conclusions

The production of mature biofilms in a laboratory setting is important for *in vitro* and *in vivo* research applications. More specifically, planktonic bacteria used in *in vitro* or *in vivo* studies may not be suitable indicators of what might occur in a biofilm community or biofilm-related infection, respectively. Thus, the indications from this study that biofilms grown in the CDC biofilm reactor reach maturity are important as they suggest that these biofilms may be applied in future investigations that, for example, might involve the prevention of biofilm-related infections that surround orthopaedic devices or other implant materials.

Acknowledgments

This material is based upon work supported by the Office of Research and Development, Rehabilitation R&D Service, Department of Veterans Affairs, Salt Lake City, UT, and the Albert and Margaret Hofmann Chair and the Department of Orthopaedics, University of Utah School of Medicine, Salt Lake City, UT. The project described was also supported

by Grant Number R01 AR057185-02 from the National Institute of Arthritis and Musculoskeletal and Skin Diseases (NIAMS) section of the National Institutes of Health (NIH). The authors also acknowledge the help of Dr. Matt DeLong and Dr. Randy Polson for their technical assistance in obtaining SEM images from the NOVA NanoSEM 600.

References

Ammendolia, M.G., Di Rosa, R., Montanaro, L., Arciola, C.R. & Baldassarri, L. (1999). Slime production and expression of the slime-associated antigen by staphylococcal clinical isolates. *J Clin Microbiol* **37**(10), 3235–3238.

Christensen, B.E. & Characklis, W.G. (1990). Physical and chemical properties of biofilms. In *Biofilms*, Characklis, W.G. & Marshall, K.C. (Eds.), pp. 93–130. New York: John Wiley.

Costerton, J.W. (2007*a*). Bacterial attachment to surfaces. In *The Biofilm Primer*, Eckey, D.C. (Ed.), pp. 36–43. Berlin: Springer.

Costerton, J.W. (2007*b*). Genetic efficiency of biofilms. In *The Biofilm Primer*, Eckey, D.C. (Ed.), pp. 74–75. Berlin: Springer.

Costerton, J.W. (2007*c*). The predominance of biofilms in natural and engineered ecosystems. In *The Biofilm Primer*, Eckey, D.C. (Ed.), pp. 5–13. Berlin: Springer.

Costerton, J.W. (2007*d*). Tertiary structures formed within the matrices of biofilms. In *The Biofilm Primer*, Eckey, D.C. (Ed.), pp. 27–34. Berlin: Springer.

Costerton, J.W., Geesey, G.G. & Cheng, K.-J. (1978). How bacteria stick. *Sci Am* **238**(1), 86–95.

Costerton, J.W., Stewart, P.S. & Greenberg, E.P. (1999). Bacterial biofilms: A common cause of persistent infections. *Science* **284**(5418), 1318–1322.

Cvitkovitch, D.G. (2001). Genetic competence and transformation in oral streptococci. *Crit Rev Oral Biol Med* **12**(3), 217–243.

De Beer, D., Srinivasan, R. & Stewart, P.S. (1994). Direct measurement of chlorine penetration into biofilms during disinfection. *Appl Environ Microbiol* **60**(12), 4339–4344.

Erlandsen, S.L., Kristich, C.J., Dunny, G.M. & Wells, C.L. (2004). High-resolution visualization of the microbial glycocalyx with low-voltage scanning electron microscopy: Dependence on cationic dyes. *J Histochem Cytochem* **52**(11), 1427–1435.

Fassel, T.A. & Edminston, C.E. (1999). Bacterial biofilms: Strategies for preparing glycocalyx for electron microscopy. *Methods Enzym* **310**(1), 194–203.

Goeres, D.M., Loetterle, L.R., Hamilton, M.A., Murga, R., Kirby, D.W. & Donlan, R.M. (2005). Statistical assessment of a laboratory method for growing biofilms. *Microbiology* **151**(Pt. 3), 757–762.

Jiang, X. & Pace, J.L. (2006). Microbial biofilms. In *Biofilms, Infection and Antimicrobial Therapy*, Pace, J.L., Rupp, M.E. & Finch, R.G. (Eds.), pp. 3–19. Boca Raton, FL: Taylor & Francis Group.

Little, B., Wagner, P., Ray, R., Pope, R. & Scheetz, R. (1991). Biofilms: An ESEM evaluation of artifacts introduced during SEM preparation. *J Industr Microbiol* **8**(4), 213–222.

Litzler, P.-Y., Benard, L., Barbier-Frebourg, N., Vilain, S., Jouenne, T., Beucher, E., Bunel, C., Lemeland, J.-F. & Bessou, J.-P. (2007). Biofilm formation on pyrolytic carbon heart valves: Influence of surface free energy, roughness, and bacterial species. *J Thoracic Cardiovasc Surg* **134**(4), 1025–1032.

Martinkova, L., Uhnakova, B., Patek, M., Nesvera, J. & Kren, V. (2008). Biodegradation potential of the genus Rhodococcus. *Environ Int* **35**(1), 162–177.

Modin, O., Fukushi, K. & Yamamoto, K. (2008). Simultaneous removal of nitrate and pesticides from groundwater using a methane-fed membrane biofilm reactor. *Water Sci Technol* **58**(6), 1273–1279.

Nickel, J.C., Ruseska, I., Wright, J.B. & Costerton, J.W. (1985). Tobramycin resistance of *Pseudomonas aeruginosa* cells growing as a biofilm on urinary catheter material. *Antimicrob Agents Chemotherapy* **27**(4), 619–624.

Priester, J.H., Horst, A.M., Van De Werfhorst, L.C., Saleta, J.L., Mertes, L.A.K. & Holden, P.A. (2007). Enhanced visualization of microbial biofilms by staining and environmental scanning electron microscopy. *J Microbiol Methods* **68**(3), 577–587.

Pringault, O. & Garcia-Pichel, F. (2000). Monitoring of oxygenic and anoxygenic photosynthesis in a unicyanobacterial biofilm, grown in benthic gradient chamber. *FEMS Microbiol Ecol* **33**(3), 251–258.

Schaudinn, C., Stoodley, P., Kainović, A., O'Keeffe, T., Costerton, B., Robinson, D., Baum, M., Ehrlich, G. & Webster, P. (2007). Bacterial biofilms, other structures seen as mainstream concepts. *Microbe* **2**(5), 231–237.

Schmitt, J. & Flemming, H.-C. (1999). Water binding in biofilms. *Water Sci Technol* **39**(7), 77–82.

Thar, R. & Kuhl, M. (2002). Conspicuous veils formed by vibrioid bacteria on sulfidic marine sediment. *Appl Environ Microbiol* **68**(12), 6310–6320.

Uhlinger, D.J. & White, D.C. (1983). Relationship between physiological status and formation of extracellular polysaccharide glycocalyx in *Pseudomonas atlantica*. *Appl Environ Microbiol* **45**(1), 64–70.

APPENDIX E

EXPERIMENTAL MODEL OF BIOFILM IMPLANT-RELATED OSTEOMYELITIS TO TEST COMBINATION BIOMATERIALS USING BIOFILMS AS INITIAL INOCULA

245
Society For Biomaterials

Experimental model of biofilm implant-related osteomyelitis to test combination biomaterials using biofilms as initial inocula

Dustin L. Williams,[1,2,3] Bryan S. Haymond,[1,2,3] Kassie L. Woodbury,[1,4] J. Peter Beck,[1,3] David E. Moore,[1] R. Tyler Epperson,[1] Roy D. Bloebaum[1,2,3]

[1]George E. Wahlen Department of Veterans Affairs Medical Center, Salt Lake City, Utah
[2]Department of Bioengineering, University of Utah, Salt Lake City, Utah
[3]Department of Orthopaedics, University of Utah, Salt Lake City, Utah
[4]School of Medicine, University of Utah, Salt Lake City, Utah

Received 23 November 2011; accepted 3 February 2012
Published online in Wiley Online Library (wileyonlinelibrary.com). DOI: 10.1002/jbm.a.34123

Abstract: Currently, the majority of animal models that are used to study biofilm-related infections use planktonic bacterial cells as initial inocula to produce positive signals of infection in biomaterials studies. However, the use of planktonic cells has potentially led to inconsistent results in infection outcomes. In this study, well-established biofilms of methicillin-resistant *Staphylococcus aureus* were grown and used as initial inocula in an animal model of a Type IIIB open fracture. The goal of the work was to establish, for the first time, a repeatable model of biofilm implant-related osteomyelitis, wherein biofilms were used as initial inocula to test combination biomaterials. Results showed that 100% of animals that were treated with biofilms developed osteomyelitis, whereas 0% of animals not treated with biofilm developed infection. The development of this experimental model may lead to an important shift in biofilm and biomaterials research by showing that when biofilms are used as initial inocula, they may provide additional insights into how biofilm-related infections in the clinic develop and how they can be treated with combination biomaterials to eradicate and/or prevent biofilm formation. © 2012 Wiley Periodicals, Inc. J Biomed Mater Res Part A: 00A:000–000, 2012.

Key Words: planktonic, biofilm, initial inocula, animal model, infection

How to cite this article: Williams DL, Haymond BS, Woodbury KL, Beck JP, Moore DE, Epperson RT, Bloebaum RD. 2012. Experimental model of biofilm implant-related osteomyelitis to test combination biomaterials using biofilms as initial inocula. J Biomed Mater Res Part A 2012:00A:000–000.

INTRODUCTION

After a careful literature review, it appears that currently, the majority of animal models that are used to study biofilm-related infection use planktonic bacterial cells as initial inocula to produce positive signals of infection.[1–24] The expectation has been that planktonic bacteria would, depending on the animal model, attach to host tissue or a medical device and subsequently form a biofilm. These animal models have been crucial in the development of novel therapeutic agents to treat and prevent biofilm-related and other infections. However, although the value of these animal models cannot be underestimated, the use of planktonic bacteria as initial inocula has provided inconsistent results in the repeatability of infection development. More specifically, results have shown that when planktonic cells are used as initial inocula, without any antimicrobial intervention, rates of infection are inconsistent between ~47 and 100%.[1–24] In addition to these inconsistencies, these models have potentially limited biomaterials scientists, clinicians, and other investigators from obtaining additional insights into the effect that bacteria might have if they contaminate a site while residing in well-established, mature biofilms.

In 1978, Costerton et al.[25] provided a general hypothesis that bacteria in nature reside predominantly in the biofilm phenotype. Since that time, data have indicated that 99.9% of bacteria in natural ecosystems reside in the biofilm phenotype.[26] Similar data have been derived from samples that have been collected from patients, retrieved medical devices, and other sources.[27–33] Moreover, the Centers for Disease Control has stated that 60% of all infections are biofilm-related.[34] A public announcement of The National Institutes of Health placed that estimate at 80% (see announcement PA-07-288). In addition to these estimates, chronic wounds are now considered to be the result of acute infection that begins with biofilm contamination as opposed to a nonhealing wound that is later

Correspondence to: D. L. Williams; e-mail: dustin.williams@utah.edu
Contract grant sponsor: Office of Research and Development, Rehabilitation R&D Service, Department of Veterans Affairs Medical Center, Salt Lake City, UT
Contract grant sponsor: National Institute Of Arthritis And Musculoskeletal And Skin Diseases; contract grant number: R01AR057185

contaminated.[35–38] A review article has been published discussing this concept of using biofilms as initial inocula.[39]

Based on these observations and information, the authors hypothesized that a sizeable portion of biofilm-related infections, including those that accompany the use of medical devices, may be the result of contamination with bacteria residing in biofilms from natural ecosystems as opposed to planktonic bacteria contaminating a site. If supported, this hypothesis would suggest that using biofilms as initial inocula, as opposed to planktonic bacteria to model clinically relevant infection scenarios, may provide deeper insight into how biofilm-related infections may be treated and eradicated using current or novel therapies, such as antimicrobial eluting coatings.

In an attempt to address the sporadic nature of biofilm infection development in animal models, wherein planktonic cells are used as initial inocula, the goal of this work was to test the above hypothesis and establish a reproducible experimental model of biofilm implant-related osteomyelitis in sheep. More specifically, in this study, biofilms of methicillin-resistant *Staphylococcus aureus* (MRSA) were grown on the surface of polyetheretherketone (PEEK) membranes using a modified CDC biofilm reactor.[40,41] These biofilms were placed in apposition to the proximal medial aspect of a sheep tibia, on the bare cortical surface stripped of periosteum, and subsequently covered by a simulated fracture fixation plate. As such, this study modeled a massively contaminated Type IIIB Gustilo open fracture, wherein, in a worst case clinical scenario, biofilms from natural ecosystems may contaminate a wound site and be compressed between bone and a fracture fixation plate.

MATERIALS AND METHODS

Biofilm growth

For this study, a fresh, clinical isolate of MRSA was used. This isolate was collected from the knee of an infected patient and passaged less than three times on Columbia blood agar. The isolate was confirmed to be one that formed biofilms as indicated by the presence of the *ica*ADBC gene cluster, black colony growth on Congo Red agar, and direct imaging of its growth on PEEK membranes using scanning electron microscopy (SEM). To grow the biofilms on PEEK membranes, a modified CDC biofilm reactor was used. The development and repeatability of growing biofilms in this reactor, as well as SEM images of the biofilms, have been published previously.[40,41]

In short, biofilms were grown by first inoculating the reactor with 500 mL of modified brain heart infusion (BHI) broth that contained 1 mL of a 0.5 McFarland standard of the MRSA isolate. In this instance, a 0.5 McFarland standard equated to $\sim 10^7$ cells/mL. Following inoculation, the reactor was incubated on a hot plate set at 34°C for a 24-h period. After the initial 24-h growth period, a flow of dilute (10%) BHI broth was flowed through the reactor for an additional 24 h using a peristaltic pump set at a rate of 6.94 mL/min. With the hot plate set at 34°C, the broth temperature was 30.2°C ± 0.7°C during the first 24 h and 30°C ± 0.8°C during the second 24 h.

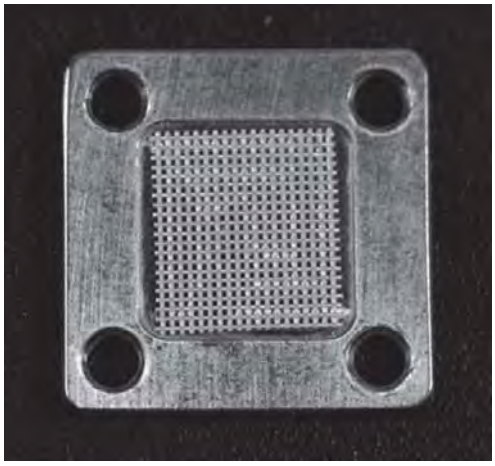

FIGURE 1. Photograph of a 316L stainless steel plate. The well machined out of the underside was used to hold a PEEK membrane (shown in well).

After the 48-h growth period, eight PEEK membranes (the reactor held a total of eight membranes) containing MRSA biofilms were removed from the reactor, rinsed 3× in sterile PBS and transferred to 5 mL of BHI broth. The biofilms were then transported to the surgical suite for inoculation into animals. Two surgeries were performed on any given surgery day, which required the use of four PEEK membranes (two per animal). At the end of each surgery day, the remaining four PEEK membranes were used to quantify the number of bacteria that were present. Each PEEK membrane was found to have an average of $5.05 \times 10^9 \pm 2.07 \times 10^9$ (9.67 ± 0.18 when $\log_{10}$ transformed) colony forming units (CFU) of bacteria. These numbers were not significantly different from the previously published numbers of bacteria that grew on these PEEK membranes.

The quantification process to determine the number of bacteria was published previously. In brief, PEEK membranes were vortexed for 1 min, sonicated for 10 min, and plated on tryptic soy agar using a 10-fold dilution series to quantify the number of CFU per membrane.

Stainless steel plates

To model a clinically relevant material that is used in fracture fixation plates, 316-L stainless steel (SS) plates were used as simulated fracture fixation plates. Each plate was machined to 2 × 2 cm with a height of 1.85 mm. The plates had a hole, measuring 2.7 mm in diameter, drilled in each corner. On the underside of each plate, a well was machined to a depth of 300 μm with 1.2 cm × 1.2 cm dimensions. The purpose of this well was to provide a contained area to place a PEEK membrane (Fig. 1). Before implantation, plates were cleaned and passivated following American Society of Testing and Materials standard F86-04 and then sterilized by autoclave.

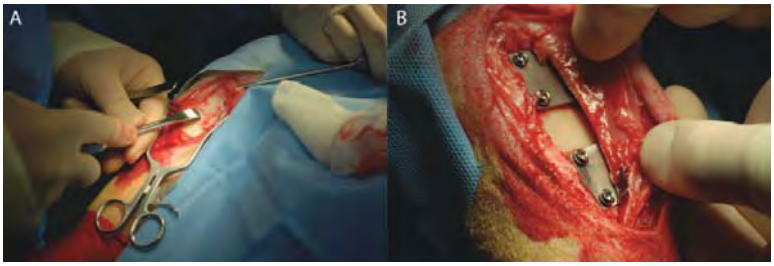

FIGURE 2. A: Photograph of the proximal medial aspect of the right tibia demonstrating removal of a 2 × 5 cm area of periosteum using a periosteal elevator. A template was used in each sheep to standardize the 2 × 5 cm area that was removed. B: Photograph of the final construct with two stainless steel plates secured to the proximal medial aspect of the tibia. There was a ~ 1 cm gap between the two plates, and each of the plates had a PEEK membrane in the underside well in direct apposition to the bare cortical bone surface. [Color figure can be viewed in the online issue, which is available at wileyonlinelibrary.com.]

Surgical procedure and postsurgical monitoring

All animal work was performed with approval from the Institutional Animal Care and Use Committee and the Environmental Health and Safety department at the University of Utah. For this study, 2–3-year-old female Columbia Cross sheep, weighing 90 ± 20 kg, were selected. This species of sheep had a flat area of bone on the proximal medial aspect of the tibia with a surface area that was suitable for securing of the plates with transcortical screws. A total of $n = 10$ sheep were used in this study with $n = 5$ being treated with biofilm to serve as positive controls of infection (Group 1) and $n = 5$ serving as negative controls of infection (Group 2). The five negative control sheep were treated with PEEK membranes that had been run through the modified CDC biofilm reactor without bacterial inoculation.

Before surgery, the sheep were fasted for >12 h. Because the goal of this work was to develop a positive signal of infection, no antibiotics were administered. Sheep were initially anesthetized using an intravenous (IV) injection of either ketamine (5 mg/kg) and diazepam (0.5 mg/kg) or propofol (3–7 mg/kg) to allow for endotracheal tube intubation. Following intubation, the sheep were placed in the supine position and maintained under anesthesia with isoflurane to effect (ranged from ~2 to 3%). An IV catheter was placed in the left forelimb, and 0.9% saline was administered at a rate of 10 mL/kg/h. Veterinary surgical and equipment technicians monitored the sheep's heart rate, temperature, carbon dioxide and oxygen levels, and respiration throughout the procedure.

The right hind limb of each sheep was circumferentially clipped free of hair/wool, from immediately above the hoof to the groin, and then scrubbed and prepped with betadine and alcohol treatment. The hoof was isolated in a sterile rubber glove and wrapped with sterile VetWrap (Fisher Scientific). After sterile draping, the proximal medial aspect of the leg and the region of the incision were treated with Chloraprep (Fisher Scientific) solution to further sterilize the skin.

An anterior midline sagittal incision was made from the region of the tibial tuberosity and extending distally, parallel to the anterior margin of the tibia. This incision was placed away from the plate and biofilm implantation site to avoid contamination of the site during wound healing. Dissection was carried medially and posteriorly, close to the bone, lifting the skin with the attached subcutaneous tissues from the surface of the medial tibial flare.

Because this study modeled a Type IIIB Gustilo open fracture—which may consist of periosteal stripping, bone exposure, and massive contamination—a 2 × 5-cm area of periosteum was removed from the proximal medial aspect of each sheep tibia [Fig. 2(A)]. On the bare cortical surface, the positions of a proximal and distal plate were templated by sequentially drilling and placing transcortical screws through each plate. The screws were not tightened at this stage. This technique allowed compensating for any irregularity in the "flat surface" of the tibia, tapped each hole, and prevented thread stripping in the thin bone. This prepositioning avoided spurious contamination of the site when placing the infectious biofilm.

A PEEK membrane (with or without biofilm, depending upon the animal group) was aseptically removed from the 5 mL of BHI broth using sterile forceps. The corner of the membrane was touched against a sterile towel, removing excess broth but not biofilm, and preventing broth from contaminating the surgical field. The membrane was placed into the well of a SS plate, and the fluid that remained on the membrane allowed it to adhere to the metal plate due to fluid cohesive forces.

Using careful, aseptic technique, the SS plate/PEEK membrane construct was placed in apposition to the tibia with the PEEK membrane residing between the bone and plate. Each plate was secured to the bone using 2.7 mm diameter × 10 mm length cortical bone screws (self-tapping; catalog #ST270.10, Veterinary Orthopaedic Implants). This process was performed twice in each sheep, such that each sheep was treated with two PEEK membranes and two plates [Fig. 2(B)]. The rationale for using two plates was to have one available for microbiological analysis and one for histological analysis at the end of the study. To the best of the surgeons' ability, the two plates had a space of ~1 cm between them; however, anatomical variation existed amongst the sheep and not all were able to maintain exactly 1 cm of space between them.

After plate placement, a swab of the cortical bone surface was collected to determine if bacteria had already begun to dislodge away from the biofilm on the PEEK membrane. The surgical site was closed with interrupted 2–0 Vicryl (catalog no. J339H, Ethicon) subcutaneous sutures and a running subcuticular 2–0 Proline (catalog no. 8533H, Ethicon) suture. A swab of the incision site was taken to determine if bacteria were present on the skin. Before wrapping the surgical site, the leg was cleaned with saline and isopropyl alcohol to kill bacteria that may have been present on the skin. This helped to reduce the risk of cross contamination throughout the animal facility and between animals.

For postoperative analgesia, each sheep was given an epidrual dose of morphine (0.1 mg/kg), and two fentanyl patches (100 μg/h) were placed in a shaved area on the left forelimb. An injection of flunixin (1.1 mg/kg) was administered to diminish inflammation. Postanesthesia monitoring extended until the animals could stand on their own as well as eat and drink.

Surgical follow up

Throughout the course of the study, each sheep was monitored by the authors' team and a veterinarian in the animal quarters to assess any symptoms of pain and distress. Under veterinary supervision, animals that showed signs of pain or distress were treated with Buprenex (0.01 mg/kg) or additional fentanyl patches. If excessive inflammation was present, they were further treated with rimadyl (4.4 mg/kg).

Using a clinical grading system, based on the hallmarks of infection: calor (heat), rubor (redness), dolor (pain), and tumor (swelling), the sheep were monitored daily for a 12-week period for these signs of infection. A daily rectal temperature of each sheep was also taken. The animals were also monitored for limping, lethargy, irritability, and going "off feed" and/or water. Based on these criteria, a four-tiered clinical grading system was established.

Grade I, or no infection, consisted of the signs of healing normally seen with surgical trauma and that resolved within 1–2 weeks of surgery. These signs included slight redness at the surgical site, mild warmth (to the touch), mild inflammation, a closed suture line, healed within 2 weeks, the sheep eating and drinking, a normal rectal temperature (for these sheep normal temperature was between 101.5 and 102.8°F), and no signs of distress or limping. A Grade II infection included increased redness, a warmer surgical site with moderate inflammation, evidence of suture line dehiscence, irritable behavior, normal temperature, and not limping. Sheep were euthanized if they displayed signs of a Grade III infection. This grade was characterized by significant redness and palpable heat at the surgical site, an open suture line with drainage, significant inflammation, tenderness, lethargy, fever, off feed and/or water, and positive bacterial growth on wound culture. A Grade IV infection was defined, but never allowed to develop in any of the animals. This included excessive heat, excessive inflammation, purulent drainage, implant exposure, excessive limping, local tenderness, off feed and/or water, lethargy, and fever.

Bone labeling

As stated by Bloebaum et al.,[42] "fluorochrome labeling is a well-established method of measuring the mineral apposition rate (MAR), at which osteoid matrix, produced by osteoblast cells, is deposited and mineralized to form new bone."

In this study, calcein fluorochrome (catalog no. C-0875, Sigma-Aldrich) was used as a nonantibacterial agent to label bone and to calculate the MAR, that is, the growth rate of the sheep bone. The method by which this works is after the calcein is injected, it is taken up by osteoblast cells and released into the matrix of newly forming bone. After processing, calcein fluorochrome can be observed in tissue samples as they are imaged using an excitation wavelength of 495 nm and emission of 515 nm. The imaging that was performed in this study is described in the "MAR analysis" section below.

Calcein was prepared in reverse osmosis water to a final concentration of 30 mg/mL. The pH was adjusted to 7.2–7.4, filtered using a 0.22-μm filter for sterility, and the solution administered IV at 0.33 mL/kg of body weight. Two separate injections were given: one 16 days and one 5 days before the established 12-week end point of each sheep to create a double label in the bone. The infected sheep that were euthanized before the 12-week end point did not receive calcein injection.

Euthanasia and microbiological sample collection

Sheep were euthanized at the end of 12 weeks, or once a Grade III infection was determined to exist. To euthanize, animals were initially sedated with an IV injection of ketamine (5 mg/kg) and diazepam (0.5 mg/kg) in order to collect a 5-mL blood sample for microbiological analysis. Euthanasia was then performed by IV injection of beuthenasia (1 mL/4.5 kg) solution.

A swab of the incision site ($\sim$1 cm^2 area) was taken and streaked onto Columbia blood agar for semiquantitative analysis. More specifically, 1+ growth was defined as having growth in the first zone of streaking, 2+ having growth in the second zone, and 3+ having growth in the third zone. The agar plate was incubated overnight at 37°C. Next, the skin at and surrounding the incision site was prepped using chlorhexidine/isopropyl alcohol antiseptic. A scalpel was used to aseptically reopen the incision site, and a swab of the subdermal tissue was collected to determine if bacteria had penetrated into the soft tissues superficial to the plates and PEEK membranes. This swab was also cultured on Columbia blood agar.

One of the SS plates was randomly selected, and the underlying PEEK membrane was removed and placed into 5 mL of 10% BHI broth. The sample was vortexed for 1 min, sonicated for 10 min, and allowed to recover in the broth at room temperature for 20 min (to allow the bacteria to convert from the biofilm to planktonic phenotype) before performing a 10-fold dilution series to quantify the number of CFU/PEEK membrane.

The SS plate that had been removed was then secured to the bone once again, so that radiographs could be taken.

The tibia was then disarticulated and used for gross photographic and radiographic analysis.

Gross photography/radiography

Gross photography of the soft tissues and bone was collected throughout the sampling/dissection process. Radiographs were obtained using a cabinet X-ray system (43855A Model, Faxitron X-Ray Corporation) set at 70 kV for 21/2 min.

Tissue embedment/sectioning

After radiographic imaging, all the soft tissue was dissected from the bone with the exception of the tissue that was directly over the undisturbed SS plate. The sample was then fixed in modified Karnovsky's fixative using 3 × 24 h changes. Following fixation, the bone was rinsed in reverse osmosis water for 10 min and cut into two sections separating the two SS plates from one another. The plate that had been removed in order to access the PEEK membrane for microbiology was again removed, and the biofilm on the underlying bone imaged with SEM. The remaining bone section, with plate and PEEK membrane intact, was used for histological analysis.

After cutting, both bone samples were placed in 70% ethanol for 24 h to initially dehydrate them. The bone for SEM imaging was further dehydrated by hand using ascending concentrations (from 70 to 95 to 100%) of ethanol, then coated with gold using a Hummer 6.2 sputter coater, and imaged using SEM.

The bone sample for histology was also dehydrated using increasing concentrations of ethanol. However, this was performed in a Tissue-Tek VIP (Miles Scientific) instrument. It was then placed into a solution of 80% methylmethacrylate and 20% *N*-butyl (the combination of these two solutions is referred to as Solution A) and mixed for 5 days to infuse the tissues. The Solution A was poured out, and a fresh aliquot of Solution A, mixed with 2.5 g/L of perkadox (the catalyst for polymerization), was added to the sample. The sample was kept in a dessicator at 4°C for 7 days. Finally, 5 g/L of perkadox was added to another batch of fresh Solution A and exchanged for the used mixture in the container, and the sample was kept in a desiccator at 4°C for an additional 9 days. Samples were then placed in a new container, and Solution A with 5 g/L of perkadox was added and polymerized in 2 cm layers using ultraviolet light. Each layer required 48 h to fully polymerize. The final product resulted in a polymethylmethacrylate (PMMA) embedded sample containing the bone, PEEK membrane, SS plate, and soft tissue regions.

Once embedded, tissue samples were cut using a band saw to remove excess PMMA and isolate the area of interest. Samples were further sectioned into ~2 mm sections using a diamond blade water saw. Radiographs of the sections were obtained following the same procedure outlined earlier. One face of a section was then polished and gold coated for SEM analysis.

SEM analysis

Scanning electron microscopy (SEM) analysis was performed using a JEOL 6100 LaB_6 filament SEM to qualitatively examine bone and/or biofilm morphology in the region, where a SS plate/PEEK membrane construct was implanted. For those bone samples that had the SS plate removed, secondary electron images were collected of the cortical bone surface to examine the morphology of the bone and/or biofilm where the PEEK membrane had been present. For those samples that were sectioned in PMMA, backscatter electron (BSE) images were collected to examine the varying levels of mineralization, how the infection influenced the periosteal response in bone, and cortical bone activity.

MAR analysis

The procedure for collecting MAR data was based on the published work of Bloebaum et al.[42] In short, after sample sections had been imaged using SEM, the polished surfaces were glued to a slide and further ground to ~50–60 μm thickness for MAR analysis. Images were first collected using a mercury lamp Nikon Labophot microscope to detect the presence of calcein double-labeled osteons of the host bone. Three slides from each sheep were analyzed. From each slide, five osteons were randomly selected in the cortical/periosteal bone region beneath a SS plate, and a total of eight measurements were made along the span of each double label using ImagePro Plus software. The MAR of bone was calculated using the formula:

$$\text{MAR } (\mu\text{m/day}) = \Sigma_x(e)(\pi/4)/nt$$

where Σ_x is the sum of all the measurements between double labels, e is the micrometer calibration factor (μm), $(\pi/4)$ is the obliquity correction factor, n is the total number of measurements, and t is the time interval between calcein injections expressed in days.

Histology

For histological analysis, sample slides were further ground to a thickness of 40–50 μm and stained with H&E stain. For H&E staining, Mayer's solution was preheated to 50–55°C. Slides were placed in the Mayer's solution for 5 min, rinsed, and dried. Slides were then placed in Clarifier for 4 min, rinsed, placed in Bluing Reagent for 4 min, rinsed again, and dried with a Kimwipe. Finally, slides were counterstained by dripping acid fuschin/5% acetic acid solution for 35–45 s and dipped in 100% ethanol for 30 s.

Macroscopic images of slides were collected using a Nikon SMZ800 macroscope. Higher magnification images were collected using a Nikon Eclipse E600 microscope. Using a modified histopathologic grading scale of Smeltzer et al.,[43] an outside observer, who was blinded to the samples in the study, examined the slides to determine what level of osteomyelitis was present in the bone and or surrounding tissue regions. Osteomyelitis was indicated by the presence of bacteria, as determined by the microbiological analysis, in conjunction with chronic inflammation and bone necrosis. Cortical bone growth/response was not an indicator of infection as it was present in all five sheep from Group 1 and three from Group 2. Thus, it appeared to be a normal bone response to the surgical trauma and

TABLE I. Histological Parameters and Scoring System

Intra- and periosseous chronic inflammation
0 Not present
1 Minimal to mild chronic inflammation with no significant intramedullary fibrosis
2 Moderate to severe chronic inflammation with no significant intramedullary fibrosis
3 Minimal to mild chronic inflammation with significant intramedullary fibrosis
4 Moderate to severe chronic inflammation with significant intramedullary fibrosis
Bone necrosis
0 No evidence of necrosis
1 Single focus of necrosis without sequestrum formation
2 Multiple foci of necrosis without sequestrum formation
3 Single focus of sequestrum
4 Multiple foci of sequestra
Cortical bone response
0 No cortical bone response
1 Cortical bone growth that does not extend beyond plate border
2 Cortical bone growth that begins to extend beyond plate border
3 Cortical bone growth that covers a plate part way
4 Cortical bone growth that covers a plate entirely

implantation. The modified Smeltzer et al.[43] grading scale is provided in Table I.

Statistical analyses

From a Kaplan–Meier survival curve, a Log-Rank test was used to examine the statistical significance in survival times between those sheep treated with biofilm and those that were not. A separate Log-Rank test was used to compare the time it took for animals in both groups to become infected. Time to infection differed from survival time, because some sheep in Group 1 survived the full 12 weeks of the study, but displayed signs of infection very early on.

Because the number of bacteria collected from PEEK membranes of those sheep in Group 1 were not normally distributed, the nonparametric Mann–Whitney *U* test was used, as opposed to a Student's *t* test, to compare the number of bacteria that were collected on the PEEK membranes of Group 1 and Group 2 animals. In all instances, an alpha level of 0.05 was established to define statistical significance. All statistical data were analyzed using SPSS 17.0 software.

RESULTS

Surgical follow up

A survival curve including each of the 10 sheep in this study was plotted using a Kaplan–Meier survival curve [Fig. 3(A)]. Two of the five sheep in the biofilm-treated sheep (Group 1) were euthanized at 3 weeks due to a Grade III infection. The other three survived to the 12-week end point, but each of those three sheep displayed Grade II signs of infection during the 12-week monitoring period. Furthermore, each of the five sheep in Group 1 displayed signs of inflammation and abscess formation between day 4 and 11 after surgery. In contrast, all five of those sheep in Group 2 survived to the 12-week end point with minimal acute inflammation and no signs of infection at any point in the study. The Log-Rank test indicated that the difference in survival among the two groups was not significant ($p = 0.184$). However, when time to infection was analyzed, there was a significant difference ($p = 0.002$) between the groups [Fig. 3(B)]. This difference corroborated with the microbiological data.

Microbiology

Microbiological data showed that PEEK membranes collected from Group 1 sheep contained an overall log density of 5.32 ± 5.41 $\log_{10}$ CFU/PEEK membrane. No bacteria were detected on the PEEK membranes of Group 2 sheep. When compared using the Mann–Whitney *U* test, this difference was statistically significant ($p = 0.008$).

All the swabs taken from all animals showed between 1+ and 2+ growth of normal flora bacteria at the incision site. In three of five of the Group 1 sheep, subdermal swabs

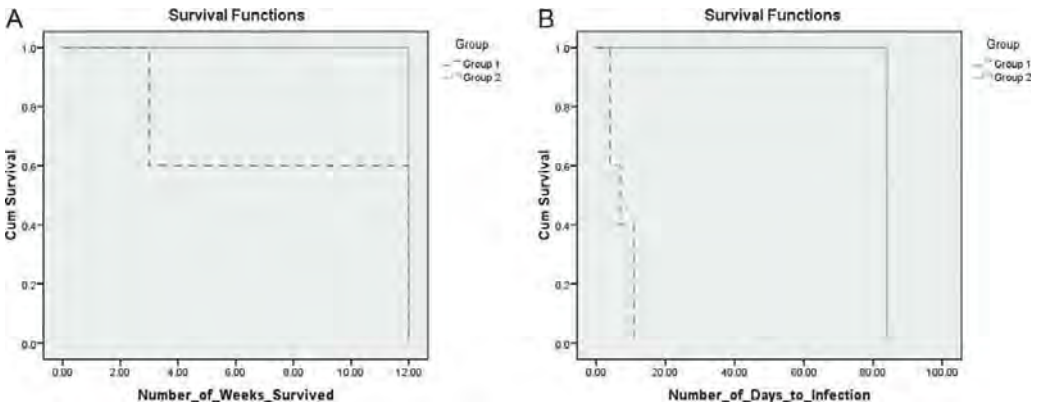

FIGURE 3. A: Kaplan–Meier survival curve for each sheep in Group 1 and Group 2. B: Kaplan–Meier curve of the time it took for each sheep to display signs of infection.

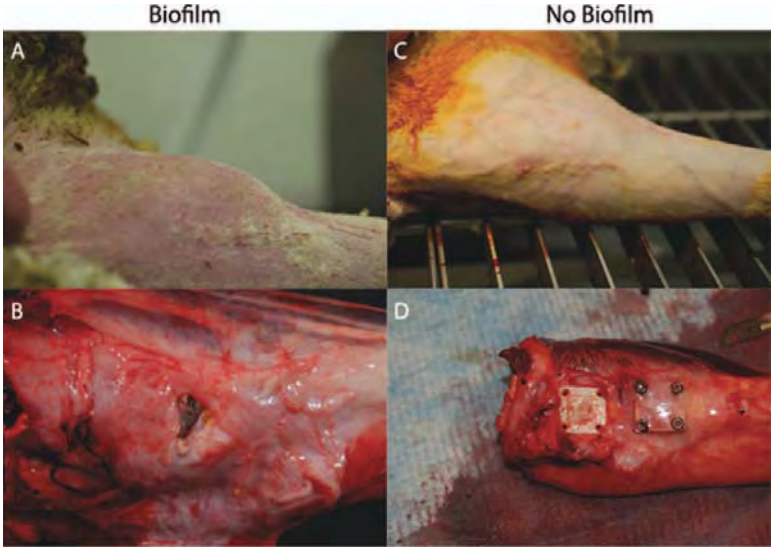

FIGURE 4. Left column: photographs of a sheep treated with biofilm. Right column: photographs of a sheep not treated with biofilm. A: Representative photograph of the proximal medial aspect of a sheep tibia from Group 1 that suffered from infection. In this particular sheep, this abscess developed on day 11 postsurgery. B: Once the skin was resected from the infected sheep shown in Figure 4A, pus could be seen as well as a significant cortical bone/periosteal response in the infected region that showed signs of osteomyelitis. This sheep had positive growth for MRSA. C: Additional photograph of a sheep tibia from Group 2. No abscess formation was seen in any of the sheep from Group 2. D: Once the skin was resected away from the sheep tibia shown in Figure 4C, a thin, fibrous membrane was observed to have grown over the stainless steel plates. In addition, the bone had grown up to the edges of the plates and no further (Grade 0 cortical bone growth). The plate that was removed was used for microbiological analysis. No bacteria were detected in/on the tissues or on the PEEK membrane. [Color figure can be viewed in the online issue, which is available at wileyonlinelibrary.com.]

detected 2+ growth of bacteria in the tissues surrounding the SS plates, whereas swabs taken of the remaining two sheep detected no growth of bacteria. All the culture swabs collected from Group 2 sheep were negative for growth.

These data indicated that the microbiological findings correlated with the clinical observations of the sheep, wherein those treated with biofilm (Group 1) suffered a Grade II or higher infection, and those not treated with biofilm (Group 2) did not suffer from infection.

Notably, when removing the SS plates for microbiological analysis, it was observed that in each of the five Group 1 sheep, the bone screws had become completely loose, and, in one animal, the plates had even shifted position. This was due to bone resorption around the screws, which was a result of infection as indicated by SEM analysis and histological results (see below). No screw or plate loosening was observed in Group 2 sheep, and it was also interesting to observe that in Group 2 sheep, the cortical bone began to grow on/attach to the PEEK membranes, which made it difficult to remove them for quantification. In contrast, the PEEK membranes in the infected sheep had no attachment of bone to them and were easily removed.

Gross photography/radiography

Gross photographs of the sheep limbs provided evidence that an abscess formed in the surgical area of Group 1 sheep, whereas no abscess formation was seen in sheep from Group 2 (Fig. 4). Furthermore, signs of infected tissue, including pus and significant inflammatory and cortical bone response, could be seen in Group 1 sheep once the skin was resected [Fig. 4(B)]. In contrast, only a thin membrane of tissue grew over the plates in Group 2 sheep with minimal periosteal/cortical bone response.

Radiographic evidence also suggested that in Group 1 sheep, "moth eaten," osteomyelitic bone was visible [Fig. 5(A)]. This result was particularly apparent in the microradiographs that were taken of bone sections after they had been embedded and cut [Fig. 5(B)]. From these sections, a significant cortical bone response and an endosteal response indicative of responsive new bone formation could be seen in Group 1 sheep. No such response was seen in Group 2 [Fig. 5(C,D)].

SEM analysis

Because of the natural complexity of the cortical bone surface of sheep and components that resembled bacteria, it was difficult to confirm that there were biofilm dwelling bacteria on the cortical bone surface of Group 1 sheep using secondary electron SEM imaging. Although it did appear that the bone surfaces of Group 1 sheep had more degradation and trauma when compared with the bone surfaces of Group 2 sheep, the differences were not deemed substantial

FIGURE 5. Left column: radiographs of a sheep treated with biofilm. Right column: radiographs of a sheep not treated with biofilm. A: Macroradiograph of the tibia of the sheep photographed in Figure 4(A). From this radiograph, the authors were able to detect signs of "moth eaten," osteomyelitic bone. Similar radiographs were collected from all sheep in Group 1. B: Once the bone was embedded and sectioned, microradiographs of the same sheep from (A) indicated that in addition to "moth eaten" cortical bone, a significant endosteal response was also present, suggesting that infection was present in the medullary canal. C: No "moth eaten" bone was detected in the radiograph of the sheep tibia from Figure 4(C). This same result was seen in all of the sheep from Group 2. D: Microradiographs of the embedded, sectioned samples from the sheep presented in (C) suggested that there was no endosteal or cortical bone response. [Color figure can be viewed in the online issue, which is available at wileyonlinelibrary.com.]

enough to support any conclusions. On the other hand, BSE images of the bone sections were much more indicative of bone trauma and infection.

More specifically, in Group 1 sheep, BSE images indicated that there was a considerable amount of bone resorption directly underneath the SS plate [Fig. 6(A)] and near the bone screws [Fig. 6(B)], which supported the observation mentioned earlier that these screws were loose, whereas no signs of bone resorption were apparent in any sheep from Group 2 [Fig. 6(C,D)]. Furthermore, a much larger gap was seen between the cortical bone surface and plate of Group 1 sheep when compared with Group 2. More specifically, the distance from the bone to the plate surface in Group 2 was ~20–50 μm, whereas in Group 1, the gap was much larger and ranged from 200 to 800 μm. As will be seen in the histopathological results, this larger gap in Group 1 sheep was due to fibrous tissue formation and chronic inflammation—which the microbiology confirmed to be the result of infection.

MAR analysis

MAR results indicated that in Group 1 sheep, the average bone remodeling rate was ~1.5 μm/day. In Group 2 sheep, the average rate was ~1.2 μm/day. Images of double labels in the periosteal regions of Group 1 sheep showed that an intense remodeling response was present [Fig. 7(A)].

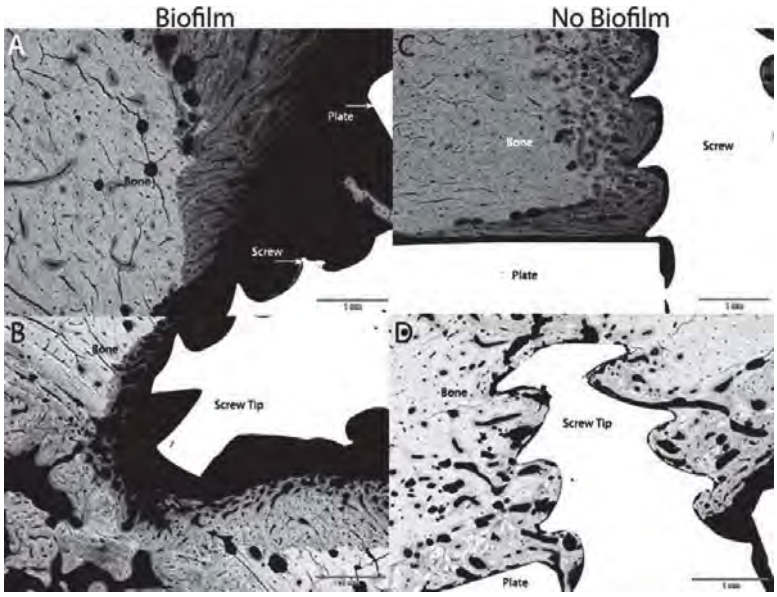

FIGURE 6. Left column: BSE images of a sheep treated with biofilm. Right column: BSE images of a sheep not treated with biofilm. Original magnification for all images was 20×. A: Representative BSE image of a cortical bone surface underneath a stainless steel plate of an infected sheep. Note the resorption away from the bone screw and plate itself as well as the abnormal morphology (wispy, moth-eaten appearance) of the bone, which was believed to be a result of infection. Darker bone was indicative of bone that was not yet mineralized, but rather, undergoing remodeling. B: Additional BSE image from the same sheep as (A) with bone resorption occurring in the distal area of the bone screw. C: Additional representative BSE image of cortical bone beneath a stainless steel plate in a sheep that was not infected. Note the smooth, morphologic difference in this bone compared to that of bone shown in (A). This bone grew up to the surfaces of the bone screw and plate with normal bone morphology. D: BSE image of the distal region of a bone screw in a sheep from Group 2. No signs of resorption were present.

However, typical double labels of osteons were seen in the cortical bone regions [Fig. 7(B)]. No significant response was seen in the periosteal regions of sheep in Group 2, and osteon structures were present in the cortical bone region indicative of remodeling [Fig. 7(C,D)]. Notably, calcein double labels further indicated bone viability.

Histology

Sections stained with H&E showed that there was an observable difference between the bone and soft tissues of Group 1 and Group 2 sheep. More specifically, when compared with the modified Smeltzer et al.[43] histopathological grading scale, the three sheep in Group 1 that survived to the 12-week endpoint displayed signs of a Grade 4 osteomyelitis as indicated by moderate to severe chronic inflammation with significant intramedullary fibrosis and multiple foci of sequestra (Fig. 8). These sheep also displayed Grade 3 cortical bone growth. The other two sheep in Group 1, which survived to 3 weeks, displayed Grades 3–4 osteomyelitis with Grade 2 cortical bone growth. None of the five sheep in Group 2 showed signs of osteomyelitis and were scored with a Grade 0 osteomyelitis. However, three of the five sheep in Group 2 did display Grade 2 cortical bone growth, whereas the other two were scored with Grade 0 cortical bone growth. Taken together, these results suggested that cortical bone growth/response could have been due to surgical trauma or the presence of infection; yet, a notable difference in bone morphology was present in those that were infected versus those that had a response due to surgical trauma. More specifically, those that had infection showed signs of "moth eaten" bone that had jagged edges due to resorption/bacterial presence, whereas those with a cortical bone response due to surgical trauma had woven bone formation with little indication that resorption was occurring.

DISCUSSION

Using biofilms as initial inocula in this study addressed at least three major limitations, which have been reviewed previously,[39] that may accompany the use of planktonic bacteria in animal models of infection, such as those that are designed to develop combination products of biomaterial coatings and other antimicrobials. (1) Planktonic cells may be cleared by the immune system more readily than cells residing in a biofilm. Thus, when planktonic cells are used in *in vivo* models, it may be that they are eradicated before they can form biofilms. As mentioned, this may contribute to the low reproducibility for the induction of osteomyelitis. (2) It is becoming ever more evident that planktonic bacterial cells are more susceptible to antibiotics than those

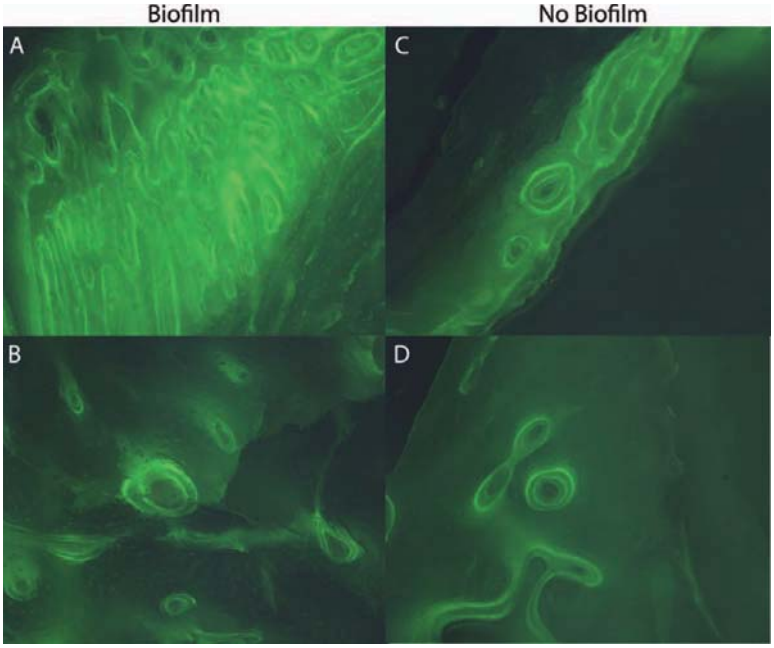

FIGURE 7. Left column: double-label images of sheep bone treated with biofilm. Right column: double-label images of sheep bone not treated with biofilm. Original magnification of all images was 20×. A: Image of calcein double labels in a region directly underneath a stainless steel plate of an infected sheep. This type of remodeling was indicative of bone that was attempting to remodel in the presence of infection. B: Cortical bone region more distal to the stainless steel plate than the image collected in (A). This image indicated that in addition to areas of intense remodeling, there were areas of typical bone remodeling within the cortical bone of sheep that were infected. C: For comparison, this image of calcein double labels was taken in the same region as the image from (A), but in a sheep that was not infected. D: Also for comparison, this image of calcein double labels was taken in the same region as (B), but in a sheep that was not infected. [Color figure can be viewed in the online issue, which is available at wileyonlinelibrary.com.]

residing in a biofilm. If antibiotics are administered prophylactically immediately following inoculation, they may affect planktonic bacteria more effectively and rapidly than they would biofilm bacteria. (3) When planktonic bacteria are added to the body, the possibility exists for them to be dispersed rapidly away from the site of initial inoculation due to the presence of flowing fluids in the body. This could dilute the concentration of bacteria per given area—potentially making it easier for the body to handle the bacterial load and prevent attachment to tissue or a medical device.

Notably, osteomyelitis developed in all five sheep from Group 1 of this study treated with biofilm, which strongly supported the hypothesis that using biofilms as initial inocula would cause infection. The hypothesis was further supported, and the data made significantly stronger by the fact that none of the sheep from Group 2 became infected. This 100 versus 0% rate of infection provided a promising outcome for future tests of combination biomaterials for device development to be performed in a repeatable fashion using this model.

The biofilms in this study appeared to have a gradual adverse clinical effect on the sheep. More specifically, osteomyelitis developed slowly and persisted without significant signs of distress in three of five of the animals in Group 1. This may be similar to biofilm-related infections that are seen clinically. In patients, biofilm-related infections can take months or years to develop and may persist without significant morbidity or mortality.[32] This may be due to the quiescent nature of biofilms and the fact that they have already established a community. Planktonic bacteria have yet to develop a community, and it appears that their "goal" in nearly every ecosystem is to find a location to colonize and then begin to develop a biofilm community.[44]

Importantly, there were no sclerosing agents used in this study to promote the development of osteomyelitis, whereas in previous studies, these noxious agents have been commonly used to initially kill bone and/or tissue with the intent to make it more susceptible to infection.[45–48] In addition, the model in this study also appeared to circumvent the problem of low reproducibility for the induction of osteomyelitis, which was cited by Gaudin et al.[49] as an important limitation of animal models of osteomyelitis.

In two of the sheep from Group 1, bacteria were not detected in the surrounding tissue regions of the SS plate. This was likely due to the limited area of sampling with the swab culture technique. Bacteria may not have been in

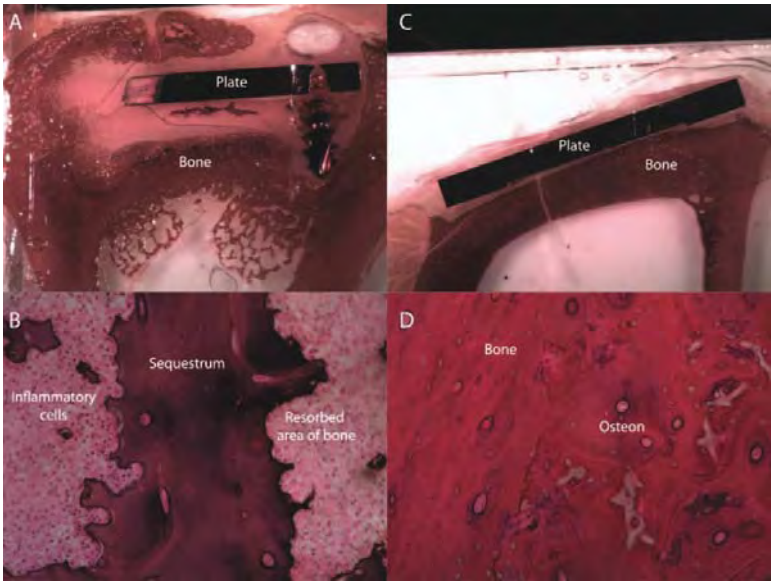

FIGURE 8. Left column: images of H&E-stained bone sections from a sheep treated with biofilm. Right column: images of H&E-stained bone sections from a sheep not treated with biofilm. A: Macroscopic image of bone from an infected sheep. Note the significant cortical bone response, the gap between the plate and bone surface, the endosteal bone response and the focus of sequestrum in the periosteal region. Taken together, these tissue responses were indicators that infection was present. Original magnification was 10×. B: Microscopic image of the sequestrum seen in (A). The sequestrum had a jagged surface (sign of resorption) and large amounts of inflammatory cells in its surroundings; indicators that bacteria were present and that chronic inflammation had persisted. Original magnification was 20×. C: Macroscopic image of bone from a sheep that was not infected. Note the apparent differences in tissue morphology between this sample and that from the infected sheep. Original magnification was 10×. D: Image of a similar region of as that analyzed in (B). Note the lack of sequestrum, resorption or chronic inflammation. In contrast, this bone had normal lamellar structure. Original magnification was 20×.[Color figure can be viewed in the online issue, which is available at wileyonlinelibrary.com.]

those tissue regions and thus were not detected. However, bacteria were collected from the PEEK membranes of both of these sheep, which corroborated with the SEM, MAR, and histopathological data—all of which supported the conclusion that infection had developed.

At least three limitations accompanied this study and will need to be addressed with future work. First, these results are based on the use of a single species of microorganism, and although the outcomes are hypothesized to be similar with other biofilm forming organisms, different organisms may lead to different results. More specifically, although *S. aureus* is a common cause of metal, device-related infections,[50] a wide variety of other organisms can cause biofilm-related infections including *Pseudomonas aeruginosa*, *Enterococcus faecalis*, coagulase negative staphylococci, *Escherichia coli*, *Acinetobacter baumanii*, *Klebsiella pneumoniae*, and others. Second, these results will need to be confirmed with other material types. For example, at least one study has shown that titanium implants have reduced infection outcomes when compared with SS.[51] Third, as this was a developmental model to test the ability of biofilms to cause infection, antibiotics were not used. However, if this were a clinical scenario, prophylactic antibiotics would have accompanied the implantation of the devices. Thus, future work will be needed to address these limitations.

In conclusion, to the authors' knowledge, this is the first animal model using biofilms as initial inocula to produce a positive signal of reproducible biofilm-related infection. As such, the model provides a promising outcome in that it may be used by future researchers and clinicians to use a reproducible model to examine the therapeutic potential of novel systemic antimicrobials and/or antimicrobial coatings on biomedical devices to treat and prevent biofilm-related osteomyelitis as well as other biofilm-related infections. It may be that the use of this and similar animal models using biofilms as initial inocula will result in an important shift in the field of biofilm research that adds onto the work that has been done with planktonic bacteria. This shift may lead to the development of novel antimicrobial therapies, such as coatings on devices, that could help prevent biofilm-related infections in a more effective manner. In short, the development of this experimental model may have tremendous implications in the future of biofilm implant-related infection treatment strategies as well as other biofilm-related infections.

The content is solely the responsibility of the authors and does not necessarily represent the official views of the

National Institute of Arthritis and Musculoskeletal and Skin Diseases or the National Institutes of Health. This study was also supported by the Albert and Margaret Hofmann Chair and the Department of Orthopaedics, University of Utah School of Medicine, Salt Lake City, UT. The authors thank Mr. and Mrs. George and Lisa Etheridge, Mr. and Mrs. Jim and Maria Hess, and Dr. Richard E. and Mrs. Susan Jones for their generous donations. Finally, the authors thank the technical team of the Bone and Joint Research Lab for their help in processing samples before analysis, as well as the animal care team, surgical technicians, and veterinary staff at the University of Utah animal facility.

REFERENCES

1. Buret A, Ward KH, Olson ME, Costerton JW. An *in vivo* model to study the pathobiology of infectious biofilms on biomaterial surfaces. J Biomed Mater Res 1991;25:865–874.
2. Cirioni O, Mocchegiani F, Ghiselli R, Silvestri C, Gabrielli E, Marchionni E, Orlando F, Nicolini D, Risaliti A, Giacometti A. Daptomycin and rifampin alone and in combination prevent vascular graft biofilm formation and emergence of antibiotic resistance in a subcutaneous rat pouch model of staphylococcal infection. Eur J Vasc Endovasc Surg 2010;40:817–822.
3. Lambe DW Jr, Ferguson KP, Mayberry-Carson KJ, Tober-Meyer B, Costerton JW. Foreign-body-associated experimental osteomyelitis induced with *Bacteroides fragilis* and *Staphylococcus epidermidis* in rabbits. Clin Orthopaed Relat Res 1991;266:285–294.
4. Darouiche RO, Farmer J, Chaput C, Mansouri M, Saleh G, Landon GC. Anti-infective efficacy of antiseptic-coated intramedullary nails. J Bone Joint Surg 1998;80:1336–1340.
5. Darouiche RO, Mansouri MD. Dalbavancin compared with vancomycin for prevention of *Staphylococcus aureus* colonization of devices in vivo. J Infect 2005;50:206–209.
6. Darouiche RO, Mansouri MD, Gawande PV, Madhyastha S. Antimicrobial and antibiofilm efficacy of triclosan and dispersin B combination. J Antimicrob Chemother 2009;64:88–93.
7. Darouiche RO, Mansouri MD, Zakarevicz D, AlSharif A, Landon GC. In vivo efficacy of antimicrobial-coated devices. J Bone Joint Surg 2007;89:792–797.
8. Davis SC, Ricotti C, Cazzaniga A, Welsh E, Eaglstein WH, Mertz PM. Microscopic and physiologic evidence for biofilm-associated wound colonization in vivo. Wound Repair Regen 2008;16:23–29.
9. Dohar JE, Hebda PA, Veeh R, Awad M, Costerton JW, Hayes J, Ehrlich GD. Mucosal biofilm formation on middle-ear mucosa in a nonhuman primate model of chronic suppurative otitis media. Laryngoscope 2005;115:1469–1472.
10. Elasri MO, Thomas JR, Skinner RA, Blevins JS, Beenken KE, Nelson CL, Smeltzer MS. *Staphylococcus aureus* collagen adhesin contributes to the pathogenesis of osteomyelitis. Bone 2002;30:275–280.
11. Fernandez-Hidalgo N, Gavalda J, Almirante B, Martin M-T, Onrubia PL, Gomis X, Pahissa A. Evaluation of linezolid, vancomycin, gentamicin and ciprofloxacin in a rabbit model of antibitoic-locl technique for *Staphylococcus aureus* catheter-related infection. J Antimicrob Chemother 2010;65:525–530.
12. Hansen LK, Berg K, Johnson D, Sanders M, Citron M. Efficacy of local rifampin/minocycline delivery (AIGISRX®) to eliminate biofilm formation on implanted pacing devices in a rabbit model. Int J Artif Organs 2010;33:627–635.
13. Hart E, Azzopardi K, Taing H, Graichen F, Jeffery J, Mayadunne R, Wickramaratna M, O'Shea M, Nijagal B, Watkinson R, et al. Efficacy of antimicrobial polymer coatings in an animal model of bacterial infection associated with foreign body implants. J Antimicrob Chemother 2010;65:974–980.
14. Keeling WB, Myers AR, Stone PA, Heller L, Widen R, Back MR, Johnson BL, Bandyk DF, Shames ML. Regional antibiotic delivery for the treatment of experimental prosthetic graft infections. J Surg Res 2009;157:223–226.
15. Li B, Brown KV, Wenke JC, Guelcher SA. Sustained release of vancomycin from polyurethane scaffolds inhibits infection of bone wounds in a rat femoral segmental defect model. J Control Release 2010;145:221–230.
16. Lucke M, Schmidmaier G, Sadoni S, Wildemann B, Schiller R, Haas NP, Raschke M. Gentamicin coating of metallic implants reduces implant-related osteomyelitis in rats. Bone 2003;32:521–531.
17. Mayberry-Carson KJ, Tober-Meyer B, Smith JK, D.W.Lambe J, Costerton JW. Bacterial adherence and glycocalyx formation in osteomyelitis experimentally induced with *Staphylococus aureus*. Infect Immun 1984;43:825–833.
18. Reid SD, Hong W, Dew KE, Winn DR, Pang B, Watt J, Glover DT, Hollingshead SK, Swords WE. *Streptococcus pneumoniae* forms surface-attached communities in the middle ear of experimentally infected chinchillas. J Infect Diseas 2009;199:786–794.
19. Zou G-Y, Shen H, Jiang Y, Zhang X-L. Synergistic effect of a novel focal hyperthermia on the efficacy of rifampin in Staphylococcal experimental foreign-body infection. J Int Med Res 2009;37:1115–1126.
20. Brin YS, Golenser J, Mizrahi B, Maoz G, Domb AJ, Peddada S, Tuvia S, Nyska A, Nyska M. Treatment of osteomyelitis in rats by injection of degradable polymer releasing gentamicin. J Control Release 2008;131:121–127.
21. Xie Z, Liu X, Jia W, Zhang C, Huang W, Wang J. Treatment of osteomyelitis and repair of bone defect by degradable bioactive borate glass releasing vancomycin. J Control Release 2009;139:118–126.
22. Krasko MY, Golenser J, Nyska A, Nyska M, Brin YS, Domb AJ. Gentamicin extended release from an injectable polymeric implant. J Control Release 2007;117:90–96.
23. Williams D, Bloebaum R, Petti CA. Characterization of *Staphylococcus aureus* strains in a rabbit model of osseointegrated pin infections. J Biomed Mater Res A 2008;85:366–370.
24. Chou TGR, Petti CA, Szakacs J, Bloebaum RD. Evaluating antimicrobials and implant materials for infection prevention around transcutaneous osseointegrated implants in a rabbit model. J Biomed Mater Res A 2010;92:942–952.
25. Costerton JW, Geesey GG, Cheng KJ. How bacteria stick. Sci Am 1978;238:86–95.
26. Wimpenny J, Manz W, Szewzyk U. Heterogeneity in biofilms. FEMS Microbiol Rev 2000;24:661–671.
27. Lawrence JR, Korber DR, Hoyle BD, Costerton JW, Caldwell DE. Optical sectioning of microbial biofilms. J Bacteriol 1991;173:6558–6567.
28. Geesey GG, Richardson WT, Yeomans HG, Irvin RT, Costerton JW. Microscopic examination of natural sessile bacterial populations from an Alpine Stream. Canad J Microbiol 1977;23:1733–1736.
29. James GA, Swogger E, Wolcott R, Pulcini Ed, Secor P, Sestrich J, Costerton JW, Stewart PS. Biofilms in chronic wounds. Wound Repair Regen 2008;16:37–44.
30. Feazel LM, Baumgartner LK, Peterson KL, Frank DN, Harris JK, Pace NR. Opportunistic pathogens enriched in Showerhead biofilms. Proc Natl Acad Sci USA 2009;106:16393–16399.
31. Dowd SE, Sun Y, Secor PR, Rhoads DD, Wolcott BM, James GA, Wolcott RD. Survey of bacterial diversity in chronic wounds using pyrosequencing, DGGE, and full ribosome shotgun sequencing. BMC Microbiol 2008;6:43.
32. Gristina AG, Costerton JW. Bacteria-Laden biofilms: A hazard to orthopedic prostheses. Infect Surg 1984;3:655–662.
33. Marrie T, Nelligan J, Costerton J. A scanning and transmission electron microscopic study of an infected endocardial pacemaker lead. Circulation 1982;66:1339–1341.
34. Costerton JW. Cystic fibrosis pathogenesis and the role of biofilms in persistent infection. Trends Microbiol 2001;9:50–52.
35. Serralta VW, Harrison-Balestra C, Cazzaniga AL, Davis SC, Mertz PM. Lifestyles of bacteria in wounds: Presence of biofilms? Wounds 2001;13:29–34.
36. Mertz PM. Cutaneous biofilms: Friend or foe? Wounds 2003;15:129–132.
37. Percival SL, Bowler PG. Biofilms and their potential role in wound healing. Wounds 2004;16:234–240.

38. James G, Swogger E, deLancey-Pulcini E. Biofilms in chronic wounds. In: Costerton JW, editor. The Role of Biofilms in Device-Related Infections. Heidelberg: Springer; 2009. p11–14.
39. Williams DL, Costerton JW. Using biofilms as initial inocula in animal models of biofilm-related infections. J Biomed Mater Res B 2011;00B:000–000.
40. Williams DL, Haymond BS, Bloebaum RD. Use of delrin plastic in a modified CDC biofilm reactor. Res J Microb 2011;6:425–429.
41. Williams DL, Woodbury KL, Haymond BS, Parker AE, Bloebaum RD. A modified CDC biofilm reactor to produce mature biofilms on the surface of PEEK membranes for an in vivo animal model application. Curr Microbiol 2011;62:1657–1663.
42. Bloebaum RD, Willie BM, Mitchell BS, Hofmann AA. Relationship between bone ingrowth, mineral apposition rate, and osteoblast activity. J Biomed Mater A 2007;81:505–514.
43. Smeltzer MS, Thomas JR, Hickmon SG, Skinner RA, Nelson CL, Griffith D, Thomas R, Parr J, Evans RP. Characterization of a rabbit model of *Staphylococcal osteomyelitis*. J Orthopaed Res 1997; 15:414–421.
44. O'Toole G, Kaplan HB, Kolter R. Biofilm formation as microbial development. Annu Rev Microbiol 2000;54:49–79.
45. Mendel V, Simanowski HJ, Scholz HC. Synergy of HBO2 and a local antibiotic carrier for experimental osteomyelitis due to *Staphylococcus aureus* in rats. Undersea Hyperb Med 2004;31: 407–416.
46. Mendel V, Reichert B, Simanowski HJ, Scholz HC. Therapy with hyperbaric oxygen and cefazolin for experimental osteomyelitis due to *Staphylococcus aureus* in rats. Undersea Hyperb Med 1999;26:169–174.
47. Lambotte JC, Thomazeau H, Cathelineau G, Lancien G, Minet J, Langlais F. Tricalcium phosphate, an antibiotic carrier: A study focused on experimental osteomyelitis in rabbits. Chirurgie 1998; 123:572–579.
48. Kaarsemaker S, Walenkamp GH, vd Bogaard AE. New model for chronic osteomyelitis with *Staphylococcus aureus* in sheep. Clin Orthopaed Relat Res 1997;339:246–252.
49. Gaudin A, Valle GAD, Hamel A, Mabecque VL, Miegeville A-F, Potel G, Caillon J, Jacqueline C. A new experimental model of acute osteomyelitis due to methicillin-resistant *Staphylococcus aureus* in rabbit. Lett Appl Microbiol 2011;52:253–257.
50. Harris LG, Richards RG. Staphylococci and implant surfaces: A review. Injury 2006;37:S3–S14.
51. Arens S, Schlegel U, Printzen G, Ziegler WJ, Perren SM, Hansis M. Influence of materials for fixation implants on local infection. J Bone Joint Surg (British) 1996;78B:647–651.

REFERENCES

1. Parker V. Antony van Leeuwenhoek. Bulletin of the Medical Library Association 1965;53:442-447.

2. Prescott LM. Microbiology New York: McGraw-Hill; 2002. p 1-16.

3. Fracastoro G. Contagion, Contagious Diseases and Their Treatment. In: Brock TD, editor. Milestones in Microbiology: 1546 to 1940. Washington: Prentice-Hall, Inc.; 1546. p 69-75.

4. Roncalli AR. The History of Italian Parasitology. Veterinary Parasitology 2001;12(98(1-3)):3-30.

5. Maloy S, Schaechter M. The Era of Microbiology: A Golden Phoenix. International Microbiology 2006;9:1-7.

6. ZoBell CE. The Effect of Solid Surfaces Upon Bacterial Activity. Journal of Bacteriology 1943;46(1):39-56.

7. Costerton JW, Geesey GG, Cheng KJ. How Bacteria Stick. Sci Am 1978;238(1):86-95.

8. Costerton JW. The Predominance of Biofilms in Natural and Engineered Ecosystems. In: Costerton JW, Editor. The Biofilm Primer. Heidelberg: Springer; 2007. p 5-13.

9. Geesey GG, Richardson WT, Yeomans HG, Irvin RT, Costerton JW. Microscopic Examination of Natural Sessile Bacterial Populations From an Alpine Stream. Canadian Journal of Microbiology 1977;23(12):1733-1736.

10. Darouiche RO. Treatment of Infections Associated with Surgical Implants. The New England Journal of Medicine 2004;350:1422-1429.

11. Costerton JW, Irvin RT. The Bacterial Glycocalyx in Nature and Disease. Annual Review of Microbiology 1981;35:299-324.

12. Choo MH, Jr DRH, Gersh BJ, Maloney JD, Merideth J, Pluth JR, Trusty J. Permanent Pacemaker Infections: Characterization and Management. The American Journal of Cardiology 1981;48:559-564.

13. Costerton JW, Irvin RT, Cheng KJ. The Role of the Bacterial Surface Structures in Pathogenesis. CRC Critical Reviews in Microbiology 1981;8:303-338.

14. Sugarman B, Musher D. Adherence of Bacteria to Suture Materials. Proceedings of the Society for Experimental Biology and Medicine 1980;167(2):156-160.

15. Jara FM, Toledo-Pereyra L, Jr JWL, Jr DJM. The Infected Pacemaker Pocket. The Journal of Thoracic and Cardiovascular Surgery 1979;78(2):298-300.

16. Gristina AG, Costerton JW. Bacteria-Laden Biofilms: A Hazard to Orthopedic Prostheses. Infections in Surgery 1984;3:655-662.

17. Marrie T, Nelligan J, Costerton J. A Scanning and Transmission Electron Microscopic Study of an Infected Endocardial Pacemaker Lead. Circulation 1982;66:1339-1341.

18. Nickel JC, Ruseska I, Wright JB, Costerton JW. Tobramycin Resistance of *Pseudomonas aeruginosa* Cells Growing as a Biofilm on Urinary Catheter Material. Antimicrobial Agents and Chemotherapy 1985;27(4):619-624.

19. Gerard LP, Ceri H, Gibb AP, Olson M, Sepandj F. MIC Versus MBEC to Determine the Antibiotic Sensitivity of *Staphylococcus aureus* in Peritoneal Dialysis Peritonitis. Peritoneal Dialysis International 2010;30(6):652-656.

20. Wolcott RD, Ehrlich GD. Biofilms and Chronic Infections. Journal of the American Medical Association 2008;299(22):2682-2684.

21. Wolcott RD, Rumbaugh KP, James G, Schultz G, Phillips P, Yang Q, Watters C, Stewart PS, Dowd SE. Biofilm Maturity Studies Indicate Sharp Debridement Opens a Time-Dependent Therapeutic Window. Journal of Wound Care 2010;19(8):320-328.

22. Anderl JN, Franklin MJ, Stewart PS. Role of Antibiotic Penetration Limitation in *Klebsiella pneumoniae* Biofilm Resistance to Ampicillin and Ciprofloxacin. Antimicrobial Agents and Chemotherapy 2000;44(7):1818-1824.

23. Gibbons RJ, Houte Jv. Bacterial Adherence in Oral Microbiology Ecology. Annual Review of Microbiology 1975;29:19-42.

24. Lawrence JR, Korber DR, Hoyle BD, Costerton JW, Caldwell DE. Optical Sectioning of Microbial Biofilms. Journal of Bacteriology 1991;173:6558-6567.

25. Stoodley P. Liquid Flow Through Biofilm Channels. Volume 2012. http://www.biofilm.montana.edu/resources/movies/1994/1994m02.html: Montana State University Center for Biofilm Engineering; 1994.

26. de Beer D, Stoodley P. Relation Between the Structure of an Aerobic Biofilm and Transport Phenomena. Water Science Technology 2005;32:11-18.

27. Erlandsen SL, Kristich CJ, Dunny GM, Wells CL. High-resolution Visualization of the Microbial Glycocalyx with Low-Voltage Scanning Electron Microscopy: Dependence on Cationic Dyes. Journal of Histochemistry and Cytochemistry 2004;52(11):1427-1435.

28. Williams DL, Bloebaum RD. Observing the Biofilm Matrix of *Staphylococcus epidermidis* ATCC 35984 Grown Using the CDC Biofilm Reactor. Microscopy and Microanalysis 2010;16:143-152.

29. Nichols WW, Dorrington SM, Slack MPE, Walmsley HL. Inhibition of Tobramycin Diffusion by Binding to Alginate. Antimicrobial Agents and Chemotherapy 1988;32(4):518-523.

30. Walters MC, Roe F, Bugnicourt A, Franklin MJ, Stewart PS. Contributions of Antibiotic Penetration, Oxygen Limitation, and Low Metabolic Activity to Tolerance of *Pseudomonas aeruginosa* Biofilms to Ciprofloxacin and Tobramycin. Antimicrobial Agents and Chemotherapy 2003;47(1):317-323.

31. Borriello G, Werner E, Roe F, Kim AM, Ehrlich GD, Stewart PS. Oxygen Limitation Contributes to Antibiotic Tolerance of *Pseudomonas aeruginosa* in Biofilms. Antimicrobial Agents and Chemotherapy 2004;48(7):2659-2664.

32. Mandell GL. Interaction of Intraleukocytic Bacteria and Antibiotics. The Journal of Clinical Investigation 1973;52:1673-1673.

33. Gilbert P, Collier PJ, Brown MRW. Influence of Growth Rate on Susceptibility to Antimicrobial Agents: Biofilms, Cell Cycle, Dormancy, and Stringent Response. Antimicrobial Agents and Chemotherapy 1990;34(10):1865-1868.

34. Narten M, Rosin N, Schobert M, Tielen P. Susceptibility of *Pseudomonas aeruginosa* Urinary Tract Isolates and Influence of Urinary Tract Conditions on Antibiotic Tolerance. Current Microbiology 2012;64(1):7-16.

35. Balaban NQ. Persistence: Mechanisms for Triggering and Enhancing Phenotypic Variability. Current Opinion in Genetics and Development 2011;21(6):768-775.

36. Hausner M, Wuertz S. High Rates of Conjugation in Bacterial Biofilms as Determined by Quantitative In Situ Analysis. Applied and Environmental Microbiology 1999;65(8):3710-3713.

37. Lederberg J, Tatum EL. Gene Recombination in *Escherichia coli*. Nature 1946;158(4016):529-564.

38. Lujan SA, Guogas LM, Ragonese H, Matson SW, Redinbo MR. Disrupting Antibiotic Resistance Propagation by Inhibiting the Conjugative DNA Relaxase. PNAS 2007;104(30):12282-12287.

39. Costerton JW. Control of all Biofilm Strategies and Behaviours. In: Eckey C, editor. The Biofilm Primer. New York: Springer; 2007. p 85-105.

40. Williams DL, Woodbury KL, Haymond BS, Parker AE, Bloebaum RD. A Modified CDC Biofilm Reactor to Produce Mature Biofilms on the Surface of PEEK Membranes for an In Vivo Animal Model Application. Current Microbiology 2011;62(6):1657-1663.

41. Morita Y, Sobel ML, Poole K. Antibiotic Inducibility of the MexXY Multidrug Efflux System of *Pseudomonas aeruginosa*: Involvement of the Antibiotic-Inducible PA5471 Gene Product. Journal of Bacteriology 2006;188(5):1847-1855.

42. Tran TD, Kwon HY, Kim EH, Kim KW, Brilles DE, Pyo S, Rhee DK. Heat-Shock Protein ClpL/HSP100 Increases Penicillin Tolerance in *Streptococcus pneumoniae*. Advances in Oto-rhino-laryngology 2011;72:126-128.

43. Livorsi DJ, Stenehjem E, Stephens DS. Virulence Factors of Gram-Negative Bacteria in Sepsis With a Focus on *Neisseria meningitidis*. Contributions to Microbiology 2011;17:31-47.

44. Nostro PL, Ninham BW, Nostro AL, Pesavento G, Fratoni L, Baglioni P. Specific Ion Effects on the Growth Rates of *Staphylococus aureus* and *Pseudomonas aeruginosa*. Physical Biology 2005;2(1):1-7.

45. Leslie M. Microbiology. Germs Take a Bite Out of Antibiotics. Science 2008;320(5872):33.

46. Fleming A. On the Antibacterial Action of Cultures of a Penicillium, With Special Reference to Their Use in the Isolation of *Bacillus influenzae*. Reviews of Infectious Diseases 1929;2(1):129-139.

47. Ligon BL. Penicillin: Its Discovery and Early Development. Seminars in Pediatric Infectious Diseases 2004;15(1):52-57.

48. Zimmer C. Evolution: The Triumph of an Idea. New York: Harper Collins; 2001.

49. Mah MW, Memish ZA. Antibiotic Resistance: An Impending Crisis. Saudi Medical Journal 2000;21(12):1125-1129.

50. Murray CK. Epidemiology of Infections Associated With Combat-Related Injuries in Iraq and Afghanistan. Journal of Trauma 2008;64:S232-S238.

51. Owens BD, John F. Kragh J, Macaitis J, Svoboda SJ, Wenke JC. Characterization of Extremity Wounds in Operation Iraqi Freedom and Operation Enduring Freedom. Journal of Orthopaedic Trauma 2007;21:254-257.

52. Balaban N, Ren D, Givskov M, Rasmussen TB. The Problem: Untreatable Bacterial Infections. In: Balaban N, editor. Control of Biofilm Infections by Signal Manipulation. Berlin Heidelberg: Springer; 2008. p 1-11.

53. Melnick M. Drug-Resistant Superbug Shows Up in Three U.S. States. TIME 2010.

54. FoxNews.com. Europe in the Grip of Drug-Resistant Superbugs. Volume 2012: FoxNews; 2011.

55. Levy SB, Marshall B. Antibacterial Resistance Worldwide: Causes, Challenges and Responses. Nature Medicine 2004;10:S122-S129.

56. Diekema DJ, BootsMiller BJ, Vaughn TE, Woolson RF, Yankey JW, Ernst EJ, Flach SD, Ward MM, Franciscus CLJ, Pfaller MA and others. Antimicrobial Resistance Trends and Outbreak Frequency in United States Hospitals. Clinical Infectious Diseases 2004;38(1):78-85.

57. Williams DL, Costerton JW. Using Biofilms as Initial Inocula in Animal Models of Biofilm-Related Infections. Journal of Biomedical Materials Research Part B 2011;00B:000-000.

58. Costerton JW. Cystic Fibrosis Pathogenesis and the Role of Biofilms in Persistent Infection. Trends in Microbiology 2001;9(2):50-52.

59. Harris LG, Richards RG. Staphylococci and Implant Surfaces: A Review. Injury 2006;37:S3-S14.

60. Costerton JW. Biofilm Theory Can Guide the Treatment of Device-Related Orthopaedic Infections. Clinical Orthopaedics and Related Research 2005;437:7-11.

61. Hetrick EM, Schoenfisch MH. Reducing Implant-Related Infections: Active Release Strategies. Chemical Society Reviews 2006;35(9):780-790.

62. Serralta VW, Harrison-Balestra C, Cazzaniga AL, Davis SC, Mertz PM. Lifestyles of Bacteria in Wounds: Presence of Biofilms? Wounds 2001;13(1):29-34.

63. Mertz PM. Cutaneous Biofilms: Friend or Foe? Wounds 2003;15:129-132.

64. James G, Swogger E, deLancey-Pulcini E. Biofilms in Chronic Wounds. In: Costerton JW, editor. The Role of Biofilms in Device-Related Infections. Heidelberg: Springer; 2009. p 11-14.

65. Gustilo RB, Merkow RL, Templeman D. The Management of Open Fractures. The Journal of Bone and Joint Surgery 1990;72:299-304.

66. Gustilo RB, Mendoza RM, Williams DN. Problems in the Management of Type III (Severe) Open Fractures: A New Classification of Type III Open Fractures. The Journal of Trauma 1984;24(8):742-746.

67. Johnson EN, Burns TC, Hayada RA, Hospenthal DR, Murray CK. Infectious Complications of Open Type III Tibial Fracture Among Combat Casualties. Clinical Infectious Diseases 2007;45:409-415.

68. Forsberg JA, Potter BK, Cierny G, Webb L. Diagnosis and Management of Chronic Infection. The Journal of the American Academy of Orthopaedic Surgeons 2011;19:S8-S19.

69. Anglen JO. Wound Irrigation in Musculoskeletal Injury. The Journal of the American Academy of Orthopaedic Surgeons 2001;9:219-226.

70. Torsvik V, Goksoyr J, Daae FL. High Diversity in DNA of Soil Bacteria. Applied and Environmental Microbiology 1990;56(3):782-787.

71. Bakken LR. Separation and Purification of Bacteria from Soil. Appl Environ Microbiol 1985;49(6):1482-1487.

72. Wimpenny J, Manz W, Szewzyk U. Heterogeneity in Biofilms. FEMS Microbiology Review 2000;24(5):661-671.

73. CDC. Injury in the United States: 2007 Chartbook. 2007.

74. CDC. NCHS Data on Injuries. 2004.

75. Petrisor B, Jeray K, Schemitsch E, Hanson B, Sprague S, Sanders D, Bhandari M. Fluid Lavage in Patients with Open Fracture Wounds (FLOW): An International Survey of 984 Surgeons. BMC Musculoskeletal Disorders 2008;9:7.

76. Bhandari M, Schemitsch EH, Adili A, Lachowski RJ, Shaughnessy SO. High and Low Pressure Pulsatile Lavage of Contaminated Tibial Fractures: An In Vivo Study of Bacterial Adherence and Bone Damage. Journal of Orthopaedic Trauma 1999;13(8):526-533.

77. Bhandari M, Guyatt GH, Swiontkowski MF, Schemitsch EH. Treatment of Open Fractures of the Shaft of the Tibia. The Journal of Bone and Joint Surgery 2000;82-B:62-68.

78. Gustilo RB, Anderson JT. Prevention of Infection in the Treatment of One Thousand and Twenty-Five Open Fractures of Long Bones: Retrospective and Prospective Analyses. The Journal of Bone and Joint Surgery 1976;58:453-458.

79. Lambert EW, Simpson RB, Marzouk A, Unger DV. Orthopaedic Injuries Among Survivors of USS Cole Attack. Journal of Orthopaedic Trauma 2003;17(6):436-441.

80. Buret A, Ward KH, Olson ME, Costerton JW. An *In Vivo* Model to Study the Pathobiology of Infectious Biofilms on Biomaterial Surfaces. Journal of Biomedical Materials Research 1991;25(7):865-874.

81. Cirioni O, Mocchegiani F, Ghiselli R, Silvestri C, Gabrielli E, Marchionni E, Orlando F, Nicolini D, Risaliti A, Giacometti A. Daptomycin and Rifampin Alone and in Combination Prevent Vascular Graft Biofilm Formation and Emergence of Antibiotic Resistance in a Subcutaneous Rat Pouch Model of Staphylococcal Infection. European Journal of Vascular and Endovascular Surgery 2010;40(6):817-822.

82. Lambe DW, Ferguson KP, Mayberry-Carson KJ, Tober-Meyer B, Costerton JW. Foreign-Body-Associated Experimental Osteomyelitis Induced With *Bacteroides fragilis* and *Staphylococcus epidermidis* in Rabbits. Clinical Orthopaedics and Related Research 1991;May(266):285-294.

83. Darouiche RO, Farmer J, Chaput C, Mansouri M, Saleh G, Landon GC. Anti-Infective Efficacy of Antiseptic-Coated Intramedullary Nails. The Journal of Bone and Joint Surgery 1998;80(9):1336-1340.

84. Darouiche RO, Mansouri MD. Dalbavancin Compared with Vancomycin for Prevention of *Staphylococcus aureus* Colonization of Devices In Vivo. Journal of Infection 2005;50(3):206-209.

85. Darouiche RO, Mansouri MD, Gawande PV, Madhyastha S. Antimicrobial and Antibiofilm Efficacy of Triclosan and Dispersin B Combination. Journal of Antimicrobial Chemotherapy 2009;64(1):88-93.

86. Davis SC, Ricotti C, Cazzaniga A, Welsh E, Eaglstein WH, Mertz PM. Microscopic and Physiologic Evidence for Biofilm-Associated Wound Colonization In Vivo. Wound Repair and Regeneration 2008;16(1):23-29.

87. Dohar JE, Hebda PA, Veeh R, Awad M, Costerton JW, Hayes J, Ehrlich GD. Mucosal Biofilm Formation on Middle-Ear Mucosa in a Nonhuman Primate

Model of Chronic Suppurative Otitis Media. The Laryngoscope 2005;115(8):1469-1472.

88. Elasri MO, Thomas JR, Skinner RA, Blevins JS, Beenken KE, Nelson CL, Smeltzer MS. *Staphylococcus aureus* Collagen Adhesin Contributes to the Pathogenesis of Osteomyelitis. Bone 2002;30(1):275-280.

89. Fernandez-Hidalgo N, Gavalda J, Almirante B, Martin M-T, Onrubia PL, Gomis X, Pahissa A. Evaluation of Linezolid, Vancomycin, Gentamicin and Ciprofloxacin in a Rabbit Model of Antibiotic-Lock Technique for *Staphylococcus aureus* Catheter-Related Infection. Journal of Antimicrobial Chemotherapy 2010;65(3):525-530.

90. Hansen LK, Berg K, Johnson D, Sanders M, Citron M. Efficacy of Local Rifampin/Minocycline Delivery (AIGISRX®) to Eliminate Biofilm Formation on Implanted Pacing Devices in a Rabbit Model. International Journal of Artificial Organs 2010;33(9):627-635.

91. Hart E, Azzopardi K, Taing H, Graichen F, Jeffery J, Mayadunne R, Wickramaratna M, O'Shea M, Nijagal B, Watkinson R and others. Efficacy of Antimicrobial Polymer Coatings in an Animal Model of Bacterial Infection Associated with Foreign Body Implants. Journal of Antimicrobial Chemotherapy 2010;65(5):974-980.

92. Keeling WB, Myers AR, Stone PA, Heller L, Widen R, Back MR, Johnson BL, Bandyk DF, Shames ML. Regional Antibiotic Delivery for the Treatment of Experimental Prosthetic Graft Infections. Journal of Surgical Research 2009;157(2):223-226.

93. Li B, Brown KV, Wenke JC, Guelcher SA. Sustained Release of Vancomycin from Polyurethane Scaffolds Inhibits Infection of Bone Wounds in a Rat Femoral Segmental Defect Model. Journal of Controlled Release 2010;145(3):221-230.

94. Lucke M, Schmidmaier G, Sadoni S, Wildemann B, Schiller R, Haas NP, Raschke M. Gentamicin Coating of Metallic Implants Reduces Implant-Related Osteomyelitis in Rats. Bone 2003;32(5):521-531.

95. Mayberry-Carson KJ, Tober-Meyer B, Smith JK, D.W. Lambe J, Costerton JW. Bacterial Adherence and Glycocalyx Formation in Osteomyelitis Experimentally Induced with *Staphylococus aureus*. Infection and Immunity 1984;43(3):825-833.

96. Reid SD, Hong W, Dew KE, Winn DR, Pang B, Watt J, Glover DT, Hollingshead SK, Swords WE. *Streptococcus pneumoniae* Forms Surface-Attached Communities in the Middle Ear of Experimentally Infected Chinchillas. The Journal of Infectious Diseases 2009;199(6):786-794.

97. Zou G-Y, Shen H, Jiang Y, Zhang X-L. Synergistic Effect of a Novel Focal Hyperthermia on the Efficacy of Rifampin in Staphylococcal Experimental Foreign-Body Infection. The Journal of International Medical Research 2009;37(4):1115-1126.

98. Brin YS, Golenser J, Mizrahi B, Maoz G, Domb AJ, Peddada S, Tuvia S, Nyska A, Nyska M. Treatment of Osteomyelitis in Rats by Injection of Degradable Polymer Releasing Gentamicin. Journal of Controlled Release 2008;131(2):121-127.

99. Xie Z, Liu X, Jia W, Zhang C, Huang W, Wang J. Treatment of Osteomyelitis and Repair of Bone Defect by Degradable Bioactive Borate Glass Releasing Vancomycin. Journal of Controlled Release 2009;139(2):118-126.

100. Krasko MY, Golenser J, Nyska A, Nyska M, Brin YS, Domb AJ. Gentamicin Extended Release from an Injectable Polymeric Implant. Journal of Controlled Release 2007;117(1):90-96.

101. Williams D, Bloebaum R, Petti CA. Characterization of *Staphylococcus aureus* Strains in a Rabbit Model of Osseointegrated Pin Infections. J Biomed Mater Res A 2008;85(2):366-70.

102. Chou TGR, Petti CA, Szakacs J, Bloebaum RD. Evaluating Antimicrobials and Implant Materials for Infection Prevention Around Transcutaneous Osseointegrated Implants in a Rabbit Model. Journal of Biomedical Materials Research part A 2009;Online.

103. Bucki R, Sostarecz AG, Byfield FJ, Savage PB, Janmey PA. Resistance of the Antibacterial Agent Ceragenin CSA-13 to Inactivation by DNA or F-Actin and its Activity in Cystic Fibrosis Sputum. Journal of Antimicrobial Chemotherapy 2007;60:535-545.

104. Chin JN, Rybak MJ, Cheung CM, Savage PB. Antimicrobial Activities of Ceragenins Against Clinical Isolates of Resistant *Staphylococcus aureus*. Antimicrobial Agents and Chemotherapy 2007;51(4):1268-1273.

105. Lai X-Z, Feng Y, Pollard J, Chin JN, Rybak MJ, Bucki R, Epand RF, Epand RM, Savage PB. Ceragenins: Cholic Acid-Based Mimics of Antimicrobial Peptides. Accounts of Chemical Research 2008;41(10):1233-1240.

106. Epand RF, Pollard JE, Wright JO, Savage PB, Epand RM. Depolarization, Bacterial Membrane Composition, and the Antimicrobial Action of Ceragenins. Antimicrobial Agents and Chemotherapy 2010;54(9):3708-3713.

107. Li C, Lewis MR, Gilbert AB, Noel MD, Scoville DH, Allman GW, Savage PB. Antimicrobial Activities of Amine- and Guanidine- Functionalized Cholic Acid Derivatives. Antimicrobial Agents and Chemotherapy 1999;43(6):1347-1349.

108. Savage PB. Multidrug-Resistant Bacteria: Overcoming Antibiotic Permeability Barriers of Gram-Negative Bacteria. Annals of Medicine 2001;33(3):167-171.

109. Savage PB. Design, Synthesis and Characterization of Cationic Peptide and Steroid Antibiotics. European Journal of Organic Chemistry 2002;2002(5):759-768.

110. Williams DL, Haymond BS, Bloebaum RD. Use of Delrin Plastic in a Modified CDC Biofilm Reactor. Research Journal of Microbiology 2011;6:425-429.

111. Noe A. Extremity Injury in War: A Brief History. The Journal of the American Academy of Orthopaedic Surgeons 2006;14:S1-S6.

112. Daniels IR. Historical Perspective on Health. Semmelweis: A Lesson to Relearn? The Journal of the Royal Society for the Promotion of Health 1998;118(6):367-370.

113. Best M, Neuhauser D. Ignaz Semmelweis and the Birth of Infection Control. Quality and Safety in Health Care 2004;13(3):233-234.

114. Bauer J. The Tragic Fate of Ignaz Philipp Semmelweis. California Medicine 1963;98:264-266.

115. Lister J. The Classic: On the Antiseptic Principle in the Practice of Surgery. Clinical Orthopaedics and Related Research 1867;468:2012-2016.

116. Lambert RA. The Comparative Resistance of Bacteria and Human Tissue Cells to Certain Common Antiseptics. The Journal of Experimental Medicine 1916;24(6):683-688.

117. Taylor HD, Austin JH. The Solvent Action of Antiseptics on Necrotic Tissue. The Journal of Experimental Medicine 1918;27(1):155-164.

118. Austin JH, Taylor HD. Behavior of Hypochlorite and of Chloramine-T Solutions in Contact with Necrotic and Normal Tissues In Vivo. The Journal of Experimental Medicine 1918;27(5):627-633.

119. Kozol RA, Gillies C, Elgebaly SA. Effects of Sodium Hypochlorite (Dakin's Solution) on Cells of the Wound Module. Archives of Surgery 1988;123(4):420-423.

120. Heggers JP, Sazy JA, Stenberg BD, Strock LL, McCauley RL, Herndon DN, Robson MC. Bactericidal and Wound-Healing Properties of Sodium Hypochlorite Solutions: The 1991 Lindberg Award. The Journal of Burn Care and Rehabilitation 1991;12(5):420-424.

121. Summers WC. Bacteriophage Research: Early History. In: Kutter E, Sulakvelidze A, editors. Bacteriophages. Boca Raton: CRC Press; 2005. p 5-28.

122. Lara HH, Garza-Trevino EN, Ixtepan-Turrent L, Singh DK. Silver Nanoparticles are Broad-Spectrum Bactericidal and Virucidal Compounds. Journal of Nanobiotechnology 2011;9:30.

123. Grass G, Rensing C, Solioz M. Metallic Copper as an Antimicrobial Surface. Applied and Environmental Microbiology 2011;77(5):1541-1547.

124. Amin RM, Mohamed MB, Ramadan MA, Verwanger T, Krammer B. Rapid and Sensitive Microplate Assay for Screening the Effect of Silver and Gold Nanoparticles on Bacteria. Nanomedicine (London, England) 2009;4(6):637-643.

125. Raad I, Reitzel R, Jiang Y, Chemaly RF, Dvorak T, Hachem R. Anti-Adherence Activity and Antimicrobial Durability of Anti-Infective-Coated Catheters Against Multidrug-Resistant Bacteria. Journal of Antimicrobial Chemotherapy 2008;62(4):746-750.

126. Salcido RS. Silver: An Old Wine in a New Bottle. Advances in Skin and Wound Care 2006;19(9):472-474.

127. Spear M. Silver: An Age-Old Treatment Modality in Modern Times. Plastic Surgical Nursing 2010;30(2):90-93.

128. Alexander JW. History of the Medical Use of Silver. Surgical Infections 2009;10(3):289-292.

129. Martin-Bates A. Tying All Together. Trauma 2008;10(2):103-108.

130. Viets HR. A Score of Significant Papers Published in the *Journal* During the Last Hundred and Fifty Years. The New England Journal of Medicine 1962;266(1):23-28.

131. Sartin JS. J. Marion Sims, the Father of Gynecology: Hero or Villain? Southern Medical Journal 2004;97(5):500-505.

132. Elgayyar M, Draughon FA, Golden DA, Mount JR. Antimicrobial Activity of Essential Oils from Plants Against Selected Pathogenic and Saprophytic Microorganisms. Journal of Food Protection 2001;64(7):1019-1024.

133. Zaika LL. Spices and Herbs: Their Antimicrobial Activity and its Determination. Journal of Food Safety 1988;9(2):97-118.

134. Lee DS, Sinno S, Khachemoune A. Honey and Wound Healing: An Overview. American Journal of Clinical Dermatology 2011;12(3):181-190.

135. Yuen MF, Tam S, Fung J, Wong DK, Wong BC, Lai CL. Traditional Chinese Medicine Causing Hepatotoxicity in Patients with Chronic Hepatitis B Infection: A 1-Year Prospective Study. Alimentary Pharmacology and Therapeutics 2006;24(8):1179-1186.

136. Mandal S, DebMandal M, Saha K, Pal NK. In Vitro Antibacterial Activity of Three Indian Spices Against Methicillin-Resistant *Staphylococcua aureus*. Oman Medical Journal 2011;26(5):319-323.

137. Kim J, Pitts B, Stewart PS, Camper A, Yoon J. Comparison of the Antimicrobial Effects of Chlorine, Silver Ion, and Tobramycin on Biofilm. Antimicrobial Agents and Chemotherapy 2008;52(4):1446-1453.

138. Okano M, Nomura M, Hata S, Okada N, Sato K, Kitano Y, Tashiro M, Yoshimoto Y, Hama R, Aoki T. Anaphylactic Symptoms Due to Chlorhexidine Gluconate. Archives of Dermatology 1989;125(1):50-52.

139. Oda T, Hamasaki J, Kanda N, Mikami K. Anaphylactic Shock Induced by an Antiseptic-Coated Central Nervous Catheter. Anesthesiology 1997;87(5):1242-1244.

140. Payne RJH, Jansen VAA. Phage Therapy: The Peculiar Kinetics of Self-Replicating Pharmaceuticals. Clinical Pharmacology and Therapeutics 2000;68:225-230.

141. Moretti EW, Ofstead CL, Kristy RM, Wetzler HP. Impact of Central Venous Catheter Type and Methods on Catheter-Related Colonization and Bacteraemia. The Journal of Hospital Infection 2005;61(2):139-145.

142. Lockhart SP, Rushworth A, Azmy AA, Raine PA. Topical Silver Sulphadiazine: Side Effects and Urinary Excretion. Burns, Including Thermal Injury 1983;10(1):9-12.

143. Liu XS, Zola JC, McGinnis DE, Squadrito JF, Zeltser IS. Do Silver Alloy-Coated Catheters Increase Risk of Urethral Strictures After Robotic-Assisted Laparoscopic Radical Prostatectomy? Urology 2011;78(2):365-367.

144. Levy SB. Antibacterial Household Products: Cause for Concern. Emerging Infectious Diseases 2001;7(3 Suppl):512-515.

145. Zasloff M. Magainins, A Class of Antimicrobial Peptides from *Xenopus* Skin: Isolation, Characterization of Two Active Forms, and Partial cDNA Sequence of a Precursor. Proceedings of the National Academy of Sciences of the United States of America 1987;84:5449-5453.

146. Hancock REW, Scott MG. The Role of Antimicrobial Peptides in Animal Defenses. PNAS 2000;97(16):8856-8861.

147. Hancock RE, Sahl H-G. Antimicrobial and Host-Defense Peptides as New Anti-Infective Therapeutic Strategies. Nature Biotechnology 2006;24:1551-1557.

148. Hancock REW, Rozek A. Role of Membranes in the Activities of Antimicrobial Cationic Peptides. FEMS Microbiology Review 2002;206(2):143-149.

149. Jenssen H, Hamill P, Hancock RE. Peptide Antimicrobial Agents. Clinical Microbiology Reviews 2006;19(3):491-511.

150. Giuliani A, Pirri G, Nicoletto SF. Antimicrobial Peptides: An Overview of a Promising Class of Therapeutics. Central European Journal of Biology 2007;2(1):1-33.

151. Hoff Wvt, Veerman ECI, Helmerhorst EJ, Amerongen AVN. Antimicrobial Peptides: Properties and Applicability. Biological Chemistry 2001;382:597-619.

152. Fantner GE, Barbero RJ, Gray DS, Belcher AM. Kinetics of Antimicrobial Peptide Activity Measured on Individual Bacterial Cells Using High-Speed Atomic Force Microscopy. Nature Nanotechnology 2010;5(4):280-285.

153. Yocum RR, Rasmussen JR, Strominger JL. The Mechanism of Action of Penicillin. Penicillin Acylates the Active Site of *Bacillus stearothermophilus* D-Alanine Carboxypeptidase. The Journal of Biological Chemistry 1980;255(9):3977-3986.

154. Herzberg O, Moult J. Bacterial Resistance to Beta-Lactam Antibiotics: Crystal Structure of Beta-Lactamase from *Staphylococcus aureus* PC1 at 2.5 A Resolution. Science 1987;236(4802):694-701.

155. Chongsiriwatana NP, Patch JA, Czyzewski AM, Dohm MT, Ivankin A, Gidalevitz D, Zuckerman RN, Barron AE. Peptoids That Mimic the Structure, Function, and Mechanism of Helical Antimicrobial Peptides. PNAS 2008;105(8):2794-2799.

156. Beckloff N, Laube D, Castro T, Furgang D, Park S, Perlin D, Clements D, Tang H, Scott RW, Tew GN and others. Activity of an Antimicrobial Peptide Mimetic against Planktonic and Biofilm Cultures of Oral Pathogens. Antimicrobial Agents and Chemotherapy 2007;51(11):4125-4132.

157. Nagant C, Feng Y, Lucas B, Braeckmans K, Savage P, Dehaye JP. Effect of a Low Concentration of Cationic Steroid Antibiotic (CSA-13) on the Formation of a Biofilm by *Pseudomonas aeruginosa*. Journal of Applied Microbiology 2011;111(3):763-772.

158. Polat ZA, Savage PB, Genberg C. *In Vitro* Amoebicidal Activity of a Ceragenin, Cationic Steroid Antibiotic-13, Against *Acanthamoeba castellanii* and Its Cytotoxic Potential. Journal of Ocular Pharmacology and Therapeutics 2011;27(1):1-5.

159. Leszczynska K, Namiot A, Cruz K, Byfield FJ, Won E, Mendez G, Sokolowski W, Savage PB, Bucki R, Janmey PA. Potential of Ceragenin CSA-13 and Its Mixture with Pluronic F-127 as Treatment of Topical Bacterial Infections. Journal of Applied Microbiology 2011;110(1):229-238.

160. Nagant C, Tre-Hardy M, El-Ouaaliti M, Savage P, Devleeschouwer M, Dehaye JP. Interaction Between Tobramycin and CSA-13 on Clinical Isolates of *Pseudomonas aeruginosa* in a Model of Young and Mature Biofilms. Applied Microbiology and Biotechnology 2010;88(1):251-263.

161. Howell MD, Streib JE, Kim BE, Lesley LJ, Dunlap AP, Geng D, Feng Y, Savage PB, Leung DY. Ceragenins: A Class of Antiviral Compounds to Treat Orthopox Infections. Journal of Investigative Dermatology 2009;129(11):2668-2675.

162. Zilberman M, Elsner JJ. Antibiotic-Eluting Medical Devices for Various Applications. Journal of Controlled Release 2008;130:202-215.

163. Buchholz HW, Engelbrecht H. Uber die Depotwirkung einiger Antibiotica bei Vermischung mit dem Kunstharz Palacos. Journal de Chirurgie 1970;11:511-515.

164. Rushton DN, Brindley GS, Polkey CE, Browning GV. Implant Infections and Antibiotic-Impregnated Silicone Rubber Coating. Journal of Neurology, Neurosurgery, and Psychiatry 1989;52:223-229.

165. Schierholz JM, Steinhauser H, Rump AFE, Berkels R, Pulverer G. Controlled Release of Antibiotics From Biomedical Polyurethanes: Morphological and Structural Features. Biomaterials 1997;18:839-844.

166. Kelm J, Regitz T, Schmitt E, Jung W, Anagnostakos K. In Vivo and In Vitro Studies of Antibiotic Release From and Bacterial Growth Inhibition by Antibiotic-Impregnated Polymethylmethacrylate Hip Spacers. Antimicrobial Agents and Chemotherapy 2006;50(1):332-335.

167. Weiss BD, Weiss EC, Haggard WO, Evans RP, McLaren SG, Smeltzer MS. Optimized Elution of Daptomycin from Polymethylmethacrylate Beads. Antimicrobial Agents and Chemotherapy 2009;53(1):264-266.

168. Shi M, Kretlow JD, Nguyen A, Young S, Baggett LS, Wong ME, Kasper FK, Mikos AG. Antibiotic-Releasing Porous Polymethylmethacrylate Constructs for Osseous Space Maintenance and Infection Control. Biomaterials 2010;31:4146-4156.

169. Anderson EM, Noble ML, Garty S, Ma H, Bryers JD, Shen TT, Ratner BD. Sustained Relesae of Antibiotic from Poly(2-Hydroxyethylmethacrylate) to Prevent Blinding Infections After Cataract Surgery. Biomaterials 2009;30(29):5675-5681.

170. Solberg BD, Gutow AP, Baumgaertner MR. Hydroxyapatite Cement in Treating Osteomyelitis in a Rat Model. Journal of Orthopaedic Trauma 1999;13(2):102-106.

171. Stigter M, Bezemer J, Groot Kd, Layrolle P. Incorporation of Different Antibiotics into Carbonated Hydroxyapatite Coatings on Titanium Implants, Release and Antibiotic Efficacy. Journal of Controlled Release 2004;99:127-137.

172. Li H, Fairfax MR, Dubocq F, Darouiche RO, Rajpurkar A, Thompson M, Tefilli MV, Dhabuwala CB. Antibacterial Activity of Antibiotic Coated Silicone Grafts. The Journal of Urology 1998;160(5):1910-1913.

173. Fei J, Yu H-j, Pan C-j, Zhao C-h, Zhou Y-g, Wang Y. Efficacy of a Norvancomycin-Loaded, PDLLA-Coated Plate in Preventing Early Infection of Rabbit Tibia Fracture. Orthopedics 2010;33(5):310.

174. Kalicke T, Schierholz J, Schlegel U, Frangen TM, Koller M, Printzen G, Seybold D, Klockner S, Muhr G, Arenas S. Effect on Infection Resistance of a Local Antiseptic and Antibiotic Coating on Osteosynthesis Implants: An In Vitro and In Vivo Study. Journal of Orthopaedic Research 2006;24:1622-1640.

175. Price JS, Tencer AF, Arm DM, Bohach GA. Controlled Release of Antibiotics From Coated Orthopedic Implants. Journal of Biomedical Materials Research 1996;30:281-286.

176. Rasic Z, Schwarz D, Adam VN, Sever M, Lojo N, Rasic D, Matejic T. Efficacy of Antimicrobial Triclosan-Coated Polyglactin 910 (Vicryl* Plus) Suture for Closure of the Abdominal Wall After Colorectal Surgery. Collegium Antropologicum 2011;35(2):439-443.

177. Galal I, el-Hindawy K. Impact of Using Triclosan-Antibacterial Sutures on Incidence of Surgical Site Infection. American Journal of Surgery 2011;202(2):133-138.

178. Ranucci M, Isgro G, Giomarelli PP, Pavesi M, Luzzani A, Cattabriga I, Carli M, Giomi P, Compostella A, Digito A and others. Impact of Oligon Central Venous

Catheters on Catheter Colonization and Catheter-Related Bloodstream Infection. Critical Care Medicine 2003;31(1):52-59.

179. Bologna RA, Tu LM, Polansky M, Fraimow HD, Gordon DA, Whitmore KE. Hydrogel/Silver Ion-Coated Urinary Catheter Reduces Nosocomial Urinary Tract Infection Rates in Intensive Care Unit Patients: A Multicenter Study. Urology 1999;54(6):982-987.

180. Corral L, Nolla-Salas M, Ibanez-Nolla J, Leon MA, Diaz RM, Martin MC, Iglesia R, Catalan R. A Prospective, Randomized Study in Critically Ill Patients Using the Oligon Vantex Catheter. The Journal of Hospital Infection 2003;55(3):212-219.

181. Justinger C, Slotta JE, Schilling MK. Incisional Hernia After Abdominal Closure with Slowly Absorbable Versus Fast Absorbable, Antibacterial-Coated Sutures. Surgery 2011;Epub ahead of print.

182. Chen SY, Chen TM, Dai NT, Fu JP, Chang SC, Deng SC, Chen SG. Do Antibacterial-Coated Sutures Reduce Wound Infection in Head and Neck Cancer Reconstruction? European Journal of Surgical Oncology 2011;37(4):300-304.

183. Fraenkel D, Rickard C, Thomas P, Faoagali J, George N, Ware R. A Prospective, Randomized Trial of Rifampicin-Minocycline-Coated and Silver-Platinum-Carbon-Impregnated Central Venous Catheters. Critical Care Medicine 2006;34(3):668-675.

184. Arvaniti K, Lathyris D, Clouva-Molyvdas P, Haidich AB, Mouloudi E, Synnefaki E, Koulourida V, Georgopoulos D, Gerogianni N, Nakos G and others. Comparison of Oligon Catheters and Chlorhexidine-Impregnated Sponges with Standard Multilumen Central Venous Catheters for Prevention of Associated Colonization and Infections in Intensive Care Unit Patients: A Multicenter, Randomized, Controlled Study. Critical Care Medicine 2012;40(2):420-429.

185. Storch M, Perry LC, Davidson JM, Ward JJ. A 28-Day Study of the Effect of Coated VICRYL* Plus Antibacterial Suture (Coated Polyglactin 910 Suture with Triclosan) on Wound Healing in Guinea Pig Linear Incisional Skin Wounds. Surgical Infections 2002;3:S89-S98.

186. Schierholz JM, Rump AF, Pulverer G, Beuth J. Anti-Infective Catheters: Novel Strategies to Prevent Nosocomial Infections in Oncology. Anticancer Research 1998;18(5B):3629-3638.

187. Fuchs T, Stange R, Schmidmaier G, Raschke MJ. The Use of Gentamicin-Coated Nails in the Tibia: Preliminary Results of a Prospective Study. Archives of Orthopaedic and Trauma Surgery 2011;131(10):1419-1425.

188. Darouiche RO, Mansouri MD, Zakarevicz D, AlSharif A, Landon GC. In Vivo Efficacy of Antimicrobial-Coated Devices. The Journal of Bone and Joint Surgery 2007;89(4):792-797.

189. Wolter CE, Hellstrom WJ. The Hydrophilic-Coated Inflatable Penile Prosthesis: 1-Year Experience. The Journal of Sexual Medicine 2004;1(2):221-224.

190. Darouiche RO. Antimicrobial Coating of Devices for Prevention of Infection: Principles and Protection. The International Journal of Artificial Organs 2007;30(9):820-827.

191. Darouiche RO, Berger DH, Khardori N, Robertson CS, M.J. Wall J, Metzler MH, Shah S, Mansouri MD, Cerra-Stewart C, Versalovic J and others. Comparison of Antimicrobial Impregnation with Tunneling of Long-Term Central Venous Catheters: A Randomized Controlled Trial. Annals of Surgery 2005;242(2):193-200.

192. Darouiche RO, Mansouri MD, Meade R. In-Vitro and In-Vivo Activity of Antimicrobial-Coated Prosthetic Heart Valve Sewing Cuffs. The Journal of Heart Valve Diseases 2002;11(1):99-104.

193. Gaudin A, Valle GAD, Hamel A, Mabecque VL, Miegeville A-F, Potel G, Caillon J, Jacqueline C. A New Experimental Model of Acute Osteomyelitis Due to Methicillin-Resistant *Staphylococcus aureus* in Rabbit. Letters in Applied Microbiology 2011;52(3):253-257.

194. Gilmore BF, Hamill TM, Jones DS, Gorman SP. Validation of the CDC Biofilm Reactor as a Dynamic Model for Assessment of Encrustation Formation on Urological Device Materials. Journal of Biomedical Materials Research Part B 2010;93B(1):128-140.

195. Horii T, Kobayashi M, Sato K, Ichiyama S, Ohta M. An In-Vitro Study of Carbapenem-Induced Morphological Changes and Endotoxin Release in Clinical Isolates of Gram-negative Bacilli. Journal of Antimicrobial Chemotherapy 1998;41:435-442.

196. Cohen J, McConnell JS. Antibiotic-Induced Endotoxin Release. Lancet 1985;2(8463):1069-1070.

197. Ginalska G, Osinska M, Uryniak A, Urbanik-Sypniewska T, Belcarz A, Rzeski W, Wolski A. Antibacterial Activity of Gentamicin-Bonded Gelatin-Sealed Polyethylene Terephthalate Vascular Prostheses. European Journal of Vascular and Endovascular Surgery 2005;29(4):419-424.

198. Fernandez ICS, Mei HC, Metzger S, Grainger DW, Engelsman AF, Nejadnik MR, Busscher HJ. In Vitro and In Vivo Comparisons of Staphylococcal Biofilm

Formation on a Cross-Linked Poly(ethylene glycol)-Based Polymer Coating. Acta Biomaterialia 2010;6(3):1119-1124.

199. Antoci V, Adams CS, Parvizi J, Ducheyne P, Shapiro IM, Hickok NJ. Covalently Attached Vancomycin Provides a Nanoscale Antibacterial Surface. Clinical Orthopaedics and Related Research 2007;461:81-87.

200. Baier RE, Meyer AE, Natiella JR, Natiella RR, Carter JM. Surface Properties Determine Bioadhesive Outcomes: Methods and Results. Journal of Biomedical Materials Research 1984;18(4):327-355.

201. Gottenbos B, Busscher HJ, Mei HCVD, Nieuwenhuis P. Pathogenesis and Prevention of Biomaterial Centered Infections. Journal of Materials Science 2002;13(8):717-722.

202. Guarner F, Malagelada J-R. Gut Flora in Health and Disease. Lancet 2003;361:512-519.

203. Spapen HD, Doom KJv, Diltoer M, Verbrugghe W, Jacobs R, Dobbeleir N, Honore PM, Jorens PG. Retrospective Evaluation of Possible Renal Toxicity Associated with Continuous Infection of Vancomycin in Criticially Ill Patients. Annals of Intensive Care 2011;19(1):26.

204. Sanders WE, Sanders CC. Toxicity of Antibacterial Agents: Mechanism of Action on Mammalian Cells. Annual Review of Pharmacology and Toxicology 1979;19:53-83.

205. Uhthoff HK, Poitras P, Backman DS. Internal Plate Fixation of Fractures: Short History and Recent Developments. Journal of Orthopaedic Science 2006;11(2):118-126.

206. Levin PD. The Effectiveness of Various Antibiotics in Methyl Methacrylate. Journal of Bone and Joint Surgery (British) 1975;57(2):234-237.

207. Miclau T, Dahners LE, Lindsey RW. In Vitro Pharmacokinetics of Antibiotic Release From Locally Implantable Materials. Journal of Orthopaedic Research 1993;11(5):627-632.

208. Zhao G, Hochwalt PC, Usui ML, Underwood RA, Singh PK, James GA, Stewart PS, Fleckman P, Olerud JE. Delayed Wound Healing in Diabetic (db/db) Mice with *Pseudomonas aeruginosa* Biofilm Challenge-A Model for the Study of Chronic Wounds. Wound Repair and Regeneration 2010;18(5):467-477.

209. Miller E, Kutter E, Mosig G, Arisaka F, Kunisawa T, Ruger W. Bacteriophage T4 Genome. Microbiology and Molecular Biology Reviews 2003;67(1):86-156.

210. Cerca N, Jefferson KK, Oliviera R, Pier GB, Azeredo J. Comparative Antibody-Mediated Phagocytosis of *Staphylococcus epidermidis* Cells Grown in a Biofilm or in the Planktonic State. Infection and Immunity 2006;74(8):4849-4855.

211. Leid JG, Willson CJ, Shirtliff ME, Hassett DJ, Parsek MR, Jeffers AK. The Exopolysacharide Alginate Protects *Pseudomonas aeruginosa* Biofilm Bacteria from IFN-γ-Mediated Macrophage Killing. The Journal of Immunology 2005;175:7512-7518.

212. Donlan RM. Biofilms Associated with Medical Devices and Implants. In: Jass J, Surman S, Walker J, editors. Medical Biofilms: Detection, Prevention, and Control; 2003. p 29-96.

213. Melchior MB, Fink-Gremmels J, Gaastra W. Comparative Assessment of the Antimicrobial Susceptibility of *Staphylococcus aureus* Isolates from Bovine Mastitis in Biofilm Versus Planktonic Culture. Journal of Veterinary Medicine Part B 2006;53:326-332.

214. Krizek TJ, Robson MC, Kho E. Bacterial Growth and Skin Graft Survival. Surg Forum 1967;18:518.

215. Ceri H, Olson ME, Morck DW, Storey DG. Minimal Biofilm Eradication Concentration (MBEC) Assay: Susceptibility Testing for Biofilms. In: Pace JL, Rupp ME, Finch RG, editors. Biofilms, Infection, and Antimicrobial Therapy. Boca Raton: CRC Press; 2006. p 257-269.

216. Costerton JW. The Microbiology of the Healthy Human Body. In: Costerton JW, editor. The Biofilm Primer. Heidelberg: Springer; 2007. p 107-128.

217. Brandt C, Hott U, Sohr D, Daschner F, Gastmeier P, Ruden H. Operating Room Ventilation With Laminar Airflow Shows No Protective Effect on the Surgical Site Infection Rate in Orthopedic and Abdominal Surgery. Annals of Surgery 2008;248:695-700.

218. Sponseller PO, Shah SA, Abel MF, Newton PO, Letko L, Marks M. Infection Rate after Spine Surgery in Cerebral Palsy Is High and Impairs Results. Clinical Orthopaedics and Related Research 2010;468:711-716.

219. Kaltsas DS. Infection After Total Hip Arthroplasty. Annals of the Royal College of Surgeons of England 2004;86:267-271.

220. Tate A, Yazdany T, Bhatia N. The Use of Infection Prevention Practices in Female Pelvic Medicine and Reconstructive Surgery. Current Opinion in Obstetrics and Gynecology 2010;22:408-413.

221. Pozo JLD, Patel R. Infection Associated with Prosthetic Joints. The New England Journal of Medicine 2009;361:787-794.

222. Zimmerli W. Prosthetic-Joint-Associated Infections. Best Practice & Research Clinical Rheumatology 2006;20(6):1045-1063.

223. Thomas JG, Nakaishi LA. Managing the Complexity of a Dynamic Biofilm. The Journal of the American Dental Association 2006;137:10S-15S.

224. Grice EA, Kong HH, Renaud G, Young AC, Bouffard GG, Blakesley RW, Wolfsberg TG, Turner ML, Segre JA. A Diversity Profile of the Human Skin Microbiota. Genome Research 2008;18:1043-1050.

225. Kloos WE, Musselwhite MS. Distribution and Persistence of *Staphylococcus* and *Micrococcus* Species and Other Aerobic Bacteria on Human Skin. Applied Microbiology 1975;30(3):381-395.

226. Simon GL, Gorbach SL. Intestinal Flora in Health and Disease. Gastroenterology 1984;86(1):174-193.

227. Stephen AM, Cummings JH. The Microbial Contribution to Human Faecal Mass. Journal of Medical Microbiology 1980;13:45-56.

228. Fry DE, Fry RV. Surgical Site Infection: The Host Factor. AORN Journal 2007;86(5):801-814.

229. Hendley JO, Ashe KM. Effect of Topical Antimicrobial Treatment on Aerobic Bacteria in the Stratum Corneium of Human Skin. Antimicrobial Agents and Chemotherapy 1991;35(4):627-631.

230. Edwards R, Harding KG. Bacteria and Wound Healing. Current Opinion in Infectious Diseases 2004;17:91-96.

231. Robson MC, Heggers JP. Bacterial Quantification of Open Wounds. Military Medicine 1969;134:19-24.

232. Bernthal NM, Stavrakis AI, Billi F, Cho JS, Kremen TJ, Simon SI, Cheung AL, Finerman GA, Lieberman JR, Adams JS and others. A Mouse Model of Post-Arthroplasty *Staphylococcus aureus* Joint Infection to Evaluate *In Vivo* the Efficacy of Antimicrobial Implant Coatings. PLoS One 2010;5(9):e12580.

233. Bowler PG. The 10^5 Bacterial Growth Guideline: Reassessing Its Clinical Relevance in Wound Healing. Ostomy Wound Management 2003;49:44-53.

234. Smeltzer MS, Thomas JR, Hickmon SG, Skinner RA, Nelson CL, Griffith D, Thomas R. Parr J, Evans RP. Characterization of a Rabbit Model of Staphylococcal Osteomyelitis. Journal of Orthopaedic Research 1997;15:414-421.

235. Connell JL, Wessel AK, Parsek MR, Ellington AD, Whiteley M, Shear JB. Probing Prokaryotic Social Behaviors with Bacterial "Lobster Traps". mBio 2010;1(4):e00202-00210.

236. Percival SL, Bowler PG. Biofilms and Their Potential Role in Wound Healing. Wounds 2004;16:234-240.

237. Okuda K, Ishihara K, Nakagawa T, Hirayama A, Inayama Y, Okuda K. Detection of *Treponema denticola* in Atherosclerotic Lesions. Journal of Clinical Microbiology 2001;39(3):1114-1117.

238. Chiu B. Multiple Infections in Carotid Atherosclerotic Plaques. American Heart Journal 1999;138(5 Pt 2):S534-S536.

239. Goeres DM, Loetterle LR, Hamilton MA, Murga R, Kirby DW, Donlan RM. Statistical Assessment of a Laboratory Method for Growing Biofilms. Microbiology 2005;151:757-762.

240. Jiang X, Pace JL. Microbial Biofilms. In: Pace JL, Rupp ME, Finch RG, editors. Biofilms, Infection, and Antimicrobial Therapy. Boca Raton: CRC Press; 2006.

241. Rode TM, Langsrud S, Holck A, Moretro T. Different patterns of biofilm formation in Staphylococcus aureus under food-related stress conditions. Int J Food Microbiol 2007;116(3):372-83.

242. Pitt WG, Ross SA. Ultrasound Increases the Rate of Bacterial Cell Growth. Biotechnology Progress 2003;19(3):1038-1044.

243. Buckingham-Meyer K, Goeres DM, Hamilton MA. Comparative Evaluation of Biofilm Disinfectant Efficacy Tests. Journal of Microbiological Methods 2007;70:236-244.

244. Smith JB, McIntosh GH, Morris B. The Traffic of Cells Through Tissues: A Study of Peripheral Lymph in Sheep. Journal of Anatomy 1970;107(1):87-100.

245. Hulterstrom AK, Berglund A, Ruyter IE. Wettability, Water Sorption and Water Solubility of Seven Silicone Elastomers Used for Maxillofacial Prostheses. Journal of Materials Science 2008;19:225-231.

246. Cross AD. Inroduction to Practical Infra-Red Spectroscopy. London: Butterworths Scientific Publications; 1960. 80 p.

247. Abbasi F, Mirzadeh H, Katbab A-A. Bulk and Surface Modification of Silicone Rubber for Biomedical Applications. Polymer International 2002;51(10):882-888.

248. Abbasi F, Mirzadeh H. Adhesion Between Modified and Unmodified Poly(dimethylsiloxane) Layers for a Biomedical Application. International Journal of Adhesion and Adhesives 2004;24(3):247-257.

249. Orhan JB, Parashar VK, Flueckiger J, Gijs MA. Internal Modification of Poly(dimethylsiloxane) Microchannels With a Borosilicate Glass Coating. Langmuir 2008;24(16):9154-9161.

250. Khorasani MT, Mirzadeh H, Kermani Z. Wettability of Porous Polydimethylsiloxane Surface: Morphology Study. Applied Surface Science 2004;242(3-4):339-345.

251. McHale G, Newton MI, Shirtcliffe NJ. Dynamic Wetting and Spreading and the Role of Topography. Journal of Physics: Condensed Matter 2009;21(46):464122.

252. Quere D. Rough Ideas on Wetting. Physica A: Statistical Mechanics and Its Applications 2002;313(1-2):32-46.

253. McCrum NG, Buckley CP, Bucknall CB. Principles of Polymer Engineering. New York: Oxford University Press; 1997. 242-245 p.

254. Bergstrom JS, Boyce MC. Mechanical Behavior of Particle Filled Elastomers. Rubber Chemistry and Technology 1999;72:633-656.

255. Schinabeck MK, Ghannoum MA. Pathogenesis of IMD Related Infections. In: Pace JL, Rupp ME, Finch RG, editors. Biofilms, Infection, and Antimicrobial Therapy. Boca Raton: CRC Press; 2006. p 42-45.

256. Sousa C, Teixeira P, Oliveira R. Influence of Surface Properties on the Adhesion of *Staphylococcus epidermidis* to Acrylic and Silicone. International Journal of Biomaterials 2009:718017.

257. Brady RA, Leid JG, Calhoun JH, Costerton JW, Shirtliff ME. Osteomyelitis and the Role of Biofilms in Chronic Infection. FEMS Immunology & Medical Microbiology 2007;52(1):13-22.

258. Healy B, Freedman A. ABC of Wound Healing. Infections 2006;332:838.

259. Bloebaum RD, Willie BM, Mitchell BS, Hofmann AA. Relationship Between Bone Ingrowth, Mineral Apposition Rate, and Osteoblast Activity. Journal of Biomedical Materials Research part A 2007;81A(2):505-514.

260. Dykstra MJ. Modified Karnovsky's Fixative. A Manual of Applied Techniques for Biological Electron Microscopy. New York: Springer; 1993. p 21.

261. Emmanual J, Hornbeck C, Bloebaum RD. A Polymethyl Methacrylate Method for Large Specimens of Mineralized Bone with Implants. Biotechnic & Histochemistry 1987;62(6):401-410.

262. Sanderson C, McGee M, Bloebaum RD. Polypropylene Containers for Safe and Predictable Embedding of Specimens in PMMA. Journal of Histotechnology 1990;2:131-133.

263. Bloebaum RD, Higgins HW, Koller KE. A Method for Cemented Bone Interface Examination Without Polymethylmethacrylate Embedment. Journal of Histotechnology 2006;4:229-231.

264. Koller KE, Epperson RT, Bloebaum RD. Deparaffinizing Soft-Tissue Sections for Elemental Analysis of Wear Particulate. Journal of Histotechnology 2006;4:233-235.

265. Isaacson BM, Brunker LB, Brown AA, Beck JP, Burns GL, Bloebaum RD. An Evaluation of Electrical Stimulation for Improving Periprosthetic Attachment. Journal of Biomedical Materials Research Part B 2011;97B(1):190-200.

266. Arens S, Schlegel U, Printzen G, Ziegler WJ, Perren SM, Hansis M. Influence of Materials for Fixation Implants on Local Infection. Journal of Bone and Joint Surgery (British) 1996;78-B(4):647-651.